Nuclear EGFR Modulation of DNA repair

by

Gianmaria Liccardi

A thesis submitted to the University College London for the degree of Doctor of Philosophy

April 2011

CRUK Drug-DNA Interaction Research Group

Department of Oncology

Cancer Institute

University College London

72 Huntley street, London WC1E 6BT, UK

I, Gianmaria Liccardi, confirm that the work presented in this thesis is my own. Where information has been derived from other sources, I confirm that this has been indicated in the thesis with appropriate referencing. The most significant part of this work has been recently published in:

> **Gianmaria Liccardi**, John A. Hartley, Daniel Hochhauser; EGFR Nuclear Translocation Modulates DNA Repair following Cisplatin and Ionizing Radiation Treatment. Cancer Research, February 1, 2011 71:1103-1114

Hence some figures of the result chapters have been taken from the published manuscript of which I am the first Author. The article has been included at the end of this thesis for further referencing.

In loving memory of my auntie Giulia

ABSTRACT

Overexpression of the epidermal growth factor receptor (EGFR) is associated with resistance to chemotherapy and radiotherapy. EGFR involvement, in repair of radiation-induced DNA damage, is mediated by association with the catalytic subunit of DNA protein kinase (DNAPKcs). This study investigated the role of EGFR nuclear import, and its association with DNAPKcs, on DNA repair following treatment either with cisplatin or ionizing radiation (IR). EGFR- null murine NIH3T3 cells were transfected with wild type or with mutated EGFR (mutations found in human cancers L858R, EGFRvIII and mutations in the EGFR nuclear localization signal (NLS) sequence NLS123, LNLS123). Comet assay analysis, which measures unhooking of cisplatin crosslinks and repair of IR induced strand breaks, demonstrated that wtEGFR and EGFRvIII completely repair cisplatin and IR induced DNA damage. Immunoprecipitation studies show that repair is associated with the binding of both wtEGFR and EGFRvIII to DNAPKcs, which increases by 2- fold 18 hours following cisplatin treatment. Confocal analysis and proximity ligation assay indicated that this association takes place both in the cytoplasm and in the nucleus resulting in a significant increase of DNA-PK kinase activity. Intermediate levels of repair as shown by the L858R construct with impaired nuclear localization demonstrated that EGFR kinase activity is partially involved in repair but is not sufficient to determine EGFR nuclear expression. EGFR-NLS mutants showed impaired nuclear localization and impaired DNAPKcs association resulting in significant inhibition of DNA repair and down-regulation of DNA-PK kinase activity.

Our data suggest that EGFR nuclear localization is required for the modulation of cisplatin and IR induced DNA damage repair. The EGFR-DNAPKcs binding is triggered by cisplatin or IR and not by EGFR nuclear translocation *per se*.

Understanding mechanisms regulating EGFR subcellular distribution in relation to DNA repair kinetics will be a critical determinant of improved molecular targeting and response to therapy.

ACKNOWLEDGEMENTS

My first and foremost thanks go to my supervisors: Prof. John Hartley, and Prof. Daniel Hochhauser. I cannot express enough my gratitude for giving me the opportunity to carry out my PhD under your insightful supervision. Thank you for giving me the freedom to develop my own ideas, for the pressure, the support, for the critical discussion and for making sure my work stayed focus… most of the time… I also would like to thank all the members of the lab: those present at the moment and those that have witnessed only a portion of this incredible experience: you all have contributed somehow to my PhD and I can associate at least one unforgettable memory to each and every one of you. Nevertheless there are some members in particular that deserve a special thank. To Dr. Konstantinos Kiakos for being a friend, for the gossips, the fiffis, for the fun and for being there when I needed a friend in the lab: thank you. To Dr. Raisa Vuononvirta: thank you for your friendship, suggestions, honesty and for the nights out with lab: those will be hard to forget. To Valeria Santoro: thank you for the coffees, the lunches, for being a real friend and a great person. A great thanks also to those that understand our code words (I shall not mention them for obvious reasons)… you know who you are… some of the funniest moments of my PhD are linked to those words and I really hope they will stay as a legacy… beside the science of course…

I also would like to thank Nicole Hartig, Berna Demiray and Anne Roehrig for their support, friendship and for keeping me company during the latest (or earliest) time of the day in the lab. A special thank goes to the Cancer Institute graduate tutor, Dr. Julie Olszewski for her great work with the PhD students of the Cancer Institute and for being always very helpful and ready to listen when most needed. A huge thanks goes to Lucia Christodulides for her help in the most critical moments of my PhD, for her honesty and support. You have been an icon during these years.

Special thanks go to my friends Mauro Proserpio and Antonio Gaglioti. Thank you for your sincere friendship, for the nights out, for coming to the lab on the countless Saturdays and Sundays waiting for my experiments to finish before going out. Thank you.

Life would have most definitely been not the same without Francesco Piazza. I will never be grateful enough for the inspiration, for your patience, support, for putting up

with me on the bad days and also… on the good days, but most importantly for keeping me sane during this incredible journey. You have been a rock in my life and this has helped me reaching this destination in one piece.

Most of all, I am deeply grateful to my parents: Maria Guida and Giovanni Liccardi and to my sister Dr. Ilaria Liccardi, for their support, encouragement, love, guidance, for giving me all the opportunities that some people only dream of, for being the best family a son and brother can hope and for teaching me that no matter what comes I can always find the strength to stand up and keep walking. Without you I would have never been able to study abroad and for this I owe you everything I have accomplished so far. Special thanks also go to the rest of my family for believing in me, for their love and thoughts. I love you all very much.

Finally, thank you God for watching over me and bless me with such a wonderful life.

COMMUNICATION

PRESENTATIONS

- **Poster presentation**. Liccardi G., Hartley, A. J., Hocchauser D., Studies of EGFR nuclear expression. International PhD meeting, Amsterdam, Netherlands, April 2008
- **Poster presentation**. Annual meeting, Cancer Institute, UCL, London UK July 2008
- **Poster presentation**. Annual meeting, Cancer Institute, UCL, London UK July 2009.
- **Poster presentation**. Graduate competition, UCL, London UK March 2009.
- **Poster presentation**. AACR annual meeting, Washington DC, USA April 2010.
- **Oral presentation**. Annual conference, Cancer Institute, London, UK. July 2010.
- **Poster presentation**. 22nd EORTC-NCI-AACR Symposium on Molecular Targets and Cancer Therapeutics, Berlin, Germany. November 2010.
- **Poster presentation**. EACR, Genes and Cancer, Warwick, UK, December 2010

PUBLICATIONS

- **Gianmaria Liccardi**, John A. Hartley, Daniel Hochhauser; EGFR Nuclear Translocation Modulates DNA Repair following Cisplatin and Ionizing Radiation Treatment. Cancer Research, February 1, 2011 71:1103-1114

TABLE OF CONTENTS

INDEX OF THE FIGURES

INDEX OF THE TABLES

ABBREVIATIONS

Abl	Abelson
AP-2	adaptor protein 2
APTX	Aprataxin
ATM	Ataxia Telangiectasia Mutated homolog protein
ATP	Adenosine TriPhosphate
ATR	Ataxia Telangiectasia and Rad3 related protein
Bad	Bcl-2-associated death promoter
Bax	Bcl-2–associated X protein
Bcl-2	B-cell CLL/lymphoma 2
BER	Base Excision Repair
bp	base pair
BSA	Bovine serum albumin
BRCT	BRCA1 Carboxyl Terminus
cAMP	Cyclic adenosine monophosphate
cavME	cavoelae mediated endocytosis
Cbl	Casitas B-lineage lymphoma protein
CCPs	clathrin coated pits
Cdc	Cell division cycle
CDDP	*cis*-diamminedichloroplatinum(II), cisplatinum or cisplatin
Cdk	Cyclin-dependent kinases

cDNA	complementary DNA
CHK1/2	Choline Kinase
COMET	Single-cell gel electrophoresis
COX-2	CycloOxygenase 2
CT	Carboxy-terminal
DMEM	Dulbecco Modified Eagle's Minimal Essential Medium
DMSO	DiMethyl SulfOxide
DNA	Deoxyribose Nucleic Acid
DNA-PK	DNA-dependent Protein Kinase comples
DNAPKcs	DNA-dependent Protein Kinase catalytic subunit
DSB	Double strand break
dNTP	deoxyNucleoside triphosphate
ECD	Extracellular Domain
ECL	Enhanced chemoilluminescence
EDTA	EthyleneDiamine Tetraacetic Acid
EGF	Epidermal Growth Factor
EGFR	HER1 or ErbB1, Epidermal Growth Factor Receptor
EGFRvIII	Epidermal Growth Factor Receptor variant III
ELISA	Enzyme-Linked ImmunoSorbent Assay
ER	Endoplasmic Reticulum
ErbB2	HER2 or ErbB2/neu, Epidermal Growth Factor Receptor 2
ErbB3	HER3, Epidermal Growth Factor Receptor 3

ErbB4	HER4, Epidermal Growth Factor Receptor 4
ERCC	Excision Repair Cross-Complementing
ERK1/2	Extracellular signal-Regulated Kinase
FA	Fanconi Anemia
FANCA	Fanconi Anemia Complementation group A
FANCC	Fanconi Anemia Complementation group C
FANCD	Fanconi Anemia Complementation group D
FCS	Foetal Calf Serum
GG-NER	Global Genome Nucleotide Excision Repair
GIST	GastroIntestinal Stromal Tumors
Grb2	Growth factor receptor-bound protein 2
GSK-3	Glycogen Synthase Kinase 3
Gy	Gray (irradiation unit)
H2AX	variant of the histone H2A
HR	Homologous Recombination
HRP	HorseRadish Peroxidase
ICL	Interstrand CrossLinks
IF	ImmunoFluorescence
IR	Ionizing Radiation
i-NOS	Inducible nitric oxide synthase
IP3	Inositol triphosphate
JAK	Janus kinase

JNK	C-jun N-terminal kinase
kDa	kiloDaltons
Kb	kilobase
L	Leucine
L858R	EGFR mutant bearing substitution of the Leucine 858 into Arginine
LNLS123	L858R bearing the NLS123 mutation
M1	EGFR mutant bearing the mutation of the first cluster of Arginine into Alanine
M12	EGFR mutant bearing the mutation of the first and second cluster of basic amino acid residues into Alanine
MAPK	Mitogen Activated Protein Kinase
MDM2	Murine Double Minute 2 protein
MEK1/2	MAPK/ERK kinase
MRE11	Meiotic Recombination 11
MRN	MRE11/NBS1/RAD51
mTOR	mammalian Target Of Rapamycin
n	degree of freedom
NBS1	Nijmegen Breakage Syndrome 1
NER	Nucleotide Excision Repair
NFkB	nuclear factor kappa-light-chain-enhancer of activated B cells
NHEJ	Non Homologous End-Joining
NLS	Nuclear Localisation Signal
NLS123	EGFR bearing the mutation of all the cluster of Arginine into Alanine

NRGs	Neuregulins
NSCLC	Non Small Cell Lung Cancer
OD	Optical Density
OTK	Oncogenic Tyrosine Kinase
p	level of significance
PY	Phospho tyrosine
P	proline
PARP	Poly (ADP-Ribose) Polymerase
PBS	Phosphate Buffered Saline
PCNA	Proliferating Cell Nuclear Antigen
PCR	Polymerase Chain Reaction
PDGFR	Platelet-derived Growth Factor Receptor
PDK1/2	Phosphoinositide Dependent Kinase
PI	Propidium Iodide
PI3K	PhosphatidylInositol-3 Kinase
PIKK	Phosphatidylinositol-3 kinase-related kinases
PIP_2	PhosphatidylInositol bisPhosphate
PIP_3	PhosphatidylInositol (3,4,5)-trisPhosphate
PKB	Protein Kinase B (Akt)
PLC-γ	Phospholipase C subunit γ
PKC	Protein Kinase C
PNK	PolyNucleotide Kinase

PTB	Phospho Tyrosine Binding domain
PTEN	Phosphatase and TENsin homolog
mRNA	messenger RiboNucleic Acid
R	Arginine
ROS	Reactive oxygen species
RT	Room temperature
RTK	Receptor tyrosine kinase
RPA	Replication Protein A
RT-PCR	Reverse Transcriptase PCR
S	Serine
S473	Serine 473
SCID	Severe combined immunodeficient
SCLC	Small cell lung cancers
SDS	Sodium dodecylsulphate
scFv	single chain variable Fragment
SD	Standard Deviation
SE	Standard Error
SH2	Src homology 2
SOS	Son of sevenless
SSB	Single strand break
Src	V-src sarcoma (Schmidt-Ruppin A-2) viral oncogene homolog
STAT	Signal Transducer and Activator of Transcription

T308	Threonine 308
TBS	Tris buffered saline
TBS-T	Tris buffered saline Tween
TCR	Transcription Coupled Repair
TGF	Transforming Growth Factor
TK	Tyrosine Kinase
TKD	Tyrosine kinase domain
TKIs	Tyrosine kinase inhibitors
TOPO2α	Topoisomerase IIα
TP53	Tumour suppressor p53
UV	UltraViolet
VEGF	Vascular Endothelial Growth Factor
Y	Turosine
XPA	Xeroderma Pigmentosum A

CHAPTER 1:

GENERAL

INTRODUCTION

1.1 CANCER EPIDEMIOLOGY

According to the world health organization (WHO) more than 11 million people are diagnosed with cancer every year. It is the leading cause of death worldwide accounting for 7.4 million deaths in 2004 and 7.9 million deaths in 2007 (around 13% of all deaths). The main types of Cancer leading to overall cancer mortality are lung (1.3 million deaths/year), stomach (803000 deaths), colorectal (639000), liver (610000), breast (519000). It has been estimated that deaths from cancer will rise with an estimated 12 million deaths in 2030.

1.2 CANCER AETIOLOGY

1.2.1 The molecular origin of Cancer

In contrast to genetic disorders where a single gene mutation is sufficient to cause disease, cancer is a multi-step process (Hanahan & Weinberg, 2000). Tumorigenesis stems from an acquired abnormal cellular growth and unregulated cellular replication (Croce, 2008). Cumulative mutations within oncogenes, tumour suppressor genes and stability genes arise from chromosomal translocation, gene amplifications or intragenic mutations. These induce gene product over expression or constitutive activation leading to cancer and its progression (Vogelstein & Kinzler, 2004). Missense mutations, deletions, insertions or epigenetic silencing that reduce tumour suppressor activation and/or expression lead to unregulated cellular replication (Martin, 2003).

Eukaryotic cells have evolved a complex system to respond to their environment and needs. Correct cellular replication is indispensable to maintain integrity of the genome within one cell and throughout its progeny (DePinho, 2000). Stability genes or caretakers family of genes comprise DNA repair genes and genes involved in mitotic recombination or chromosomal segregation. These genes minimise genetic alteration but when inactive, mutations in other genes occur at a higher rate. Every gene can be a target of increased mutation rate, but only mutations in oncogenes and tumour suppressors can confer selective growth advantage over non-mutated cells (Vogelstein & Kinzler, 2004).

Germline mutations of these genes result in hereditary predisposition to cancer (Merlo et al, 2006; Shackleton et al, 2009). The mutations of these genes in somatic cells result in tumours. The first somatic mutation in an oncogene or tumour suppressor that causes

clonal expansion initiates the neoplastic process. Following mutations result in additional rounds of clonal expansion and therefore tumour progression (Hanahan & Weinberg, 2000)

1.2.2 Cancer Heterogeneity confers resistance to treatments

According to the clonal evolution theory a tumour can grow, mutate and undergo different selective pressures acquiring a fundamental diversity both between cancer types and within an individual tumour. This model holds that such secondary or tertiary genetic alterations confer a selective advantage that allows individual clones to out-compete other clones and acquire differences in clinical behaviour, in the response to therapy and in their resistance potential (Nowell, 1976). In contrast to this approach the cancer stem cell model suggests that some cancers are driven by a small population subset of cancer cells (Dick, 2008). As a normal stem cell differentiates into phenotypically different cells, it has been shown that also cancer cells may undergo a series of epigenetic changes that result in a progeny with a limited proliferative potential and irreversible loss of tumorigenic capacity. These non-tumorigenic cells compose the bulk of a tumour (Shackleton et al, 2009). While these two models are not mutually exclusive in cancers that follow the stem cells model (cancer stem cell will generate a progeny in a clonal evolution fashion) (Williams et al, 2007), the heterogeneity of cancers that do not follow the stem cell model is only due to clonal evolution. The main difference between the two models is that the heterogeneity proposed by the clonal evolution model suggests that all cells within a cancer have the potential to contribute to disease progression and therefore all cells must be eliminated to cure the disease (Shackleton et al, 2009). In contrast the cancer stem cell origin suggests that only a specific subset population of cancer stem cells needs to be eradicated (Dick, 2008). Difficulty of eliminating all the tumorigenic cells before even one reaches growth advantage (clonal evolution model) and the difficulty of reaching cancer stem cells and distinguish them from non tumorigenic cells make clinical management difficult. This and the clear understanding of which cancers follow which model are central to improve successfulness of targeted therapy.

1.3 CANCER TREATMENTS

Surgery, radiation therapy (RT), hormonal therapy and chemotherapy are the major treatments for cancer. Radiotherapy is based on the use of ionising radiation (IR) and

specifically targets a limited area of a tumour. Chemotherapy is a more systemic approach, usually utilized to treat larger or spread tumours. The majority of patients affected by cancer will receive some form of RT or chemotherapy as a single therapy or in combination as a concomitant therapy, or adjuvant after surgical removal of a tumour. It has been reported that the assessment of the contributions of different modalities to cure rates, of those cured, 11% are cured by chemotherapy, 40% are cured by RT and 49% are cured by surgery (Tobias J & Hochhauser D.; 2010).

1.3.1 Radiotherapy

Standard radiotherapy is applied by the usage of high photons X-rays produced by linear accelerators. Following the first observation that IR reduced the viscosity of DNA in solution (Dikomey & Franzke, 1986a), IR has been shown to induce single and double DNA strand breaks (SSBs, DSBs) and covalent bonds leading to DNA-protein crosslinks (Dikomey & Franzke, 1986b) and DNA-DNA crosslinks (Jackson & Bartek, 2009; Szumiel, 2008; Ward, 1995). In a mammalian cell 1 Gray (Gy) of IR has been estimated to produce 1000 SSBs, 30-40 DSBs and around 3000 base damages (being a single strand break the consequence of 2.7 base damages) (Ward, 1995). DSBs are known to be the most lethal type of damage and even 1 unresolved DSB could cause cell death (Jackson & Bartek, 2009; Jeggo & Lavin, 2009). IR-induced DNA damage is not randomly distributed throughout the genome of an exposed cell (Olive & Banath, 2006). Due to the high local energy deposition via a radiation particle track, the damage produced (comprising 1 or more DSBs, associated SSBs, base damages and crosslinks) is all clustered within about 10 base pairs (Glei et al, 2009). Because of its complexity, this type of clustered damage is less repairable than sparse damage throughout the genome.

1.3.1.1 Radiotherapy unspecificty

Therapeutic usage of X-rays requires high voltage varying from 50kVto 30 MeV. As the voltage increases, X-rays of shortage wavelength are also produced (Collins, 2004). Although these have a greater penetration within the tissues, the radiation energy deposited at any depth of tissue falls off exponentially leading to irradiation of the superficial area of the tumour and beyond it (the tumour free tissue surrounding it). This represents the major limiting factor of Radiation therapy (McArt et al, 2009). The

effects of RT depend on two main factors: oxygenation of the tumour tissue and tumour repopulation following treatment.

1.3.1.1.1 Oxygenation

Well oxygenated tissues are more radiosensitive than those that are anoxic. This is because RT produces free oxygen radical adding a great deal of DNA damage to what IR has already produced *per se.* Cancer cells often display increased glycolysis and CO_2 production resulting in acidification and production of a hypoxic environment. Hypoxic cancer cells require higher doses of radiation compared to anoxic cells because lack of oxygen impedes formation of free radicals. Reduction of tumour bulk via RT results in relieve of vascular obstruction allowing blood supply and greater sensitivity to subsequent doses of irradiation due to the oxygenation effect (Azqueta et al, 2009; Fyles et al, 1998; Masunaga et al, 2009).

1.3.1.1.2 Repopulation

Tumour repopulation during, or at the end of, the course of RT can take place via regeneration of the radioresistant stem cells. Resistance to RT is usually acquired via: a) DNA induced damage, b) the binding of free radicals by glutathione and other sulfryd molecules, c) the increased glutathione S transferase and other enzymes that eliminate free radicals and inhibit expression of anti apoptotic proteins (Bentzen, 2003; Gao et al, 2010; Schmidt-Ullrich et al, 1999).

1.3.2 Chemotherapy

The majority of current anticancer drugs exert their effects by targeting and reducing enhanced cellular proliferation and division of cancer cells. Recently, the design of drugs that target invasion, metastasis and vascularisation of tumour cells has been also a major focus of cancer therapy (Helleday et al, 2008). Cell cycle and cellular division can be targeted in several ways:

- Targeting DNA directly with DNA damaging drugs
- Direct targeting of the cell division with inhibitors of the mitotic spindles that prevent equal division of DNA to the two daughter cells
- Targeting the growth signals that promote entry of the cell into the cell cycle via hormonal manipulation

- Targeting the signalling pathway that control growth, proliferation and division

The majority of the drugs in use today fall in the first two categories. Highly replicating cells, like cancer cells, can undergo increased cellular death by attempting to replicate over damaged DNA. The capability of cancer cells to overcome/bypass this obstacle suggests that DNA repair pathways efficacy can modulate the effects of chemotherapeutic drugs. In some cancers the inherited inactivation of these pathways is one of the contributing factors of carcinogenesis (Middleton & Margison, 2003). Paradoxically, tumour progression has been associated in some instances with activation and enhancement of the DNA repair pathways and in some other cases their inactivation has also been associated with chemoresistance. These features make DNA repair mechanisms and their modulators a promising target for cancer therapy (Darzynkiewicz et al, 2009; Fojo, 2001; Helleday et al, 2008).

Anticancer drugs can be grouped according to type of DNA damage induced as described in Fig 1.1. Only the most relevant drugs to this study have been reviewed.

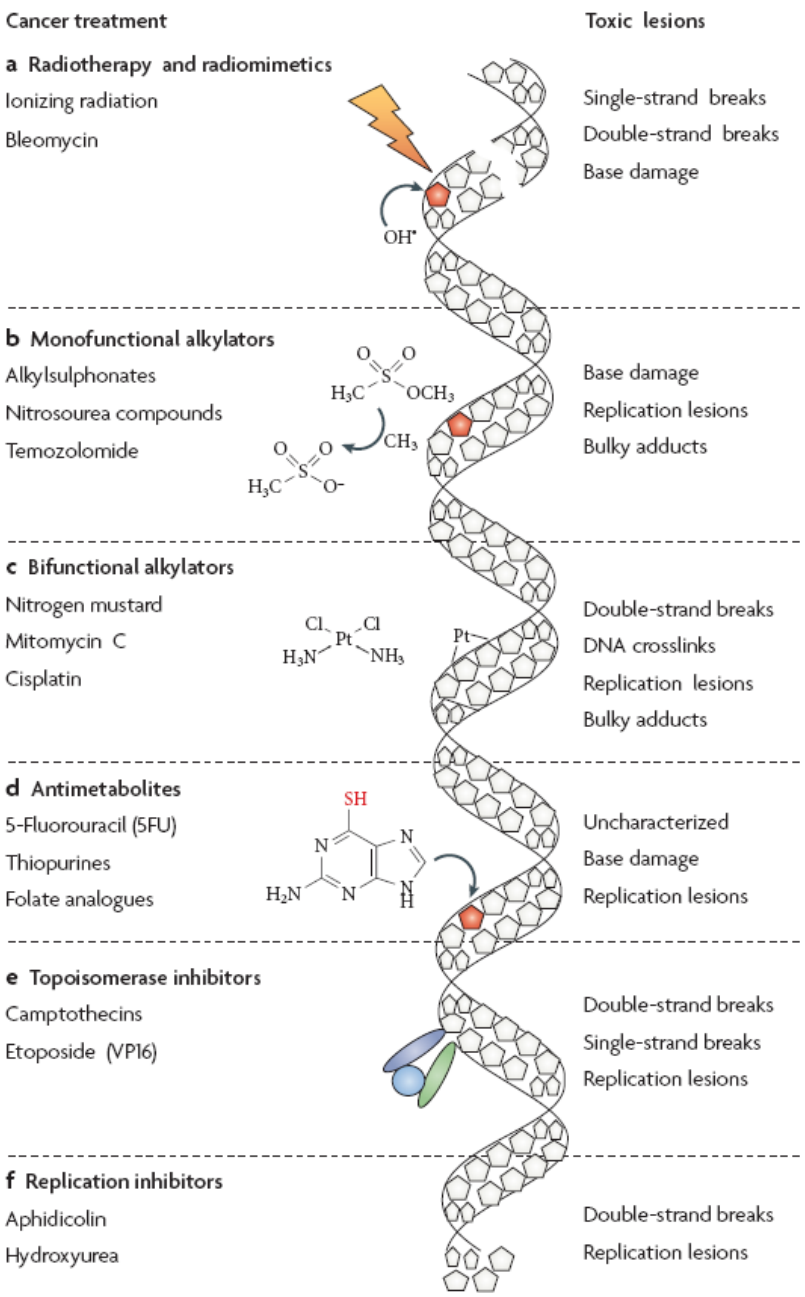

Figure 1.1: Summary of the toxic lesions produced by Cancer Treatment and the pathways engaged to repair them. The diagram shows the type of treatment together with the chemical structure of the most representative molecules (left), the toxic lesion correspondent to the treatment and the major DNA repair pathway involved (right). The diagram was taken from (Helleday et al, 2008).

1.3.2.1 Alkylating Agents

These drugs induce a type of lesion that interferes with the replication fork progression via the production of a chemical modification (adduct) of the DNA bases. Adducts are generally created by the covalent binding of the drug alkyl group ($R\text{-}CH_2$) to chemical moieties in DNA after being metabolized in the body (McCune & Slattery, 2002). Alkylating agents are categorized in Monofunctional alkylators with one active moiety that modifies single bases and Bifuctional alkylating agents that have two reactive sites and usually crosslink DNA with protein and/or crosslink two DNA bases within the same DNA strand (intrastrand cross-links) or on opposite DNA strands (interstrand cross-links). The cross-link is dependent on the chemical structure of the drug which determines 1) the length of DNA that it affects, 2) the type of adduct on the opposite strand and 3) the sequence of bases that is most favourable for the binding. Therefore, alkylating agent's damage is highly chemical selective explaining the different responses in different tumours (Lind & Ardiet, 1993).

Examples of monofunctional alkylators are: Alkysulphonates, Nitrosourea compounds, Temozolomide. Nitrogen mustards, Mytomicin C and Cisplatin are bifunctional alkylators (Chabner & Roberts, 2005).

1.3.2.1.2 Cisplatin

Cisplatin (cis-Diamine dichloroplatinum (II)) or cis-DPP (Fig 1.2) is one of the most used antitumour drugs today. Its anticancer properties were only noticed in the middle 1960 by Rosenberg and co-workers when they realized that platinum electrodes released platinum complexes by redox reactions that provoked complete inhibition of cellular division in Escherichia coli (Cepeda et al, 2007). Cisplatin is a neutral, square planar molecule of platinum (II) bound to two chloride and two ammonia groups, where the chloride molecules are in the cis-geometry(Wang & Lippard, 2005). When administrated intravenously, quickly diffuses into tissues binding primarily to plasma proteins. Due to the strong reactivity of platinum against sulphur and thiol groups of amino acids such as cysteine, nearly 90% of platinum in the blood is bound to albumin and other proteins leading to the inactivation of the majority of cisplatin.

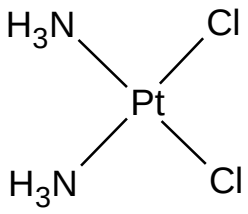

Figure 1.2: Structure of cisplatin. Cisplatin (*cis*-diamminedichloroplatinum(II), CDDP) is an inorganic compound with a planar structure.

The loss of chloride groups is required for the binding to genomic DNA (gDNA). In the blood, the chloride concentration is high (100mM) whereas upon entering cells, where it is lower (30mM), the chloride groups are replaced by water molecules. This cationic aquated mono, $[Pt(H_2O)Cl(NH_3)_2]^+$, and diaquo, $[Pt(H_2O)_2(NH_3)_2]^{+2}$, species of cisplatin are very reactive with nucleophilic sites on macromolecules . The N7 atoms of guanine (G) and adenine (A) located in the major groove of the double helix are the most accessible and reactive sites for platinum binding to DNA due to their high nucleophilicity and accessibility (Cepeda et al, 2007; Wang & Lippard, 2005). Interestingly only 10% of the covalently bound cell-associated cisplatin is found in the gDNA and about 75-85% of the drug binds to proteins, RNA, thiol-containing peptides, and other cellular components rich in nucleophilic sites such as cytoskeletal microfilaments (Akaboshi et al, 1992). The formation of the crosslinks inhibits DNA replication and transcription, by stalling the replication machinery at the site of the crosslink that can bend the double helix towards the major groove or even unwind it (Martin et al, 2008). Recognition of the damage, failure to unhook the crosslink, replication machinery stall, indirect further damage produced by the crosslinks and activation of other signalling pathways contribute towards cisplatin cytotoxicity (Jakupec et al, 2003; Kartalou & Essigmann, 2001a; Kartalou & Essigmann, 2001b).

Cisplatin is a widely used chemotherapeutic agent for a large number of cancers it is effective in ovarian cancer, bladder cancer, lymphoma and non small-cell carcinoma of the bronchis. It is active in osteosarcoma, oesophagogastric cancer, squamos cancer of the head and neck. It has been used in combination with radiotherapy and other chemotherapeutic agents in cancer that have shown resistance to treatment (Borst et al, 2008), (Tobias & Hochhauser 2010), (Savage et al, 2009).

1.3.3 Hormonal therapy

The drugs utilized for this approach aim at targeting the endocrine function by affecting steroid hormones and their antagonists. This leads to a modulation of the tumour growth. They are divided into two classes: antagonists or competitive antagonists of the estrogen receptor (mainly used in breast cancer) and glucorticoids. The first group induces a G-S transition arrest resulting in cell death the second group targets protein synthesis leading to apoptosis (Prat & Baselga, 2008).

1.4 DNA DAMAGE AND REPAIR

Exogenous and endogenous damage agents that cause different types of DNA damage constantly threaten the human genome (De Bont & van Larebeke, 2004; Shrivastav et al, 2008). These are:

Byproducts of normal cellular metabolism:

- Hydrolysis is a cause of spontaneous DNA depurination, reactive oxygen species that cause DNA breaks (Li et al, 2000)
- Replication defects can cause mismatches and replication fork collapses resulting in strand breaks (Paques & Haber, 1999).

Environmental agents:

- ultraviolet light (UV) (De Bont & van Larebeke, 2004),
- ionizing radiation (IR) (Azevedo et al)
- Genotoxic chemicals (Branzei & Foiani, 2008).

As previously explained this constant induction of DNA damage and the inherited mutation within the sequence of key genes can affect the integrity of the genome and induce tumorigenesis. In order to protect themselves from the consequences of this damage, cells have evolved DNA damage repair systems, which recognise the different type of damage and activate specific repair pathways that will repair the DNA lesions (Zhou & Elledge, 2000). Activation of DNA repair pathways often induces a cell cycle arrest to allow sufficient time to completely repair the DNA lesions; however improper repair can take place mostly due to the large extent of the damage. This causes inheritable permanent mutations to the daughter cells and oncogenesis or sometimes programmed cell death (Moynahan & Jasin, 2010). For example, recognition of unrepaired DSBs can cause either activation of apoptosis or improper chromosome

segregation resulting in chromosome aberrations such as deletions, translocations, and ultimately oncogenesis (Lobrich & Jeggo, 2007; Selvanayagam et al, 1995).

The next section will illustrate the different DNA repair mechanisms, their impact on the cell cycle and the mechanism of cellular death triggered by DNA damage.

Fig 1.3 summarises the cellular response to DNA damage.

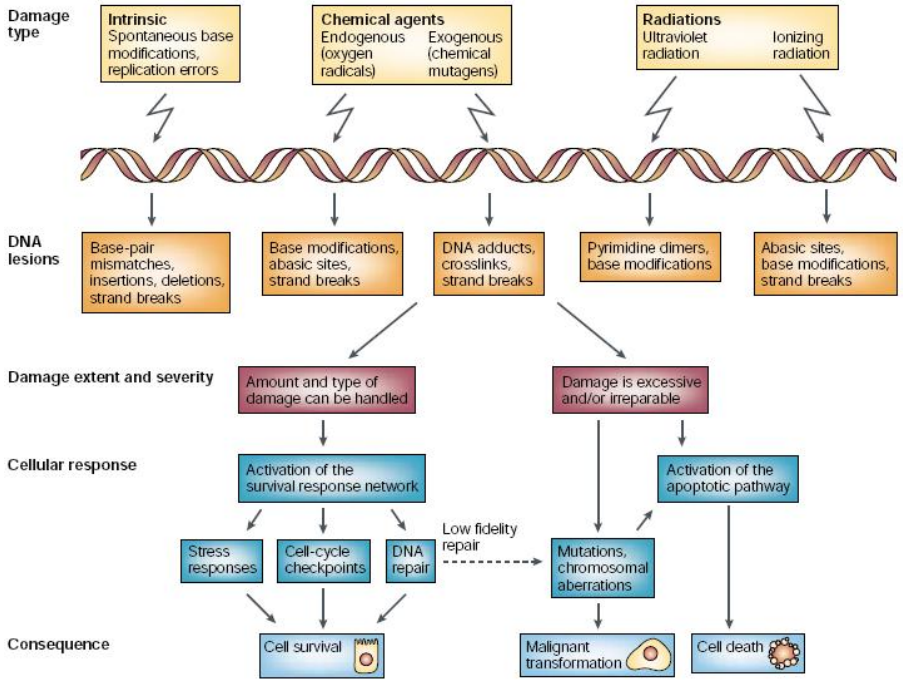

Figure 2.3: Cellular response to DNA damage. Different types of damage are dealt by the cell in different ways. The diagram shows the cellular response to DNA damage and its consequences. The diagram was taken from (Shiloh, 2003).

1.4.1 Nucleotide excision repair (NER)

It is the most versatile and most ubiquitous repair mechanism. It recognizes a wide variety of unrelated DNA lesions such as 6-4 pyrimidone photoproducts, benzo[a]pyrene DNA adducts induced by cigarettes smoke, cyclobutane pyrimidine dimers induced by UV and cisplatin adducts (Bessho et al, 1997; De Silva et al, 2000; De Silva et al, 2002). There are two subsets of the NER pathway, global genomic repair (GGR), also called short patch, and transcription-coupled repair (TCR), long patch, which only differ in the recognition of the damage (Nojima et al, 2005; Tornaletti, 2009). In its simplest form NER involves four steps: 1) recognition of the damage and formation of a pre-incision complex, 2) asymmetric incision at the 5' and 3' of the lesion to produce a short oligo containing the single stranded damaged DNA 3) Repair by utilizing the undamaged complementary strand 4) ligation of the newly synthesized

strand to complete the repair of DNA (Hoeijmakers, 2001). While in GGR XPC/HR23B is the major DNA lesion recognition complex, in TCR the damage is recognized by the arrest of the elongating RNA polymerase (RNAP) at the site of the lesion. The recognition of the lesion triggers the recruitment of the transcription factor II H (TFIIH). TFIIH is a nine subunit complex two of which, XPB and XPD, are DNA helicases that unwind the DNA damaged duplex. Once the strands are unwound and the damages site inaccessible, XPF-ERCC1and XPG are recruited to make the 5' and 3' excision on each site of the lesion creating a 22-30 base oligonucleotide. Using the opposite undamaged strand replication factor C (RFC), PCNA, DNA polymerase δ or ε, DNA ligase I and RPA, gap fill the excised strand and ligate the synthesized oligonucleotide to the DNA strand (Andressoo et al, 2005; Andressoo et al, 2006; Hoeijmakers, 2001; Hoeijmakers, 2007; Hoeijmakers, 2009; Mitchell et al, 2003). Fig 1.4 summarise the pathway.

1.4.2 Base excision repair (BER)

It is mainly involved in the repair of DNA damage cause by cellular metabolism. BER recognizes mainly DNA damage occurring during cellular metabolism as a result of reactive oxygen species, hydrolysis, methylation and deamination. In addition BER is employed by the formation of a SSB following IR (Swartzlander et al; Swartzlander et al, 2010).

Normally glycosilases flip the damaged base out of the helix forming an abasic site (hydrolysis per se forms and abasic site). At this stage the endonuclease APE1 makes an incision at the damaged strand and DNA polβ removes the 5' baseless sugar residue and allows the XRCC1 protein to synthesize the damaged base. DNA Ligase 3 seals the strand break completing the repair. If the long patch pathway is activated, DNA pol δ/ε and PCNA produce an incision and re-synthesize 2-10 bases, FEN1 endonuclease cleaves the displaced DNA fragment and DNA Ligase I seals it to the DNA strand. Some BER lesions can cause block of transcription, which will be dealt by the TCR (Hoeijmakers, 2007). Usually when BER is utilized for the repair of a SSB, the poly ADP ribose polymerase-1 (PARP1) and PNK are recruited to the site of the damage to prevent any unwanted recombination event and signal for BER initiation (Griffiths et al, 2009). Fig 1.5 shows the steps of this pathway.

1.4.3 Mismatch repair (MMR)

It is a highly conserved mechanism, strand specific which is initiated by the recognition of mismatched or unmatched DNA base pairs or insertion-deletion of loops. Mammalian MMR involves the family members of the E. coli MutS and MutL. Heterodimer formation of the human MutS homolog 2 and homolog 6 (hMSH2/6) also called hMutSα recognizes mismatches and single base loops (Zdraveski et al, 2002). Insertion or deletion loops are usually recognized by the hMSH2/3 (hMutSβ) (Sugawara et al, 1997). Formation of other heterodimeric complexes of the hMutL-like proteins hMLH1/hPMS2 (hMutLα) and hMLH1/hPMS1 (hMutLβ) interact with the MSH complexes and the replication factors either to contact the replication machinery or to stabilize the MSH complexes on the lesion. Following recognition of the damage strand discrimination of the newly synthesized (containing the mismatch) strand is probably based on physical contact with the nearby replication machinery (Martin et al, 2008). Excision of a DNA fragment past the mismatch and its degradation are carried out by RPA, PCNA, RFC, exonuclease1 and endonuclease FEN1(Hoeijmakers, 2001). Correct synthesis is mediated by the activity of polδ/ε. Fig 1.6 shows a diagram of the pathway.

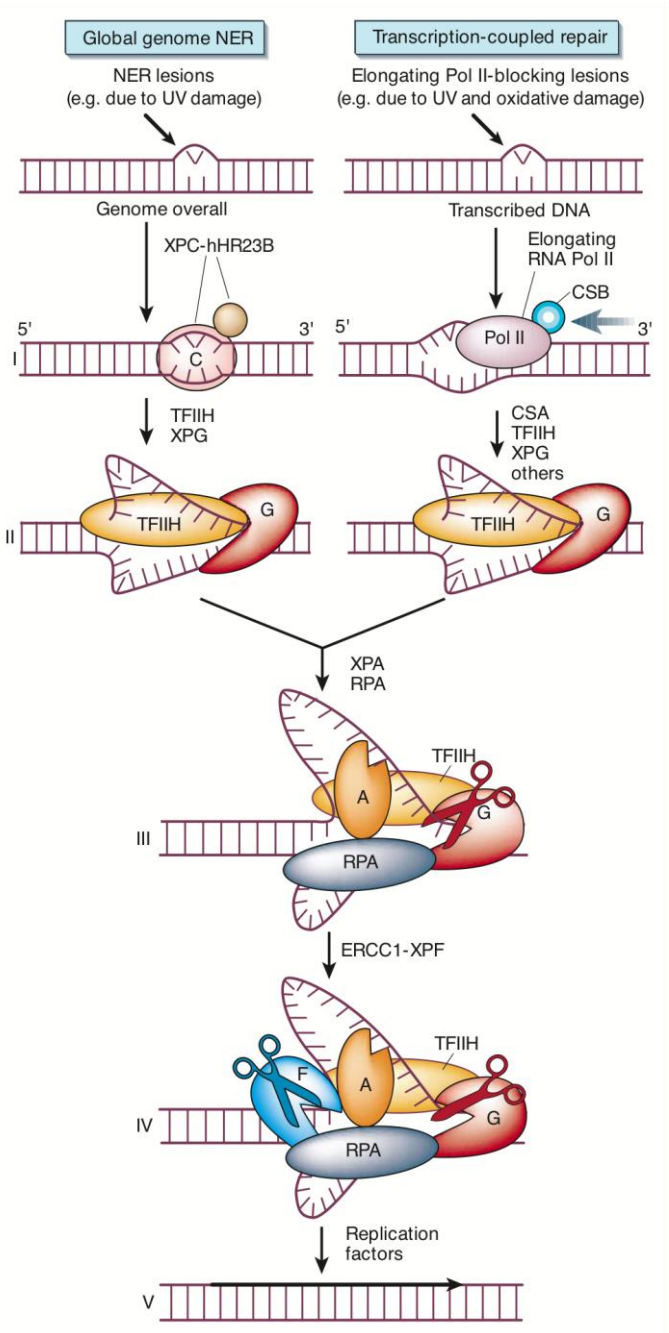

Figure 1.4: Nucleotide excision repair. The diagram shows the different steps and the molecules involved in this repair pathway (Hoeijmakers, 2001).

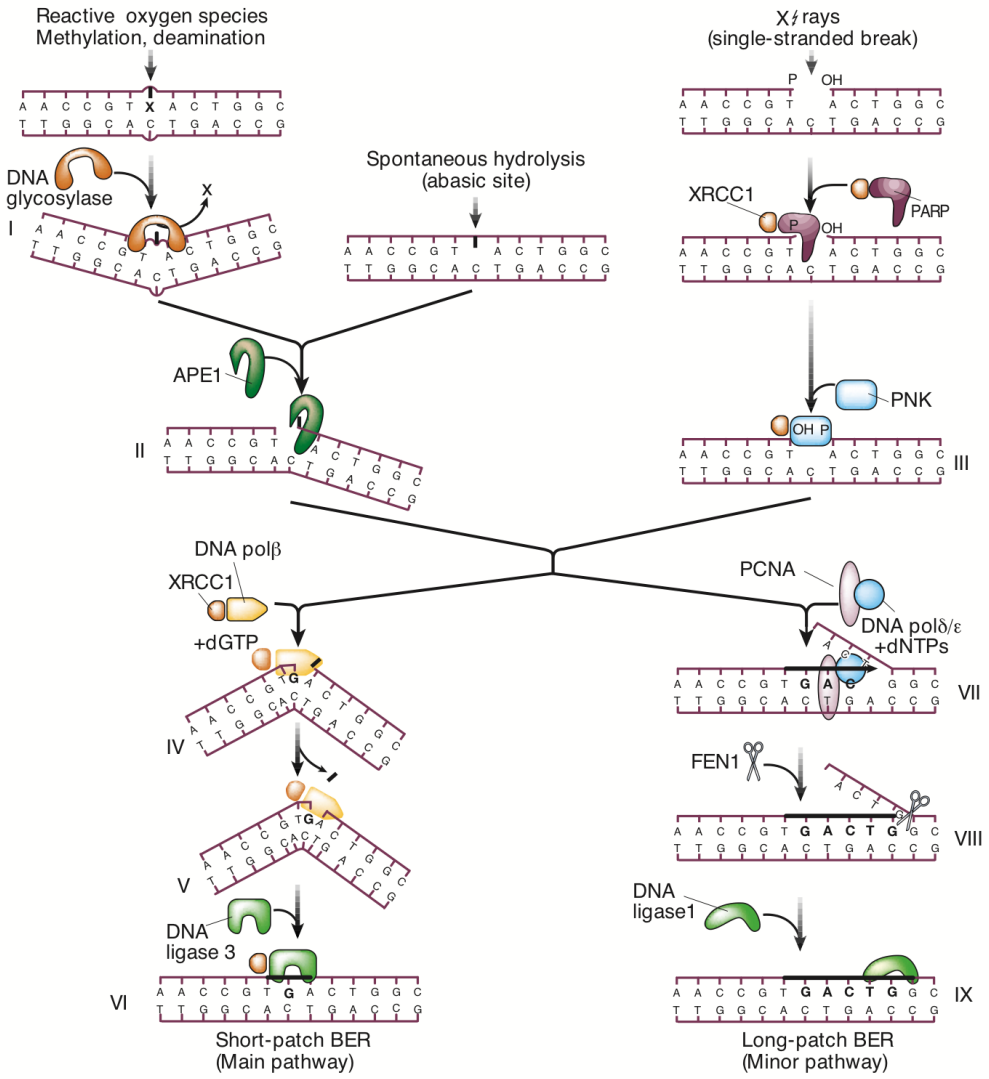

Figure 1.5: Base excision repair (BER) pathways. (Hoeijmakers, 2001)

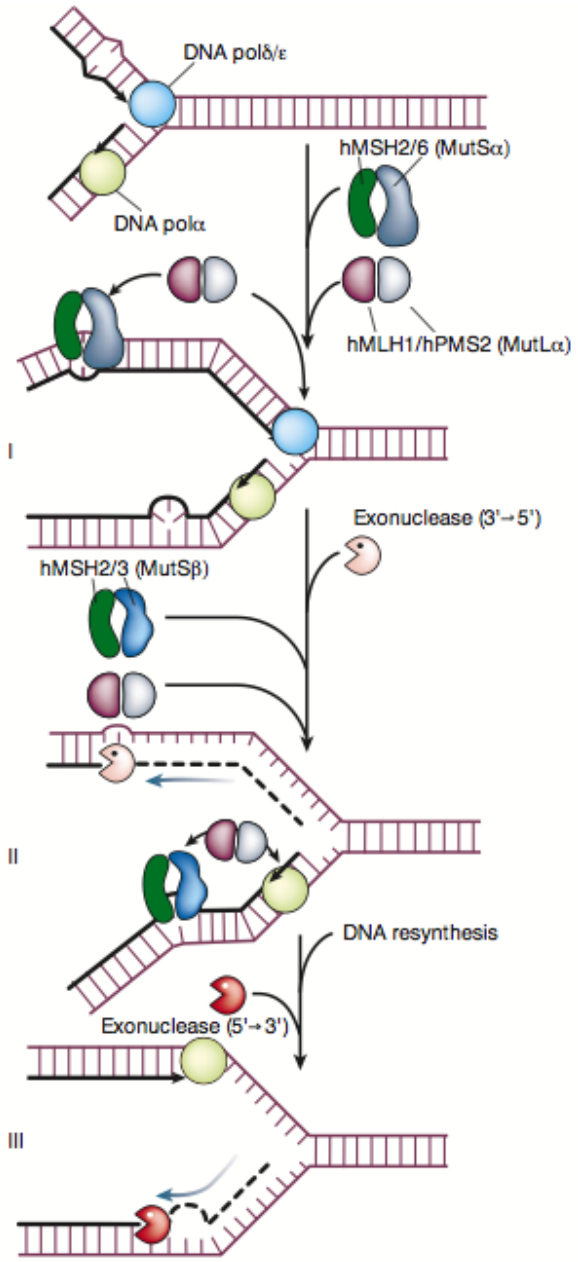

Figure 1.6 Mismatch repair (MMR) pathway. Hoeijmakers J.H., Nature 2001

1.4.4 Double strand breaks repair pathways: Nonhomologous end joining and Homologous recombination.

1.4.4.1 Double strand breaks causes and consequences

DSB are naturally generated in the cells when the replication fork encounters a DNA nick or blocking lesion. DSBs can be classified in Physiological DSBs and Pathological DSBs. Physiological DSBs are those that arise from programmed genome rearrangement (yeast mating switch type, V(D)J recombination, antigen receptor gene rearrangement and meiosis). Pathological double strand breaks are those produced by oxidative free radicals, IR, replication across another lesion, inadvertent nuclear enzyme action at a fragile site, topoisomerase failure, and physical stress imposed on the chromosome during mitosis (Caldecott, 2008). Normally during oxidative respiration mitochondria convert from 0.1-1% of the oxygen to superoxide (O_2^-). Superoxide dismutase in the mitochondrion (SOD2) and in the cytosol (SOD1) converts this into hydroxyl free radicals, which react with DNA causing single strand breaks. Two closely spaced SSBs give rise to a DSB. Each hour around 10^{22} ROS are produced in the human body (10^9 per hour per cell). Environmental IR, such as γ-rays and X-rays, is also a cause of DSBs. Only at seas level around 300 million IR particles pass through each person per hour. These create free radicals that cluster around DNA generating 1 DSB for every 25 SSBs (De Bont & van Larebeke, 2004). Despite being the most mutagenic form of DNA damage, mammals have evolved a way to exploit the formation of DSBs to control biological processes and maintain heterogeneity. In addition to the action of topoisomerases II that induce the formation of DSBs to decatenate the DNA strands, DSBS occur also to initiate rearrangement during maturation of immunoglobulin genes and are central in the recombination events between homologs during meiotic prophase I (McKinnon & Caldecott, 2007).

The failure to repair or missrepair DSBs can result in cellular death or in large-scale chromosome deletions, translocations, and fusions enhancing genome instability and induce carcinogenesis. This is one of the main reasons why chemical agents such as Topoisomerase poisons, other chemotherapeutic drugs and IR therapy while inducing substantial damage to eradicate cancer cells may induce, at the same time, secondary malignancies, by targeting the genome integrity of non cancer cells (Jeggo & Lobrich, 2007; Khanna & Jackson, 2001).

1.4.4.2 Double strand breaks repair pathways

Two major pathways in diploid cells repair DSBs. The most common form of repair is the homology-directed repair or homologous recombination (HR), which requires long sequence of homology to repair the damage. The second, but mostly developed in non-dividing haploid organisms and diploid organism is the nonhomologous end joining (NHEJ), which does not require the presence of a homologous strand to repair the DSB (Shrivastav et al, 2008). Although still active area of investigation, it s generally accepted that during S phase the physical vicinity of the sister chromatids provides the homology required for activation of HR. During S/G2 transition if a homolog is not present NHEJ will be used to repair the break and outside of this phase NHEJ is the only possible option. The issue of homologue proximity and the possible competition among the components of these pathways are yet to be fully understood (Allen et al, 2003). Recent studies have suggested the DNA ligase IV complex may be responsible to suppress the HR initiation step, leading to NHEJ activation (Shrivastav et al, 2008).

1.4.4.2.1 Non-homologous end joining (NHEJ)

Accurate and mostly precise on simple breaks such as blunt ends, this pathway rejoins the two damaged ends of the DNA break in a sequence independent fashion (van Gent & van der Burg, 2007). Although described as non homologous a small region of homology (1-6bp) can facilitate the strand break rejoining (van Gent & van der Burg, 2007). It requires Ku heterodimer (Ku70 and Ku80) which binds to the reciprocal DNA ends through is ring shape structure. This complex has mainly the function of a scaffold to assemble the other components of the pathways at the DNA termini. One of the first enzymes to be recruited is the DNA dependent kinase catalytic subunit (DNAPKcs). This serine-threonine 460kDa protein forms a so-called synaptic complex that holds the two ends of the broken DNA molecule together. Together with Ku70/80 it forms a holeo-enzyme complex called DNAPK (Hammel et al, 2010). Usually in presence of DNA blunt ends or complementary 5’ phosphate and 3’ hydroxyl group, the auto-phosphorylation of DNAPKcs allows juxtapositioning of the DNA ends that become available for ligation by the DNA ligase IV complex containing XRCC4 and XLF cofactors (Weterings & Chen, 2007). In many cases, ends cannot be precisely rejoined because of aberrant 3’phoshate groups, 5’ hydroxyl groups damaged backbone sugar residues and damaged DNA bases. These ends require processing before ligation takes

place. This process can be mediated by different proteins according to the different type of DNA ends fromed at the site of the break. Polynucleotide kinase (PNK) interacts with DNA ligase IV in presence of 3' phosphate groups and 5' hydroxyl groups and recruits ancillary components such aprataxin (APTX) and PNK-APTX like factor (PALF) for additional 3' nuclease activity (van Gent & van der Burg, 2007). Artemis nuclease activity is involved in the resolution of difficult DSBs. Following binding and phosphorylation by DNAPKcs, Artemis exerts a diverse array of nuclease activity including 5' and 3' endonuclease activity, hairpin opening activity in addition to its own 5' exonulease activity. In presence of aberrant DNA ends DNAPKcs phosphorylates Werner helicase (WRN) whose nuclease activity is required for their processing (Stracker et al, 2009). Despite the great flexibility shown by the XFL:XRCC4:DNA ligase IV to ligate across gaps with incompatible ends there are 2 members of the Polymerase X family Polymerase μ and λ that can fill the 5'single stranded extensions. Their activity is well suited in the NHEJ pathway as Pol μ is capable of both template dependent and independent synthesis and Pol λ has more flexibility than replicative polymerases (Lieber, 2010; Shrivastav et al, 2008).

There are several other factors shown to be required for the repair of difficult DSBs by the NHEJ. These are: the MRE11/RAD50/NBS1 (MRN) complex, MDC1, 53BP1 and ATM kinase. While the MRN complex may be implicated in keeping the DNA ends together, or in close proximity, MDC1, 53BP1 and phosphorylation of the histone variant H2AX seems to be required to the formation of this complex in foci fashion. ATM is one of the major kinase of H2AX following formation of DSBs therefore it has been suggested that ATM would induce the creation of chromatin microenvironment that allows the formation of the MRN foci. Fig 1.7 shows the most significant steps of the NHEJ pathway (Lieber, 2010).

1.4.4.2.2 Homologous Recombination (HR)

It is an error free repair process that requires homologous sequence of the sister chromatid. All the homology directed repair is initiated by a 5'-3' resection at the DSB end and ATM activation mediated by the Mre11/Rad50 and Nsb1 (MRN; Mre11-Rad50-Xrs2) complex that creates a single stranded DNA (Branzei & Foiani, 2008). From here, three main homology-directed repair pathways could take place. These are: Synthesis-dependent strand annealing, double Holliday-Junction and single strand

annealing (Helleday et al, 2008). Following resection, in the synthesis-dependent strand-annealing subpathway, Rad51 with help of a numerous group of proteins (BRAC2, RAD52, RAD54, RAD54B and also RAD51 paralogues RAD51B, RAD51C, RAD51D, XRCC2 and XRCC3) forms the nucleoprotein filament that searches for the homolog and initiates strand invasion (Shrivastav et al, 2008). The base pairing of the homolog and the invading strand creates a DNA heteroduplex that displaces one of the DNA strands forming a D-loop that enlarges as the synthesis proceeds. The annealed 3' strand is then elongated via repair synthesis mediated by polymerase η (pol η). Several lines of evidence have suggested that pol η is involved in HR, however several other polymerases can compensate in his absence. Synthesis must continue beyond the original point of break to restore the missing information at the break point. On the other side of the D-loop an X -like structure, called the Holliday Junction, is formed at the border of the intersection between the invading strand and the homolog (Moynahan & Jasin, 2010). In order to release the newly synthesized strand the Holliday junction has to slide towards the same direction of the synthesis in a process referred as branch migration. WRN, BLM, p53, RAD54, BLAP75, hMSH2, hMSH6 have all been shown to be able to modulate the sliding and the direction of the junction. This is necessary to allow release of the new strand however the sliding process and the regulating mechanism are not fully understood (Helleday et al, 2007). Once free, the released strand is bound by RPA and if the opposite end of the DSB is similarly fixed then simple annealing will take place via the help of Rad52 or possibly p53. Presence of damaged bases or the extent of the synthesis my lead to flaps, gaps. In this case XPF/ERCC1 endonuclease activity is employed and the gaps are filled by the activity of other proteins such as DNA ligase I, PCNA and pol δ/ε (Adair et al, 2000; Batty & Wood, 2000).

Sometimes there is the possibility that a double Holliday junction forms at either side of the D-loop. This normally happens when the opposite strand anneals to the D-loop and also starts synthesis creating a double intersection. If the cleavage that release these heteroduplexes is made at the holliday junctions then flanking sequences continuity of the DSBs will be preserved otherwise it will result in a cross over event.

If at the sides of the DSBs two adjacent repeat sequences are present, single strand annealing may be utilized to resolve the DSBs. This is a process facilitated by rad52 and RPA but Rad51-independent. If this HR subpathway is initiated then the sequence

between the repeats will be inevitably lost as well as one of the repeats. In the literature this sub pathway is also referred as an unintentional consequence of the need to create a single stranded DNA to initiate synthesis- dependent strand annealing. Fig 1.8 shows the steps of this pathway (Evers et al, 2010; Helleday et al, 2007; Shrivastav et al, 2008).

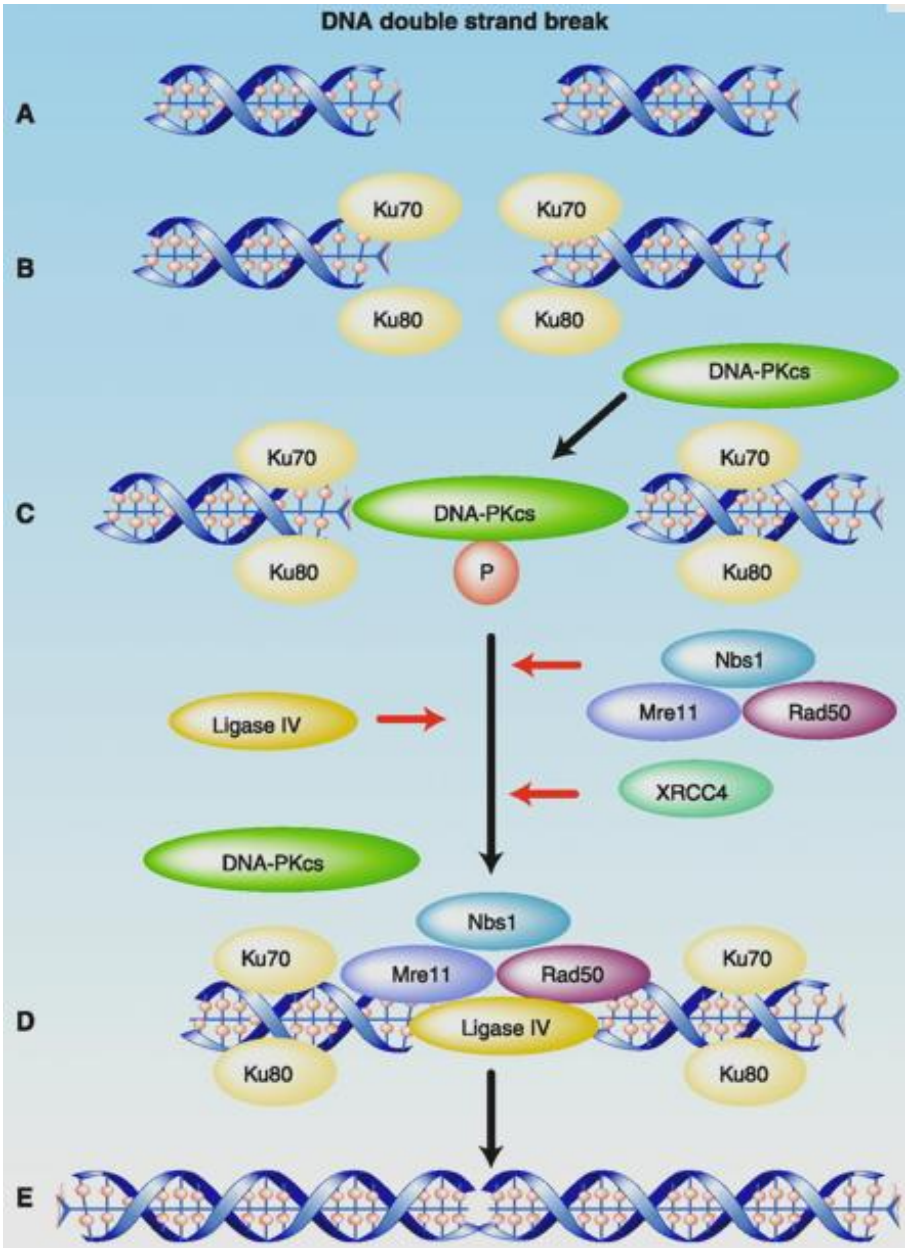

Figure 1.7: Non Homologous end joining (NHEJ) pathway. (Chen & Nirodi, 2007)

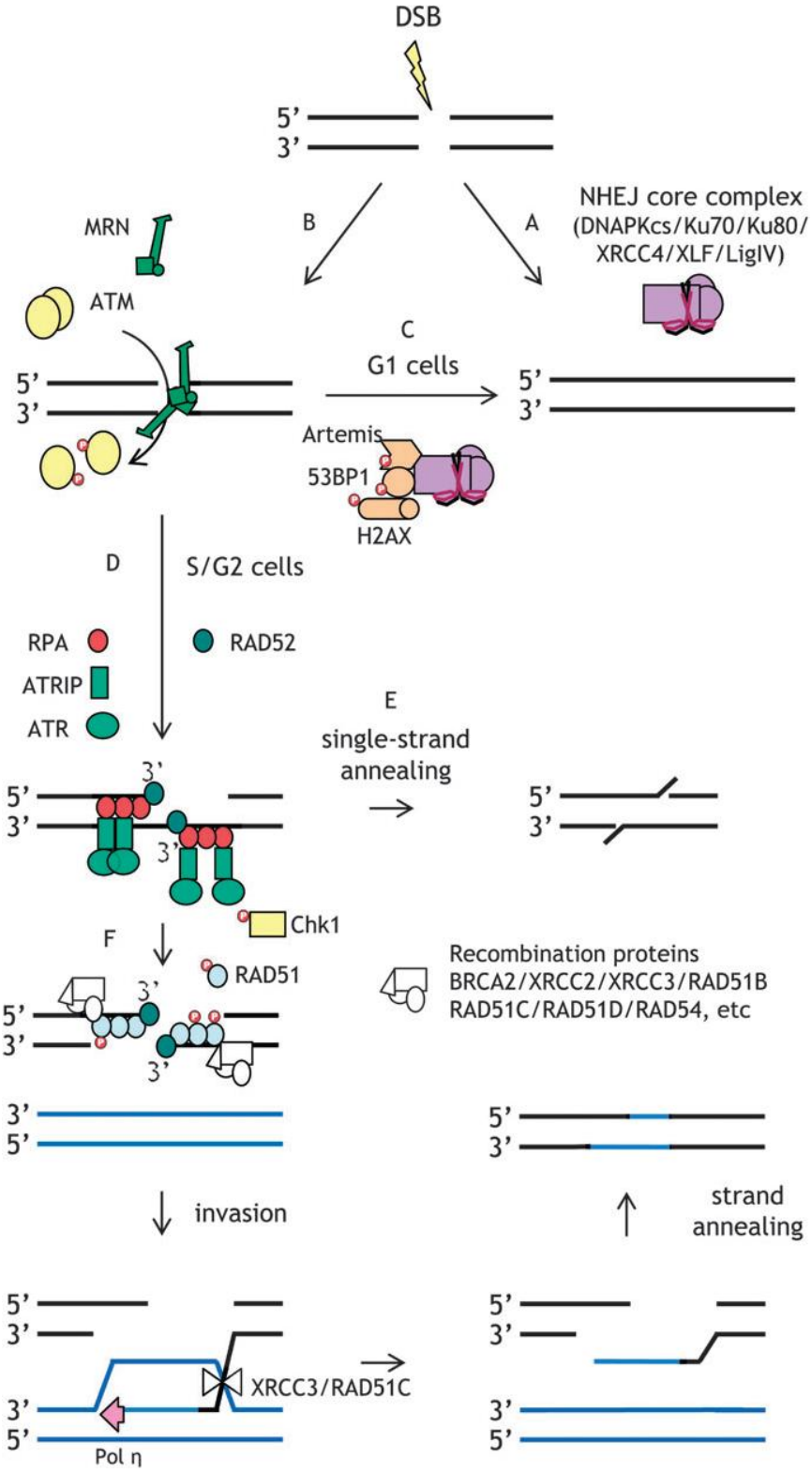

Figure 1.8: Homologous recombination (HR) pathway. (Helleday, 2010)

1.5 DNAPKcs

1.5.1 Structure

The product of the PRDK gene is a 4128 amino acids polypeptide of 469 kDa. It is the largest protein kinase in biology and a member of the phosphoinositide 3-kinase-likefamily (PIKK) of protein kinases. DNAPKcs is specifically activated by double stranded DNA ends of different configurations. DNAPKcs alone has a dissociation constant of $3x10^{-9}$ M for blunt DNA ends. In presence of Ku at the DNA ends, the affinity is higher with a dissociation constant of $3x10^{-11}$ M. DNAPKcs N-terminal extends from amino acid 1-2908 (about 250 kDa) and contains a putative DNA-binding domain, a leucine rich region and a series of HEAT repeats (huntingtin, elongation factor 3, A subunit of protein phosphatase 2A and TOR1). The C- terminal region contains a FAT [FRAP (FKBP12-rapamycin-associated-protein) ATM (ataxia-talangiectasia mutated), TRRAP (transactivation/transformation-domain-associated-protein)] domain (amino acids 2908-3539), the PIKK domain (3645-4029) and the FATC domain (4906-4128). Cells that lack DNAPKcs expression have been shown to be radiosensitive and also have defects in V(D)J recombination. In addition mammals with DNAPKcs also showed severe combined immunodeficiency (SCID) (Lieber, 2010).

1.5.2 DNAPKcs involvement in repair

Despite its capability to bind DNA alone, DNAPKcs recruitment to damaged DNA is Ku dependent. The binding of these two proteins is mediated by a conserved region in the extreme C-terminus region of Ku and C-terminal region of DNAPKcs. By translocating inwards, away from the DNA damaged ends, Ku allows DNAPKcs interaction to the DNA, providing sufficient space for two DNAPKcs molecules to bind to the DNA termini and interact in a synaptic complex that hold the ends tight together. The DNAPKcs-Ku-DNA complex is referred as the DNAPK complex, known to be the most central component of the NHEJ pathway (Collis et al, 2005; DiBiase et al, 2000). Although DNAPK phosphorylates Ku70, Ku80, XRCC4, XLF, Artemis and DNA ligase IV in vitro there is no evidence that these phosphorylation events are required *in vivo* for NHEJ (Douglas et al, 2005; Sibanda et al, 2010). The only *in vivo* validated substrate of DNAPK is DNAPKcs itself. Noteworthy is that the Ku component of DNAPK can only load or unload DNA therefore the kinase activity of the complex is mediated by its only

kinase component, DNAPKcs (Chan et al, 2002). There are 16 phosphorylation sites identified to contribute to DNAPKcs autophosphorylation in response to DNA damage.

1.5.3 DNAPKcs phosphorylation

The most *in vivo* characterized and IR inducible and DNAPK-dependent sites are the ABCDE cluster (Ser^{2612},Ser^{2624}, Thr^{2609}, Thr^{2620}, Thr^{2628}, Thr^{2647}) and Ser^{2056}, Thr^{3950}. In addition IR-induced phosphorylation of Ser^{2612} Thr^{2628} and Thr^{2647} occurs following inhibition of the related protein ATM. In contrast other studies have shown that both ATM and ATR can phosphorylate Ser^{2612}, Thr^{2609}, Thr^{2628} and Thr^{2647} in response to IR or UV. Cell type, cell cycle stage and the extent of the DNA damage may be the determining factors that induce *in vivo* DNAPKcs phosphorylation by DNAPK or ATM or ATR. Proteomic screen have also revealed additional *in vivo* phosphorylation site (Ser^{2674}, Ser^{2675}, Ser^{2677}, Ser^{3205}) but the kinase responsible and the consequences of these events have not been yet determined (Chan et al, 2002; Collis et al, 2005; Sibanda et al, 2010). *In vitro* studies of DNAPKcs autophosphorylation have revealed that this process induces loss of kinase activity and dissociation of the phosphorylated DNAPKcs from KU-DNA. This suggests that the phosphorylation event may regulate the assembly/disassembly of the DNAPK complex (Bailey et al, 2004; Chen et al, 2005). Further studies have shown autophosphorylation of DNAPKcs is required for its release from DSB *in vivo* since DNAPKcs kinase dead, and autophosphorylation defective DNAPKcs are maintained longer at the site of DNA damage. DNAPKcs autophosphorylation can be highly complex *in vivo* because although it may be required for disassembly of the complex, phosphorylation at other regions, enhances the rate of HR and can either positively or negatively regulate DNA processing (Gu et al, 2010).

1.6 DNA REPAIR REGULATION THROUGH THE CELL CYCLE

Although the activation of a specific DNA repair pathway depends on the type of DNA lesion and its recognition, cell cycle is also a determining factor in this choice. Certain repair mechanisms can only take place during one phase of the cells cycle. NER factors will be usually required to repair SSB lesions in G1 cells (Branzei & Foiani, 2008). In contrast, DSBs are repaired by HR during S phase because of the presence of an intact and accessible sister chromatid but during the remaining phases of the cycle, being the chromatin already highly condensed, repair will be undertaken by NHEJ (Shrivastav et al, 2008). The recognition of the damage, the cell cycle and the DNA repair mechanisms

are highly linked and clearly dependent from each other. In order to maintain genome stability and integrity cells have evolved two important checkpoints during the cell cycle also called restriction points where DNA integrity is checked and damaged DNA is repaired to assure correct transmission of the genetic information. In presence of DNA damage, cells integrate DNA repair pathways with transcription, signalling, and apoptosis in a tightly regulated network called the DNA damage response (DDR) orchestrated by the checkpoint proteins. Recognition of damage usually becomes an activating signal that checkpoint transducers amplify to downstream targets activating DNA repair systems, cell cycle arrest, and apoptosis (Jackson, 2009). Central components of the checkpoint machinery are the PI3K related proteins ATM, ATR and DNAPKcs. ATM and DNAPKcs respond to the presence of DSBs whereas ATR is activated by SSBs and stalled replication forks. These proteins are usually recruited by interacting directly with their partners, NBS1, ATRIP and Ku respectively. ATM and ATR target many substrates including the checkpoint kinase 2 (CHK2) and checkpoint kinase 1 (CHK1) (Lobrich & Jeggo, 2007). While CHK2 activation is exclusively ATM dependent, CHK1 is activated by ATR is mediated by the protein Claspin and also indirectly by ATM that activates ATR. CHK1 and CHK2 target cyclin dependent kinases (CDK) whose activation modulates the cell cycle progression by regulating the cell cycle checkpoints (Branzei & Foiani, 2008). As mentioned above these restriction points often induce cell cycle arrest to allow repair of damaged DNA before the synthesis of the cell cycle and prior to enter mitosis. Thus they control the transition to the most important phases of the cell cycle: G1/S and G2/M.

The next sections will briefly review the cell cycle checkpoints, their role in recognising DNA damage and the consequence of unreparable damage

1.6.1 Cell cycle checkpoints

The interaction of three families of proteins regulates the checkpoints of the cell cycle: CDKs, cyclins and the cyclin dependent kinase inhibitors (CKI). Each of these components is made of a great array of molecules and sub family members that are differentially activated during the cell cycle. Cyclins expression is mediated by transcriptional control and destroyed by ubiquitin mediated proteolysis, CDKs requires cyclin binding to relieve the obstruction of their catalytic site and CKI inhibits the binding of the cyclin and CDKs rendering the CDKs inactive (Lee et al, 2008; Wojda, 2000).

As shown in Fig 1.9 each cyclin preferentially binds to a specific CDK. An important substrate of the CDKs is the retinoblastoma protein pRb, which, in its hypophosphorylated status, binds and inactivates the transcription factor E2F. RB phosphorylation by the CDK-cyclin active complex, releases E2F which mediates transcription of genes such as the DNA polymerase α and thimidine kinase allowing transition in S phase (Nevins, 2001). There are two main families of CKIs. The INK4 family (inhibitor of cyclin dependent kinase 4) family ($p15^{INK4}$, $p16^{INK4}$, $p18^{INK4}$, $p19/p14^{ARF}$), which specifically binds to CDK4 and CDK6 and the Cip/Kip family ($p21^{Cip1/WAF1}$, $p57^{Kip2}$, $p27^{kip1}$), which have a wider specificity and bind to the CDK-cyclin complex rather than CDK alone (Shan et al, 1996).

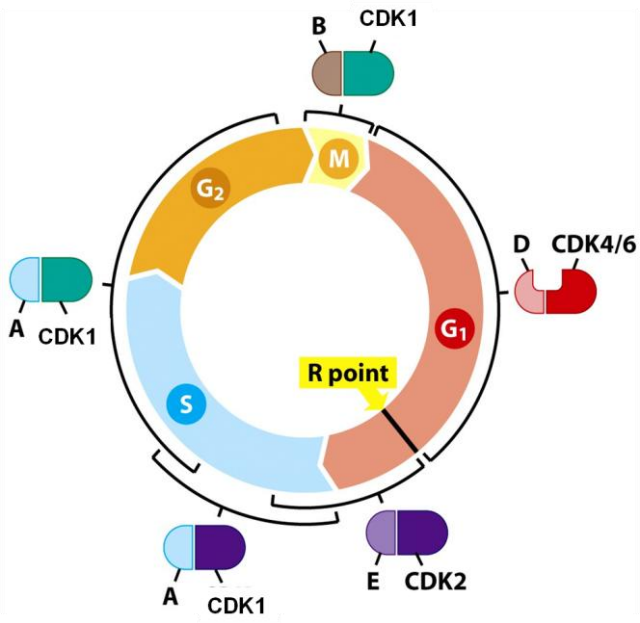

Figure 1.9: Changes in cycle dependent kinase and cyclins during the cell cycle. The diagram outlines the production of cyclins during the different phases of the cell cycle and the correspondent CDK binding partner. The picture is taken from: The Biology of Cancer (© Garland Science 2007).

1.6.1.1 Cell cycle arrest

G1-S arrest is usually initiated by ATM and mediated by direct activation of CHK2 and direct/indirect activation of p53 (Shiloh, 2003). While CHK2 induces activation and consequent degradation of CDC25A, p53 induces transcription of $p21^{Cip1/WAF1}$. Both p21 and CDC25A inhibit the CDK2/cyclinE complex formation and its mediated pRb phosphorylation(Lobrich & Jeggo, 2007; Meek, 2009). S phase arrest arises following ATR recognition of SS DNA due to collapsed or stalled replication forks replication

blocks. Subsequent activation of CHK1 induces phosphorylation and degradation of CDC25A. This prevents the initiation of a new replication origin and slows down replication (Zhou & Elledge, 2000). G2 cell cycle arrest is regulated via the inactivation of Cdk1 kinase (also known as Cdc2) (van Vugt et al, 2005). DSBs formation induces direct recruitment of ATM and indirect recruitment of ATR by the ATM strand resection. They activate CHK1 and CHK2 respectively inducing CD25A degradation and promote stabilization of p53 and consequent induction of p21. The phosphorylation of CDK1 and the inhibition of the complex formation with CyclinB induce the G2 arrest. Also, p27 and Wee1 have been shown to induce CDK1 inhibition. Fig 1.10 shows a summary of the above mentioned cell cycle arrest (Bassermann & Pagano, 2010).

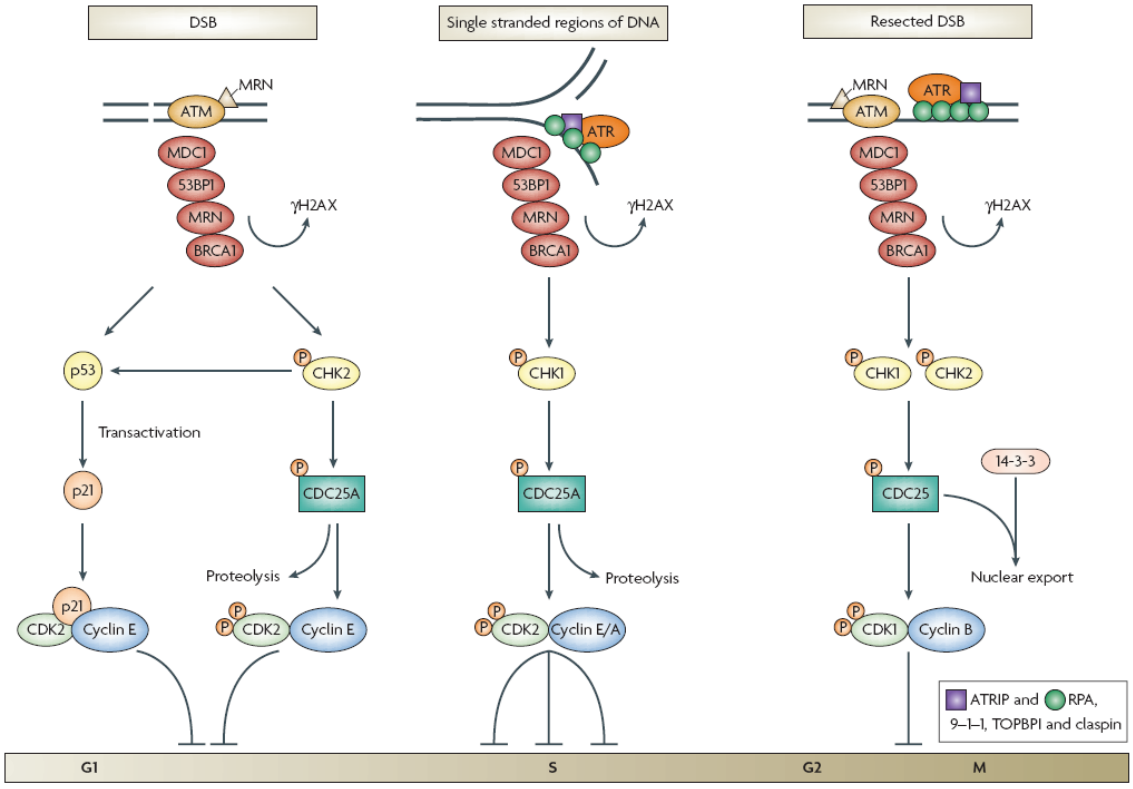

Figure 1.10: Mammalian signalling activating cell cycle check points following DSBs formation. The diagram shows the different response to DSBs according to the different cell cycle phase. ATM responds mainly to DSBs whereas ATR to SSBs. The recruitment of the MRN complex amplifies the signal and involves the transducer kinases CHK1 and CHK2. In turn these transducers regulate inhibition of the cell cycle by inhibiting the cyclin/CDK complex formation. The diagram was taken from (Lobrich & Jeggo, 2007).

1.6.2 Apoptosis

Despite all the activity and the tight network of pathways that aims at the repair of unwanted damage, cells have methods to detect defects and commit suicide. This is because tissue remodelling is too energetically expensive to sustain and the severity of DNA damage can become harmful for the rest of the body. There are two main pathways that can lead to cellular death: apoptosis and necrosis (Gramaglia et al, 2004). Apoptosis, also called programmed cell death, is a gene directed programme that requires protein synthesis. Although a clear example of tissue remodelling during embryogenesis, apoptosis also takes place in adult cells. Apart from the unsustainable DNA damage, also the sudden withdrawal of growth stimulatory signals that halt the cell cycle and promote death signals can trigger apoptosis (Lowe & Lin, 2000). Two families of proteins are central for the apoptotic process to complete: caspases and the B-cell lymphoma-2 (BCL-2) family of proteins. Indeed many studies have shown the involvement of many kinases including receptor proteins in the activation of apoptosis, but one of the most known apoptosis initiator is the tumour suppressor gene p53. Its pro-apoptotic activity is exerted via the transcription of members of the BCL-2 family such as Bax and Apaf1, that, together with Bad and cytochrome C, activate caspase 9 leading to the activation of several member of the caspase family of proteins (Miyashita et al, 1994). Caspase are large proteases synthesized as inactive precursors (pro-caspases). Their activation is triggered by the cleavage at aspartate residues within their protein sequence. In other words the activated proteases are themselves caspases that activate a series of proteolytic events that initiate the appearance of different caspases (Tsujimoto, 2003).

The balance of anti apoptotic BCL-2 protein and the pro apoptotic protein BAX is determined by p53 and growth factors. P53 induces BAX transcription and inhibits transcription of the Bcl2 gene resulting in equilibrium in favour of BAX complexes. BAX stimulates cytochrome C release from mitochondria which activates pro-caspase 9 by binding to Apaf (Lo et al, 2005c). The cytochrome C/procaspase9/Apaf complex is also known as the Apoptosome (Shi, 2002). Caspase 9 also activates downstream caspases such as caspase 1, which digests actin, caspase 6 which digests nuclear lamin and caspase 3 that leads to the activation of DNAse. Withdrawal of growth factors induces apoptosis by the activation of the BCL-2 death associated promoter (Bad). During proliferation phosphorylated Bad is bound to the protein 14-3-3 that inhibits Bad pro-apoptotic activity (Adrain & Martin, 2009). Growth factors indirectly maintain Bad

phosphorylation via the activation of a member of the PI3K pathway, protein kinase B (Akt). In absence of growth factors Bad is dephosphorylated and following dissociation from 14-3-3 it binds BCL2 blocking its inhibitory effect on cell death. P53 seems to be involved in the activation of the Akt pathway responsible for Bad inactivation (Breen et al, 2007). Necrosis is commonly seen in the centre of solid tumours. Usually low or poor nutrient supply determines disruption of the energy dependent ion channels. The consequent increase in cell volume and loss of membrane integrity induces the activation of proteases and nucleases. This type of cellular lysis is often associated with an inflammatory response. Fig 1.11 shows the complexity of the apoptotic pathway (Weisz et al, 2007).

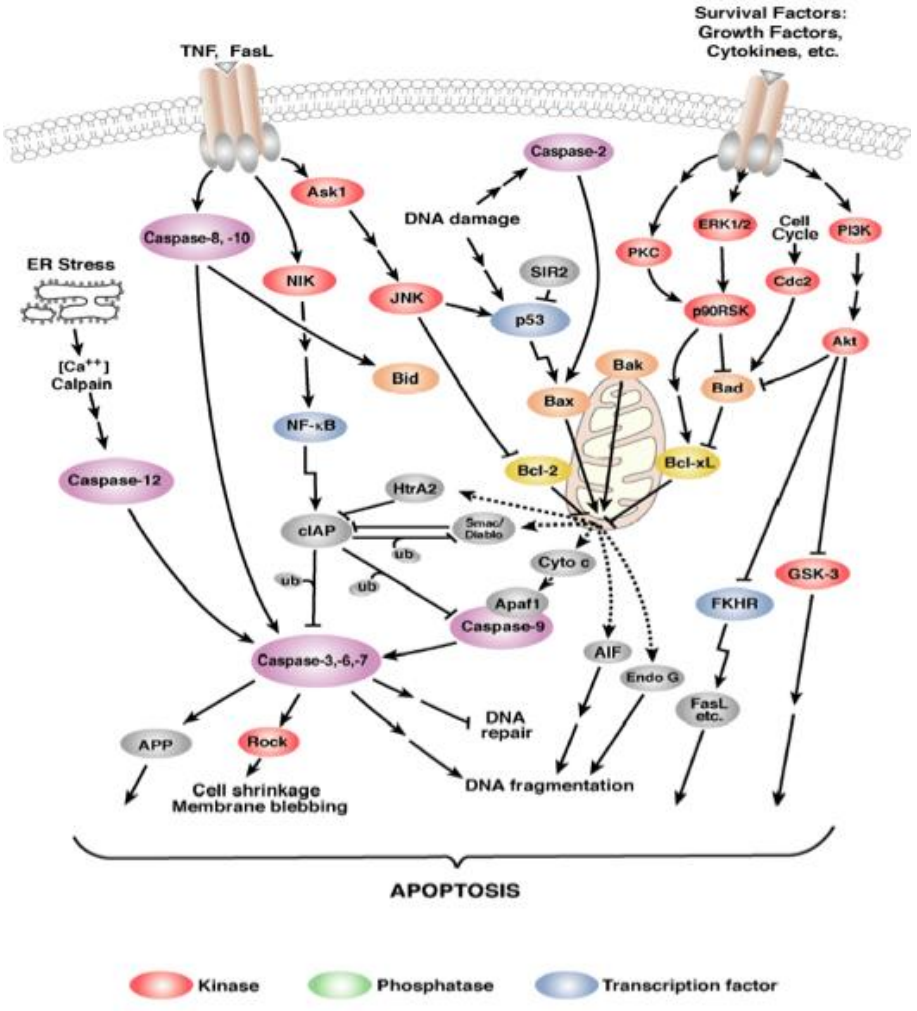

Figure 1.11: Apoptosis signalling pathway (www.cellsignal.com).

1.7 CELLULAR SIGNALLING AND CANCER

Despite the presence of an extensive array of molecules and mechanisms, evolved to protect cells from DNA damage and prevent its incorporation and transmission, cells still manage to acquire somatic mutations developing into malignancies. Interestingly, not even the induction of further DNA damage within these same cells via the usage of genotoxic agents and RT is, most of the time, sufficient to kill cancer cells (Savage et al, 2009). One of the main aims of cancer therapy is to achieve tumour control with less toxicity. Targeting aberrant oncogenic factors or pathways that are specific to cancer cells has shown improvement in the outcome of cancer therapies without increasing toxicity (Nyati et al, 2006). The concept of resistance to treatments and to the innate cellular defence mechanisms is incredibly vast and the attempt to give a comprehensive picture, fair to all the molecules involved in these processes, would require volumes. This section is going to review the role of receptor tyrosine kinases and in particular the role of the epidermal growth factor receptor (EGFR) in tumorigenesis, cancer signalling and resistance to therapy. This is necessary to understand the role of molecular targeted therapy within cancer management and the importance of a better understanding of cellular mechanism following radiotherapy or chemotherapy to design more efficient molecular target therapies.

1.7.1 Oncogenic Receptor Tyrosine kinases (RTK)

Growth factor and RTKs coordinate, through a complex system of signalling network, cellular survival, apoptosis, proliferation, differentiation and migration.

There are 58 known RTKs in mammals distributed in 20 subfamilies and despite sharing a lot of structural homology and downstream signalling pathways each RTK associates uniquely to these pathways contributing to an enormous combinatorial complexity (Lemmon & Schlessinger, 2010). All RTKs have a ligand binding domain in the extracellular region, a single transmemebrane helix, and a cytoplasmic domain containing the kinase domain and an additional carboxyl (C-) terminal and juxtamembrane regions. Their mechanism of activation, topology and downstream signalling pathways are conserved from the nematode *Caenorhabditis elegans* to humans (Amit et al, 2007b). Mutation in RTKs and aberrant activation of their signalling pathways have been linked to diseases such as diabetes, inflammation, bone disorders angiogenesis and arterosclerosis. Nearly 30% of the RTKs are involved in cancer or tumorigenesis via exerting their oncogenic potential (Bublil & Yarden, 2007;

Katz et al, 2007; Seger et al, 2008). Their aberrant activation is mediated by four main molecular mechanisms: autocrine activation, chromosomal activation, overexpression, or gain of functional mutations (Amit et al, 2007b). One of the main characteristics of RTKs and also one of the properties that renders them central in understanding and designing new molecular targets is their functional robustness, shown by their capability to maintain output reproducibility despite input variation (Citri & Yarden, 2006).

1.7.1.1 The EGF receptor family

The ERBB family of protein takes its name from their homology to the erythroblastoma viral gene product v-erb. It comprises four receptors: ERRB1-4, also known as HER1-4, and 13 polypeptide extracellular ligands which all contain a conserved epidermal growth factor (EGF) domain. All four receptor are transmembrane glycoproteins whose activation takes place via ligand binding and/or homo or heterodimerisation (Bublil & Yarden, 2007). The vertebrate family of receptors evolved from the single ligand-receptor pair expressed in nematodes. While in worms there is only one single EGF-like ligand (LIN-3), drosophila expresses four stimulatory ligands and one inhibitory ligand called ARGOS. The function of this family of receptor is also very well conserved across the species. In worms, EGFR controls vulva development, differentiation of the male tail and posterior-ectoderm development, the drosophila. Likewise, the Drosophila EGF receptor (DER) controls the development of several organs during embryogenesis and the mammalian ERBBs control organogenesis in multiple epithelial tissues (Amit et al, 2007b).

1.7.1.1.1 The evolution of the mammalian ERBB network

The origin of the first ERBB receptor must have been the result of a gene fusion event that linked a cytoplasmic tyrosine kinase to a cell surface receptor. Amino acid sequence analysis of the four ERBB has revealed that a gene duplication event must have occurred to generate two ancestral receptors, the ERBB1/ERBB2 precursor and the ERBB3/ERBB4 precursor. Following subsequent gene duplication these precursors generated the 4 ERBB proteins. In parallel to the evolutionary events that lead to the segregation of 4 receptors, the vertebrate ligands also segregated into the ERBB1 ligands and the ERBB3/ ERBB4 ligands (Fig 1.12) (Amit et al, 2007b).

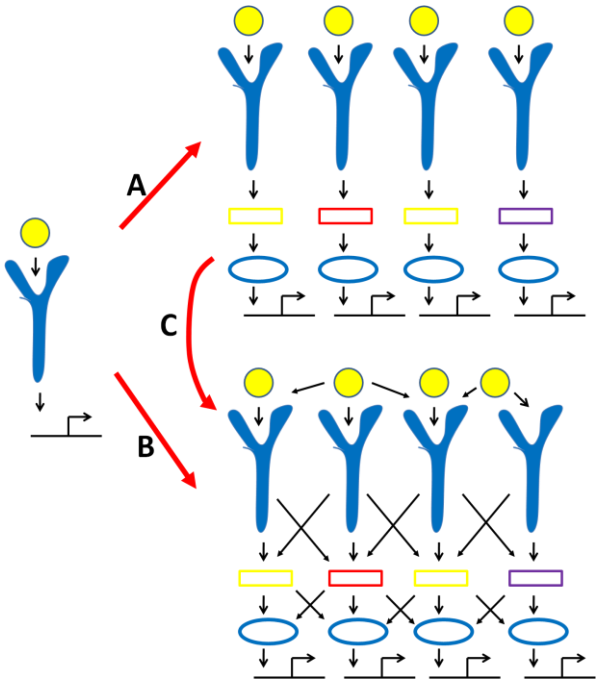

Figure 1.12: Evolution of ERBB signalling. From a single vertical cascade of signalling events, mediated by one receptor in invertebrate primordial specie (left), three scenarios may have evolved. Option A describes two events of RTK duplication leading to 4 cascades contributing to gene expression remaining isolated from each other. In option B the four cascades interact and establish a complex bow tie of layered signalling network. Evolution from invertebrates may have preferred directly option B or the transit from option A (Option C). There is no evidence of evolutionary stability of option A. Fig rearranged from (Amit et al, 2007b).

1.7.1.2 ERBB ligands

The epidermal growth factor (EGF), transforming growth factor alpha (TGF-α) and amphiregulin (AR) bind selectively to EGFR. Betacellulin (BTC), heparin-binding EGF (HB-EGF) and epiregulin (EPR) bind to ERBB1 and ERBB4. The third classes of ligands, the neuregulins (NRG1-4) bind and activate ERBB3 and ERBB4. ERBB2 lacks ligand association but it is known to be the most preferred partner for other ERBB interactions. The majority of the ERBB ligands are synthesized as type-1 transmembrane proteins. The mature and soluble form of the ligand is released into the cellular matrix following protease cleavage by members of the ADAM family (A disintegrin And Metalloproteinases) of metalloproteinases (Zhou et al, 2006). Each member of this family recognizes at least one feature of the EGF like motif of a ligand. This motif is made up of 6 spatially conserved cysteine residues (CX7 CX4-5 CX10-13 CXCX8 C) that forms three peptide loops through the formation of disulfide bonds by the interaction of C1-C3, C2-C4, and C5-C6 (Nakamura et al, 2000). In some cases

(HB-EGF, TGF-α, AR and BTC) the ligand binding molecule is not cleaved from the membrane and can function even if tethered to the plasma membrane through adjacent receptor bearing cells (juxtacrine signalling) (Klein et al, 2004; Lemmon, 2009; Lemmon & Schlessinger; Lemmon & Schlessinger, 2010; Ozcan et al, 2006).

1.7.1.3 ERBB2

Heterodimers containing HER2 have stronger signal output because of the larger subset of phosphoproteins that HER2 can bind, and the higher affinity and broader specificity that these heterodimers have with different ligands (Lazzara & Lauffenburger, 2009). Also the endocytosis rate of the HER2 heterodimers is slower compared to the other ERBBs and usually, rather than degraded; they are reshuffled back to the plasma membrane (Madshus & Stang, 2009). The analysis of the HER2 structure has also shown that differently from the other ERBBs the dimerisation loop of ERBB2 is constitutively extended even in a monomeric state (i.e. resembles the same conformation adopted by ligand bound EGFR)(Alvarado et al, 2009; Bose & Zhang, 2009). The very strong interaction between the extracellular domains I and III render the ligand binding domain inaccessible by ligands. For these reasons ERBB2 is mostly recognized as a non autonomous amplifier (Fig 1.13) (Seger et al, 2008).

1.7.1.4 ERBB3

ERBB3 is a kinase defective, non-autonomous receptor forming three functional heterodimers. It evades ligand induced degradation and in association with ERBB2 activates strongly PI3K (Fig 1.13) (Sergina et al, 2007; Shi et al).

1.7.1.5 ERBB4

ERBB4 is an autonomous receptor that shares many features with EGFR. In addition to sharing most of their ligands ERBB4 recruits some of the most characterised interacting partner of EGFR (Shc, Grb2 and STAT5) (Qiu et al, 2008) (Fig1.13). The incapability of recruiting a ubiquitin ligase, induces a slow receptor down-regulation. Proteolytic cleavage of ERBB4 cytoplasmic domain translocates the truncated receptor (discussed below) to the nucleus and might exert transcriptional activity (Zaczek et al, 2005).

1.7.1.6 Robustness of the ERBB signalling

The ERBBs proteins owe their specific robustness to 1) the network architecture interfacing with several sources of input that diverges through a conserved core into several outputs 2) their modularity which configures this family into quasi autonomous sub systems, 3) an intrinsic positive and negative feedback control that maintains input balances and allows their dynamic interaction, 4) their redundancy and 5) the induction of buffering mechanisms that enable damaged components of the system to maintain, to a certain extent, their function (for example the recruitment of chaperones to maintain protein stability) (Fig1.14)(Citri & Yarden, 2006),(Amit et al, 2007b),(Amit et al, 2007a).

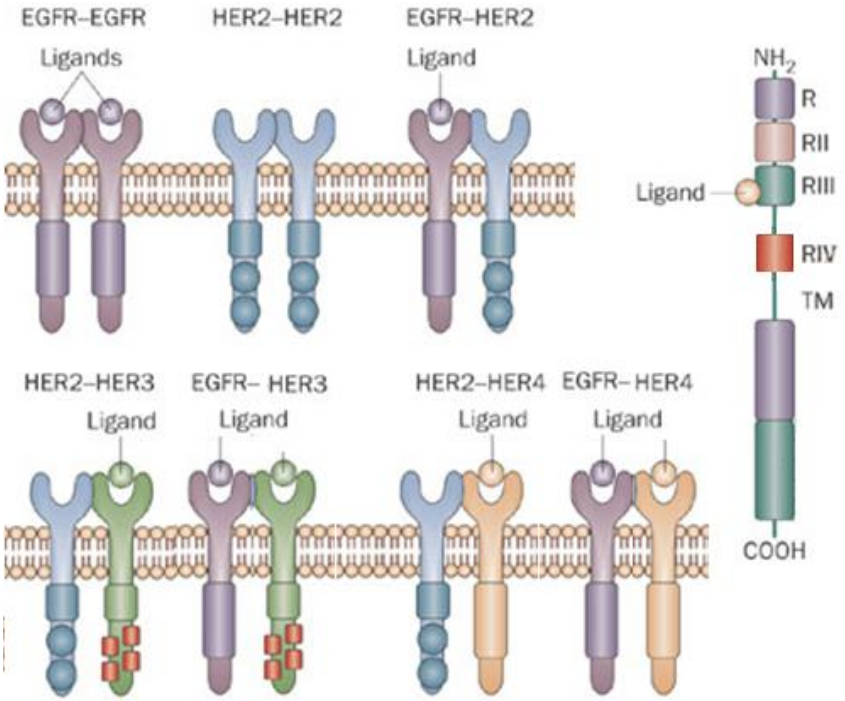

Figure 1.13: ERBB family. ERBB structure and domains and their choice of binding partner are shown. Each receptor, except HER3, relies on homo or hetero dimerisation for activation. No ligand for HER2 has been identified. The structure of the ERBB receptor is shown on the right. The figure is a modified version of (Linardou et al, 2009).

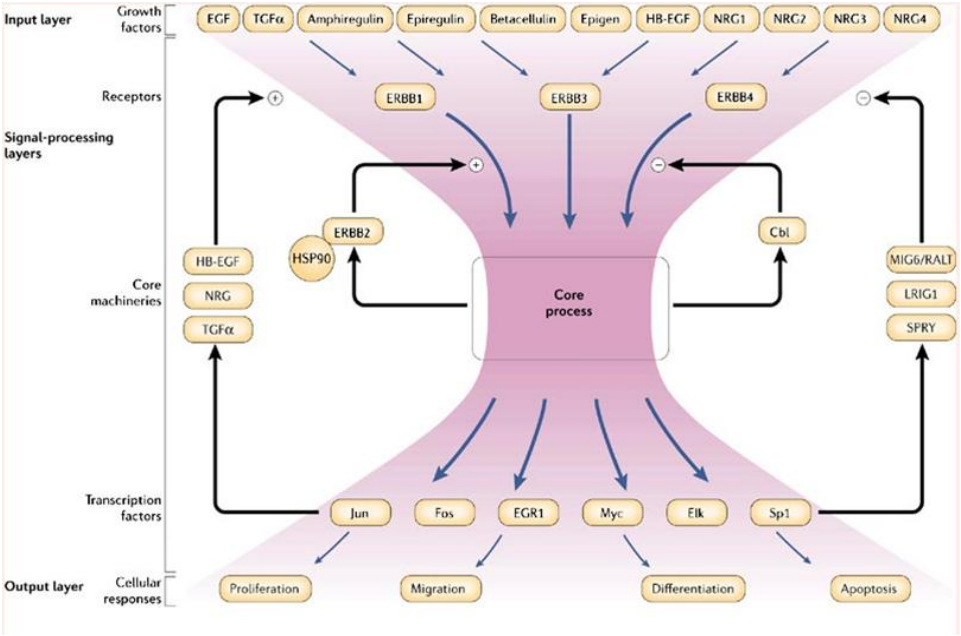

Figure 1.14: ERBB ligand perspective and network robustness. This is a simplified version of the bow-tie architecture of the ERBB family of RTK. The heart of the system is a core process consisting of various interactions among the downstream kinases of the ERBB receptors while interfacing with three ERBB and a large group of redundant ligands. The result of the core output is gene expression through the activation of transcription factors that produce different cellular responses. The robustness of the system is guaranteed by the modularity (inter-activation of kinases), by the functional redundancy together with a stringent control. ERBB2 (left side of the core) functions as a +ve regulator. Heterodimerization of ERBB2 with any other ERBB reinforces and prolongs the signal output. (Right) ERBB2 is chaperoned and also suppressed by the Heat shock protein 90 (HSP90). (Left) ubiquitin ligase E2 Cbl controld the -ve feedback. The bistability of this network is mediated by the transcription of ERBB ligands (positive input) or negative regulators (MIG6/RALT, SPRY, LRIG1). The figure was taken from (Citri & Yarden, 2006).

1.8 EPIDERMAL GROWTH FACTOR RECEPTOR

1.8.1 Structure

EGFR is synthesized from a 1210 residue polypeptide precursor. Following cleavage of the N-terminal sequence a 175kDa transmembrane glycoprotein consisting of one single polypeptide chain of 1186 amino acids is inserted into the cell membrane (Fischer et al, 2003). The sequence identity with the other members of the EGFR family varies from 37% identity (53% of similarity) with ERBB3 and 49% identity (64% of similarity) with ERBB2 (Jorissen et al, 2003; Lemmon & Schlessinger, 2010). It is characterized by three domains: the extracellular ligand binding domain or ectodomain (642 amino acids) a single transmembrane helix domain (23 amino acids) and intracellular domain

subdivided into three regions 1) the juxtamembrane domain (50 amino acids) 2) the kinase domain and 3) the carboxyl tail (542 amino acids). While the kinase domain has the highest sequence identity with other tyrosine kinases (average of 59-81%) the carboxyl terminal domains share the lowest identity (average of 12-30%) (Fiske et al, 2009; Klein et al, 2004).

1.8.1.1 EGFR ligand binding domain

The extracellular region of EGFR contains four domains (I-IV). Domains I and III are each about 160 amino acids in length comprising a B-helix LRR solenoid like structure and together they bind to activating ligands. Domains II and IV are cysteine rich domain both consisting of around 150 amino acids, held together by one or two disulfide bonds (Lemmon, 2009). The x ray structure (Fig 1.15) of the extracellular domain revealed that a protruding structure form the domain II makes contact with domain II of the other dimerising receptor suggesting that the dimerisation is entirely receptor dependent (Bublil & Yarden, 2007). Differently from all the other receptor tyrosine kinases, the EGFR ligand contacts two distinct sites within one single dimerising molecule (domains I and III) rather than crosslinking two separate molecules into a single receptor molecule (Lemmon & Schlessinger, 2010) Following the ligand binding EGFR extracellular domain undergoes a conformational change which releases the dimerisation arm in domain II (Chang et al, 2009; Hubbard, 2009; Jura et al, 2009). Before ligand binding, this arm is completely buried by intramolecular interaction with domain IV (Lemmon, 2009). This tethered conformation stabilizes the receptor and autoinhibits ligand binding and dimerisation (Dawson et al, 2007; Mattoon et al, 2004). Ligand binding disrupts the tether (Mattoon et al, 2004) allowing the dimerisation arm II to interact with a second ligand bound receptor molecule (Dawson et al, 2007).

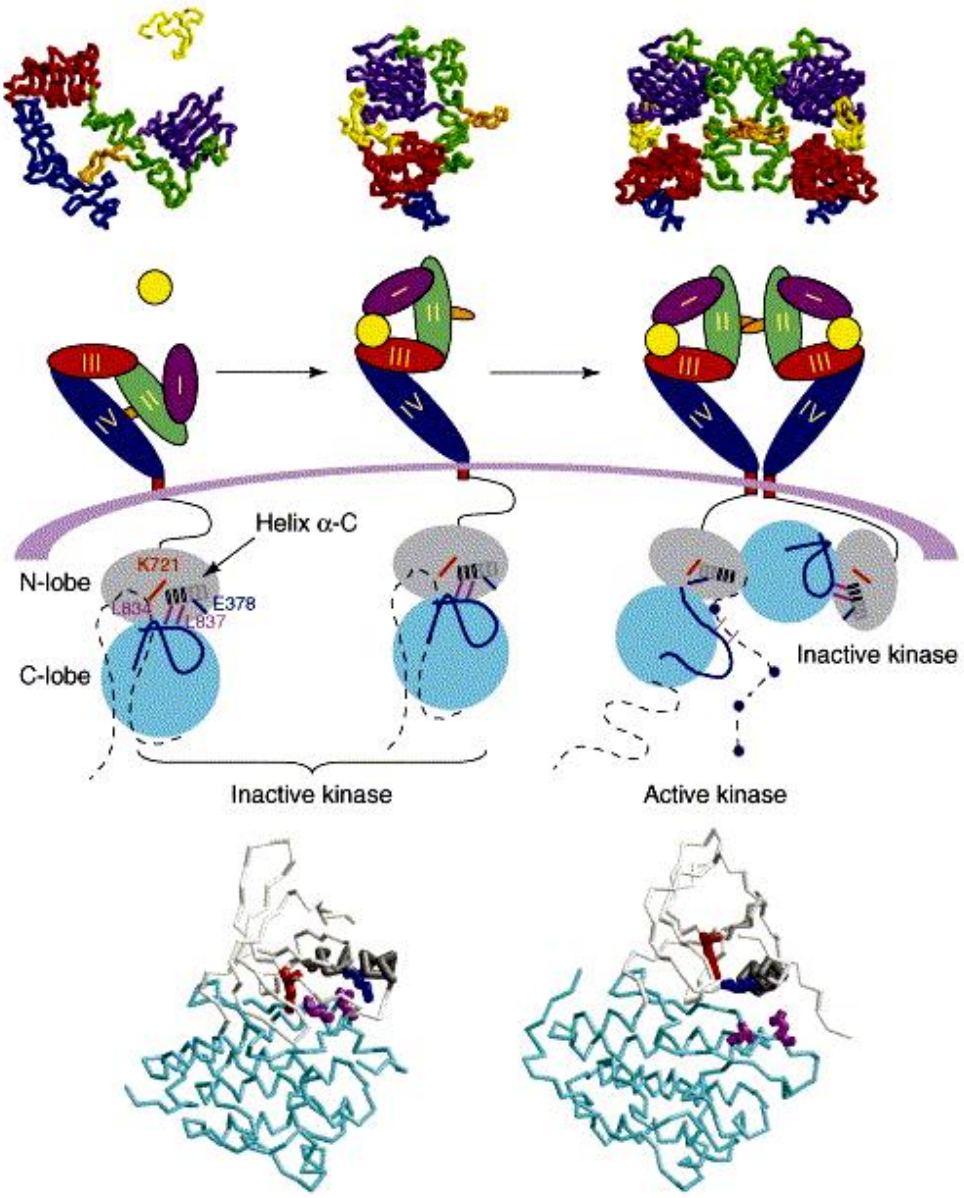

Figure 1.15: EGF receptor activation. Both 3 dimensional and schematic representation of the EGFR receptor are depicted in colour co-ordination. Ligand binding mediates the kinase activation by inducing EGFR dimerisation. In the inactive kinase both L834 (L858) and L837 (L861) are buried inside the domain facing the α-C helix, preventing the formation of a salt bridge between the E378 and the K721. Dimerisation induces the juxtaposition of the C lobe of an activator receptor to the N-lobe of the receiver. The orientation of the L834 and L837, now facing the surface of the kinase, allows contact with the C-tail of the activating kinase. The α-C helix change in orientation allows the formation of the salt bridge between E378 and K721 necessary to keep the kinase active conformation. In this diagram only one receptor C-tail is activated; however the flexibility of the kinase region allows two receptors to switch their position inducing each other activation. (Bublil & Yarden, 2007)

1.8.1.2 Transmembrane domain and Juxtamembrane domain

EGFR transmembrane domain is made up of one single a-helix that continues to the juxtamembrane domain. The juxtamembrane domain has a number of different regulatory functions, such as downregulation and ligand dependent internalization, basolateral sorting in polarized cells and association as a docking site for several other molecules (eps38, calmodulin and PKC) (Hubbard, 2001; Hubbard, 2004; Hubbard, 2009; Kil et al, 1999; Macdonald-Obermann & Pike, 2009; Red Brewer et al, 2009). The versatility of this domain will be further discussed in the result chapter.

1.8.1.3 Kinase domain

Each tyrosine kinase domain is uniquely cis-autoinhibited via intramolecular interactions. The phosphorylation of the activation loop is a key regulatory element in most kinases and is necessary to destabilize the cis- autoinhibitory interaction, and to stabilize the receptor into an active configuration (Bublil & Yarden, 2007; Morandell et al, 2008; Morgan & Grandis, 2009). In addition to the activation loop other kinases are relived from the autoinhibition by elements outside of the TKD(Schlessinger, 2003). One of the most common and known example is the juxtamembrane domain autoinhibition. The juxtamembrane region can make several contacts with the kinase domain, including the activation loop acting as a stabilizer of the autoinhibited conformation (example KIT) (Bose & Zhang, 2009; Hubbard, 2004; Mattoon et al, 2004). Receptor dimerisation promotes the trans-phosphorylation of key tyrosine within the juxtamembrane domain that disrupts the autoinhibitory conformation and lead to receptor activation (Lemmon, 2009). In addition to the juxtamembrane also the c-terminal domain has been shown to play a role in the auto-inhibition mechanism (Bose & Zhang, 2009). The region of the c-terminal domain containing tyrosine residues that undergoes autophosphorylation impedes access of ATP substrate to the active site within the kinase domain. Only following autophosphorylation the physical obstruction is released, and the receptor is stabilized into an active conformation (Mosesson et al, 2008). The activation loop, juxtamembrane domain and carboxyl tail are determinant for the kinase domain activation of RTKs and EGFR is not an exception. However, differently from all the other allosteric models where one autoinhibited kinase domain trans-phosphorylate the other receptor kinase domain within a dimer, EGFR adopts an allosteric model that resemble the activation of CDKs by cyclins (Lemmon & Schlessinger, 2010). The EGFR tyrosine kinas domain forms an asymmetric dimer

whereby the c lobe of one TKD (activator) contact the N lobe of the other TKD (receiver) inducing a conformational change that releases the autoinhibitory effect of the receiver (Jura et al, 2009). In this way the receiver kinase domain adopts an active conformation without the necessity to phosphorylate its activation loop. The juxtamembrane domain has been shown to play a key part in EGFR allosteric conformational change by 'exposing' the C lobe of the activator kinase in the dimer formation (Bublil & Yarden, 2007; Macdonald-Obermann & Pike, 2009; Red Brewer et al, 2009). In an inactive receptor the C-terminal region is found to obstruct the site on the Activator where the receiver juxtamembrane region docks to achieve receptor activation supporting earlier studies that have previously indentified autoinhibitory role of EGFR C-terminus (Fig 1.15) (Zhang et al, 2006).

1.8.2 Autophosphorylation

Following kinase activation, autophosphorylation of tyrosine residue within the carboxyl tails create the phosphotyrosine biding site necessary to recruit signalling molecules containing Src homology 2 (SH2) and phosphotyrosine binding (PTB) domains. The EGFR phosphotyrosine may directly recruit these proteins or indirectly via the binding to other docking proteins such as Grb2. In addition to autophosphorylation EGFR is also trans-phosphorylated by other tyrosine kinases (such as Src) providing the required docking site for the adaptors and modifiers (Gandhi et al, 2009; Gazdar & Minna, 2008; Morandell et al, 2008; Shtiegman et al, 2007; Zandi et al, 2007). Autophosphorylation is not a prerequisite for EGFR signalling as several studies have shown that signalling is stimulated also by c-terminally truncated EGFR expressed alone or in combination with other ERBB. This is because other trans-phosphorylating proteins may mediate the phosphorylation of the docking sites (Wang et al, 2007; Zandi et al, 2007). Fig 1.16 shows the different phosphorylation sites together with the kinase responsible for the phosphorylation event and the interacting protein.

Site	Kinase	Interacting protein
Y727 (Y703)	c-Src	Shc
Y764 (Y740)	c-Src	–
Y801 (Y777)	–	–
Y813 (Y789)	–	Shc
Y827 (Y803)	–	–
Y869 (Y845)	c-Src	–
Y891 (Y867)	–	SH3BP-1
Y900 (Y876)	–	–
Y915 (Y891)	c-Src	–
Y944 (Y920)	c-Src	–
Y978 (Y954)	–	Stat5 Shp2
Y998 (Y974)	–	Crk Eps15 Shc c-Src Stat5 Shp2
Y1016 (Y992)	ErbB c-Src	Shc PLCγ Shp2 RasGAP Vav2
Y1069 (Y1045)	ErbB	Cbl
Y1092 (Y1068)	ErbB c-Src Jak2	Grb2 Stat3
Y1110 (Y1086)	ErbB c-Src	Grb2 Shc Stat3
Y1125 (Y1101)	c-Src	Grb2
Y1138 (Y1114)	–	Grb2 Shc
Y1172 (Y1148)	ErbB	Gab1 Grb2 Shc PLCγ Vav2
Y1197 (Y1173)	ErbB	Gab1 Gbr2 Shc Shp1 PLCγ

Figure 1.16: Tyrosine phosphorylation site on EGFR. Diagram shows amino acid kinase inducing the phosphorylation and the interacting protein. Bold amino acids residues are numbered according to gi-29725609 and gi-2811086; in brackets according to gi-4885199 sequence. From (Morandell et al, 2008).

1.8.3 EGFR and cellular signalling

There are four main pathways activated by EGFR: the mitogen activated protein kinase (MapK) pathway, the activation of the Sarcoma (Src) family of kinases, such as the Janus Kinase and the signal transducer and activator of transcription (JAKs – STATs) pathway and the phospholipase D (PLD), the γ subunit of the Phosphoinositide phospholipase C (PLC-γ) and phosphatidylinositol-3-kinase (PI3K) lipid metabolism pathways. Each of these pathways can be activated by more than one phosphorylated tyrosine contributing to the high level of redundancy and robustness regulated by EGFR. Fig 1.17 highlights the major EGFR-phosphorylation events and their correspondent downstream signalling pathways.

1.8.3.1 EGFR activation of the MapK pathway

The key event for the activation of the downstream MapK kinase is the EGFR induced phosphorylation of the proto-oncogene Rat sarcoma (Ras). Usually EGFR autophosphorylation and kinase activation promotes the Src Homology 2 domain (SH2) mediated binding of the growth factor receptor-bound protein 2 (Grb2). Alternative the EGFR-Grb2 binding is indirectly mediated by the binding of EGFR to Sh2 that then recruits Grb2 (Grant et al, 2002; Katz et al, 2007). This adaptor protein is constitutively bound to the Ras exchange factor called Son of sevenless (Sos). The relocation of the

cytosolic Grb2/SOS complex facilitates the Ras association with SOS resulting in the exchange of Ras- bound Guanosine diphosphate (GDP) for Guanosine triphosphate (GTP), hence inducing Ras activation (Katz et al, 2007). Ras in turn activates Raf1 though a series of intermediate kinases leading to the phosphorylation of the extracellular signal-regulated kinases (Erks) Erk1 and Erk2 that catalyse the phosphorylation of transcription factor promoting proliferation (Fig1.18) (Huang et al, 2007b).

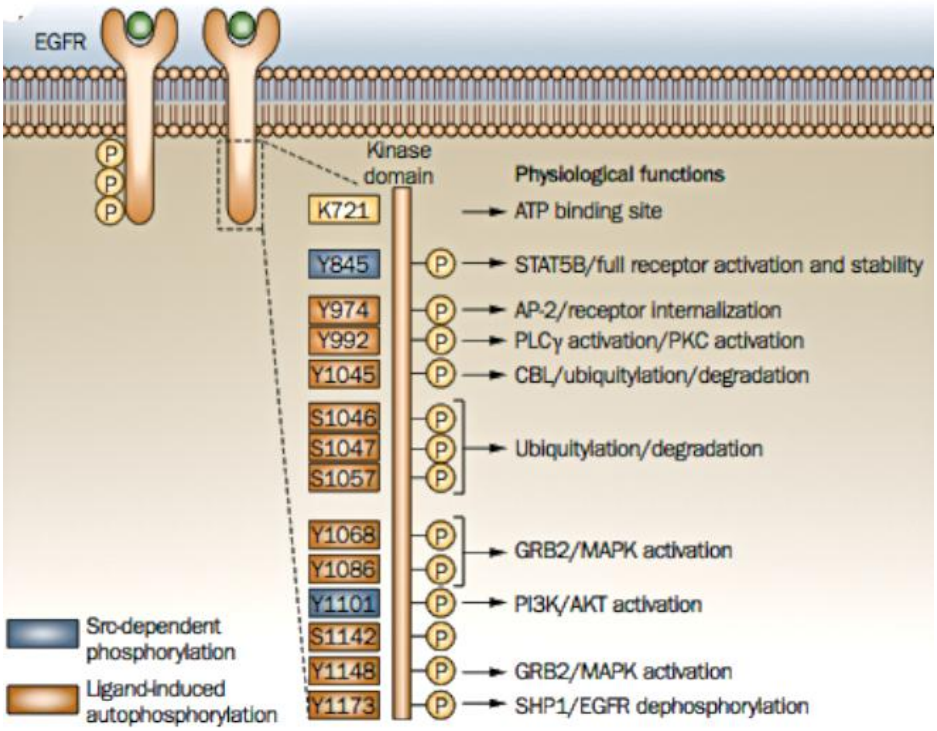

Figure1.17: Topology of EGFR residues inducing cellular signalling. The diagram enlarges a portion of the kinase domain and C-tail highlighting all the activating Tyrosine residues. Src-dependent phosphorylated tyrosines are highlighted in blue, EGF dependent tyrosine phosphorylation in orange. K721 residue, critical for the ATP binding, and phospho-groups, are shown in light yellow. Arrows point the activating kinase of the residue followed by consequent function or the activated signalling pathway. Where not indicated the activating kinase is EGFR itself. The picture was taken from (Wheeler et al, 2010).

1.8.3.2 Src family of kinases

It is still not clear whether the Src family of proteins is a signal transducer downstream of EGFR or a kinase for EGFR. The direct association of these proteins takes place via the Src SH2 domain although the EGFR binding site is not yet been recognized. Src does not bind to the major autophosphorylation sites but instead it phosphorylates Y891

and Y920 via its SH2 domain providing docking site for p85 subunit of the PI3K. The Src dependent Y845 phosphorylation has been linked to STAT5b activation however the role of this site in mitogenic signalling has been quite controversial (Fig 1.18) (Benhar et al, 2002; Yang et al, 2008).

1.8.3.3 Stat and JAK

STATs proteins are usually recruited at the intracellular domain of RTKs via the binding of STAT SH2 domain and the receptor phosphotyrosine residues. Tyrosine phosphorylation of key STAT phosphotyrosine (Y669 STAT5b, Y694 in STAT5a and Y701 in STAT1) and hetero and homodimerisation is required for STAT activation and nuclear translocation (Jorissen et al, 2003). STAT1, 3, 5 have been implicated in EGFR signalling. Differently from the other cytokine receptor EGF induced, EGFR-dependent STAT activation does not require JAK kinases. In addition STAT proteins do not bind the EGFR carboxyl tail but indeed it appears that EGFR-STATs are constitutively associated however the STAT transcriptional activity is strictly dependent on the EGFR kinase activity (Fig 1.18) (Morgan & Grandis, 2009).

1.8.3.4 Phospholipids metabolism

EGF stimulation in cells induces the production of arachinoid acid (AA), phosphatidic acid (PA) and phosphotidylinositol turnover. EGFR activates at least three of the enzymes involved in this process: phospholipase C-γ (PLC-γ), phospholipase D (PLD) and PI3-K. Despite being still obscure the mechanisms of EGFR- PLD mediated activation seems to require the physical interaction of the two proteins but tyrosine phosphorylation does not seem to be an absolute requirement. PLC-γ instead binds directly to the EGFR autophosphorylation Y1173 and Y992 residues and is consequently phosphorylated by EGFR on Y771 and Y1254 (Kamat & Carpenter, 1997). Once activated it catalyses the hydrolysis of PtdIns(4,5)-P_2 which accumulates the second messenger 1.2 diacylglycerol (DAG) and inositol 1, 3, 5, triphosphate (IP_3). The cellular role of IP_3 is to release calcium while DAG acts as a cofactor in the activation of the protein kinase C (PKC) kinase. Therefore EGFR can activate Ca^{2+}-dependent pathways such as the nuclear factor kappa-light-chain-enhancer of activated B cells (NFκB) and through the PKC indirect activation other signalling pathways such as MAPK, JUNK and possibly Na^+/H^+ exchange. PI3-Ks are members of one of the

most important family of kinases in the cell regulating proliferation, survival, adhesion, and migration (Liaw et al, 1998; Marais et al, 1998). Some members of this family are also involved in DNA repair pathways and DNA damage response. They normally catalyse the phosphorylation of the 3' positon of phosphatydilinositols and are further classified into three classes according to their substrate and lipid structure. Among these, only class I is regulated by RTKs. While the interaction of ERBB3 with PI3-K is direct and this receptor is the main activator of the pathway, EGFR requires the binding of p85 subunit that then interacts with the PI3-K-SH2 domain (Carpenter, 1993; Djordjevic & Driscoll, 2002). EGFR/ERBB3 heterodimers have been shown to activate PI3-K following EGFR ligands stimulation as well as Src induced EGFR phosphorylation (Kim et al, 1994). PI3-K produces phosphatidylinositol-3-,4,5 triphosphate (PIP_3). The most characterised target of this secondary message is the serine threonine kinase AKT (PKB) (Fig 1.18). This protein normally binds to lipids but is translocated to the plasma membrane and activated by phosphoinositide-dependent kinase 1 (PDK1) on the threonine 308 (T308) (Nicholson & Anderson, 2002). Full AKT activation is mediated by PDK-2 that phosphorylates the serine residue 473 (S473). Once fully activated, AKT localizes both in the cytosol and the nucleus where it mediates survival, evasion of apoptosis, sustained angiogenesis and replicative potential. More specifically AKT is involved in the regulation of the cell cycle by the phosphorylation of the CKI p21 and p27 that leads to their inhibition and prevents their nuclear translocation (Liang et al, 2002). Akt kinase activity has also been shown in the inactivation of the glycogen synthase and activation of glycolisis as well as glucose transport, hence playing a central role in energy metabolism. The most recognized and characterized function of this EGFR downstream target is its regulation of the anti-apoptotic signal via the NFkB and the inactivation of BAD, CASP9 and the forkhead transcription factor (Luo et al, 2003). Both EGFR and ERBB3 activation of AKT signalling, induced by ligand or IR, is a major mechanism that leads to tumour resistance against IR treatment (Engelman, 2009; Li et al, 2009; Toulany et al, 2008b).

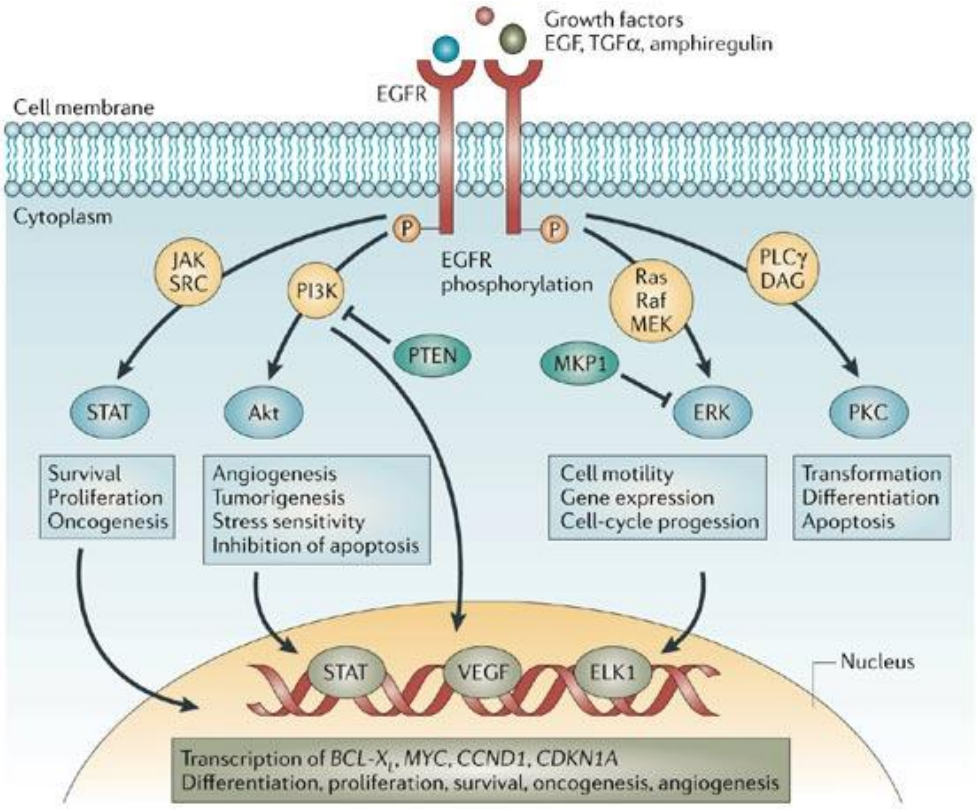

Figure 1.18: Signalling pathways activated by EGFR. The pathways do not include all the components but only the first and last member of the pathway. Cross talk is not shown for clarity. The function of each pathway is highlighted in the colour boxes. Two inhibitors (PTEN and MKP1) are shown to inhibit Pi3K and MAPK pathway respectively. The mediated transcriptional gene activation is also shown. Lawrence et al., Nature reviews Cancer 2006.

1.8.4 EGFR biological downregulation: endocytosis mediated degradation

Following activation EGFR undergoes a desensitization phase called endocytosis where the active complex of ligand-receptor is internalized and sorted either for degradation, or recycling or nuclear translocation (the latter will be further discussed later on) (Madshus & Stang, 2009). Just as important as activating cellular signalling is switching them off and although EGFR (as well as many RTKs) may spend hours or even days at the cell surface, its removal can happen within seconds after messenger stimulation (Oved & Yarden, 2002; Zwang & Yarden, 2009). In resting cells EGFR resides in lipid rafts of the cell membrane enriched in caveolins and cholesterol. Following ligand binding, EGFR exits these domains in Src dependent manner. Already within the lipid rafts the ligand bound receptor associate to coat adaptors such as adaptor protein 2 (AP2) and Eps15 involved in the endocytic machinery. EGFR endocytosis takes place through clathrin coated pits (CCPs), via cavoelae mediated endocytosis (CavME), or via

macropinocytosis (Zwang & Yarden, 2009). While EGF dependent activation induces CCPs mediated EGFR endocytosis, IR induces EGFR CavMe endocytosis. These are certainly the most described and recognized internalization routes engaged by EGFR. Fig 1.19 shows the main endocytosis pathways.

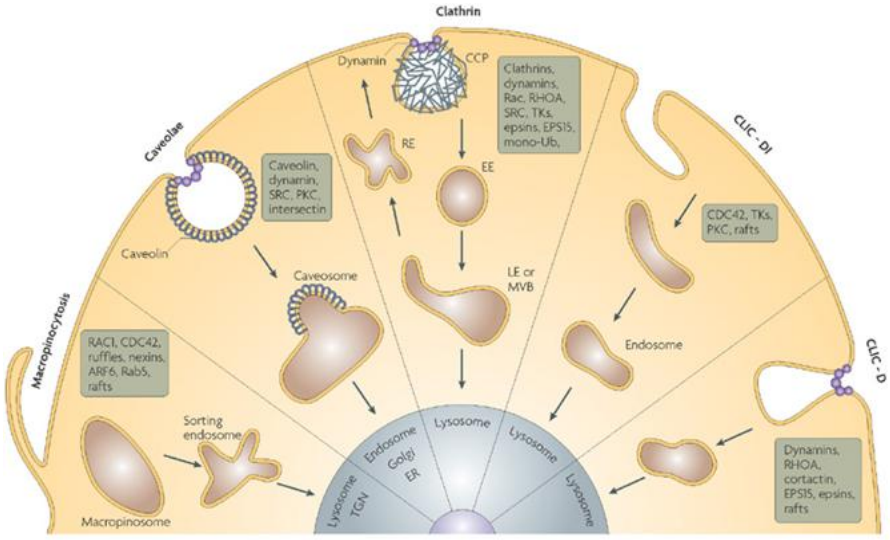

Figure 1.19: Endocytosis pathways. The diagram illustrates the different types of endocytosis, EGFR final destination and the molecular players of the respective pathways. The first three (From left to right) are the routes engaged by EGFR. The diagram was taken from (Mosesson et al, 2008).

1.8.4.1 CCps endocytosis

At the cell surface lattices made up of clathrin triskelia recruit AP2 that mediates the formation of the clathrin coated pits at the plasma membrane. Two groups of GTPases are determinant factors in this type of endocytosis: dynamins, which promote the constriction of the vesicle stalk and the Rab family members, which are involved in vesicle budding, fusion and motility (Sorkin & Goh, 2008; Zwang & Yarden, 2009). Another protein that regulates EGFR endocytosis via CCps is the ubiquitin ligase Casitas B-lineage lymphoma protein (Cbl). Cbl recruitment to active EGFR is mediated by EGFR phosphorylation on the Y1045 (Tanos & Pendergast, 2006). Once bound to the receptor via its TKB domain or through Grb2, Cbl recruits E2 molecules promoting mono, multi (several monoubiquitylated sites on the protein) or poly-ubiquitylation (several Ubiquitin (Ub) molecules on one single lysine) of EGFR either independently or concurrently (Stang et al, 2004; Woelk et al, 2007). Protein ubiquitylation is a reversible post-translational mechanism in which the 76 amino acid polypeptide ubiquitin (Ub) is attached to the ε group of the lysine residue in target proteins. The Cbl

mediated ubiquitylation is required for receptor sorting in the endosomes and subsequent sorting into the lysosomal degradative compartment (Huang et al, 2007a). Epsin-1 and Cin85 facilitate EGFR translocation from the clathrin-coated pits to the plasma membrane. Cin-85 has been found to be associated to Cbl suggesting that together they regulate EGFR endocytosis (Sigismund et al, 2008).

Following the release of internalised plasma proteins, endocytic vesicles undergo uncoating, a process mediated by the auxiliary protein Hsc70. This allows EGFR induced activation of Rab5 and membrane translocation of the early endosomes antigen1 (EEA1) determining the fusion of the vesicle with early endosomes (Massie & Mills, 2006; Mosesson et al, 2008). The endocytic process then terminates with the formation of the mutivesicular bodies (MVBs) from late endosomes by invagination of the endosomes membrane to produce intraluminal vesicles (Puri et al, 2005). MVBs then fuse with lysosome or mature into lysosomes leading to the lysis of their protein content. Three multiprotein complexes mediate the MVBs formation of EGFR-concentrated-limiting endosomal membranes: Endosomal sorting complexes required for transport I, II, III (ESCRT-I, II, III). Alternatively, EGFR can also escape the endosomal compartments via receptor recycling. While EGF-induced EGFR activation leads to endocytosis and receptor degradation, TGF-α induced-endocytosis is followed by receptor recycling (Yu et al, 2002). Recycling endosomes contain RAB4 or Rab1 GTPases, which are involved in fast and slow recycling respectively (Mosesson et al, 2003).

Protein kinase C (PKC) has been shown to be involved in recycling by inducing EGFR threonine phosphorylation. Kinsin family member 16B (KIF16B) and the cytoskeleton associated recycling or transport (CART) complex also regulate recycling by modulating the actin filaments and facilitating the trafficking to the recycling endosomes (Massie & Mills, 2006; Sorkin & Goh, 2008). Fig 1.20 shows a diagram of these events. Along with their degradative function endosomes have also been associated with signalling pathways. Endosomes contain many cellular kinases and EGFR (in particular in its oncogenic status) has been shown to stimulate survival and proliferation by interacting with internalised Ras, Shc, and Grb2, and induce oncogenesis by coupling with internalized c-Met to the STAT3 pathway (Oved & Yarden, 2002; Warren & Landgraf, 2006; Woelk et al, 2007).

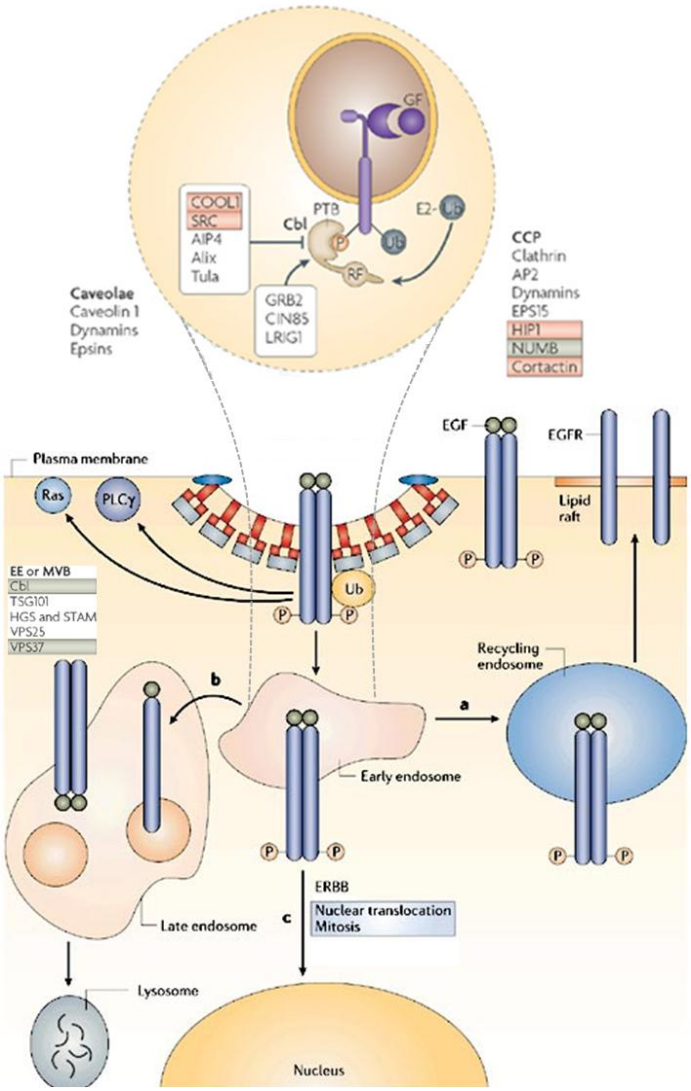

Figure1.20: EGFR life cycle. GF-activated EGFR is internalized through CCP or through caveolae, membrane sub-domains enriched in caveolin (IR stimulation). Authophosphorylated EGFR activates several signalling pathways by activating Ras and PLC γ. Central molecule to both endocytosis pathways are shown in the respective boxes. Within early endosomes (expanded circle), phosphorylated EGFR recruits Cbl. Next, Cbl recruits ubiquitin-loaded E2 molecules. This step is highly regulated, either negatively (by Rho guanine nucleotide exchange factor 7 (ARHGEF7 or COOL1) and SRC) or positively (by CIN85 and LRIG1). From the early endosome EGFR can be a) recycled back to the membrane, b) sorted into late endosomes (EE) and mutlivescicular (MVB) bodies. In this case the cytoplasmic tail is occluded to prevent further activation. Following fusion event between the late endosome and the lysosomal compartment EGFR is degraded. A third possibility consists in EGFR nuclear translocation. Escape from Cbl-mediated receptor degradation is common in tumours expressing mutant forms of receptor tyrosine kinases or Cbl. Proteins whose function is associated with oncogenesis, along with displaying aberrant expression in human tumours, are shown in red, whereas those involved in tumour suppression are shown in gray. Fig adjusted from (Mosesson et al, 2008).

1.8.4.2 Cavoelae-mediated endocytosis (CavME)

Cavoelae are specialized lipid rafts generated by the oligomerisation of the protein caveolin. The first step of this mechanism consists in the inward budding of caveolin vesicles into larger caveolin enriched organelles called caveosomes. The vesicle release is mediated by dynamins, PKC, and Src kinases(Sigismund et al, 2005; Zwang & Yarden, 2009).

1.8.5 ONCONGENIC EGFR

Despite the overwhelming network of regulatory mechanism that are employed in EGFR mediated cell signalling activation and inhibition, which increase the robustness of this system, the ERBB family and in particular EGFR represent a major player in many types of malignancies. As EGFR is involved in cell proliferation, motility and survival, an imbalanced EGFR system can easily lead to neoplastic transformation (Fischer et al, 2003). In 1980 it was found that addition of EGF to culture medium of human epidermoid carcinoma (A431) led to high yields of tyrosine phosphorylation, similarly to cells infected with oncogenic viruses. EGFR has been the first RTK to be associated with a human cancer and indeed deregulated EGFR is now associated with many human cancers. There are two main mechanisms by which the tight control of the EGFR system can be by passed: modulation of the EGFR-ligand system and by passing some of EGFR inherent controls. The first mechanism includes production of ligands in an autocrine fashion, overexpression of EGFR via gene amplification, defective downregulation of EGFR (defective endocytosis) and cross talk with heterologous receptor systems (Bublil & Yarden, 2007). The second mechanism includes the acquisition of somatic mutations, which give rise to constitutive active EGFR variants.(Gazdar, 2009a; Nyati et al, 2006)

These mechanisms of aberrant EGFR expression and activation induce an indirect deregulation of the cellular machinery (EGFR regulates its downstream kinases which then promote uncontrolled growth, proliferation, migration etc). They represent the EGFR mediated contribution towards oncogenic transformation (Fry et al, 2009; Grandal & Madshus, 2008). In addition, the activation of EGFR signalling pathways following radiotherapy and chemotherapy also play an important part in acquiring resistance and tolerance to treatment. EGFR can also directly modulate cellular survival and proliferation by translocating into the nucleus and associate with nuclear proteins regulating cell cycle, transcription and DNA repair. This section will review the

mechanisms that lead to EGFR deregulation and the molecular therapeutic attempts to inhibit EGFR in cancer cells.

1.8.5.1 Autocrine mechanisms

Both EGF and TGF-α are usually found co-expressed with EGFR in a variety of human cancers. Overexpression of TGF-α in transgenic mice induces tumour formation and also addition of EGF or TGF-α in mouse fibroblast expressing EGFR induces cellular transformation. However the effect of the ligand activation on cellular transformation is only detected when EGFR is overexpressed, as medium levels of expression do not lead to transformation (Zandi et al, 2007). Autocrine production of these ligands in EGFR overexpressed tumours (colorectal cancer, head and neck cancer squamous cell carcinoma) has shown to lead to high proliferation and worse clinical outcome. As explained above TGF-α induced EGFR activation evades CCPs mediated endocytosis and degradation maintaining therefore recycling and signalling activation (Gazdar & Minna, 2008).

1.8.5.2 EGFR overexpression

Elevated levels of EGFR expression have been correlated with increased survival in many cancer types including head and neck, bladder, ovarian, cervical and esophageal. Spontaneous receptor dimerisation, due to the numerous receptors at the membrane, induces constitutive activation resulting in ligand independent increased motility, and continuous activation of downstream signalling contributing to a more malignant phenotype (Arteaga, 2002). Increased number of EGFR molecule by gene amplification has been observed in breast carcinomas, non small-cell lung cancer (NSCLC) and particularly glioblastoma multiforme (GBM). Other mechanisms that lead to EGFR overexpression are: increased activity of the EGFR promoter or deregulation at the translational and post translational level (Gazdar & Minna, 2008). P53 has been shown to bind to the promoter of EGFR activating EGFR transcription. Therefore, as the levels of p53 are usually high in cancer cells, so the levels of the receptor will be. It has also been reported that a specific region of the EGFR gene has enhancer ability in some breast cell cancer lines over-expressing EGFR. These cell lines have also been shown to express more DNAase H1 sites in the intron 1 of the EGFR gene suggesting that chromatin structure of the EGFR regulatory regions may have a role in its

expression(Kersting et al, 2008). Again in intron1 the number of polymorphic CA dinucleotide seems to correlate with the EGFR expression (Huang et al, 2009). The higher number of polymorphic sites the lower the EGFR expression (Kang et al, 2005).

1.8.5.3 Evading degradative fate.

EGFR overexpression and over activation due to autocrine and paracrine ligand activation and by spontaneous dimerisation may saturate the capacity of the CCps and endosomal adaptors (Stang et al, 2004). A single amino acid mutation within the Cbl zinc finger domain renders the protein ligase defective therefore impairing EGFR ubiquitylation (Shtiegman et al, 2007). Indeed ERBB2 has been often associated with Hsp90, which stabilise the protein rendering it a poor substrate for lysosomal degradation; hence EGFR/ERBB2 dimer may undergo the same by pass (Yang et al, 2006). Several reports have implicated the Src family of kinases in control of Cbl half-life. Interaction with Src redirects the Cbl ubiquitin ligase activity towards itself resulting in Cbl proteosomal degradation. Therefore the uncoupling of the Cbl mechanism may be one of the facets of the EGFR-Src interaction during oncogenesis(Huang & Sorkin, 2005; Zwang & Yarden, 2009). Several ligands including EGF induce transcription of Sprouty proteins, which displace RTKs from Cbl. Ligands increase Sprouty tyrosine phosphorylation thereby sequestering Cbl from activated EGFRs (Sorkin & Goh, 2008).

1.8.5.4 EGFR mutations

The somatically acquired mutations in the EGFR gene are not randomly distributed but rather clustered in specific areas, which assumes the role of mutational hot spots. There are 1380 mutations of the EGFR gene sequenced from tumour samples. 30% (413 of 1380) are found in adenocarcinoma, 2% in NSCLC (16 of 1380). The number of sequenced EGFR mutations is incredibly high and will be categorized according to their location within the EGFR domains (Gazdar, 2009a). All the mutations are shown in Fig 1.21 and 1.22. The most relevant to this study will be discussed.

1.8.5.4.1 Extracellular mutations

Mutations of the extracellular domain are particularly found in Glioblastoma. EGFR type I, II, III variant (EGFRvI, EGFRvII, EGFRvIII) are the most known and contain deletions of exons encoding parts or the entire extracellular domain(Zandi et al, 2007).

These truncated mutants, despite having impaired ligand binding, are found constitutively active and highly tumorigenic. EGFRvI lacks most of the extracellular domain, is ligand independent and constitutively active (Pines et al). EGFRvII has an in frame deletions of 83 amino acids (exon14-15) and therefore still a capable of ligand binding. The oncogenic role of this truncated receptor is still unclear (Grandal et al, 2007). The most frequent and also most characterized mutation is the EGFRvIII also described as de2-7 EGFR or Δ2-7 EGFR which is the result of an in frame deletion of exons 2-7. These exons encode domain I and two thirds of domain II of the extracellular domain and the deletions of amino acid 2-273 results in the loss of most of the ligand binding area. Like EGFR, EGFRvIII activates the RAS/RAF/MEK/ERK pathway and Jun N-terminal kinase via PI3K (Grandal et al, 2007; Modjtahedi et al, 2003). EGFRvIII is trapped in a partially activated state which is sufficient for oncogenic signalling but not for degradation (Zandi et al, 2007). In fact despite its internalization this truncated receptor fails to be ubiquitylated promoting also intracellular oncogenic signalling. Another truncated receptor is the EGFRvIII/D12-13, which in addition to the deletion of exon 2-7, this mutant also lacks part of domain III (exon 12- 13). Besides these deletion mutants there is also the report of a mutant that contains duplication of exon 2-7: EGFR TDM/2-7. This mutant contains an extra cysteine reach domain I and part of domain II which do not impair its ligand binding dependency. Genomic analysis of the EGFR gene has revealed that both exon 1 and exon 7 contain an Alu element where DNA breaks are centred (Fenstermaker & Ciesielski, 2000). The recombination of these Alu elements have been implicated in the mechanism of deletion/duplication of the region they are flanking explaining why the extracellular domain is subject to these types of mutations (Wong et al, 1992). Fig 1.21 show a diagram of the mutation above mentioned.

1.8.5.4.2 Intracellular mutations: Kinase domain mutations

All the somatic mutation falling in this category target the residues around the adenosine triphosphate (ATP) binding pocket leading to ligand independent activation of TK activity (Gazdar, 2009a). They are divided into three classes. Class I mutation are in frame deletions in exon 19 (various sets of deletions from amino acid 746 to 753) which almost always include deletion from Leucine (L) 747 to Glutamic acid (E) 749 accounting for about 44% of all the EGFR mutations. Class II mutations comprises single point mutation which cause a missense mutation. The most characterised is the single point mutation in exon 21 of Leucine (L) 858 into Arginine (R). L858R has the

highest prevalence of any other single point mutation of the EGFR TK domain (41% of all activating mutations). To classII belongs the mutation of Glycine (G) 719 into Serine (S), Alanine (A) or (C) Cysteine (4% of all the activating mutations) (Sharma & Settleman, 2009). Other missense mutations account for another 6 % of EGFR mutations (Gazdar, 2009a). Class III mutations are in frame duplications or insertions in exon 20. This class accounts for the remaining 5% of all the activating mutations. There is a remaining portion of low frequency (<1%) mutations in exon 20 such as the Threonine (T) 783 into Alanine (A) and the Valine (V) 765 into Alanine (A) (Gandhi et al, 2009). Mutations in exon 19 and the L858R mutation represent about 90% of all the activating mutations and for this reason they are also named classical mutations(Gazdar & Minna, 2008). The L858R mutation is located next to the conserved aspartic acid-phenyalanine-glycine sequence (DFG) that has the function to stabilize the activation loop. This mutation and also the G719X (X indicates S, A or C) result in similar configuration changes which destabilizes the helical axis narrowing the ATP binding site and conferring kinase activation and higher protein stability (Gazdar et al, 2004; Murray et al, 2008; Sharma & Settleman, 2009). Fig 1.22 shows a diagram o f all the kinase mutations

1.8.5.4.3 Intracellular mutations: C- terminal mutations

These mutations target the C-terminal domain and are best described in GBM models. While EGFRvIV lacks exon 25-27, EGFRvV is truncated from amino acid 958 and lacks the rest of the C-tail (exon 25-28) (Frederick et al, 2000). EGFRTDM 18- 25 and EGFRTDM 18-26, which contain duplication of exons 18-25 and 18-26 respectively, also belong to this category. Of these four mutants, only EGFRvIV has been shown to have oncogenic properties. The removal of exon 25-27 removes the autoinhibitory regulation of the carboxyl on the TK domain resulting in constitutive kinase activity (Zandi et al, 2007). Fig 1.21 shows all the mentioned mutations.

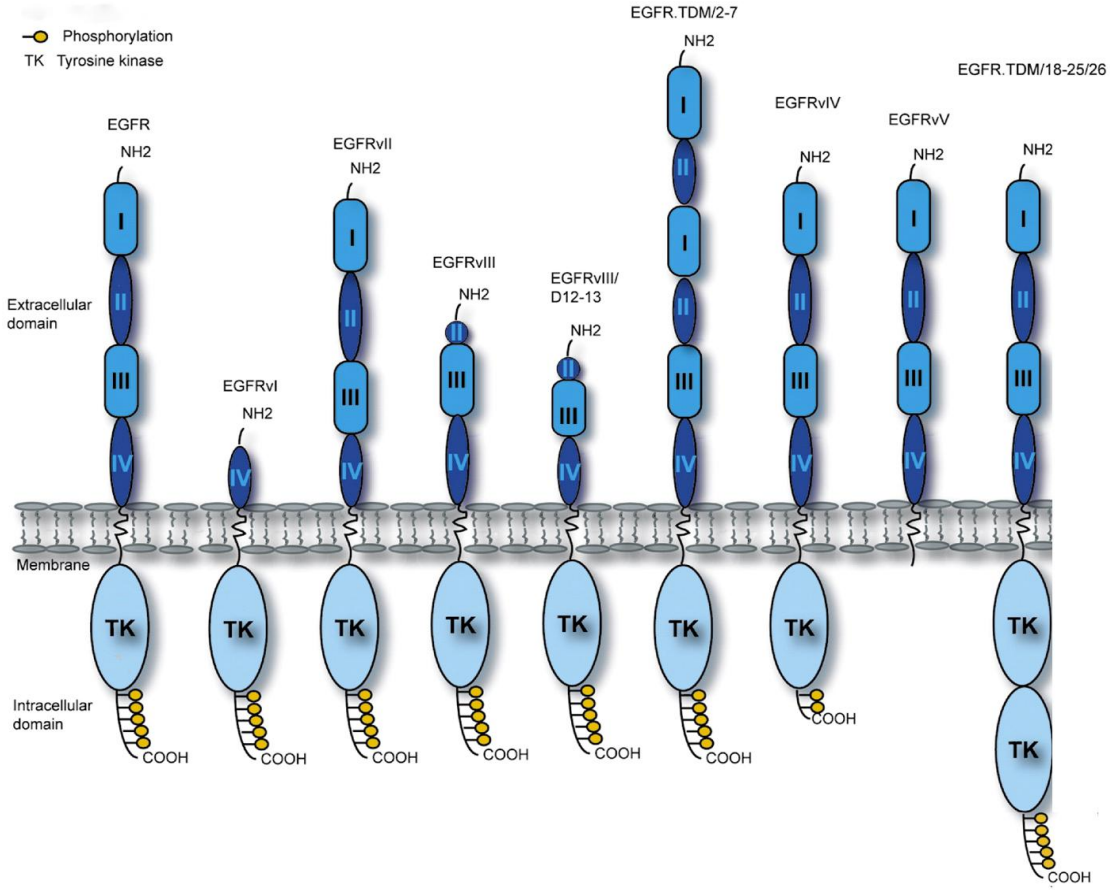

Figure 1.21: Schematic representation of EGFR mutations. From left to right: wtEGFR, deletions or duplication of EGFR (EGFRvI-EGFRvV, EGFRvIIID12-13, EGFRTDM/2-7, and EGFRTDM18-25/26). Modified from(Zandi et al, 2007).

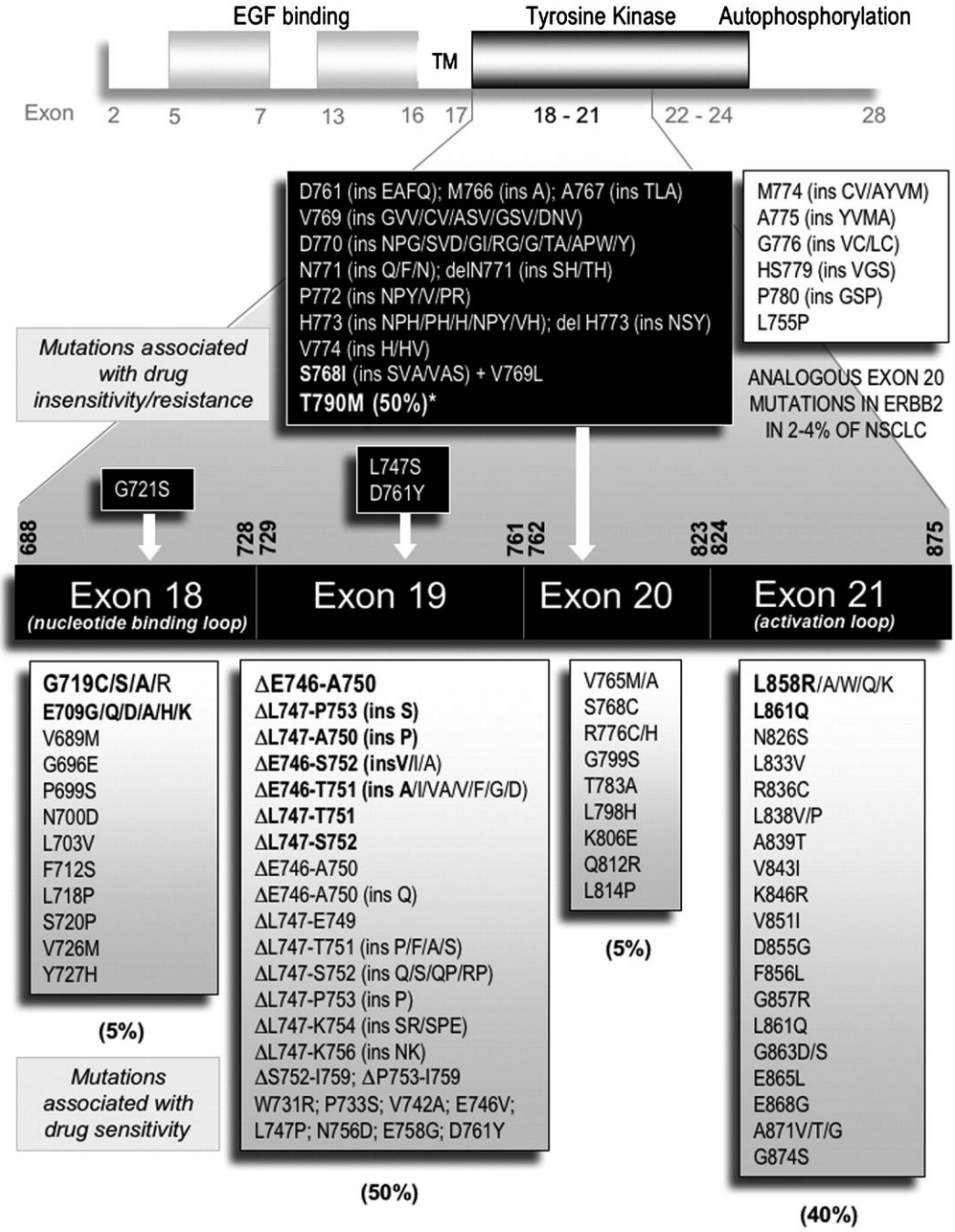

Figure 1.22: Schematic representation of EGFR mutation in the kinase domain. The cartoon shows relative position of EGF binding domain, TM, tyrosine kinase domain and the autophosphorylation domain. The relative position of the correspondent exons is also indicated. Only exons 18-21 are expanded. The list of mutations is divided in two. The bottom part shows the acquired somatic mutations that correlate with gefitinib or erlotonib sensitivity whereas the top part shows the mutation that correlate with resistance to these drugs. The most frequent mutations in both panels are shown in bold. The overall mutation frequency is also shown. This diagram has been taken from (Sharma & Settleman, 2009).

1.8.5.5 EGFR nuclear expression

In addition to the canonical role of EGFR as the initiator of the signalling events that originate at the plasma membrane in response to ligand binding, accumulating evidence from the research of several group in the past 10 years, shows that EGFR and other members of the EGFR family shuttle from the cell surface to the nucleus transducing growth, proliferation and modulation of DNA repair response. This section will illustrate the molecular mechanism that mediates nuclear translocation, the recent findings on EGFR nuclear expression and their significance in terms of tumorigenesis and resistance to chemo and radiotherapy.

1.8.5.5.1 Mechanism of nuclear translocation

The design of eukaryotic cells separates the cytosol and also its components from the nucleus via the nuclear envelope. The regulation of the transport across this cellular barrier facilitates the control of important cellular process such as gene expression, cell cycle progression, signal transduction and mediates the recognition and recruitment of a specific cytosolic protein (cargo), its translocation through the nuclear envelope an the release of the cargo in the nucleus (Lange et al, 2007). While small macromolecules <40-50 kDa can freely move across the nuclear pore complexes by diffusion, large molecules must contain a specific recognition signal (Kaffman & O'Shea, 1999; Moroianu, 1999). The carrier proteins that transport macromolecules across the nucleus are collectively referred as karyopherins (β- karyopherins or Importin β is the most representative superfamily) with those involved in the import called importins and those involved in the export called exportins (Corbett & Krebber, 2004; Lange et al, 2007). Although the majority of the cargo proteins bind directly to β- karyopherins, the interaction between them can also be mediated by the adaptor molecule importinα. The energy required for the transport is provided by the small Ras GTPases, Ran that binds and exchanges both GDP and GTP (Kaffman & O'Shea, 1999; Powers & Dasso, 2004). The constant cycling between these two bound states is determined by the Ran guanine nucleotide exchange factor (Ran GEF), and the Ran GTPase-activating protein (RanGAP). Because these modulators are segregated in different cellular compartment the different forms of Ran are also differently distributed with RanGTP in the nucleus and RanGDP in the cytosol (Kaffman & O'Shea, 1999; Madrid & Weis, 2006; Moroianu, 1999). Importin α recognizes and binds the cargo protein in the cytoplasm

linking it with the importin β. Importin β mediates the transport of the formed trimeric complex through the nuclear pore into the nucleus and dissociates by the binding of the RanGTP. This association causes a conformational change in the importin β resulting in the release of the cargo- importinα (Wente & Rout). The release of the cargo is then mediated by importin α IBB (importin β binding) domain, the nucleoporin NP2 and the export receptor Cse1/Ran GTP. The latter then recycles the importin α in the cytoplasm for another round of import (Lange et al, 2007). Fig 1.23 shows the mechanism of nuclear translocation.

1.8.5.5.2 Nuclear localisation signals

In order to discriminate among all the molecules in the cytosol, proteins destined for transport into the nucleus contain specific recognition target amino acid sequence called nuclear localisation signal (NLS). The best characterised are the classical signals: monopartite consisting of one and bipartite consisting of two stretches of basic amino acids sequences spaced by 3 or 10 stretches of amino acids. The most known examples are the monopartite signal is the SV40 large T antigen NLS (126PKKKRRV) and bipartite nucleoplasmin NLS (155KRPAATKKAGQAKKKK170) (Chuderland et al, 2008; Kaffman & O'Shea, 1999; Lange et al, 2007). The nuclear import and accumulation of the cargo is dependent on the affinity of the NLS cargo to the importinα, and on the concentration of the importinα (Zaidi et al, 2004). Importin α is composed of 10 armadillo motifs each made up of three α helices (ARM domain) and a N-terminal domain required for binding to the importin β and for cargo dissociation. The 10 armadillo motifs generate a curved molecule in which the two NLS binding sites are located within the concave faces of the molecule. Both pockets are made up of conserved tryptophan and 4 downstream asparagines. The N-terminus major pocket binds the monopartite NLS, the minor pocket binds the smaller stretch of basic amino acid residues of the bipartite NLS (Cyert, 2001; Lange et al, 2007). The cargo NLS runs anti-parallel within the curved importin α, the NLS lysine or arginine (basic) amino acids side chain lie between the conserved side chains of the tryptophans forming salt bridges with the negatively charged residues present in the binding groove. The downstream asparagines make key chain contact. The N-terminal region of the importin α contains an autoinhibitory region consisting of basic amino acids (KRR) that competes with the cargo NLS for binding (Chuderland et al, 2008; Lange et al, 2007;

Weis, 2007; Wente & Rout; Zaidi et al, 2004). During import the binding of importin β inhibits this region but once in the nucleus the two molecules dissociate allowing the autoinhibitory region to fold over and interact with the major NLS binding pocket of the importinα. Because both mono and bipartite signals bind the major pocket, the binding of the autoinhibitory domain affects the affinity of importin α to the NLS facilitating the release of the cargo in the nucleus preventing the NLS cargo to re-bind to the importin (Lange et al, 2007). Fig 1.23 shows the dynamics of the nuclear import cycle.

The import is further regulated at different levels. Cargo post translational modification may affect the affinity for the importin, both the cargo and the importin may be bound by an insoluble cellular component compromising the nuclear transfer; the nuclear pore could undergo deregulation affecting the transport (Corbett & Krebber, 2004; Lange et al, 2007; Rout & Aitchison, 2001; Strambio-De-Castillia et al; Weis, 1998; Weis, 2007; Wente & Rout).

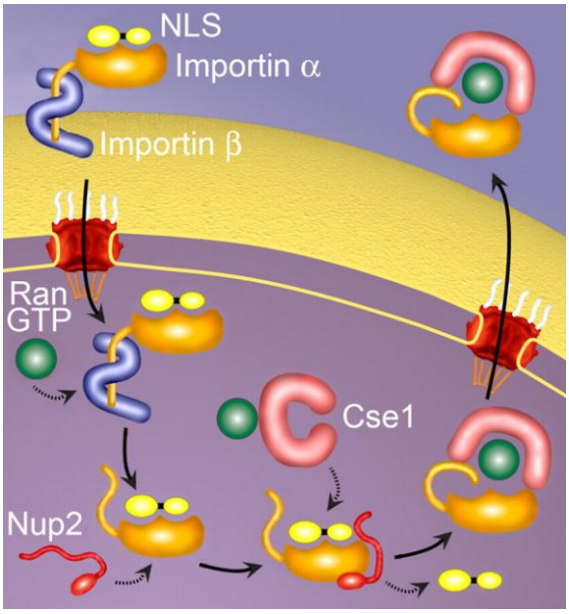

Figure 1.23: Nuclear translocation mechanism. The NLS containing cargo is bound by the heterodimeric complex importinα/importinβ in the cytoplasm. Following nuclear localisation, RanGTP induces importinβ dissociation. Nup2 and Cse1 then mediate NLS cargo release. Importin α autoinhibitory domain folds back preventing re-binding to the NLS cargo and the new Cse1/RanGTP/importinα translocates back to the cytosol. (Lange et al, 2007).

1.8.5.5.3 EGFR Nuclear translocation

Nuclear EGFR was firstly observed in hepatocytes during liver regeneration (Kamio et al, 1990; Marti et al, 1991). Many studies have now reported nuclear EGFR in the form

of uncleaved receptor in the nuclei of various tissues such as thyroid cells, ovarian epithelial cells, immortalized renal cells and also primary tumours including those of the bladder, breast, oesophagus and thyroid (Dittmann et al; Hoshino et al, 2007; Kamio et al, 1990; Lo et al, 2005b; Marti et al, 2001; Xia et al, 2009; Xu et al, 2009b). Hsu et al., that characterized the EGFR tripartite NLS 645RRRHIVRKRLLRRR657, provided the initial analysis of the mechanism of EGFR nuclear translocation in 2007. Despite not being the only characterised tripartite NLS, this type of NLS lacks a specific model of binding with importin α and the EGFR mechanism of nuclear import is still not completely understood. Sequence analysis reveals that the EGFR NLS sequence is well conserved among different species and also among the other ERBB family members with the exception of ERBB3 (Hsu & Hung, 2007). While the ERBB4 nuclear localisation takes place via sequential receptor cleavage, the mechanisms for EGFR and ERBB2 is still not clear. Ligand binding to ERBB4 or activation of PKC by phorbol esters stimulates an initial metalloproteinase mediated cleavage of ERBB4 that release the extracellular 120 kDa part of the receptor, leaving behind an 80kDA membrane bound intracellular domain that includes the kinase domain . There is now sufficient evidence showing that ADAM17 (a disentigrin and metallopeptidase 17) is responsible for this event. The 80 kDa fragment has two possible fates: it can be ubiquitylated and subsequently degraded, or further cleaved by presenilin-dependendent γ secretase that release the soluble intracellular domain within the cytoplasm which is then translocated to the nucleus (Fig 1.24) (Wells & Marti, 2002).

ERBB2 colocalises with importin β in the endosomes and form a tricomplex with it and the nucleoporin Nup358 (usually found at the cytoplasmic filaments of the nuclear pore complex) that translocates near the nuclear envelope (Wang et al, 2010b).

EGFR ligand stimulation and radiation treatment have been shown to stimulate EGFR nuclear localisation. Following activation and receptor internalization EGFR can have three possible fates: recycling, degradation or routed from the early endosomes to the Golgi and the ER by retrograde transport. This retrotranslocation would then allow binding with the importin β leading to receptor nuclear translocation (Dittmann et al, 2008a; Dittmann et al, 2010b; Hsu et al, 2009; Lo, 2010; Wang et al, 2010a; Wang et al, 2010b; Wang et al). Despite this being the only published mechanism (discussed further in chapter 3) it still unclear how EGFR (having a transmembrane domain) can pass through the aqueous channels of the NPC. One possibility, yet to be confirmed, is that it

follows the model presented by the FGFR. Differently form EGFR, FGFR undergoes a clathrin independent endocytosis, and its unusual β-sheet (rather than α-helical) transmembrane domain is known to associate unstably with membrane creating a sort of dynamic equilibrium between membrane bound and soluble cytosolic FGFR (Wang et al, 2010b). The unstable transmembrane seems to recruit chaperone-like accessory proteins that internalise the protein without requiring endosomes. The chaperone masks the hydrophobic transmembrane domain allowing the receptor to translocate to the nucleus via the association with importin β (Fig 1.25) (Wells & Marti, 2002). Another mechanism proposed for the translocation of integral membrane proteins consist in the initial insertion of integral membrane proteins into the Endoplasmic reticulum (ER) membrane where the NLS is recognized by the importins (Liao & Carpenter, 2007; Wang et al, 2010a; Wang et al, 2010c).

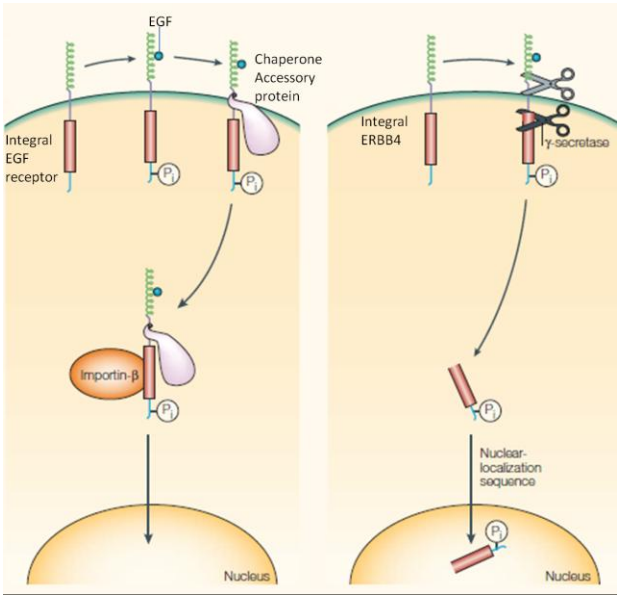

Figure 1.24 Nuclear localisation mechanisms require masking of the hydrophobic transmembrane domain. Like FGFR, EGFR may employ and accessory-like protein to internalise in the cytosol and mask the hydrophobic transmembrane domain. Nuclear translocation can take place via the binding of the importin β through the aqueous environment of the NPC. ERBB4 escapes the hydrophobicity issue by undergoing 2 γ-secretase mediated cleavages. The truncated intracellular soluble part can then easily translocate to the nucleus. (Wells & Marti, 2002)

Then the protein is directed to the inner nuclear membrane by moving through the ER membrane into a contiguous outer nuclear membrane (ONM) reaching the nuclear pore complex. This model predicts that an integral membrane protein (such as EGFR) arrives at the inner nuclear membrane (INM) by moving through the different adjacent

membranes (ER-ONM-INM) still membrane bound. This would allow its transmembrane hydrophobic domain to hide from the aqueous nuclear pore complex environment and trick its way to the nucleus. The receptor is then released from the INM by an INM sorting motif that is recognized by importin α isoform and released in the nucleoplasm (Wang et al, 2010a; Wang et al, 2010b) (Fig 1.25).

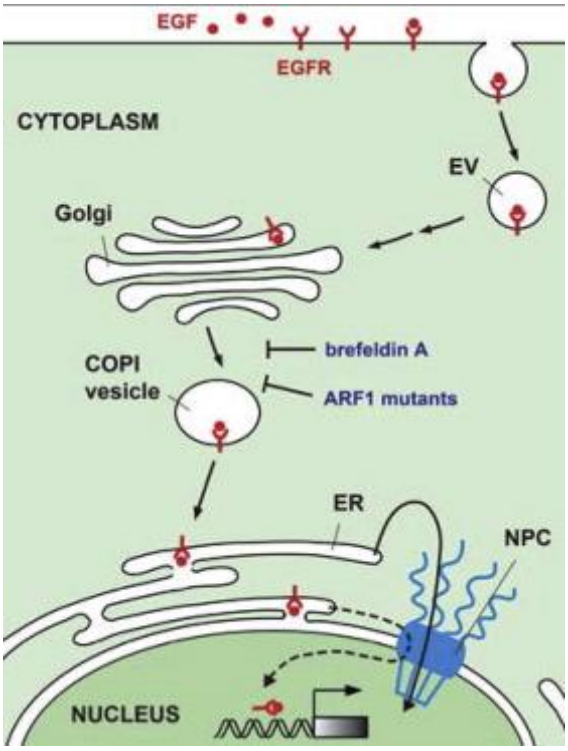

Figure 1.25: Integral membrane protein translocation to the inner nuclear membrane. Integral membrane protein are initially inserted into the ER and then via membrane interaction to the outer nuclear membrane (ONM) and the trough the nuclear pore complex (NPC) into the nucleus via the inner nuclear membrane (INM). In this way the embedded transmembrane hydrophobic domain does not have to pass through the soluble NPC environment. Inner nuclear membrane proteins (INM pr.) utilize this mechanism with the help of ribosomes. (Wang et al, 2010a)

1.8.5.5.4 EGFR modulates transcriptional regulation

During the past 10 years accumulating evidence has shown that EGFR escapes receptor internalization and degradation and that it translocates into the nucleus not only in response to ligand binding, but also following ionizing radiation heat shock, H_2O_2 and chemotherapy. Upon EGF stimulation EGFR translocates to the nucleus and binds to A-T- reach regions (ATRS) working as a transcription co-factor via its functional trans-activation domain (Lin et al, 2001). Nuclear EGFR binds the proximal region of the promoters of several important genes: cyclinD1 (Lo et al, 2006a), involved in cell cycle progression and inducible nitric oxide synthase (iNOS) (Lo et al, 2005a; Lo & Hung,

2006), TWIST and cyclooxygenase-2 (COX-2) (Husvik et al, 2009; Lo et al, 2010; Xu et al, 2009a). The binding of EGFR to STAT proteins has been shown to compensate its inability to directly bind DNA (due to the lack of a DNA binding domain). Nuclear EGFR cooperates with STAT3 to upregulate expression of COX-2 and iNOS genes, with E2F1 to activate transcription of the B-MYB gene (an important regulator of cellular proliferation) (Hanada et al, 2006). In addition the physical association of EGFR with STAT5 has been shown to enhance the expression of the AURORA-A gene (Hung et al, 2008) (Fig 1.26). Increased expression of Aurora-A is involved in centrosome amplification and microtubule disorder. Another mechanism that shows EGFR mediated gene regulation is its recently shown interaction with the Mucin1 (MUC1) (Bitler et al, 2010). This interaction promotes chromatin-bound EGFR and colocalisation of EGFR with phosphorylated RNA polymerase II (Huo et al).

1.8.5.5.5 EGFR modulation of DNA repair

In addition to the transcriptional regulator function nuclear EGFR has been involved in DNA repair. Recent studies have shown that EGFR is normally present in the perinuclear region of the cells and that following IR treatment it is internalized in the nuclear compartments and binds DNAPKcs and the regulatory subunit ku70 (Wheeler et al, 2010). This interaction has been shown to correlate with DNAPKcs T2609 phosphorylation and enhanced DNAPK kinase activity (Dittmann et al, 2010b). The resulting modulation in both formation of γ-H2AX foci, which are involved in the recognition of damaged DNA, and the slower DNA repair kinetics suggested that EGFR modulates the repair kinetics of DNA strand breaks following IR via the association with DNAPKcs (Dittmann et al, 2008a; Dittmann et al, 2008b; Rodemann et al, 2007; Wang & Hung, 2009). In addition the role of EGFR in DNA repair was also shown by the activated nuclear EGFR dependent Y211 phosphorylation of the proliferation cell nuclear antigen (PCNA) that is essential for the DNA sliding clamp involved in both DNA replication and DNA repair (Wheeler et al, 2010). This showed that nuclear EGFR tyrosine kinase activity could also regulate proliferation and DNA repair by regulating PCNA function.

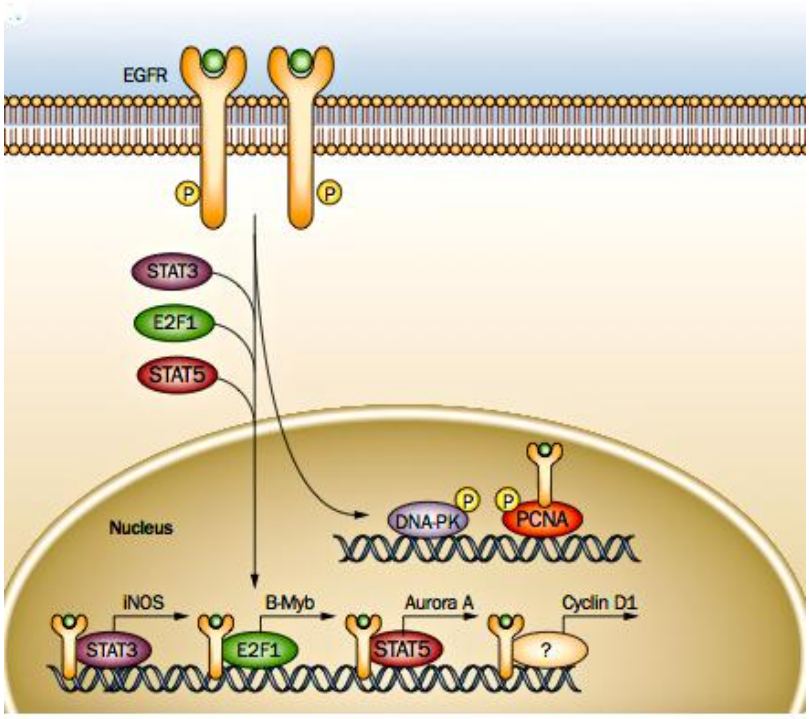

Figure 1.26: EGFR nuclear activity. The diagram shows the binding partner utilised by EGFR to modulate transcription of iNOS, B-Myb, Aurora A. Cyclin D1 is the only gene for which an EGFR binding partner is still unidentified. The arrow also shows EGFR modulation of DNA repair by association with DNAPKcs and PCNA. (Wheeler et al, 2010)

1.8.5.5.6 EGFR radio-protector function

Indeed, EGFR involvement in response to IR treatment is the most understood (Gazdar, 2009a; Nyati et al, 2006). EGFR mediates three important stages to overcome IR induced DNA damage. Following IR the very early response (1-4 h) is mediated by EGFR nuclear translocation, binding with DNAPKcs, and enhanced DNA repair (Rodemann et al, 2007). Exposure to radiation induces a first round of rapid cell death in a caspase3 mediated apoptosis fashion that precedes cell division. Then a second cell death phase occurs due the unrepaired DSBs that emerge from the radiation induced cell cycle arrest (Rodemann et al, 2007). Experimental evidence has shown that radiation induced EGFR activation protects cells from apoptosis by the activation of the AKT anti apoptotic signalling pathway (second phase 4-24 h) (Chen & Nirodi, 2007; Feng et al, 2007; Toulany et al, 2007; Toulany et al, 2008a; Toulany et al, 2006; Toulany et al, 2008b; Wang & Greene, 2005). The third phase of EGFR mediated radioprotection is shown by EGFR ligand-independent phosphorylation and activation of the Ras/Raf/Mek/Erk and STAT signalling that offer a critical survival advantage by

promoting repopulation and tumour progression (>24 h) (Baumann et al, 2007; Russo et al, 2009; Ruzzo et al; Toulany et al, 2006). Fig 1.27 shows the EGFR radioprotective model.

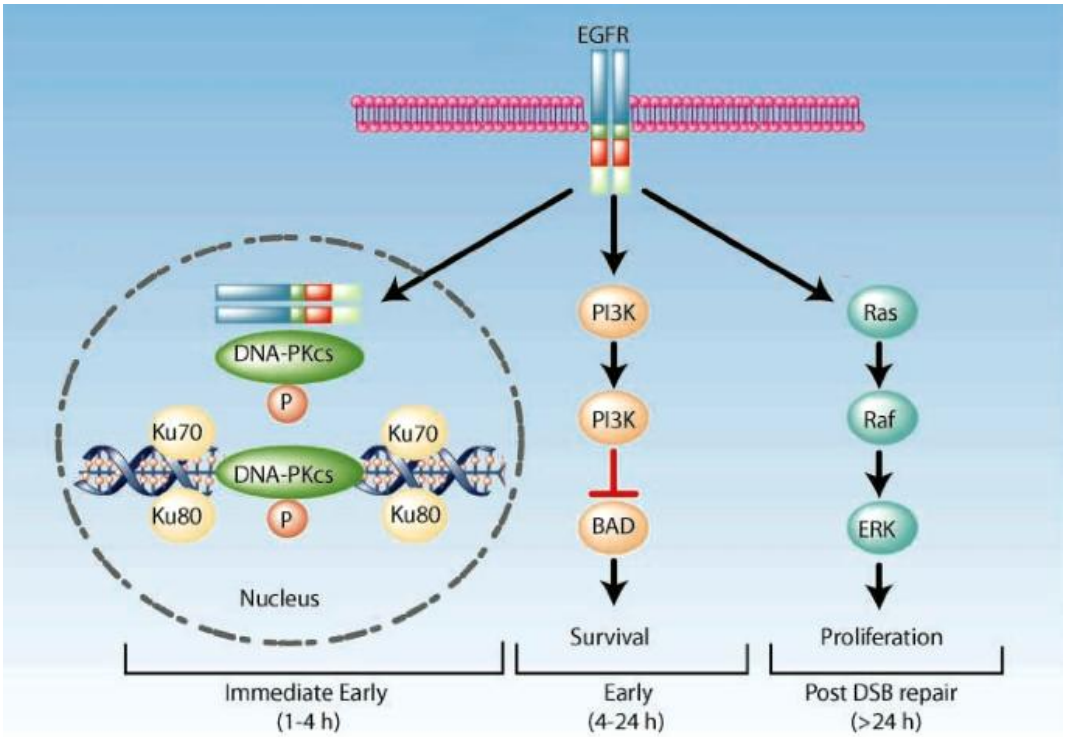

Figure 1.27: A model of EGFR radioprotection. EGFR radioprotection can be didvided into three phases. 1) Immediate early: EGFR translocates to the nucleus and enhance DNA response. 2) Early: EGFR mediates antiapoptotic signalling via activation of AKT. 3) Post DSB repair: EGFR mediates tumour progression and repopulation by activation of the MAPK pathway. Chen D. J. et al, Clinical cancer research 2007

Expression of nuclear EGFR correlates with overall survival in breast cancer, with significant increase if local recurrence and decrease in disease free survival in oropharyngeal squamos cell carcinoma. Interestingly in a study of small cohort of esophageal cancer patients nuclear located phosphorylated EGFR was correlated with higher tumour node metastasis, nodal metastasis and poor treatment outcome (Gazdar, 2009a) (Epperly et al, 2006; Ibrahim et al, 1999; Psyrri et al, 2008; Reiter et al). Nuclear expression of EGFRvIII has been correlated with invasive breast cancer, brain tumour and prostate cancer (Andersen et al, 2009; Golding et al, 2009; Lo et al, 2010; Mukherjee et al, 2009; Viana-Pereira et al, 2008). In addition in hormone refractory prostate cancer EGFRvIII nuclear expression was associated with decreased time to death from biochemical relapse and decreased overall survival (Wheeler et al, 2010). In

glioblastoma the nuclear association of EGFRvIII with STAT3 upregulates iNOS and also found to mediate the EGFRvIII induce glial transformation (de la Iglesia et al, 2008; Lo; Lo et al, 2010; Wheeler et al). The inhibition of EGFR nuclear trafficking by means of molecular inhibitors (discussed below) has shown suppression of cyclinD1 expression and also tumour growth and has also shown induced radiosensitivity (Agelaki et al, 2009).

1.8.5.6 EGFR targeted therapy

Despite the great variety of anticancer treatments (listed above) the overall prognosis for cancers such as lung cancers still remains 5 years survival rate of 15% of all stages. In addition the high toxicity of the drugs together with poor tissue conservation also has been for many years the big disadvantage of conventional therapy(Hynes & Lane, 2005). The development of EGFR targeted therapy stems from two important observations. Tumour cells harbouring oncogenic EGFR alleles acquire dependency on the survival signals transduced by the hyperactive, over-expressed EGFR such that acute disruption leads to rapid death of tumour cells (Arteaga, 2002). Many cancer are not only accompanied by over expressed EGFR and over activation of its down stream signalling pathways but the majority of the most aggressive forms of cancer show EGFR somatically acquired mutations which express a gain of function and also nuclear EGFR (Gazdar & Minna, 2008; Wheeler et al). The design of EGFR targeting molecules has generated a great deal of interest following the observation that the acquired mutations may predict the sensitivity for tyrosine kinase inhibitors and therefore allow a more specific design of cancer therapy and that the abrogation of EGFR nuclear translocation has been shown to correlate with better therapy response.

There are two main approaches utilized to inhibit EGFR activation: 1) targeting the ligand binding domain by use of monoclonal antibodies which inhibit dimer formation and kinase activation leading to subsequent receptor degradation and 2) targeting kinase domain by using Tyrosine kinases inhibitors which compete with ATP for the binding of the activating ATP pocket domain leading to inhibition of kinase activity and consequent inhibition of downstream signalling pathways (Debucquoy et al).

1.8.5.6.1 EGFR inhibitors

These types of inhibitors are mainly reversible inhibitors although irreversible kinase inhibitors have also been synthesized. Some act by mimicking the tyrosine moiety and

attaching to the binding region a non-phosphorilable peptide, other instead target downstream signals by targeting the binding site of intracellular adaptor proteins.

1.8.5.6.1.1 Tyrosine kinase inhibitors

Reversible TKI are: Gefitinib, Erlotonib, Lapatinib, Imatinib, Dasanitib, BMS-599626 and AEE788 (Gazdar, 2009a; Gazdar, 2009b). Erlotonib is a selective low molecular weight inhibitor that (like gefitinib) competes with ATP for binding in the TK domain. In addition to the inhibitory activity exerted on EGFR, it can also target ERBB2, causing inhibition of the AKT pathway and MAPK signalling, and target the formation of ERBB2/ERBB3 dimers (Chang et al, 2007; Xu et al; Yeo et al). Lapatinib is a dual inhibitor for both EGFR and ERBB2 causing inhibition of receptor phosphorylation and of downstream signalling pathways (Carter et al, 2009; Kim et al, 2009a; Kondo et al; Wang et al, 2006). Clinical studies have shown its activity in advanced breast cancer and in advanced metastatic cancers. Both BMS-599626 and AEE788 target EGFR, ERBB2 and the vascular endothelial growth factor receptor (VEGFR). They mainly target the receptor kinase activity and inhibit cellular proliferation by heterodimerisation and downstream signalling pathways. Imatinib is a competitive inhibitor of multiple tyrosine kinases (EGFR, c-kit, platelet derived growth factor receptor (PDGFR). Dasanitib is a dual inhibitor of Src-Abl used in patients that show imatinib resistance in chronic myelogenous leukaemia (Carter et al, 2009).

1.8.5.6.1.2 Gefitinib Iressa^{TM}, ZD1839

Gefitinib is a low molecular weight anilinoquinazoline acting as a reversible ATP-competitor. Both in vitro and in vivo studies have demonstrated the efficacy of this inhibitor in blocking EGFR autophosphorylation and kinase activity (Gelibter et al, 2003; Golsteyn, 2004; Yano et al, 2003). Gefitinib has also been shown to modulate cell cycle progression by disrupting cdk2 regulation possibly by upregulation of the CKI p27kip1 (Yano et al, 2003). The antitumour activity of gefitinib has been shown in a subset of patients with NSCLC: 10% of European patients and 30% of patients from East Asia. Sequencing of the EGFR gene has shown that in those patients whose tumours exhibited EGFR mutations, the response rate to gefitinib is about 75%. Some studies also showed that EGFR activating mutations (class I and II) not only impact response rate but also progression free survival (PFS) in patients with NSCLC treated with gefitinib. The INTEREST study showed 7.0 vs 4.1 months PFS in patients with

mutation treated with gefitinib compared to those treated with docetaxel alone whereas those patients expressing wild type EGFR trended in favour of docetaxel (1.7 vs 2.6 months) (Gazdar, 2009b). A similar association was also found in the I-PASS trial, which compared first line gefitinib with carboplatin/paclitaxel in Asian patients with advanced NSCLC and with no history of smoking. In these studies those patients with mutation had a significantly longer PFS whereas those expressing wtEGFR had better PFS with chemotherapy (Armour & Watkins). The EGFR activating mutations have become independent predictors for time to treatment failure with the deletion of exon 19 and the L858R mutation being the best predictor for longer time to treatment failure (Giaccone, 2005; Morita et al, 2009; Paez et al, 2004; Pallis et al, 2007; Sequist et al, 2008; Soh et al, 2007; Sorscher, 2004; Tam et al, 2009; Ushiki et al, 2009; Zhu et al, 2008). In addition to the improvement in the regimen of NSCLC, Gefitinib has been also shown to improve survival of patients with advanced pancreatic cancer, head and neck cancer and GBM (Pedersen et al, 2005; Rossler et al, 2009; Sundberg et al, 2003). Two clinical studies of gefitinib in combination with gemcitabine and cisplatin and in combination with paclitaxel and carboplatin have not confirmed the previously obtained result in vitro (Choong et al, 2006; Giaccone et al, 2004b; Maemondo et al). Moreover, gefitinib treatment of early NSCLC has been also unsuccessful suggesting that EGFR activating mutations may be utilized as a prognostic factor rather that predictive factor for TKI efficacy (Wu et al). The controversial issues on the gefitinib efficacy can be partially resolved by two important facts. First, not all the activating mutations lead to all TKI sensitivity in fact tumours expressing the L858R mutation are significantly more sensitive to gefitinib than those expressing the G719S mutation (Chen et al, 2006). Second, tumours might have additional genetic lesions that relieve the tumour dependency on the EGFR signalling pathway. Indeed, it is largely recognized now that the efficacy of gefitinib is of limited duration due to the emergence of another somatic mutation in the tyrosine kinase domain. The Threonine 790 to Methionine (T790M) is found in about 50% of the patients that show resistance to TKI. The mechanism and the structural reconfiguration that this mutation confers to EGFR are unclear. It has been proposed that as the L858R mutations shows higher K_m for ATP and a lower K_i for gefitinib (i.e. the affinity for ATP is lower and for gefitinib is higher) the secondary mutation T790M re-establishes the affinity for the ATP resulting in a reduced potency of an ATP competitive agent (Bean et al, 2007; Costa et al, 2008; Engelman et al, 2007; Kwak et al, 2005; Tam et al, 2009). The Aspartic acid 761 to Threonine (D761T)

mutation has also been implicated in conferring TKI resistance and it has been suggesting that these mutations may weaken the interaction of the TKI with EGFR (Gazdar, 2009a; Gazdar, 2009b; Ushiki et al, 2009).

1.8.5.6.1.3 Irreversible TKI

The attempt to overcome the resistance to the T790M mutation has lead to the production of irreversible TKI. These kinases inhibitors form irreversible covalent bonds to the kinase active site by reacting with a nucleophilic cysteine residue. This irreversibly blocks the binding of ATP to the kinase domain rendering EGFR inactive. The clinically most advanced irreversible inhibitors of EGFR are HKI-272, BIBW2992 and PF00299804 (Citri et al, 2002; Engelman et al, 2007; Gazdar, 2009a; Harada et al; Kwak et al, 2005; Sebastian et al, 2005; Yu et al, 2007).

1.8.5.6.2 Monoclonal antibodies

While the TKI target EGFR intracellular domain, mAB target the extracellular domain and modulate the intracellular cascade of signalling events by interfering with the receptor homo and hetero dimerisation (Rivera et al, 2008; Schmiedel et al, 2008). The most widely used in the clinic is Cetuximab (Erbitux®, IMC-C225) (Reade & Ganti, 2009). Cetuximab is a chimeric/human antibody containing approximately 30% of murine sequences with proven second or third line efficacy in colorectal and head and neck cancer. It competes with ligand for the ligand binding site on EGFR domain III for which it has a five times greater affinity. It inhibits EGFR not only by impeding ligand binding but also by sterically prohibiting EGFR to adopt the extended active conformation (Benavente et al, 2009; Li et al, 2008; Morgan & Grandis, 2009; Vallbohmer et al, 2005).

1.9 AIMS AND OBJECTIVES

EGFR has a major role in oncogenesis, cancer progression and cancer therapy. The aim of this investigation is to study the role of nuclear EGFR in the modulation of DNA repair following IR and cisplatin treatment. To this end, the following questions will be addressed:

- Does the mutation of the EGFR NLS sequence determine impaired nuclear translocation (Chapter 3)?
- How does the NLS mutation affect EGFR? (Chapter 3)
- Does EGFR impaired nuclear translocation inhibit repair of cisplatin induced ICLs or IR induced SBs (Chapter 4)?
- How does EGFR impaired nuclear translocation inhibits repair of IR or cisplatin induced damage (Chapter 4-5)?
- What are the consequences of cisplatin damage in terms of survival (Chapter 5)?

CHAPTER 2:

MATERIALS AND METHODS

2.1 MATERIALS

2.1.1 EGF

EGF was obtained from Sigma Aldrich.

2.1.2 Cell lines and culture conditions

NIH3T3 wild type cell line were obtained from CRUK and were grown in DMEM supplemented with 10% heat inactivated (at 56^{o}C for 30 minutes) foetal calf serum, 1% of 200mM L-glutamine (Autogen Bioclear, UK), 1% of 10,000 units Penicillin – 10mg/ml Streptomycin (Sigma-Aldrich, UK) and incubated at 37^{o}C in 5% CO_2.

2.1.3 Chemotherapeutic drugs and other reagents

Clinical grade Gefitinib (Iressa, ZD 1839) was kindly provided by AstraZeneca (Macclesfield, UK). Cisplatin (DBL, Warwick, UK) were obtained from The Middlesex Hospital (UCL Hospital, London, UK). Details of the compounds used for this study are described in Table 2.1. Stock solutions were either prepared in advance or fresh prior to experiments according to stability of each compound. Cisplatin was obtained pre-diluted at the indicated concentrations from the hospital.

Compounds	Type of drug	Structure	Dilution solvent	Stock solution
Gefitinib	Quinazoline derivative inhibiting EGFR (ErbB1) tyrosine kinase activity (small molecule)	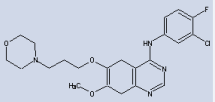	DMSO	10mM
Cisplatin	Alkylating agent – platinum compound (covalent DNA binding drug)	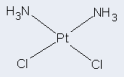	Sterile water	3.3mM

Table 2.1: Compounds used in DNA repair studies

2.1.4 Plasmids

The plasmid DNA used was the pUSEamp vector (Upstate Cell Signaling Solutions, NY, USA). Fig 2.1 shows the plasmid map.

The *wtEGFR* and the *L858R* constructs were kindly provided by Daphne Bell and Matthew Myerson from the MGH Cancer Centre, Harvard Medical School, Boston, USA.

The NLS mutant constructed during the project used the wtEGFR and the L858R plasmid as template. The two designed and SDS purified mutagenic primers (Forward 5'cctcttcatggcagcggcccacatcgttgcgaaggccacgctggcggcgctgctgcagg3' and Reverse 5'cctgcagcagcgccgccagcgtggccttcgcaacgatgtgggccgctgccatgaagagg3') were utilized according to the Site directed mutagenesis XL kit protocol (Stratagene) to change the EGFR NLS sequence 645-RRRHIVRKRTLRR- 657 into 645-AAAHIVAKATLAA-657. EGFRvIII was kindly provided by Edith Blackburn from the Department of Biosciences University of Kent, Canterbury, England.

The repair assay utilised other *EGFR* plasmids: *EGFR M1, M12 KMT ΔNLS* enconding point mutations of the EGFR NLS sequence (M1: AAAHIVRKRTLRR, M12: AAAHIVAAATLRR), the deletion of the NLS sequence (ΔNLS) and a mutation within the kinase domain (KMT: K821A). These plasmids were obtained from Prof. M.C. Hung (MD Anderson Cancer Center, USA). These constructs were all cloned into the pCDNA3.1 (Invitrogen) shown in Fig 2.2.

Table 2.2 shows the list of all the plasmids utilised in this study together with their most relevant characteristics.

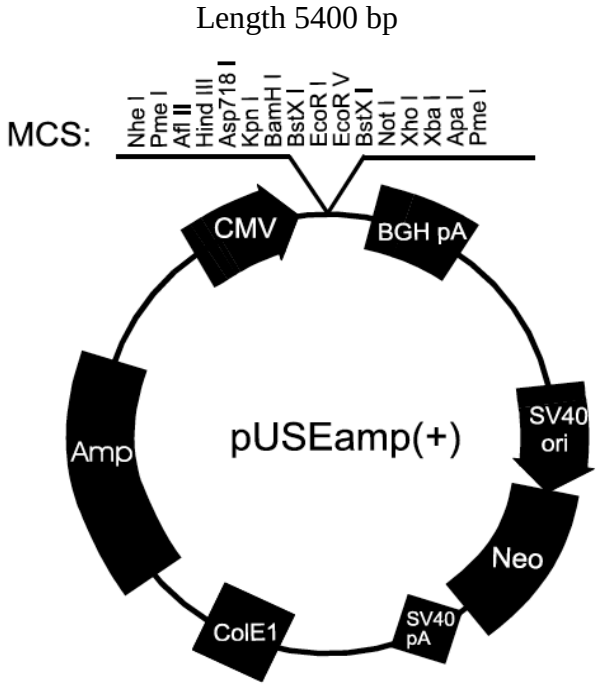

Figure 2.1: pUSEamp plasmid map. This vector was used for expressing various EGFR constructs. Picture from: Upstate Cell Signaling Solutions (www.upstate.com).

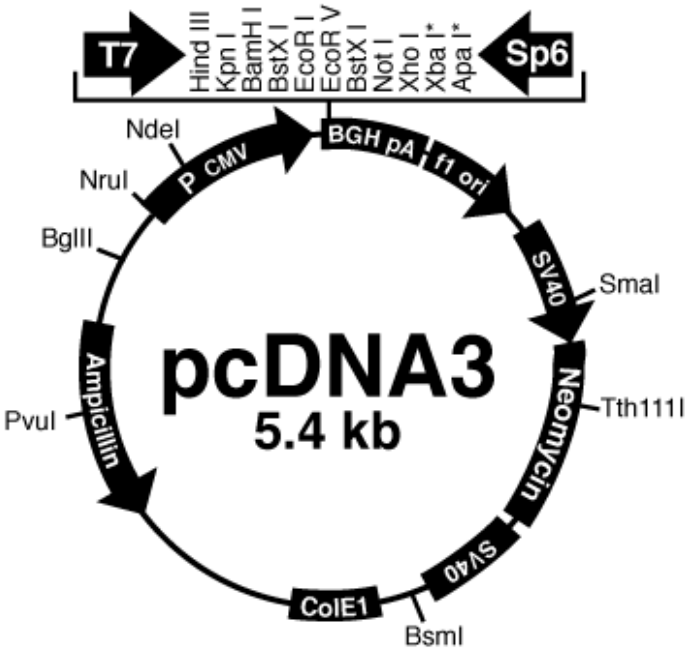

Figure 2.2: pcDNA3 plasmid map. This plasmid carries the resistance gene ampicillin and neomycin. Unique restriction sites are indicated on the plasmid. (www.invitrogen.com).

PLASMID	VECTOR	INSERT	SIZE	NLS CODING	KINASE MUTATION	ORIGIN
wtEGFR	pUSEamp	wtEGFR	9.4 Kb	RRRHIVRKRTLRR	N/A	Dr. Daphne Bell and Prof. Matthew Myerson
EGFR M1	cDNA3.1	M1	9.3 Kb	AAAHIVRKRTLRR	N/A	Prof MC Hung
EGFRM12	cDNA3.1	M12	9.3 Kb	AAAHIVAAATLRR	N/A	Prof. MC Hung
EGFR NLS123	Puse amp	NLS123	9.4 Kb	AAAHIVAKATLAA	N/A	CONTSRUCTED
EGFR ΔNLS	cDNA3.1	ΔNLS	9.3 Kb	XXXXXXXXXXXXX	N/A	Prof. MC Hung
EGFR L858R	pUSEamp	L858R	9.4Kb	RRRHIVRKRTLRR	L858R	Dr. Daphne Bell and Prof. Matthew Myerson
EGFRLNLS123	pUSEamp	LNLS123	9.4Kb	AAAHIVAKATLAA	L858R	CONSTRUCTED
EGFR KMT	cDNA3.1	KMT	9.3 Kb	RRRHIVRKRTLRR	K721/A	Prof. MC Hung
EGFRvIII	cDNA3.1	EGFRvIII	8.5Kb	RRRHIVRKRTLRR	N/A	Dr. Edith Blackburn

Table2.2: List of plasmid used in this study

2.1.5 Primers

All the primers were self designed and ordered from MWG

2.1.5.1 Mutagenic primers

PRIMER	SEQUENCE
FORWARD	5'-cctcttcatggcagcggcccacatcgttgcgaaggccacgctgg cggcgctgctgcagg-3'
REVERSE	5'-cctgcagcagcgccgccagcgtggccttcgcaacgatgtgggcc gctgccatgaagagg-3'

Table2.3: List of mutagenic primers

2.1.5.2 Sequencing primers

PRIMER	SEQUENCE
EGFR-seq1	5'-aggaaatcctgcatggcgc-3'
EGFR-seq2	5'-ccccaccacgtaccagatggatg-3'
EGFR-seq3	5'gccttgccgcaaagtgtgtaac-3'
EGFR-seq4	5'-gtgcaagcttctggagggtgagcc-3'
EGFR-seq5	5'-gtagctccagacatcactctggt-3'
EGFR-seq6	5'-gactatgtccgggaacacaaagac-3'
EGFR-seq7	5'-caacttctaccgtgccctcctgatgg-3'

Table 2.4: List of sequencing primers

2.1.5.3 Screening primers

PRIMER	SEQUENCE
EGFR-screeningF	5'-gtagctccagacatcactctggt-3'
EGFR-screeningR	5'-ggagcttgtggagcctctta-3'

Table 2.5: List of screening primers

2.2 METHODS

2.2.1 Tissue culture

2.2.1.1 Cell lines maintenance

All cell lines were grown in 75cm^2 flasks (T75), in humidity-saturated (95%) incubators (Forma Scientific, UK), at 37^{o}C with 5% CO_2. All procedures were carried out in Class II MDH biological safety cabinet (Intermed MDH, UK) using aseptic techniques (cabinet was cleaned with 70% industrial methylated spirit – IMS – as well as the equipment used inside the cabinet). Cells were routinely passage twice a week, at 80-90% confluence. As all cell lines were adherent, media was removed and cells were washed with 3ml of sterile 0.01M phosphate-buffered saline solution (PBS, Sigma-Aldrich, UK) to remove the residual serum. Cells were subsequently detached using 5ml of 1xTrypsin/EDTA (Autogen Bioclear, UK) at 37^{o}C. 5ml of complete medium was then added to inactivate the trypsin and cells were pelleted by centrifugation at 1200rpm for 5 minutes at room temperature. The supernatant was discarded and cells were resuspended in 10ml of complete medium. Cells were finally seeded into new flasks at a ratio of 1/2 to 1/5 according to the cell line. All cell lines were passaged to a maximum of 30 times, after which point fresh cells were retrieved from the liquid nitrogen stock.

2.2.1.2 Storage and retrieval from liquid nitrogen

In order to store cell lines, frozen cell stocks were prepared. Cells were grown in 175cm^2 flasks (T175) to 80% confluence. Cells were trypsinised and resuspended to a concentration of 1x10^{6}cells/ml in freezing medium (FCS containing 10% dimethylsulphoxide – DMSO – Sigma-Aldrich, UK). The cell suspension was aliquoted in 1ml cryotubes and frozen at -80^{o}C for one day. Tubes were then transferred to a liquid nitrogen tank. Cells were recovered from liquid nitrogen by thawing the cryotubes rapidly in a 37^{o}C water bath. The cell solution was added to a 25cm^2 flask (T25) containing 9ml of complete growth medium. Flasks were incubated at 37^{o}C with 5% CO_2. The medium was changed after 24 hours (once cells have re-attached to the bottom of the flask) to avoid toxicity due to the DMSO from the freezing mixture.

2.2.1.3 Cell count

Cells were counted, once resuspended in 10ml of complete growth medium (see cell line maintenance), using a haemocytometer. A haemocytometer has two chambers and each chamber has a microscopic grid etched on the glass surface (4 squares each containing 16 smaller square all connected by a 25 square grid). The chambers are overlaid with a glass coverslip that rests on pillars exactly 0.1mm above the chamber floor. 15µl of cell suspension was mixed with 15µl of trypan blue (Sigma-Aldrich, UK) in order to exclude dead cells (1 in 2 dilution). 15 µl of this Dilution was loaded into one chamber. The number of cells present in the original solution was determined by counting the number of cells within the 4 large squares. The obtained numbered was then divided by 4 (number of squares) and then multiplied by 2 (dilution 1:2). The total number of cells obtained was multiplied by $1x10^4$, giving the number of cells per ml of suspension.

2.2.1.4 Cell doubling time

NIH3T3 cells were plated to an initial cell number of $1x\ 10^5$ per $25cm^2$ flask containing 8 ml of growing media. Single flasks were utilised for each time point until confluence. Every 24 hours cells were trypsinised, centrifuged, resupended and counted. The doubling time was calculating by plotting the number of counted cells (Y) against the number of hours (X). This resulted in 1 doubling time every 20-24 hours.

2.2.2 Drug treatments

Prior to drug treatment, cells were seeded in flasks, 96 or 6 well plates and incubated at 37^oC in 5% CO_2 for 24 hours. Cells were then treated at a range of concentrations and lengths of exposure (Table 2.6). Optimal concentration was determined by the DNA repair response curve. Appropriate schedules were used for the different experiments, as outlined in the methods detailed previously.

Compounds	Lengths of exposure	Range of concentrations
Gefitinib	24 hours and when medium changed	0 and 2μM
Cisplatin	1 hour	0 – 150μM

Table 2.6: Range of concentrations and lengths of exposure for drugs used in the different experiments. The ranges of concentration indicated in the table reflect the minimum and maximum concentrations used.

2.2.3 Irradiation condition

In radiotherapy, the potency of IR is referred to the measurement of charge deposited within a tissues and usually corresponds to exposure (coulomb/kg). For living tissue the energy deposited is expressed in Gray or Gy, being 1 Gy the amount of radiation required to deposit 1 Joule of energy in 1 kg. This represents the absorbed dose. During this thesis there will be a general reference to IR, however alpha or beta, gamma rays and X-rays are all different types of ionising radiation. The biological damage produced by each of these different types is measured in Sievert. This corresponds to the absorbed dose multiplied by the quality factor which, for alpha particles is 20 while for X-rays is 1. In this study it was chosen to study the effect of X-rays. These are measured in Gy.

For irradiation conditions cells were plated at a concentration of 1 x 10^5/ml. Following 48 hours transfection, cells were serum starved for 24 hours and irradiated with 4 Gy (for the interaction and nuclear translocation studies) or 12.5 - 15Gy (for the repair studies) using the A.G.O. HS 321kV X-ray system. The x-ray machine was calibrated by a nuclear engineer to a dose rate of 4.39 Gy/min; 250 KV/12.5mA at a 30cm distance using a filter made of 0.25mm Cu and 1.00 mm Al.

2.2.4 The Comet assay

2.2.4.1 DNA damage level

Cells were plated at 10x10^4cells/ml in 25cm^2 flasks (Nunclon, VWR, UK) and incubated for 24 hours at 37^{o}C in 5% CO_2. In order to analyse DNA damage and repair, cells were treated with the appropriate chemotherapeutic drug at a range of concentrations. Drugs were left in contact with the cells for a short period of time (1 to 2 hours according to the drug) and left to incubate in drug free media (if necessary), for DNA damage to reach its peak (e.g. 9 hours for cisplatin). From this,

a fixed drug concentration was determined to treat the cell and observe the repair of drug-induced DNA damage. For IR induced strand breaks the dose producing a tail moment (see section 2.10.2) of 9-10 was used. For interstrand crosslink agents (cisplatin), the drug concentration giving about 70% decrease in tail moment (see section 2.10.2) was useed.

2.2.4.2 DNA repair study

Once the concentration was selected, fresh cells were plated at $1x10^5$ cells/ml in 6 well plates and incubated at 37^oC in 5% CO_2 for 24 hours. Cells were then treated for the appropriate time and the drug was subsequently replaced by drug free media. Cells were incubated in drug free media for various period of time in order to measure DNA damage repair. Cells were collected by trypsinisation, pelleted and resuspended in 1ml of foetal calf serum containing 10% DMSO, before to be stored at -80^oC.

2.2.4.3 Assay methodology

When studying damage caused by a crosslinking agent, cells were thawed and resuspended in ice cold media to a concentration of $2.5x10^4$cells/ml. Those cell suspensions were divided into two samples, one of which being irradiated (12.5Gy) using the A.G.O. HS 321 kV X-ray system to deliver a fixed number of random DNA strand breaks (procedure carried out on ice), immediately before analysis. For strand breaking agents, cells were thawed and diluted to a concentration of $2.5x10^4$cells/ml without any irradiation.

In both cases, the following methodology was the same. All procedures were carried out on ice and in subdued light. Cells were embedded in 1% type VII agarose (Sigma-Aldrich, UK) (1ml of agarose + 0.5ml of cell suspension) on duplicate 1% type 1A agarose (Sigma-Aldrich, UK) pre-coated microscope slides. Cells were lysed, in the dark on ice, for one hour in ice cold lysis buffer (100mM disodium EDTA, 2.5M NaCl, 10mM Tris-HCl pH 10.5) containing 1% Triton X-100 (Sigma-Aldrich, UK) added fresh. Slides were subsequently washed every 15 minutes in ice cold distilled water for 1 hour. Slides were then incubated in ice cold alkali buffer (50mM NaOH, 1mM disodium EDTA, pH 12.5) for 45minutes followed by electrophoresis in the same buffer for 25 minutes at 18 V (0.6V/cm), 250mA. The slides were finally rinsed in neutralising buffer (0.5M Tris-HCl, pH 7.5) then saline

(PBS). Slides left to dry overnight were re-hydrated for 20 minutes with distilled water and stained with propidium iodide (2.5µg/mL) for 30 minutes (in the dark) then rinsed in distilled water. Finally, slides were left to dry in a drying oven and stored.

2.2.4.4 Data analysis

Images (illustrated in Fig 2.3) were visualised using a NIKON inverted microscope with high-pressure mercury light source, 510-560nm excitation filter and 590nm barrier filter at x20 magnification. Images were captured using an on-line charge-couple device (CCD) camera and analysed using Komet Analysis software (Kinetic Imaging, Liverpool, U.K.). For each duplicate slide 25 individual cells were analysed. Tail moment for each cell was calculated using the Komet Analysis software as the product of the percentage DNA in the comet tail and the distance between the means of the head and tail distributions, based on the definition of Olive *et al.* (2002).

For strand breaks, tail moment data were analysed as a function of time post-incubation or drug concentration. Fig 2.4 illustrates the effect of a drug inducing strand breaks. Data shown in this study were the result of three independent experiments and included corresponding standard deviation bars.

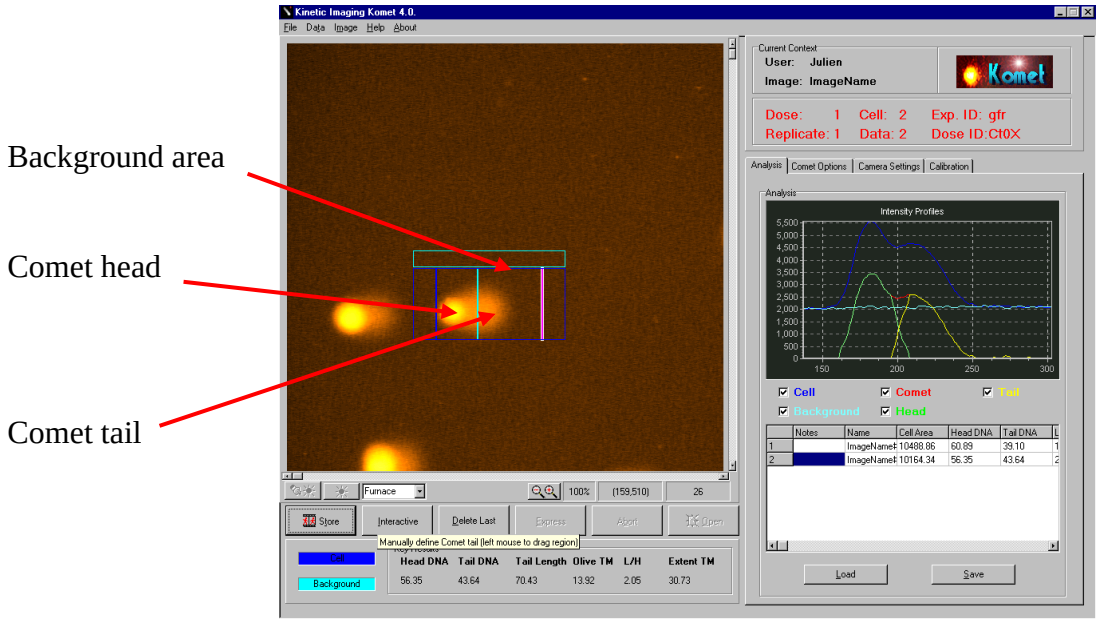

Figure 2.3: Screen display of Komet analysis software. The Fig show untreated irradiated cells. Red arrows are showing the head and the tail of comet. The background is also taken into consideration by the software for calculation of the tail moment.

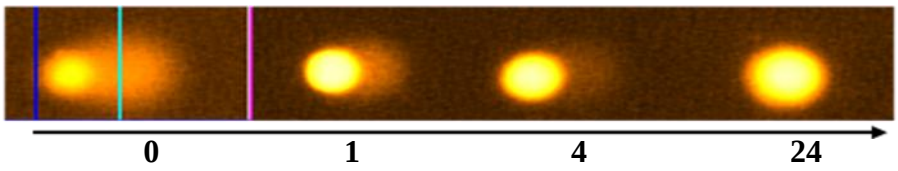

Time post-treatment (hours)

Figure 2.4: Repair of DNA damage caused by IR treatment. Comet tail appears to be reduced over time

For crosslinking agents, results were expressed as percentage decrease in tail moment compared to untreated controls calculated by the following formula (tail moment was calculated from the same software as previously described):

$$\% \text{ decrease in tail moment} = \left[1 - \left(\frac{TMdi - TMcu}{TMci - TMcu} \right) \right] \times 100$$

where TMdi = tail moment of drug-treated irradiated sample

TMcu = tail moment of untreated, unirradiated control

TMci = tail moment of untreated, irradiated control

Percentage decrease in tail moment data were the result of three independent experiments, with corresponding standard error bars. Fig 2.5 represents DNA damage repair profile of irradiated cell treated with cisplatin. The short comet tail after 9 hours is due to the presence of interstrand crosslinks, delaying the DNA migration. Hence, as crosslinks are unhooked (repaired), the comet tail in irradiated cells is restored. For cisplatin the peak of crosslinking is observed after 9 hours post-incubation.

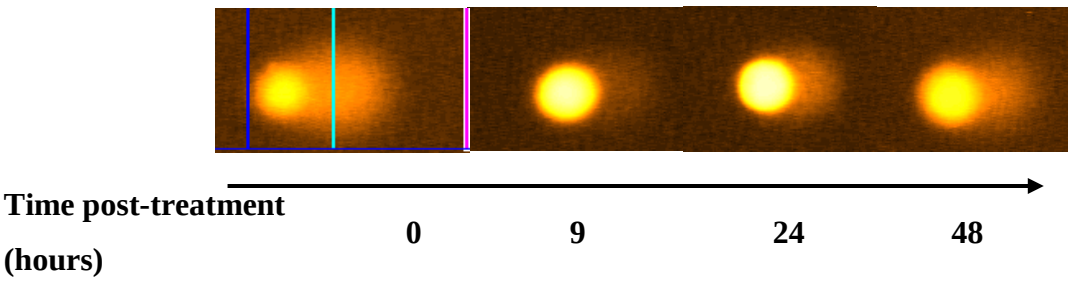

Figure 2.5: DNA damage repair profile of irradiated cells treated with cisplatin. Cells were treated with cisplatin for 1 hour and subsequently incubated in drug-free media for various times. After 9 hours crosslinking reached its maximum (60-70% crosslinks) as the tail appears much shorter (crosslinks are causing the delay in DNA migration). At 24 and 48 hours, the unhooking (repair) of cisplatin crosslinks causes the comet tail to re-elongate.

2.2.5 Statistical Analysis

The two way ANOVA and Bonferroni post tests were used for calculating the significance of the differences in unhooking crosslinks and in the repair of the DNA SBs. All the cell lines were compared to the wtEGFR expressing cell line, statistical values of $P < 0.01$ were considered significant.

2.2.6 MTT

Cells were diluted 2.5 X 10^4/ml and 500 (100μl) or 1000 (200μl) cells were plated in each well of a 96 well plate and incubated overnight in full serum media. Cells were incubated with 50 μM cisplatin for one hour in serum free media and then left in full serum media over a period of 72 hours. Following 24, 48 and 72 hours cells were incubated with 20 μl of 5mg/ml Thiazolyl Blue Tetrazolium Bromide (MTT solution) for 3 hours at 37°C. Next, the media was replaced with 200 μl Dymethil sulfoxide (DMSO). Each plate was left on the shaker for 5 minutes. Cell density was

read at 560 nm, corrected with background reading and correlated to untreated control to calculate % survival.

2.2.7 Western blotting analysis

2.2.7.1 Total protein extraction

Cells were washed twice with ice-cold PBS buffer. Sigma lysis buffer containing fresh 1.5 X protease inhibitor and 1.5 X phosphatase inhibitor (Roche, UK), was added to the cells (kept on ice) for few minutes. Then, cells were scraped using cell scrapers (VWR, UK) and left rotating for 15 minutes at 4^{o}C. Samples were then pelletted by centrifugation for 15 minutes at 4^{o}C (13,000rpm). The total cell lysate (supernatant) was placed in a fresh eppendorf tube and stored at -80°C.

2.2.7.2 Nuclear and cytoplasmic protein extraction

Nuclear and cytoplasmic separation was achieved using the Nuclear extract kit from Perbio (Cramlington, UK). Cells were grown and treated in 25cm^2 flasks (T25). Briefly, cells were washed gently twice with cold PBS and scraped in 2ml of cold PBS. Cell solutions obtained were transferred to a pre-chilled 15ml falcon tube (VWR, UK) and centrifuged 5 minutes at 500g at 4^{o}C (supernatant was discarded). Cell pellets were resuspended in 300µl of cold PBS and transferred to a cold eppendorf tube and centrifuged at 500g, 4^{o}C for 5 minutes (supernatant was discarded – all the PBS must be removed). Pellets were finally resuspended in 100µl of ice-cold CERI (Cytoplasmic Extraction Reagent I) buffer, containing protease inhibitor, and vortexed at high speed for 15 seconds. The cell suspensions were incubated 10 minutes on ice before adding 5.5µl of CERII (Cytoplasmic Extraction Reagent II) buffer. Cell solutions were vortexed for 5 seconds and incubated for 1 minute on ice. Solutions were vortexed once more for 5 seconds and centrifuged for 5 minutes at 16,000g at 4^{o}C. The supernatant corresponds to the cytoplasmic fraction and was stored at -80^{o}C (the last few microliters of supernatant were discarded to avoid contamination with the nuclear pellet).

The nuclear pellets were resuspended in 50µl of NER (Nuclear Extraction Reagent) buffer containing protease inhibitor and vortexed 15 seconds at high speed. Samples were vortexed for 15 seconds every 10 minutes for 40 minutes. Lysed nuclei were

centrifuged for 10 minutes at 16,000g at 4^{o}C and the nuclear fractions (supernatant) were stored at -80^{o}C.

2.2.7.3 Protein quantification

Once extracted, proteins were quantified using the RC DC protein assay from Bio-Rad Laboratories. This assay is based on the Lowry protocol (Lowry *et al.*, 1951), using reagents A, S and B. Briefly, 2µl of each lysate was mixed with 18µl of distilled water, then 100µl of the mix of reagent A and S (20µl of reagent S with 1ml of reagent A) was added. Finally 800µl of reagent B is added and solutions are incubated for 15 minutes at room temperature. Absorbance (OD) was measured, against a blank containing only distilled water at 750nm on a Philips spectrophotometer (Beam PU8620 Series UV/Vis single) and total protein concentration was determined with the following formula:

$$\text{Concentration in } \mu g/\mu l = OD*25$$

Once the concentration was determined, loading dye (250mM Tris HCl, pH 6.8, 500mM DTT, 10% SDS, 0.5% Bromophenol Blue, 50% glycerol and distilled water were used to make a 5 times stock) was added to 50µg of protein (volume equivalent). Samples were boiled at 70°C for 10 minutes and then stored at -20^{o}C until immunoblotting.

2.2.7.4 Immunoblotting

Samples prepared as in section 2.7.1 and 2.7.2 were centrifuged for 5 seconds and loaded onto 3-8% Tris acetate gels (Novex pre-cast gels, Invitrogen, UK), using the XCell SureLock™ Mini-Cell module (Invitrogen, UK) with NuPAGE tri-acetate SDS running buffer (60.5g Tris Base, 89.5 Tricine, 10.0g SDS and distilled water added to a volume of 1 litre were used to make a 20 times stock) in order to separate proteins at 150V, at room temperature. Proteins smaller than 40kDa were separated on 4-12% Bis-Tris gels (Novex pre-cast gels, Invitrogen, UK) using the same module as above but with MES running buffer (97.6g MES, 60.6g Tris Base, 10g SDS, 3g EDTA and distilled water added to a volume of 500ml was used to make a 20 times stock). Kaleidoscope marker (Bio-Rad, UK) was used as a size marker.

Proteins were transferred electrophoretically (35 V at RT for 2.5 hours) onto activated immobilon P membranes (Sigma-Aldrich, UK) (membranes are activated by immersion in 100% MeOH for 30 seconds, followed by 2 minute in distilled water and 5 minutes in transblot buffer), using the XCell II Blot module (Invitrogen, UK) with transblot buffer (100ml of running buffer stock x10 (30.3g Tris Base, 144.1 Glycine and distilled water to 1 litre – pH 8.3), 200ml MetOH and distilled water to 2 litre). Unbound sites on membranes were subsequently blocked using blocking buffer: 5% BSA (Bovine Serum Albumin – Sigma-Aldrich, UK) in TBS with 0.1% Tween 20 for phosphorylated proteins. Proteins were probed using the appropriate antibody (see dilutions and preparation in Table 2.7). Finally, the primary antibody was probed with HRP-conjugated polyclonal antibodies (Mouse or Rabbit – 1/2000, cell signalling – see Table 2.7) for chemiluminescence detection (ECL system, Amersham Biosciences, UK, Millipore GeHealthcare). To this end, blots were dried and incubated 5 minute shaking vigorously with ECL reagents before covering them with cling film and exposing them to Kodak X-OMAT™LS film for various times (2 seconds to 1 hour).

For all experiments using total protein lysate, α-tubulin or calnexin were used as a loading control. However, for the nuclear and cytoplasmic separation, lamin was used for the nuclear fraction and calnexin for the cytoplasmic fraction.

Antibodies	Dilutions	Dilution buffer	Supplier
Anti-EGFR	1/1000	5% BSA	Cell Signaling
Anti-phospho EGFR Y845	1/1000	5% BSA	Cell Signaling
Anti-phospho EGFR y1068	1/1000	5% BSA	Cell Signaling
Anti-DNAPKcs	1/400	5% Milk	Abcam
Anti-Akt	1/1000	5% BSA	Cell Signaling
Anti-phospho Akt (S473)	1/1000	5% BSA	Cell signaling
Anti-MAPK (p42/44)	1/1000	5% BSA	Cell signaling
Anti-phosphoMAPK	1/1000	5% BSA	Cell signaling
Anti-Calnexin	1/1000	5% BSA	Cell Signaling
Anti-LaminA/C	1/1000	5% milk	Cell Signaling
Anti-Mouse (ab6728)	1/2000	5% milk	Cell Signaling
Anti-Rabbit (ab6721)	1/2000	5% milk	Cell Signaling

Table 2.7: List of antibody

2.2.8 Immunoprecipitation

Protein Sepharose G/A™ 4 Fast Flow (Amersham Biosciences, Sweden) beads were washed as follows: 1 ml of Protein Sepharose was added to 14 ml of sterile PBS into a 15 ml falcon. The sample was mixed and then centrifuged at 5000 rpm for 5 minutes in a cold centrifuge. The supernatant was discarded at the pelleted beads were cleaned twice as described above. The beads were then resupsended in PBS with a ratio 1:4.

Stably expressing NIH3T3 cell lines were plated at 2 X 10^5 /mL or 4 X 10^5/mL in a 10 cm dish (Nunc) and left overnight before treatment. Exponentially growing cells were then left in growing medium, or treated with 50µM cisplatin for one hour in serum free media and then left in drug free growing medium for 18 hours, or serum starved for 24-36 hours or serum starved for 24-36 hours and treated with EGF (Sigma) 100ng/ml or treated with 4 gy IR and left 20 minutes in serum free media. Following appropriate treatments, approximately 5x10^6 cells were lysed on ice in 500µl of CelLytic™M Cell lysis reagent (Sigma) supplemented with Protease and

Phospahatases inhibitor (Roche) and Benzonase (Merck) according to manufacturer's protocol. Following lysis, 1.5 mg of protein sample was incubated with 2µg of anti-EGFR antibody (clone R19/48 Invitrogen) and left rotating at 4 C for 2.5 hours. Then, 10 µl (1:4 PBS) of packed A Sepharose beads (Amersham) were added and the eppendorfs were left rotating for an additional 30 minutes. Immunocomplexes were pulled down from cleared lysates with the A sepharose beads and washed 1%Triton X-100 PBS. Pulse spin centrifugation, washing and mixing was repeated three times. Following the final wash the beads were drained by vacuum suction using a 25G x5/8'' needle (Terumo) and resuspended in sample buffer for Western blot analysis.

2.2.9 Densitometric Analysis

To compare the intensity of bands produced by immunoblotting the ImageJ densitometric analysis tool was used. Briefly, blots were scanned and bands of interest were selected. Intensity was measured by calculating the plotting area of each of individual bands. Background values and control values were then detracted to determine the fold increase. Fig illustrates the methodology

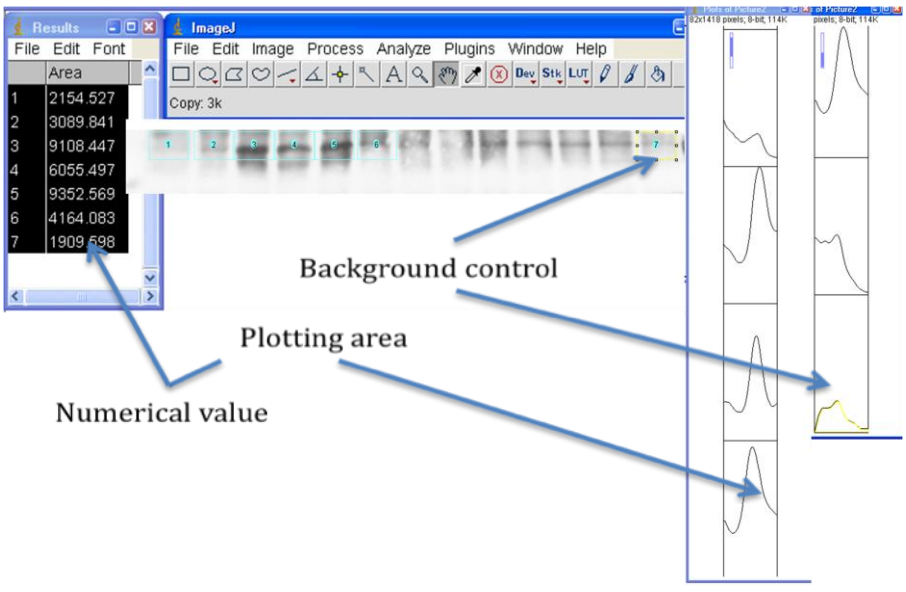

Figure 2.6: Densitometry programme

2.2.8 Cloning

2.2.8.1 Site directed mutagenesis

Primers were designed according to manufacturer protocol

Forward 5'cctcttcatggcagcggcccacatcgttgcgaaggccacgctggcggcgctgctgcagg3'

Reverse 5'cctgcagcagcgccgccagcgtggccttcgcaacgatgtgggccgctgccatgaagagg3'

Primers were designed to contain all the desired mutation flanked by 10-15 bases of correct sequence and SDS purified (MWG).

The melting temperature of the mutagenic primers was calculated according to the equation:

$$Tm= 81.5+0.41(\%GC)-675/N$$

$$=81.5+ 0.41(57)-675/22$$

$$=81.5+23.37-30.68=$$

$$= 75$$

Mutagenesis reaction:

5 µl of 10x reaction Buffer

X µl (5, 10, 20 or 50 ng) double stranded DNA template

X µl (125ng) Forward Primer

X µl (125ng) Reverse Primer

1 µl of dNTP mix

5 µl of QuikSolution

1 µl PfuUltra HF DNA polymerase (2.5U/ µl)

Cycles:

1	95 ^{o}C 2minutes	
	95 ^{o}C 1 minute	
2	60 ^{o}C 50 seconds	18 times
	68 ^{o}C 9 minutes	
3	68 ^{o}C 7 minutes	
4	4 ^{o}C 2 minutes or more	

Following the mutagenesis/ amplification, the reactions were incubated with 2 µl of DpnI (10U/µl) for 2 hours at 37 ^{o}C to digest the maternal strand. Reactions were then transformed using the XL10-Gold Ultracompetent Cells (Stratagene).

2.2.8.2 Plasmids transformation and amplification

In order to transform the plasmids into *E. coli*, 100µl of TOP10F chemically competent *E. coli* (Invitrogen, UK) was mixed with 5µl of plasmid and incubated for 15 minutes on ice. Cells were heat shocked for 90 seconds at 42^{o}C before incubation for 2 minutes on ice. 800µl of SOC medium was added and cells were pelleted for 6.5 minutes at 4,000rpm, at room temperature. Finally, 750µl of the supernatant was removed and the pellet was resuspended in the rest of the supernatant. Each transformed plasmid was plated on a pre-warmed LB (Luria-Bertani) agar plate (Invitrogen, UK), containing either 50µg/ml of ampicillin (Sigma-Aldrich, UK) or 30µg/ml of kanamycin (Sigma-Aldrich, UK) selective agent. Plates were incubated overnight at 37^{o}C. After selection, colonies were picked and grown overnight in 10ml of LB broth base (Lennox L Broth Base) medium (Invitrogen, UK) containing 50µg/ml of ampicillin (Sigma-Aldrich, UK) or 30µg/ml of kanamycin (Sigma-Aldrich, UK), in an incubator shaker (37^{o}C, 300rpm). Cells were harvested and plasmids were extracted using the QIAprep Spin Miniprep, Highspeed Maxiprep kit (Qiagen, UK) and quantified at 260nm using a NanoDrop® ND-1000 UV-Vis Spectrophotometer (NanoDrop, UK)

Following site directed mutagenesis plasmids were digested and ligated into a newly linearised backbone plasmid.

2.2.8.3 Plasmid digestion

After extraction, integrity and purity of the plasmids was checked. For the restriction reactions, 2µl of plasmid DNA was incubated with 0.5µl of the appropriate enzyme (see Table 2.8), 1.5µl of the corresponding 10x buffer (supplied with the enzyme), 1µl of 30.3mg/ml RNAseA (Sigma-Aldrich, UK) and distilled water to 15µl. Reactions were incubated for 2 hours at 37 ^{o}C and run on a 1% agarose ethidium bromide gel. The gel was electrophoresed at 100V and photographed using a dual intensity ultraviolet transilluminator coupled with camera (UVP, UK). A 1Kb DNA ladder was used to determine the size of each fragment obtained. Bands were excised and purified using the gel extraction kit from Qiagen according to manufacturer protocol.

The expected sizes were as follow: EGFR ~ 4.0Kb; pcDNA3 ~ 5.4Kb; pUSEamp ~ 5.4Kb; NLS123~ 4.0Kb; L858R ~ 4.0Kb; LNLS123 ~ 4.0Kb; M1 ~ 3.9Kb; M12~ 3.9Kb; ΔNLS ~ 3.9Kb; KMT ~ 3.9Kb, EGFRvIII ~ 3.1Kb

Plasmid	Enzyme	Supplier
wtEGFR	EcorV and XhoI	Roche
NLS123	EcorV and XhoI	Roche
L858R	EcorV and XhoI	Roche
LNLS123	EcorV and XhoI	Roche
pUSEamp	EcorV and XhoI	Roche
pcDNA3	XhoI and XbaI	Roche
M1	XhoI and XbaI	Roche
M12	XhoI and XbaI	Roche
ΔNLS	XhoI and XbaI	Roche
KMT	XhoI and XbaI	Roche
EGFRvIII	XbaI and HindIII	Roche

Table 2.8: List of enzymes used for plasmids restriction. Enzymes were chosen according to the position of the insert on the plasmid.

2.2.8.4 Ligation

Excised and purified bands were quantified at 260 nm using the nanodrop.

Ligation was carried out by using the DNA ligation Kit Ver 2.1 (Takara).

30-50 ng of linearised Vector were used per reaction. The correct amount of the insert was calculated by the equation:

(ng Vector x Kb Insert)/Kb Vector=ng Vector

This correspond to the ng of the insert necessary for a 1:1 ratio (Vector:Insert). In order to maximise the chances of successfulness Ligation reactions were always prepared using a 1:3, 1:5 and 1:8 ratio (Vector:Insert).

To the Vector:Insert initial mix was then added the correspondent volume of Solution I from the DNA ligation kit. The reaction was incubated at 16 ^{o}C for 30 minutes. Prior to transformation, 1 µl of Solution III was added to 9µl of ligation reaction to increase the number of transformants. When the initial ligation reaction over-exceeded 10 µl, ligated DNA was precipitated with ethanol and dissolved in a volume of 10 µl TE Buffer.

2.2.8.5 Colonies screening

Bacterial colonies were screened by PCR using EGFR screening primers.

Briefly, PCR reaction was prepared according to the Promega GOtaq protocol. Individual colonies were picked and gently submerged into individual tubes containing a single reaction mix to provide sufficient template DNA for PCR. The same colony was then incubated in a 1.5 ml Eppendorf (labelled accordingly) containing LB media at 37 ^{o}C over the period of the PCR amplification and gel electrophoresis. Positive colonies were then further incubated overnight at 37 ^{o}C by pouring the content of the Eppendorf in 250 ml of LB media.

2.2.8.6 Sequencing

Samples were sent for sequencing to MWG Company (Germany)

2.2.8.7 Plasmids transfection

Transfection was achieved using GeneJuice® transfection reagent (Novagen® EMD Biosciences Darmstadt, Germany). Exponentially growing NIH3T3 cells were plated in 6 well plates (Nunclon™, VWR, UK) at a concentration of 1 x10^5cells/ml (1.5 ml per well), without any antibiotics and incubated for 24 hours at 37^{o}C (5% CO_2). 3μl was vortexed with 100μl of DMEM FCS free and incubated for 5 minutes in an eppendorf. 1μg of plasmid was added to the solution and incubated at room temperature for 15 minutes. Media from the plates was removed and replaced by fresh complete media with no antibiotics. Each plasmid/GeneJuice mixture was added dropwise to one well. Cells were incubated at 37^{o}C (5% CO_2) until confluence. Cells were subsequently trypsinised (0.5ml of trypsin) and pelleted before being plated in T25 flasks with media containing antibiotics and selective agent G418 (Sigma-Aldrich, UK). Transfected cells were incubated for 3 to 4 weeks to allow clones to grow (media was regularly changed to keep selective pressure). All the clones used were grown as stable transfected cell lines, maintaining selective pressure in the media.

2.2.9 Confocal Microscopy

2.2.9.1 Immunofluorescence Staining

2 X 10^4 Stable and transfected NIH3T3 were plated on 13mm cover glass (VWR) in a 24 well plate overnight before treatment. Cells were then treated with 50μM cisplatin for one hour in serum free media and/or left growing in drug free growing medium; serum starved for 24-36 hours or/and then treated with 4 Gy IR.18 hours following the treatment with cisplatin and 20 minutes following the IR treatment cells were washed twice in ice cold PBS followed by fixing with 4% PFA for 15 minutes at room at RT. Cells were then permeabilised with PBS containing 0.5% Triton X-100 for 10 minutes washed 3X with PBS and blocked in PBS 5% BSA (Sigma) for 1 hour at room temperature. Respective primary antibodies were added as follows: anti-rabbit EGFR (1:50, clone 15F8 cell signaling) and anti-mouse DNAPKcs (1:50 AbCam) in PBS 1% BSA and incubated in a humid chamber at 4ºC overnight. Slides were then washed 3X with PBS 0.1% Triton X-100 for 10 minutes and protein expression was visualized by incubating the cells with corresponding secondary fluorescent conjugated Abs, as follows: 1:100 Alexa Fluor 647 goat anti-rabbit and 1:100 Alexa Fluor 488 goat anti-mouse (Molecular probes and Invitrogen Life Technologies) for 2 hours at RT. Fluorescent label- antibodies were added alone as negative controls. Following 3 washes with PBS 0.1% Triton X-100 Nuclei were stained using Dapi (Sigma) and mounted onto glass slides with fluorescent mounting medium (Dako). Cells were then visualised by confocal microscopy (objective X40, Leica TCS SP2). Nuclear slices images were acquired by sequential scanning using the LAS AF Lite programme.

2.2.9.2 Proximity Ligation assay

Stables NIH3T3 grown on 13 mm cover glass (VWR) were left in growing medium, or treated with 50μM cisplatin for one hour in serum free media and then left in drug free growing medium for 18 hours, or serum starved for 24-36 hours, or serum starved for 24-36 hours and treated with 4 gy IR and left 20 minutes in serum free media. Cells were washed with chilled PBS and fixed with 4% paraformaldehyde for 15 min, blocked, permeabilized, and incubated overnight with anti-rabbit EGFR (clone 15F8 cell signalling 1:50), anti-mouse DNAPKcs (AbCam 1:50) as described above. Cells were then incubated with secondary antibodies conjugated with

oligonucleotides (PLA probe minus: anti-mouse and plus: anti-rabbit) for 90 minutes at 37°C in a humidity chamber. Following 2 washes for 5 minutes with 1X PBS 0.1% Triton X-100, the hybridization solution, consisting of two oligonucleotides, was diluted in high purity water (1:5) and added to the cells for 15 minutes at 37°C. Cells were then washed once for 3 minutes to remove the hybridization solution. Next, the ligation solution was diluted in high purity water (1:5) and 1.5 μl of ligase to a final volume of 60 μl (per cover glass). The ligation reaction was then added to the cells for 15 minutes at 37°C. Following 2 washes for 2 minutes, the amplification solution was diluted in high purity water (1:5) and 0.75 μl of polymerase to a final volume of 60 μl per cover glass. The slides were then incubated for 90 minutes at 37°C. Next the cells were washed 2 times for 3 minutes and the detection solution was diluted in hi purity water (1:5) and added to the cells for 60 minutes at 37°C. Finally cells were washed 2 times with 1X PBS 0.1% Triton X-100 for 2 minutes, 1 time with 0.5 X PBS 0.05% Triton X-100 for 2 minutes, 2 time with high purity water for 2 minutes and 1 time with 70% ETOH for 1 minutes. The slides were left to dry for 3 minutes at RT and then mounted onto a glass slide with fluorescent medium (Dako). Cy3 signal amplification was utilised for the assay. Cells were then examined with a confocal microscope (objective X40, Leica TCS SP2).

2.2.10 DNA-PK Functional Assay

DNA-PK activity was detected using the Promega SignaTECT DNA-PK assay system, according to the manufacturer's protocol. The SignaTECT utilises the unique SAM^{2TM} Biotin Capture Membrane and results in high density of streptadavidin on the membrane matrix. This provides rapid, quantitative capture of biotinylated substrate molecules, based on the strong affinity of biotin for streptadavidin (Kd=10-15M). This system overcomes the problem of non-specific substrate binding by using a biotinylated DNA-PK p53 derived peptide substrate. The high binding capacity of the SAM^{2TM} Biotin capture membrane for the DNA-PK biotinylated peptide substrate and the low background observed with this system, maximises the signal-to-noise ratio. Briefly, 50μg of Benzonase treated whole-cell extract, was incubated with DNA-PK, biotinylated peptide substrate, [γ-32P] ATP, and either DNA-PK activation buffer or DNA-PK control buffer for 5 minutes at 30 ºC. Termination

buffer was added, and 10 µl of each reaction sample were spotted onto a SAM^{2TM} biotin capture membrane. The SAM2TM membrane squares were washed and dried before analysis by scintillation counting. The enzymatic activity of DNA-PK was expressed as a percentage decrease of control DNA-PK activity.

CHAPTER 3

CHARACTERISATION OF THE EGFR NLS MUTANTS

3.1 INTRODUCTION

3.1.1 EGFR endocytosis is required for receptor degradation, recycling and nuclear translocation

In resting cells the epidermal growth factor receptor (EGFR) resides at the lipid rafts of the cell membrane rich in cavoelae and cholesterol (Zwang & Yarden, 2009). Upon ligand binding EGFR exits these domains in a Src-dependent manner and releases the auto-inhibition of its catalytic function via homo or hetero-dimerisation with members of the ERBB family (Sorkin & Goh, 2008; Wang et al, 1999). The dimerised receptors trans-phosphorylate a plethora of effector molecules including MAPK and AKT (Grandal & Madshus, 2008; Puri et al, 2005). Following the stimulation of these intracellular signalling pathways EGFR is bound by the SH2 domain of Cbl leading to EGFR polyubiquitination and internalisation in the early endosomes (Mosesson et al, 2008; Tvorogov & Carpenter, 2002). The receptor endocytosis takes place through the formation of clathrin-coated pits (CCPs) or, in the presence of high doses of ligand, via cavoelae (Sigismund et al, 2005; Sorkin & Goh, 2008). Clathrin-mediated endocytosis (CME) is the major receptor internalisation pathway (Sigismund et al, 2008; Zwang & Yarden, 2009). Membrane receptors can spend limteless time at the membrane, however following activation, they will be internalised within seconds to assure immediate inactivation of the downstream signalling events (Mosesson et al, 2008; Oved & Yarden, 2002).

3.1.1.1 EGFR phosphorylation mediates nuclear translocation

Internalised EGFR can undertake three different routes: 1) recycling to the membrane in an inactive form, 2) lysosomal degradation into the late endosomes or 3) nuclear translocation (Mosesson et al, 2008; Waterman & Yarden, 2001). The decision is made according to the expression level and the activation status (Zwang & Yarden, 2009). EGFR high expression saturates the degradation machinery leading to the recycling of the receptor at the transmembrane. In addition, internalised active EGFR represents a very poor substrate for lysosomal degradation inducing EGFR sorting into the Golgi and ER leading to nuclear translocation (Liao & Carpenter, 2007). A large body of evidence has shown that EGFR, either alone or

associated to ERBB2, can be further phosphorylated once internalised into the early endosomes (Mosesson et al, 2008). This is suggested to prevent degradation and contribute further to nuclear translocation. Following sorting through the Golgi and ER, EGFR association with sec61 results in a retro-translocation to the cytosol where EGFR is stabilised following association with HSP70. Binding of importin β, mediated through the NLS sequence, translocates the receptor to the nucleus (Dittmann et al, 2008a; Hsu & Hung, 2007; Liao & Carpenter, 2007; Lo et al, 2006a).

3.1.2 EGFR NLS sequence is a functional NLS sequence

Nuclear translocation requires energy, physiological temperature, a NLS and a soluble transporter. The study of this very complex mechanism has revealed that the last two components are known to be the "conditio sine qua non" for nuclear translocation. The import takes place following three important steps: docking at the nuclear pore complex, translocation and deposition. During the docking phase the molecule that needs to be imported (the cargo molecule) binds to a soluble molecule known as importin via the recognition of the NLS sequence. Therefore in absence of one of these two components nuclear localisation is impaired.

3.1.2.1 The criteria for a functional NLS

The recognition of a NLS sequence via a bioinformatic approach is only valuable for predicting putative NLS motifs. The functionality of a NLS sequence in any protein is determined by four criteria:

1. The putative NLS sequence must be necessary for import. The transport of the cargo protein into the nucleus is therefore hindered when the sequence is deleted or altered. The most common approach to verify whether a sequence is necessary for import is to mutate the consensus residues (basic amino acids – R/K) into Alanine and verify that the nuclear translocation of the protein decreases (Hsu & Hung, 2007).
2. The sequence must be sufficient to target an unrelated protein into the nucleus. Usually this is demonstrated by fusing the putative NLS sequence to the N-terminus of the Green Fluorescent Protein (GFP) and the location of the protein is assessed visually (Hsu & Hung, 2007).

3. The protein of interest (containing the NLS) must interact with the import receptor (importins) and the interaction must be mediated via the putative NLS sequence. This is addressed by performing an *in vitro* binding experiment with the purified proteins and with RanGDP and RanGTP that, as explained in the introduction chapter, provide the energy for association and dissociation (Liao & Carpenter, 2007; Lo et al, 2006a; Lo et al, 2006b).
4. The transport machinery must be disabled to show that nuclear import of the protein of interest is mediated by a nuclear transport mechanism that can only take place via the NLS sequence (Liao & Carpenter, 2007; Lo et al, 2006a).

Table 3.1 describes the criteria met by EGFR.

Criterion	Experimental design	Research Article	Outcome
NLS mutation reduces nuclear translocation	EGFR-NLS mutants: M1: AAAHIVRKRTLRR M12: AAAHIVAAATLRR M123:RRRHIVRKRTLAA	Hsu SC. *et al.* J Biol Chem. 2007	Criterion Met
Targeting unrelated protein to the nucleus	GFP-(EGFR)NLS	Hsu SC. *et al.* J Biol Chem. 2007	Criterion Met
NLS protein must interact with importin molecule	EGFR-Importin α and Importin β interaction EGFR-sec61 interaction	Lo HW . *et al.* J Cell Biochem. 2006 Lo HW *et al.* BJC 2006 Liao HJ *et al.* Mol Biol Cell 2007	Criterion Met
Disabling transport machinery leads to inhibition of protein nuclear translocation	Importin α /β SiRNA Sec61 SiRNA RanGDP blockage	Lo HW . *et al.* J Cell Biochem. 2006 Liao HJ *et al.* Mol Biol Cell 2007	Criterion Met

Table 3.1: Experimental evidence for nuclear EGFR. The table shows individual criterion, the experimental design utilised to validate the criterion requirement and the published research article where the evidence is shown.

3.1.3 The NLS sequence affinity for the importin molecule is highly regulated

The NLS sequence is pivotal during the entire nuclear translocation mechanism because it is the only known biological signature that can successfully obtain binding with importin molecules and its success is dictated by the affinity of the NLS sequence with the importin molecule. In many cases such affinity is further

positively or negatively regulated via phosphorylation and/or via intramolecular association (Moroianu, 1999). For example, phosphorylation of the serine residue contained in the NLS of the transcription factor Pho4 reduces affinity with the importin molecule (Kaffman & O'Shea, 1999). Unphosphorylated pho4 localises to the nucleus whereas phosphorylation lowers affinity with its importin molecule triggering nuclear export and impeding re-import. Another example is the transcription factor NF-AT. Unphosphorylated NF-AT localises to the nucleus and when phosphorylated undergoes a conformational change that masks its NLS, impeding binding with the importin molecule (Zaidi et al, 2004) SWI5 is phosphorylated on three Serines, two of which lie in proximity of its NLS. Unphosphorylated SWI5 is nuclear localised whereas when phosphorylated the transcription factor is restrained in the cytoplasm (Kaffman & O'Shea, 1999; Wells & Marti, 2002). From this last study it was suggested that phosphorylation of the sites in the vicinity of the basic NLS prevents binding of the import machinery and therefore cytoplasmic localisation.

3.1.4 EGFR NLS sequence mutation

The principal aim of this study is to investigate the role of EGFR nuclear translocation in the modulation of DNA repair. In the introduction chapter the role of the EGFR acquired mutations in therapy and their importance in predicting sensitivity have been outlined. The EGFR NLS sequence is a tripartite sequence made up of three clusters of basic amino acid residues RRRHIVRKRTLRR and published data have demonstrated that mutation of the first two clusters of basic amino acids into Alanines leads to a 78% decrease in nuclear EGFR following ligand binding (Hsu & Hung, 2007). There is no published evidence investigating whether the remaining 22% of nuclear EGFR is sufficient to mediate the transcriptional-mediated EGFR nuclear function. In addition, there is no published study investigating the nuclear translocation of EGFR NLS mutants following IR (the second most studied inducer of EGFR nuclear translocation (Das et al, 2007; Dittmann et al, 2005a). For these reasons wtEGFR and EGFR L858R (L858R) mutant expressing plasmids were utilised as a background to construct two NLS-EGFR mutants bearing a mutation of all the Arginine residues into Alanine (RRRHIVRKRTLRR into AAAHIVAKATLAA): EGFRNLS123 (NLS123) and L858RNLS123 (LNLS123).

3.1.5 NIH3T3 cells as a cellular model

Stable transfection of the human EGFR into the murine fibroblast NIH3T3 cells and EGF supplementation into the growth medium were shown to be necessary and sufficient to achieve cellular transformation of this cell line (Di Fiore et al, 1987), making this system an unbiased and optimal cellular model to study the modulation of EGFR on DNA damage repair.

3.1.6 CHAPTER AIMS:

- Validation of the NIH3T3 cellular system
    - wtEGFR and L858R expression following transient transfection
- Validation of the constructed mutants
    - Sequence analysis and restriction digest to prove site directed mutagenesis
- Characterisation of the expressing EGFR constructs
    - Phosphorylation of wtEGFR and mutants following ligand binding, IR or chemotherapy
    - Activation of downstream signalling pathways following ligand induction
    - Nuclear localisation following EGF or IR stimulation

3.2 RESULTS

3.2.1 EGFR expression in NIH3T3 (EGFR null) cells

Following transient transfection of NIH3T3 cells, wtEGFR and L858R expression was confirmed via western blotting analysis over a period of 72 hours. This was necessary to determine the maximal expression of the EGFR constructs in the NIH3T3 cells. Fig 3.1 shows that EGFR expression peaks at 48 hours following transient transfection while no expression was detected in the vector control (VC) transfected cell line (Fig 3.1).

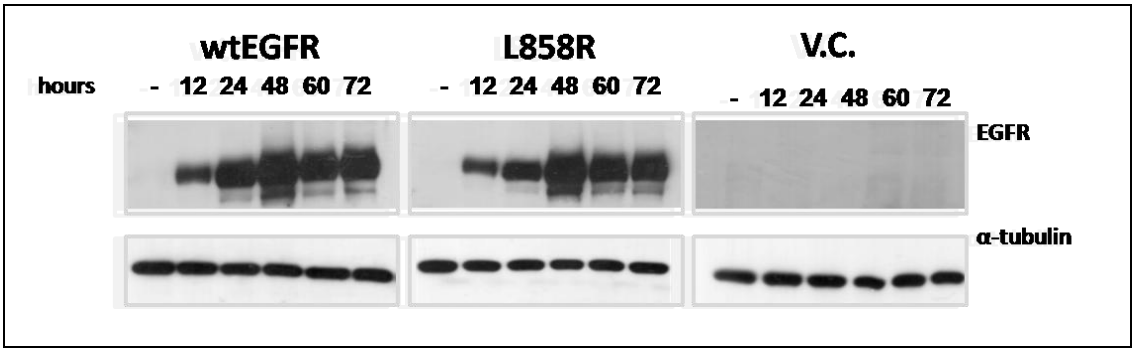

Figure 3.1: EGFR expression peak at 48 hours following plasmid transfection. NIH3T3 cells were transiently transfected with 2 μg of plasmid DNA encoding for wtEGFR or L858R or with the backbone plasmid (V.C.). Cells were seeded and lysed over a period of 72 hours. Whole cell lysates were resolved on a denaturing gel and blotted for total EGFR and α-tubulin.

3.2.2 EGFR NLS site directed mutagenesis

To examine the modulation of EGFR nuclear translocation, NLS sequence mutants (NLS123, LNLS123) were generated as described in the Materials and Methods section. The expected mutagenesis was validated via enzymatic digestion of the obtained plasmids and by sequencing. Fig 3.2A shows the result of the EcoRV-XhoI double digestion and of the EcoRI single digestion whereas Fig 3.2B and C show the nucleotide and amino acid alignment of the obtained sequences. The mutated constructs were sequenced three times to confirm correct mutagenesis and absence of any other mutation in the remaining DNA sequence.

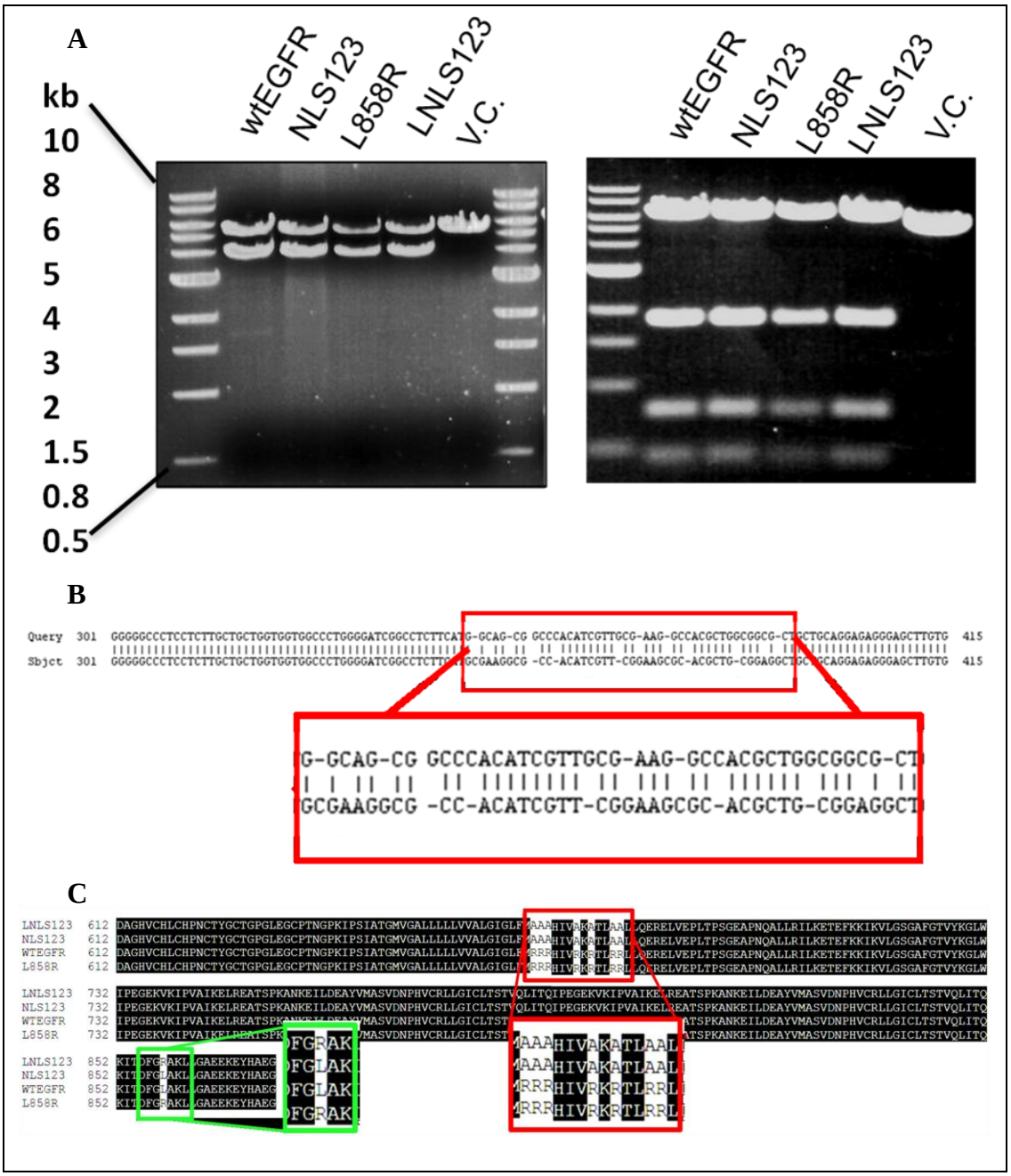

Figure 3.2: Enzymatic digestion and sequencing confirmed the NLS mutagenesis. A) In the left panel 2µg of plasmid DNA was digested with EcorV-XhoI to generate the expected fragments of 3.994 KB (EGFR cDNA) and 5.426 KB (pUSEamp) and with EcorI to generate the expected fragments of 0.02, 0.5, 0.8, 1.8 and 6.3 KB (right panel). Digested DNA was then resolved on a 1% Agarose gel and samples were visualised using a UV transilluminator. **B)** NLS123 nucleotide sequence obtained by MWG sequencing service was blasted against the Human genome database. The Fig represents a snapshot from the whole sequence alignment. **C)** The cDNA sequences obtained by the MWG sequencing service were translated into an amino acids sequence using the Expasy tool and then were aligned using the clustalW 2.0.5 multiple sequence alignment**.** The alignment file was then processed with BOXSHADE 3.21. The Fig represents a snapshot from the whole sequence alignment.

3.2.3 Mutant characterisation

3.2.3.1 EGF stimulation induces EGFR activation

The activation of EGFR upon ligand binding has been fully described in the introduction chapter. Being the EGFR specific ligand, EGF has a strong and immediate effect on EGFR dimerisation and phosphorylation. EGF is known to promote kinase autophosphorylation leading to the activation of many important cellular responses (Oved & Yarden, 2002; Toulany et al, 2007; Tvorogov & Carpenter, 2002). Physiological EGF levels typically range from 10 to 100 ng/ml (Sigismund et al, 2005) and in fact as little as 10 ng/ml can activate EGFR within minutes. It has been shown that 100 ng/ml of EGF is the dose necessary to induce EGFR nuclear translocation (Hsu & Hung, 2007). Therefore the effects of this dose on the tyrosine phosphorylation over a period of 1 hour were investigated and the activation of the downstream MAPK and AKT pathways and the timing of the nuclear translocation examined. This is necessary to elucidate the correlation of these events and the significance of their timing.

Fig 3.3A shows the western blots of NIH3T3 cells transiently transfected with wtEGFR, NLS123, L858R, LNLS123 or VC treated with 100 ng EGF over a period of 1 hour. This illustrates EGF-dependent EGFR phosphorylation and activation of MAPK and AKT downstream signalling pathways. Fig 3.3 B-D show the fold increase of Y1068 (B), AKT (C) and MAPK (D) activation.

Cells transfected with wtEGFR showed a time dependent Y1068 phosphorylation increasing 3.13-fold by 30 minutes, remaining at this level at 60 minutes. Similarly, phosphorylation of both AKT and MAPK increased 3.20 and 2.06-fold by 60 minutes. L858R transfected cells showed constitutive receptor activation and MAPK phosphorylation. In contrast, there was a 2.2-fold increase in AKT phosphorylation by 60 minutes. NLS123 transfected cells showed lack of Y1068 phosphorylation and no upregulation of either AKT or MAPK. LNLS123 expressing cells showed constitutive receptor activation, however this was reduced compared to Y1068 phosphorylation shown in wtEGFR cells. LNLS123 cells showed no upregulation of either AKT or MAPK.

In light of the lack of EGFR-Y1068 phosphorylation in the NLS123 transfected cells following EGF induction, the overall receptor phosphorylation was assessed together with the ligand dependent and independent phosphorylation in wtEGFR and EGFR mutant-expressing cell lines. Fig 3.4 shows the western blots of cells transfected with

wtEGFR, NLS123, L858R, LNLS123 or VC, treated with 100 ng/ml of EGF for 1 hour following serum starvation. The obtained cell lysates were then immunoprecipitated with anti-EGFR and total receptor phosphorylation was determined by blotting with a pan phospho-tyrosine PY99 antibody (Fig 3.4). EGF-induced activation was observed in wtEGFR transfected cells, constitutive activation in both L858R and LNLS123 transfected cells and lack of activation in the NLS123 transfected cells.

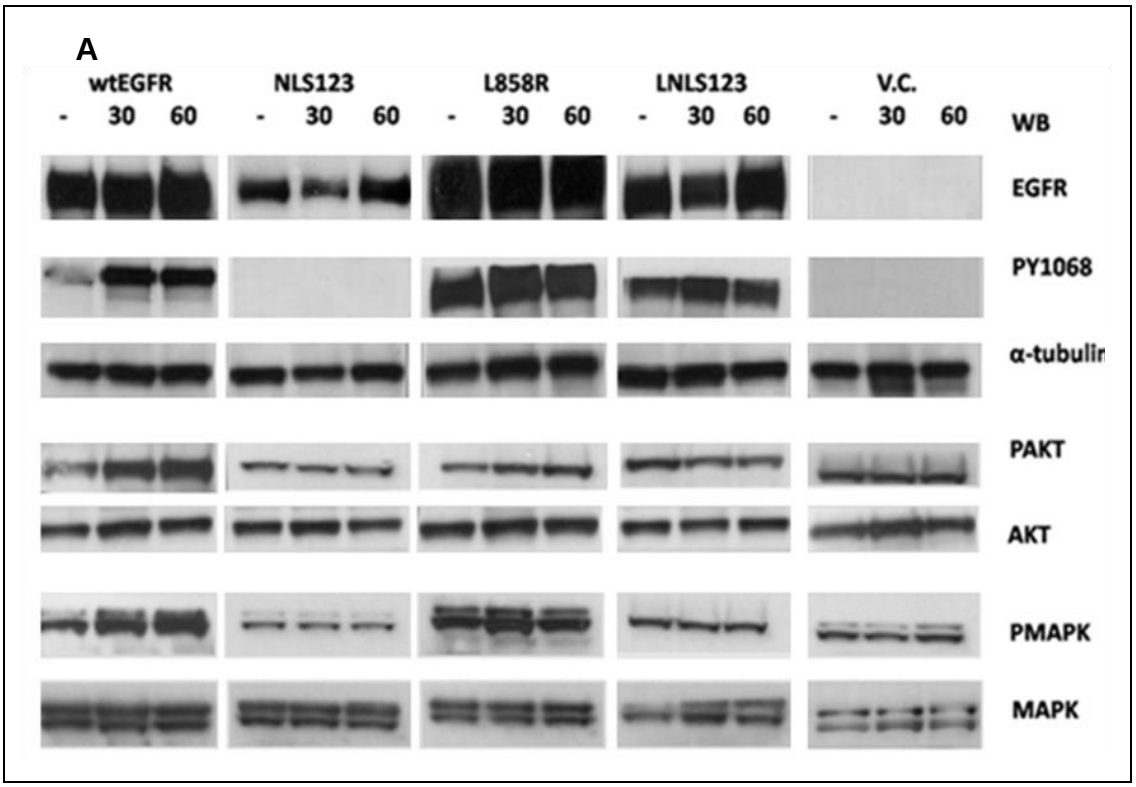

Figure 3.3 (A): EGF induces EGFR and downstream signalling activation in EGFR transfected cells. NIH3T3 cells where transfected with wtEGFR, NLS123, L858R, LNLS123 or VC 48 hours following transfection the cells were serum starved for 24 hours and then treated with EGF 100 ng/ml. Cells were collected over a period of 1 hour and 40μg of protein lysate was analysed via western blot. Samples were immunoblotted using anti EGFR, anti PY1068, anti PAKT (ser473), anti α-tubulin, anti AKT, anti PMAPK (p42-p44) and anti MAPK antibodies.

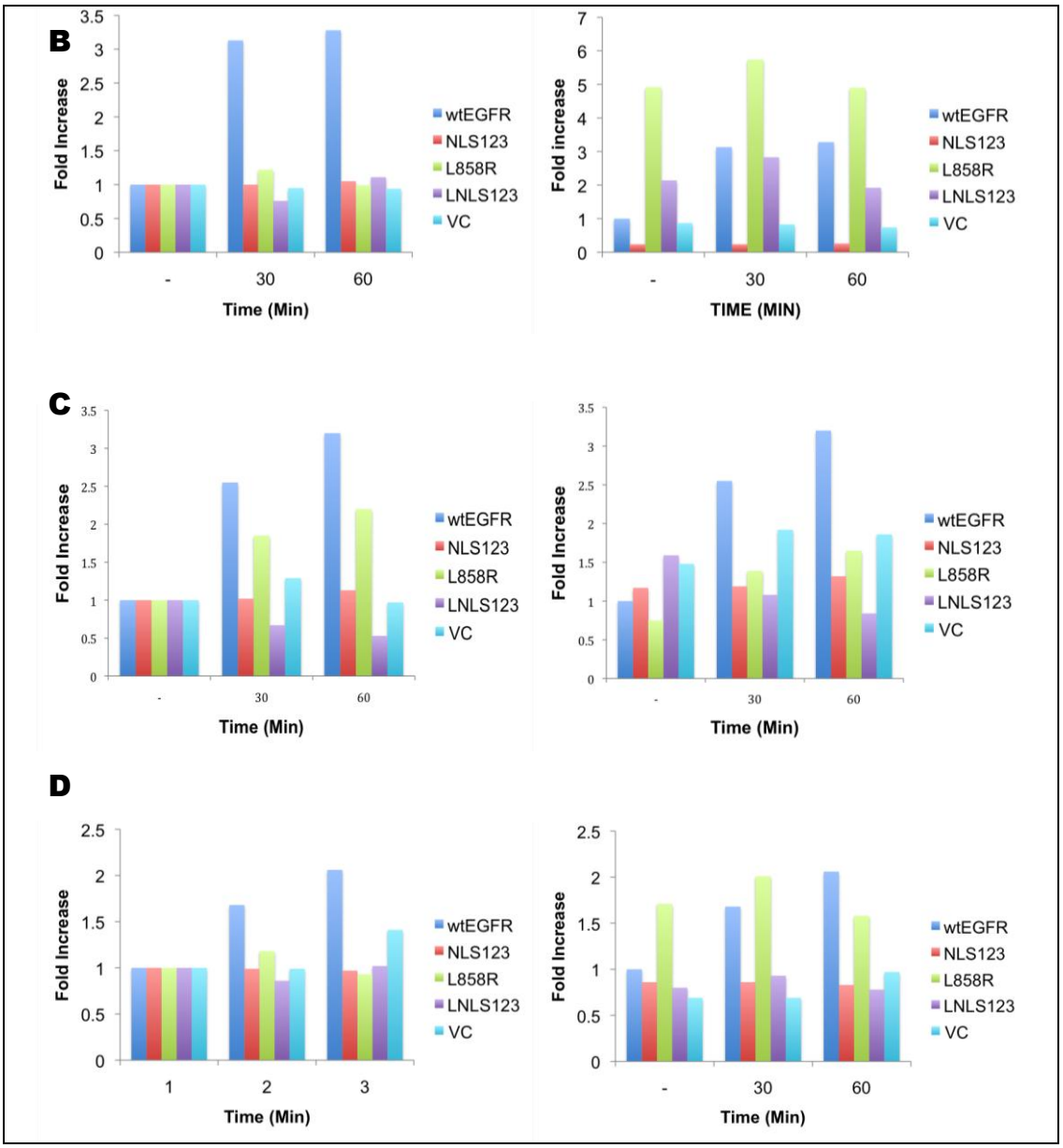

Figure 3.3 (B-D): Graphic representation of the densitometry analysis of Figure 3.4 A blots. In each lane, left graphs show the fold increase compared to their individual negative control (EGF untreated – serum starved) and right graphs show the comparison when densitometry was done compared to the untreated wtEGFR sample. In order the graphs show: the fold increase of Y1068 phosphorylation (B), AKT phosphorylation (C) and MAPK phosphorylation (D).

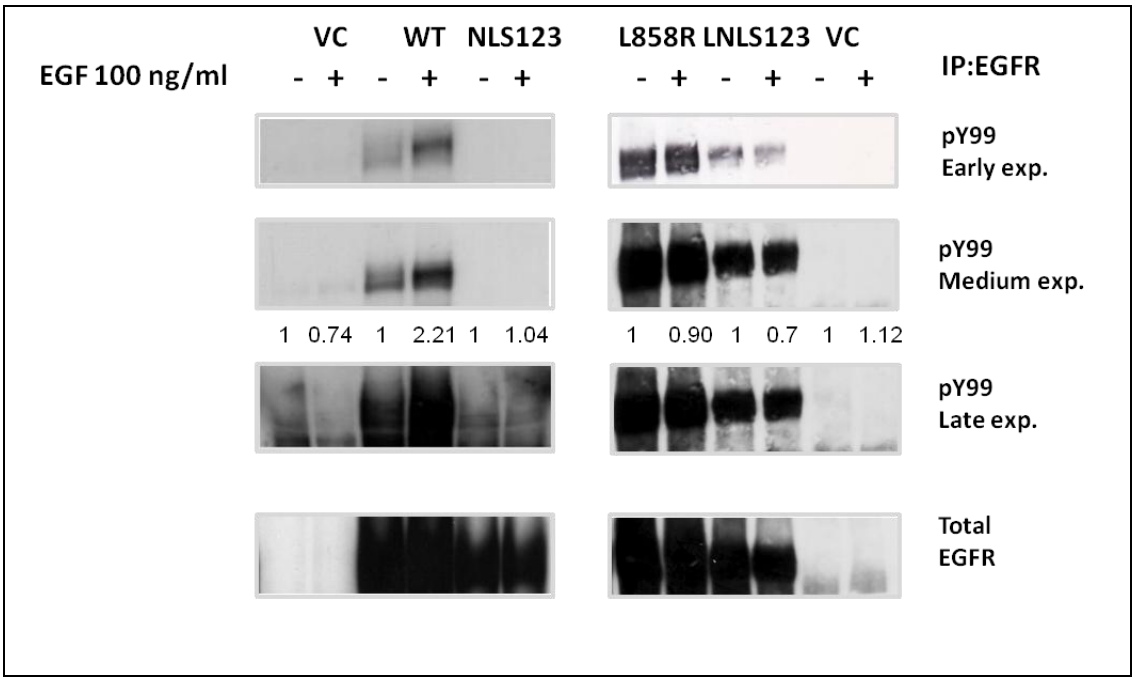

Figure 3.4: EGF treatment does not activate the EGF receptor bearing the NLS123 mutation. 60 minutes following EGF treatment 500 µg of protein lysate was used to immunoprecipitate EGFR. Samples were then analysed via western blot and immunoblotted with PY99 and for total EGFR. + indicates treated sample – indicates non-treated sample. Numbers represent fold increase calculated as a mean density of the first two exposures.

3.2.3.2 Dose-dependent cisplatin activation of EGFR

To extend our knowledge of the nature of the NLS123 mutation and its impact on the receptor phosphorylation, this study investigated the receptor activation in transiently transfected cells treated with different doses of cisplatin (Fig 3.5). This is because cisplatin has been shown to induce ligand-independent EGFR phosphorylation on the Y845 residue (Benhar et al, 2002). Since both the L858R and LNLS123 mutant receptor have shown that EGF treatment induced EGFR activation, this assay was performed only on the wtEGFR and the NLS123.

Fig 3.5 shows the western blot results of cells transfected with wtEGFR and NLS123. Following 48 hours transfection, cells were treated for one hour with cisplatin with a dose range of 10-150 µM in serum-free media. Cell lysates were then blotted with PY845 antibody that recognises ligand-independent kinase domain activation. In wtEGFR transfected cells, phosphorylation increased in a dose dependent manner peaking at 50µM cisplatin, whereas NLS123 cells showed no Y845 phosphorylation.

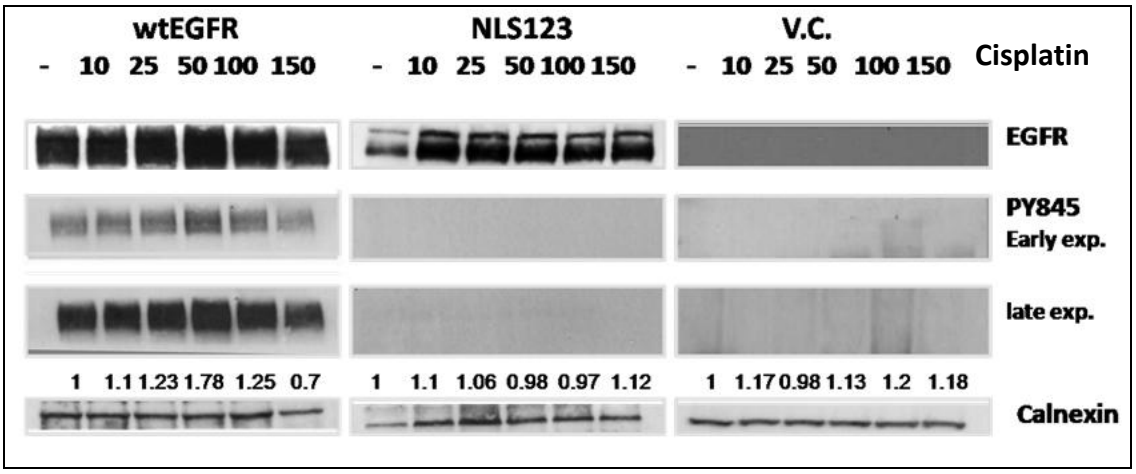

Figure 3.5: EGFR activation following cisplatin treatment. NIH3T3 cells were transfected with wtEGFR NLS123 and V.C. 48 hours following transfection cells were treated with 10, 25, 50, 100, 150 µM of cisplatin in free serum media for one hour. Cells were collected one hour following treatment and whole protein lysate was extracted. 50 µg of the protein lysate was loaded on a denaturing SDS gel and analysed via western blotting. Samples were blotted against anti EGFR, anti pY845 anti calnexin. Numbers represent mean fold increase of the PY845 density exposures compared to untreated control.

3.2.3.2.1 EGFR activation following cisplatin treatment

The lack of Y845 activation, observed in cells transfected with NLS123 following cisplatin treatment induced us to test a wider range of phosphorylation events. Since cisplatin stimulates EGFR autophosphorylation and ligand independent phosphorylation of the receptor (Benhar et al, 2002), wtEGFR and NLS123 transfected cells were treated with 50µM cisplatin for one hour in serum-free media. Cell lysates were then immunoprecipitated with anti-EGFR and blotted with the pan phosphotyrosine PY99 antibody to detect the presence of any phosphorylation event following cisplatin. Fig 3.6 shows the results of the immunoprecipitation. While cells transfected with wtEGFR showed some increased phosphorylation following cisplatin treatment (visible in the early exposure of the blot), NLS123 transfected cells showed no phosphorylation event following cisplatin as shown by the very late exposure of the blot.

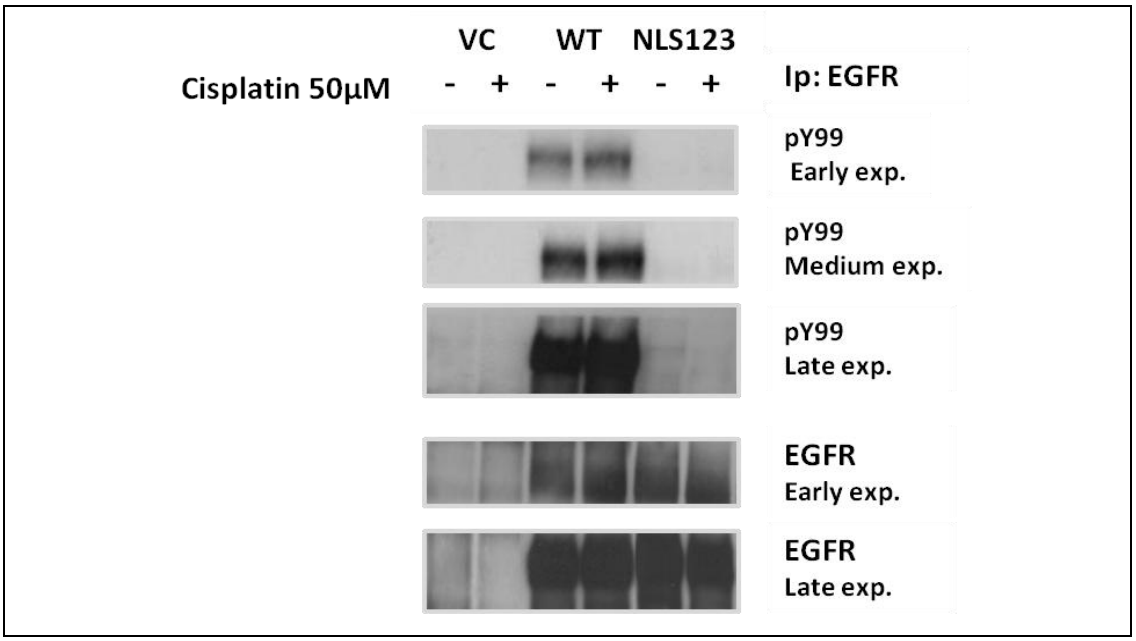

Figure 3.6: Cisplatin treatment does not activate the EGF receptor bearing the NLS123 mutation. wtEGFR, NLS123, or VC transfected NIH3T3 cells were treated with 50 µM cisplatin in serum free media, 48 hours after transfection. Cells were seeded 60 minutes following cisplatin treatment and 500 µg of the protein lysate was used to immunoprecipitate EGFR. Immunoprecipitated samples were then analysed via western blot and immunoblotted with anti PY99 or anti EGFR. + indicates treated sample – indicates non treated sample.

3.2.4 EGFR nuclear translocation is induced by ligand stimulation and by IR treatment

Several reports have shown that EGF induction or IR treatment induce EGFR nuclear translocation (Dittmann et al; Dittmann et al, 2005a; Dittmann et al, 2008a; Dittmann et al; Hsu & Hung, 2007; Lo et al, 2006a). 100 ng/ml is the EGF dose shown to induce nuclear translocation in CHO cells transfected with wtEGFR (Hsu & Hung, 2007). However, reports suggest that the EGF concentration is not strictly the determining factor for EGFR translocation (Liao & Carpenter, 2009). In a cancer cell the overexpression of EGFR is often accompanied by the autocrine production of several ligands such as EGF. Therefore 100 ng/ml is the concentration of EGF that can mostly mimic this and show the response of an EGFR over-expressing cell line (Gazdar & Minna, 2008; Zandi et al, 2007). Published evidence has also shown that 4 Gy is the IR dose sufficient to induce EGFR nuclear translocation in some of the most widely characterised EGFR over-expressing cancer cell lines including A431 and A549 (Rodemann et al, 2007). In this study the same dose has been utilised to

test wtEGFR nuclear translocation within the NIH3T3 cells and determine whether the NLS123 mutation impairs EGFR nuclear translocation.

3.2.4.1 EGF induction of EGFR nuclear translocation

NIH3T3 cells transfected with wtEGFR, NLS123, L858R and LNLS123 were used in this study. Cells were serum starved for 24 hours and then 100 ng/ml of EGF was added to the serum-free medium. Cells were then fixed with 4% PFA, 30 and 60 minutes following addition of EGF and then probed using anti-rabbit EGFR and stained using DAPI and goat anti-rabbit alexa fluor 568. Fig 3.7 shows the result of the staining of the fixed cells visualised via confocal microscopy. Cells expressing wtEGFR showed EGFR time-dependent nuclear translocation. 30 minutes following EGF stimulation wtEGFR showed cytosolic internalisation and initial nuclear expression followed by marked nuclear translocation at 60 minutes confirming published reports (Hsu & Hung, 2007; Liao & Carpenter, 2007; Liao & Carpenter, 2009; Lo et al, 2006a). In contrast, NLS123, L858R and LNLS123 transfected cells showed no EGFR nuclear translocation at either time point with clear membrane and cytosolic accumulation.

3.2.4.2 EGFR nuclear translocation induced by IR

Having established EGFR nuclear translocation following EGF stimulation in wtEGFR expressing cells and the effects of the NLS123 mutation, EGFR nuclear translocation was investigated in wtEGFR, NLS123, L858R or LNLS123 transfected cells following treatment with 4 Gy IR. Prior to irradiation, cells were starved for 24 hours.

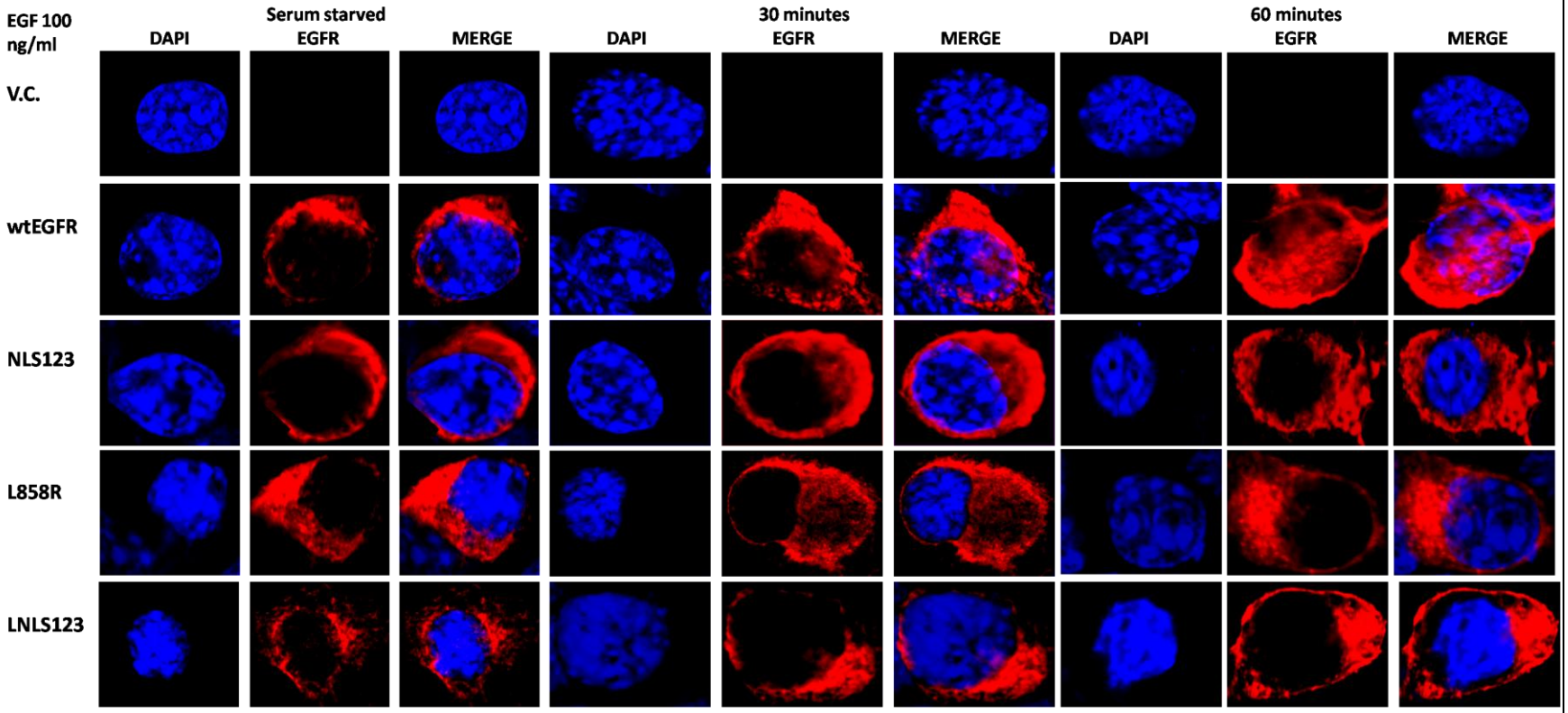

Figure 3.7: EGFR cellular localisation following EGF treatment. NIH3T3 cells transiently transfected expressing wtEGFR, NL123, L858R, LNLS123 or VC were serum starved for 24 hours, treated with 100ng/ml of EGF and then fixed with 4% PFA at 30 or 60 minutes following treatment. Cells were stained with Goat anti-Rabbit Alexa fluor 568 (EGFR),

Cells were collected over a period of 20 minutes from the time of irradiation and the cytosolic fraction was separated from the nuclear compartment. Densitometric analysis was used to quantify receptor nuclear accumulation. To normalise the densitometric data and take into account cytosolic contamination of the nuclear fraction, the ratio between the densities of cytosolic EGFR/calnexin was subtracted from the ratio between the densities of nuclear EGFR/calnexin (contamination). The ratio of cytosolic untreated EGFR/calnexin represents the physiological amount of EGFR in the cytosol in relation to the amount of cytosolic marker calnexin present in the blotted cellular extracts. By subtracting this amount from all the ratios of nuclear EGFR/calnexin it is possible to determine, and exclude, if EGFR nuclear accumulation is due to any cytosolic contamination (shown by the calnexin bands in the nucleus) and therefore the real fold increase of EGFR nuclear accumulation over time can be determined.

Fig 3.8 shows the results of samples obtained from wtEGFR transfected cells. These cells showed a time-dependent EGFR nuclear accumulation with a corresponding time-dependent cytosolic reduction. Densitometric analysis shows a 2.16-fold increase in EGFR nuclear accumulation by 20 minutes. NLS123 (Fig 3.9) and L858R (Fig 3.10) transfected cells show no EGFR nuclear accumulation over time as indicated by the densitometric values which fall below 1 following IR treatment. In both these transfected cell lines there was a time dependent accumulation of EGFR in the cytosolic fraction. LNLS123 transfected cell lines (Fig 3.11) showed lack of EGFR nuclear accumulation as indicated by the negative value. Considering the potent effect of IR on EGFR phosphorylation, the phosphorylation of the Y1068 and Y845 residues in both cellular compartments following IR was investigated in all the transfected cell lines. Cytosolic fraction from wtEGFR (Fig 3.8), L858R (Fig 3.10), LNLS123 (Fig 3.11) showed activation at both Y845 and Y1068 phosphorylation residues following IR treatment. Only the wtEGFR nuclear fraction (Fig 3.9) showed increased Y845 phosphorylation following IR treatment. NLS123 transfected cells (Fig 3.10) showed no receptor activation either in the cytosol fraction or in the nucleus.

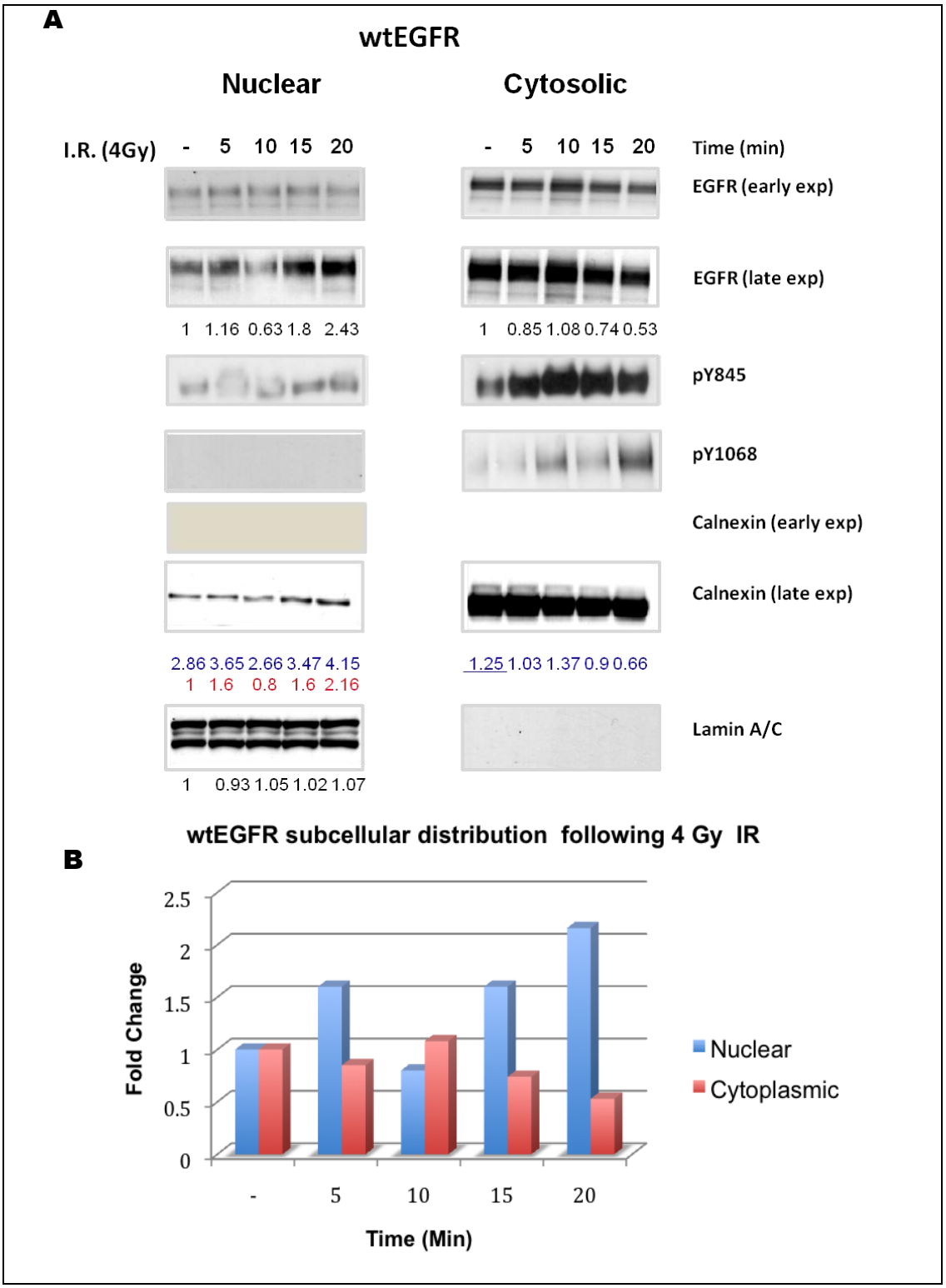

Figure 3.8: **IR induced nuclear translocation in NIH3T3 cells transiently transfected with wtEGFR.** (A) Cells were serum starved for 24 hours and then irradiated at 4 Gy. Cells were seeded 5, 10, 15, 20 minutes following treatment and nuclear fractionation was obtained. 40µg of protein lysate was loaded onto denaturing gel and bands were obtained via immunoblotting with anti EGFR, anti PY1068, anti PY845, anti Calnexin and anti Lamin A/C. Numbers (black) represent fold increase compared to untreated, (blue) EGFR/calnexin density ratio, (red) fold increase of nuclear EGFR once subtracted density of cytosolic contamination (blue underlined). (B) EGFR cellular distribution is shown in the graph.

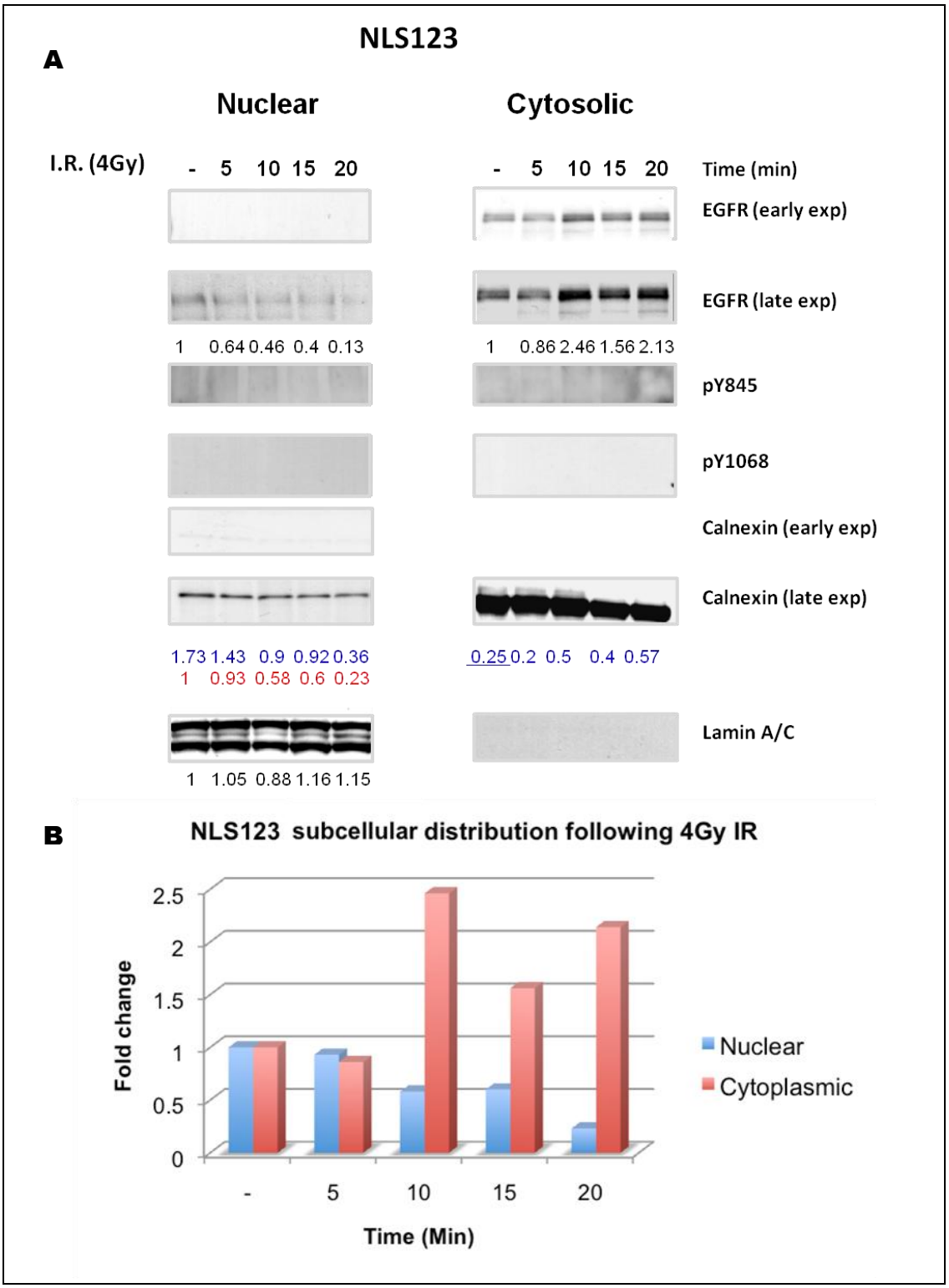

Figure 3.9: IR does not induce EGFR nuclear translocation in NIH3T3 cells transiently transfected with NLS123. Cells were serum starved for 24 hours and then irradiated at 4 Gy. Cells were seeded 5, 10, 15, 20 minutes following treatment and nuclear fractionation was obtained. 40µg of protein lysate was loaded onto denaturing gel and bands were obtained via immunoblotting with anti EGFR, anti PY1068, anti PY845, anti Calnexin and anti Lamin A/C. Numbers (black) represent fold increase compared to untreated, (blue) EGFR/calnexin density ratio, (red) fold increase of nuclear EGFR once subtracted density of cytosolic contamination (blue underlined). (B) EGFR cellular distribution is shown in the graph.

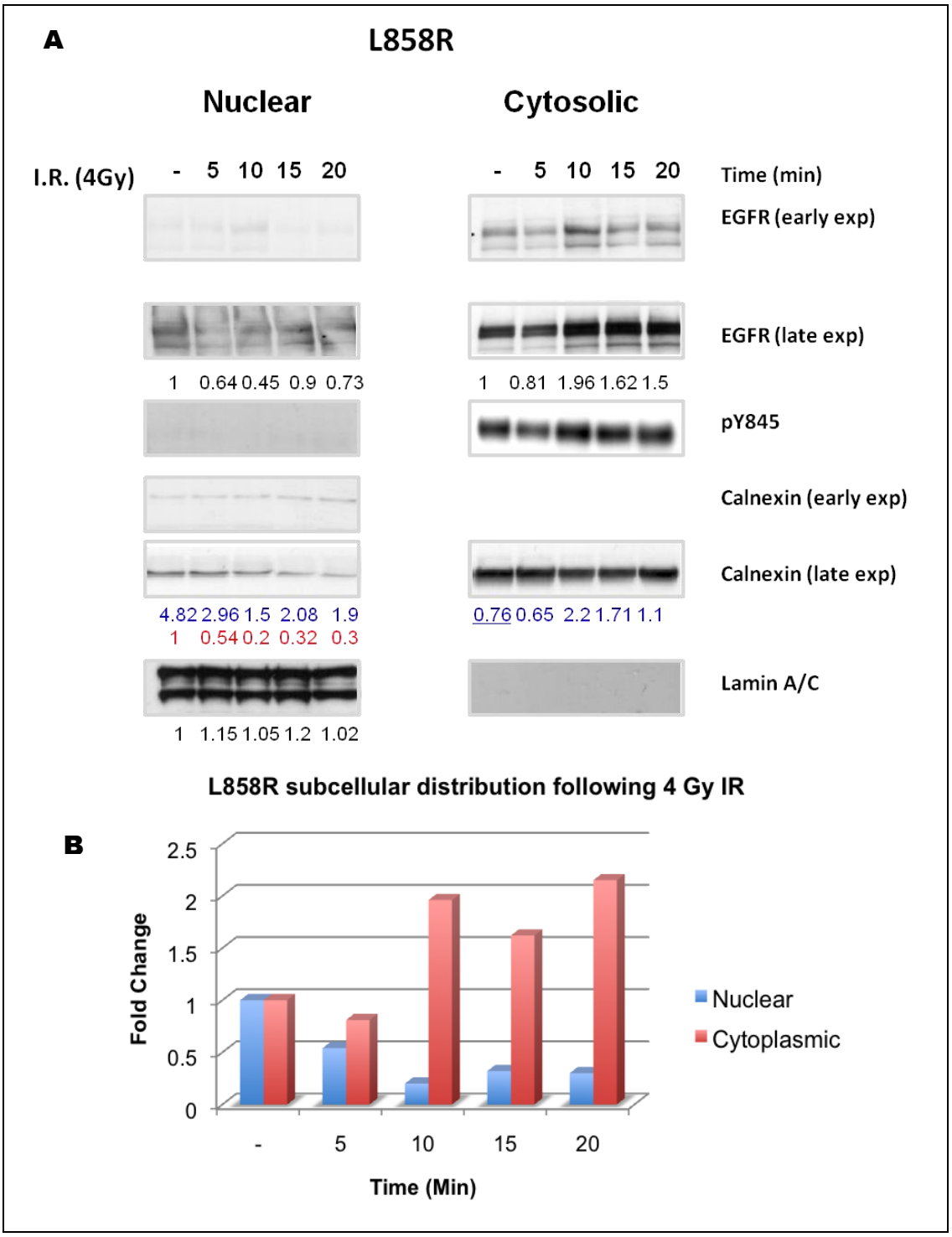

Figure 3.10: IR does not induce EGFR nuclear translocation in NIH3T3 cells transiently transfected with L858R. (A) Cells were serum starved for 24 hours and then irradiated at 4 Gy. Cells were seeded 5, 10, 15, 20 minutes following treatment and nuclear fractionation was obtained. 40µg of protein lysate was loaded onto denaturing gel and bands were obtained via immunoblotting with anti EGFR, anti PY845, anti Calnexin and anti Lamin A/C. Numbers (black) represent fold increase compared to untreated, (blue). EGFR/calnexin density ratio, (red) fold increase of nuclear EGFR once subtracted density of cytosolic contamination (blue underlined). (B) EGFR cellular distribution is shown in the graph.

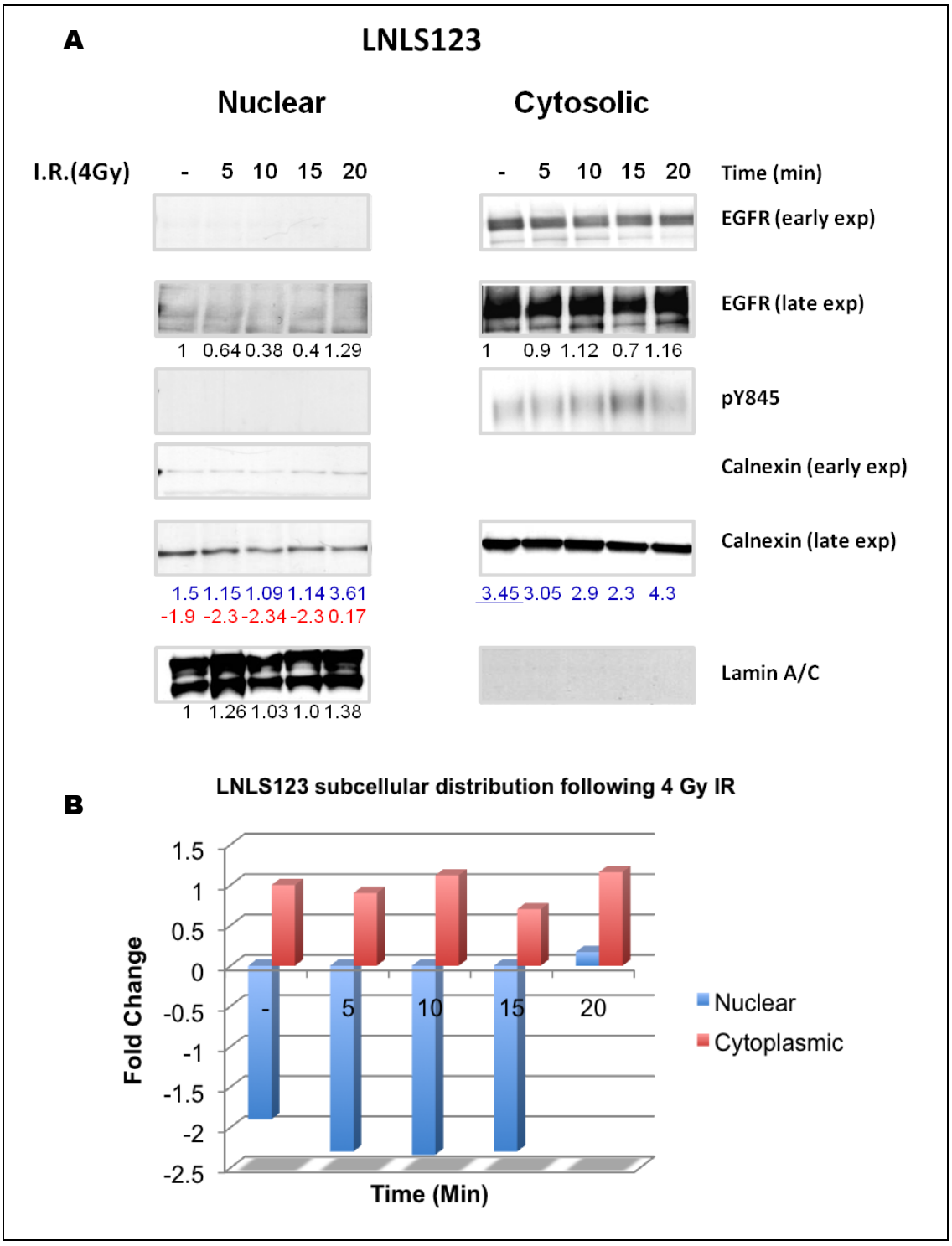

Figure 3.11: IR does not induce EGFR nuclear translocation in NIH3T3 cells transiently transfected with LNLS123. (A) Cells were serum starved for 24 hours and then irradiated at 4 Gy. Cells were seeded 5, 10, 15, 20 minutes following treatment and nuclear fractionation was obtained. 40µg of protein lysate was loaded onto denaturing gel and bands were obtained via immunoblotting with anti EGFR, anti PY845, anti Calnexin and anti Lamin A/C. Numbers (black) represent fold increase compared to untreated, (blue) EGFR/calnexin density ratio, (red) fold increase of nuclear EGFR once subtracted density of cytosolic contamination (blue underlined). (B) EGFR cellular distribution is shown in the graph.

A

wtEGFR	CYTOSOL					NUCLEAR				
TIME	0.00	5.00	10.00	15.00	20.00	0.00	5.00	10.00	15.00	20.00
ROW EGFR	8169.74	6925.03	8861.62	6089.38	4342.55	2968.50	3456.03	1884.55	5327.57	7289.57
FOLD EGFR	1.00	0.85	1.08	0.75	0.53	1.00	1.16	0.63	1.79	2.46
ROW CALNX	6532.57	6678.68	6457.89	6821.87	6559.97	1034.92	944.68	707.68	1534.63	1643.09
FOLD CALNX	1.00	1.02	0.99	1.04	1.00	1.00	0.91	0.68	1.48	1.59
						2.87				
RATION EGFR/CLNX	1.25	1.04	1.37	0.89	0.66	2.87	3.66	2.66	3.47	4.44
CORRECT MINUS THE CITO UNT EGFR/CLNX						1.62	2.41	1.41	2.22	3.19
FOLD EGFR						1.00	1.49	0.87	1.37	1.97
ROW LAMIN						4824.10	4489.57	5084.10	4947.69	5169.10
FOLD LAMIN						1.00	0.93	1.05	1.03	1.07

B

NLS123	CYTOSOL					NUCLEAR				
TIME	0.00	5.00	10.00	15.00	20.00	0.00	5.00	10.00	15.00	20.00
ROW EGFR	1545.28	1346.36	3735.67	2380.82	3548.67	1363.77	894.82	632.75	566.92	226.02
FOLD EGFR	1.00	0.87	2.42	1.54	2.30	1.00	0.66	0.46	0.42	0.17
ROW CALNX	6185.13	7402.72	7508.67	6106.48	6163.89	786.92	623.92	705.75	615.80	623.34
FOLD CALNX	1.00	1.20	1.21	0.99	1.00	1.00	0.79	0.90	0.78	0.79
RATIO EGFR/CALNX	0.25	0.18	0.50	0.39	0.58	1.73	1.43	0.90	0.92	0.36
RATIO EGFR/CALNX MINUS CYTOSOLIC UNTREAD										
RATIO						1.48	1.18	0.65	0.67	0.11
FOLD EGFR						1.00	0.80	0.44	0.45	0.08
ROW LAMIN						3259.15	3427.28	2867.46	3798.40	3747.15
FOLD LAMIN						1.00	1.05	0.88	1.17	1.15

C

L858R	CYTOSOL					NUCLEAR				
TIME	0.00	5.00	10.00	15.00	20.00	0.00	5.00	10.00	15.00	20.00
ROW EGFR	2750.43	2237.28	5409.06	4466.83	4127.83	2017.32	1290.42	914.58	1588.85	1485.99
FOLD EGFR	1.00	0.81	1.97	1.62	1.50	1.00	0.64	0.45	0.79	0.74
ROW CALNX	3581.67	3434.67	2491.43	2606.43	3790.26	418.39	434.80	607.75	760.46	785.46
FOLD CALNX	1.00	0.96	0.70	0.73	1.06	1.00	1.04	1.45	1.82	1.88
RATIO EGFR/CALNX	0.77	0.65	2.17	1.71	1.09	4.82	2.97	1.50	2.09	1.89
RATIO EGFR/CALNX MINUS CYTOSOLIC UNTREAD										
RATIO						4.05	2.20	0.74	1.32	1.12
FOLD EGFR						1.00	0.54	0.18	0.33	0.28
ROW LAMIN						6937.10	8020.23	7316.10	8241.81	7082.81
FOLD LAMIN						1.00	1.16	1.05	1.19	1.02

D

LNLS123	CYTOSOL					NUCLEAR				
TIME	0.00	5.00	10.00	15.00	20.00	0.00	5.00	10.00	15.00	20.00
ROW EGFR	8165.62	7350.74	9211.57	5563.15	9503.45	884.65	566.80	337.02	362.14	1145.04
FOLD EGFR	1.00	0.90	1.13	0.68	1.16	1.00	0.64	0.38	0.41	1.29
ROW CALNX	2369.99	2403.58	3097.58	2445.04	2223.34	585.51	490.92	307.39	317.39	316.68
FOLD CALNX	1.00	1.01	1.31	1.03	0.94	1.00	0.84	0.52	0.54	0.54
RATIO EGFR/CALNX	3.45	3.06	2.97	2.28	4.27	1.51	1.15	1.10	1.14	3.62
RATIO EGFR/CALNX MINUS CYTOSOLIC UNTREAD										
RATIO						-1.93	-2.29	-2.35	-2.30	0.17
FOLD EGFR						1.00	1.18	1.21	1.19	0.00
ROW LAMIN						6510.69	8236.13	6770.88	6560.71	9005.42
FOLD LAMIN						1.00	1.27	1.04	1.01	1.38

Table 3.2 A-D: Analysis of the densitometric values acquired via ImageJ on the cytosolic - nuclear separation blots for (A) wtEGFR, (B) NLS123, (C) L858R, (D) LNLS123.

3.3. DISCUSSION

3.3.1 EGFR expression in NIH3T3 cells

Over-expression of the EGF receptor is considered to be one of the principal characteristics of many types of cancer cells (Moasser et al, 2001). Our data showed that following transient transfection, the EGF receptor expression peaks at 48 hours remaining constant for the next 24 hours (Fig 3.1). Although sufficient receptor expression was already detectable from 12 hours following transfection, all the treatments were made 48 hours following transfection to mimic the EGFR over-expression of other cancer cells.

3.3.2 NIH3T3 cells as the most suitable cellular model

Although the plasmids utilised express human EGFR, NIH3T3 mouse fibroblast cell line was employed for this study. These cells do not express EGFR and they have been shown to become tumorigenic if cultured with EGF and overexpressing the EGF receptor (Di Fiore et al, 1987). Moreover, in addition to the intrinsic identity of the two genomes (human and mouse genome share 97% identity of their translated sequence) that have conserved the same cellular mechanisms; the necessity of employing an EGFR negative system is clearly primary. Among the other organisms whose genome has high homology to humans, the Green monkey COS7 and the hamster CHO cell lines are also EGFR negative. However, the CHO cell lines have a great practical disadvantage since there are not many commercially available antibodies or assays that guarantee cross reactivity with the hamster species rendering our molecular approach, potentially, difficult to interpret. The COS7 cells, although more closely related to humans, have not been shown to undergo transformation following over-expression of EGFR and therefore, among these three cellular systems, negative in the expression of EGFR, the mouse fibroblast NIH3T3 cell line was chosen. Despite the fact that a mouse-derived cell line cannot fully recapitulate the cellular circuits and the mechanisms of EGFR induced DNA repair regulation of human cancer cell lines, there are other biological disadvantages that have led to the NIH3T3 choice. Among the published cancer cell lines there are only two lines that do not express EGFR: ZR75 and DU4475 (Moasser et al, 2001). These cancer cell lines express HER2 and therefore the modulation of DNA repair by

another member of the ERBB family could have not been excluded. The final category, which was examined as a possible candidate for our model, includes those cancer cell lines that express EGFR and are also EGFR dependent. There are disadvantages of knocking out the existing receptor and knocking in our mutants and also the high expression of other members of the ERBB family of receptors. Moreover there are several reports showing that silencing the EGF receptor in an EGFR-dependent cell line results in spontaneous cell death (Park et al, 2009).

3.3.3 EGFR expression mediated signalling dependence in NIH3T3 cells

This chapter has confirmed that the NIH3T3 cells are EGFR negative (Fig 3.1) and also shown that upon EGFR transient expression, two main signalling pathways are activated in response to the ligand-induced upstream activation of the receptor (Fig 3.3). This demonstrates the adaptability of our cellular system and at the same time the influence of the EGF receptor on the NIH3T3 endogenous AKT and MAPK pathway (Klein & Levitzki, 2009). This was important to confirm the validity of this system to examine the EGFR modulation of DNA repair in this cell line and to compare the cellular responses in the presence of the somatic or the constructed EGFR mutants. Interestingly, despite the constitutive activation of the L858R, the densitometric analysis revealed a lower AKT and MAPK pathway compared to the activation measured in cells transfected with wtEGFR. This is a novel finding which has not been reported elsewhere. The downstream signalling activation of the L858R receptor has not been extensively analysed since this somatic mutant is often expressed together with the wtEGFR and discerning the actual activator of the signalling pathway is virtually impossible. As outlined in the Chapter1, the activation of one EGFR molecule relies on dimerisation and on the activation of the receiver kinase by the activator kinase. L858R may exert its oncogenic potential by playing the part of the activator with the wtEGFR molecule that will induce the activation of the downstream pathways. In contrast, the NLS123 showed lack of receptor phosphorylation and there was no detectable upregulation of the AKT and MAPK signalling pathways.

3.3.4 Conformational change is required for EGFR activation

The results so far reported indicate that the mutation of the NLS sequence of the EGFR receptor compromises receptor activation. The classical model of activation of

the EGFR molecule describes that symmetrical ligand binding to the ectodomains of two receptors triggers juxtaposition of their cytoplasmic kinase domains and subsequent autophosphorylation. This causes catalytic activity and formation of several docking sites for other signalling proteins (Domagala et al, 2000; Klein et al, 2004; Ozcan et al, 2006; Schlessinger, 2002). Nevertheless, studies on the EGFR juxtamembrane domain have shed new light on EGFR activation (Bae & Schlessinger, 2010; Choowongkomon et al, 2005; Lemmon & Schlessinger, 2010; Zhang et al, 2006). According to the latest published model the C-lobe of a cyclin-like "donor" molecule contacts the residues of the N lobe of an "acceptor" like molecule resulting in an allosteric activation of the acceptor molecule (Fig 3.12) (Jura et al, 2009; Lemmon & Schlessinger, 2010; Mustafa et al; Thiel & Carpenter, 2007)

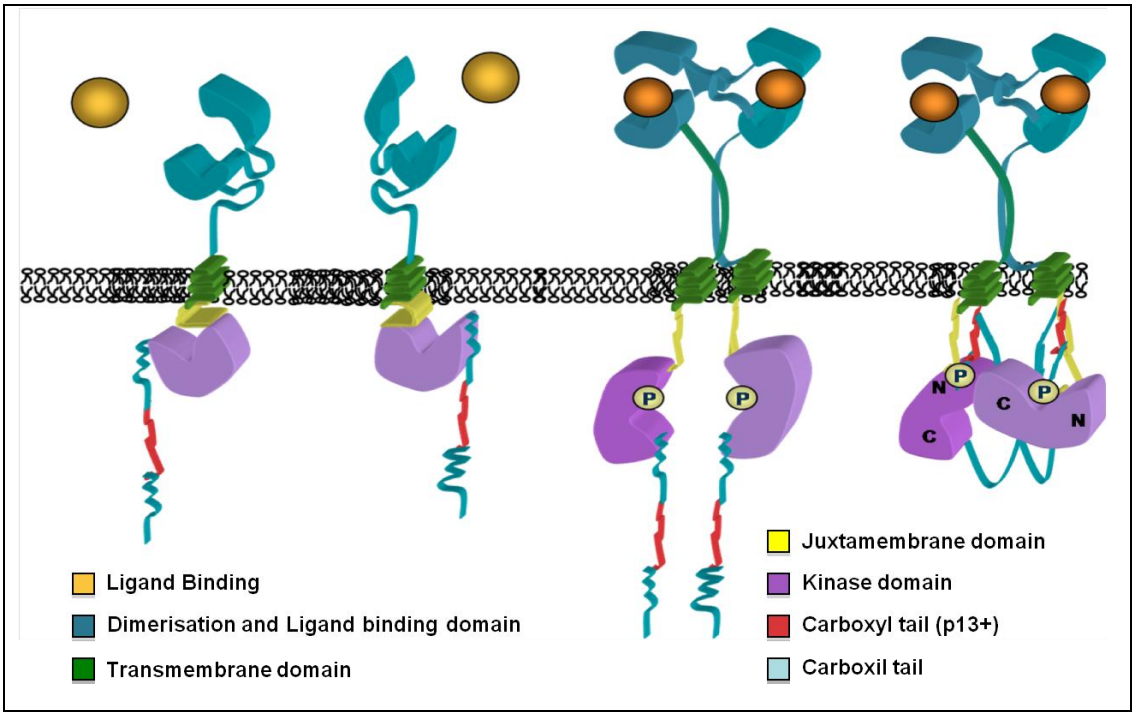

Figure 3.12: EGFR asymmetrical activation. The Fig shows the activation of the EGF receptor by the asymmetrical mode. The activation of the EGF receptor requires conformational change and dimerisation to achieve the phosphorylation of the correspondent molecule carboxyl tail. The C lobe and the N lobe of the kinase domain are marked to show how the N lobe of the first receptor comes to contact to the C lobe of the second.

3.3.5 The Juxtamembrane domain regulates the cellular fate of the receptor

The majority of the literature reports have portrayed the ligand binding domain, the kinase domain and the carboxyl tail as the most important domains. This is confirmed further by the design of EGFR-specific inhibitors. Nevertheless, despite its short length, also the Juxtamembrane domain (JX segment) contains many regulatory motives that dictate the fate of the entire receptor (Aifa et al, 2006a; Jura et al, 2009) (Fig 3.13).

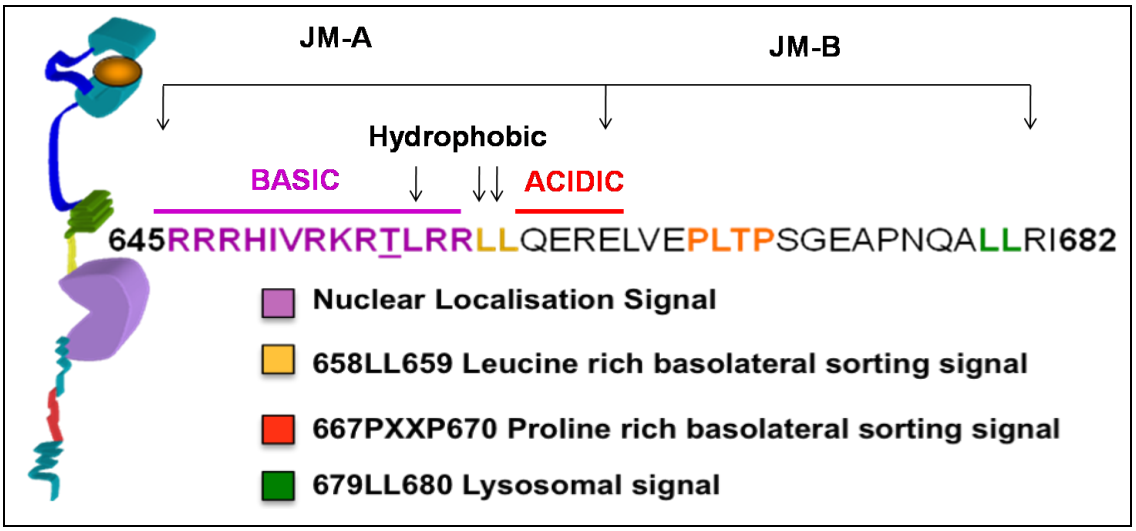

Figure 3.13: The Juxtamembrane domain sequence of the EGF receptor. The coloured amino acids highlight the four amino-acid signals present in this domain

The two basolateral signals: the dominant, proline rich core 667PXXP670, and the recessive, leucine rich 658LL659 and the lysosomal signal, 679LL680 are the residue and the motif that dictate the distribution of the molecule across the membrane and its recycling (Choowongkomon et al, 2005; Red Brewer et al, 2009). Essentially, when EGFR is inactive the only signal accessible is the basolateral dominant which recycles EGFR into an inactive form to the basolateral surface. The other signals are sterically obstructed and therefore inaccessible. This signal seems to be sufficient for targeting the receptor released at the trans Golgi to the basolateral plasma membrane and redirect the endosomal recycled receptor to the basolateral membrane (Choowongkomon et al, 2005). Upon ligand binding the lysosomal import becomes the only alternative because the homo or heterodimerisation of the molecules removes the inhibition of the lysosomal signal. The JX segments of the dimerising molecules come closer together exposing the lysosomal signal for recognition. The

active molecule following its activation is therefore degraded and recycled back to the surface membrane into an inactive state (Thiel & Carpenter, 2007).

The characterisation of the NLS mutation herein reported suggests that the NLS123 mutant is kinase dead. EGF, cisplatin or IR do not stimulate the kinase activity of the receptor, down-regulating the signalling pathways that are normally controlled by EGFR. This pattern suggests that the impairment of kinase activity observed in this mutant receptor may be the result of an obstructed conformational change that impedes the allosteric activation and the EGFR kinase-kinase juxtaposition. The NLS mutation seems therefore to be responsible for this dramatic kinase impairment.

3.3.6 The NLS sequence is a recognition sequence for the allosteric activation of the receptor

It has been shown that the 13 amino acids 645-657 (NLS sequence) containing the Threonine 654 (T654) not only represent the NLS sequence of the receptor but they are indispensable to achieve the conformational change that allows receptor dimerisation and subsequent activation. Upon ligand binding the receptor undergoes a conformational change in the intracellular domain at the site of the JX segment whereby the tyrosine kinase domain presents its carboxyl tail to the correspondent dimerised sister molecule (and vice versa) allowing a reciprocal phosphorylation of their residues (Aifa et al, 2006a; Aifa et al, 2006b). Some studies have shown that the phosphorylation of the T654 by protein kinase C (PKC) regulates the allosteric activation of the receptor. The phosphorylation of the T654 not only seems to suppress the kinase activity but also seems to re-route the receptor to the basolateral surface. The proposed model infers that this phosphorylation event may disrupt the helical structure causing the recessive basolateral signal to become accessible and to dominate over the lysosomal sorting signal (Choowongkomon et al, 2004; Dittmann et al; Macdonald-Obermann & Pike, 2009).

However, contrasting published evidence has shown that full length EGFR lacking these NLS 13 amino acids does not dimerise or autophosphorylate suggesting that the phosphorylation of T654 (residue contained in the NLS sequence) is neither necessary nor indispensable to switch off the kinase activity of the receptor and that the phosphorylation may be a consequence (rather than the reason) of the lack of the conformational change that favours this post-translational modification. The

undetected phosphorylation of the NLS123 mutant suggests that the phosphorylation of the T654 is not necessary to determine or signal the phosphorylation inhibition. However, the undetected phosphorylation of the T654 (located in the middle of the NLS sequence) could be the consequences of an obstructed protein structure which does not allow addition of a phosphate group (the juxtamembrane stretch is not accessible) or, if accessible, to the neutral charge of the NLS caused by the alanine substitution which does not attract negatively charged groups.

Truncated mutants, deprived of the extracellular region but with an intact p13 (NLS sequence is a peptide of 13 amino acids), dimerise and achieve a carboxyl tail autophosphorylation (Aifa et al, 2006b). This suggests that ligand binding is not the key component for the receptor activation. Collectively, these findings have proposed a model whereby the thirteen amino acid peptide corresponding to the NLS sequence, p13+ (mainly because the threonine residue is surrounded by basic amino acids and therefore positively charged) of the JX segment will electrostatically interact with another 13 amino acids peptide of exact but opposite charge, p13-, where the carboxyl tail faces the kinase domain of the other molecule allowing the reciprocal autophosphorylation (Aifa et al, 2006a).

3.3.7 The NLS third core of Arginine is required for dimer stabilisation

It has been recently shown that the last two arginines of the NLS sequence 656-RR-657 are responsible for adopting an α helical conformation that is indispensable for EGFR activity (Jura et al, 2009). The authors of this work compared the differential activation of these two arginines mutated into alanines (which would basically represent a charge removal) to the replacement by glycine (which would weaken the helix). The effect of the alanine substitution is smaller compared to the glycines substitution however the impairment on kinase activity of the receptor following EGF activation is significant for both.

In the model presented by Jura *et al*. 2009; the juxtamembrane segment JM-A forms an antiparallel helical dimer to allow the binding of the asymmetric kinase dimer. The JM-B allows stabilising contact between the acceptor and donor lobe; however, there is no functional involvement of this part of the Juxtamembrane domain (Fig 3.14). The model showed clearly the importance of the last core of the Arginine residues within the NLS sequence, whose mutation is probably the main responsible for the kinase inactivation of the NLS123 mutant. In the original study that has

characterised the EGFR NLS sequence, Hsu et al., showed that the mutation of the last core of basic amino acid within the EGFRNLS sequence induced only a reduction in EGFR activation (Hsu & Hung, 2007), therefore the alanine substitution of the first two cores of basic amino acids within the EGFR NLS sequence have contributed to the complete kinase inactivation of the NLS123 mutant shown in this study. This sugegsts that the mutation of all the three Arginine' cores is required to impair conformational allosteric change and consequent kinase activation.

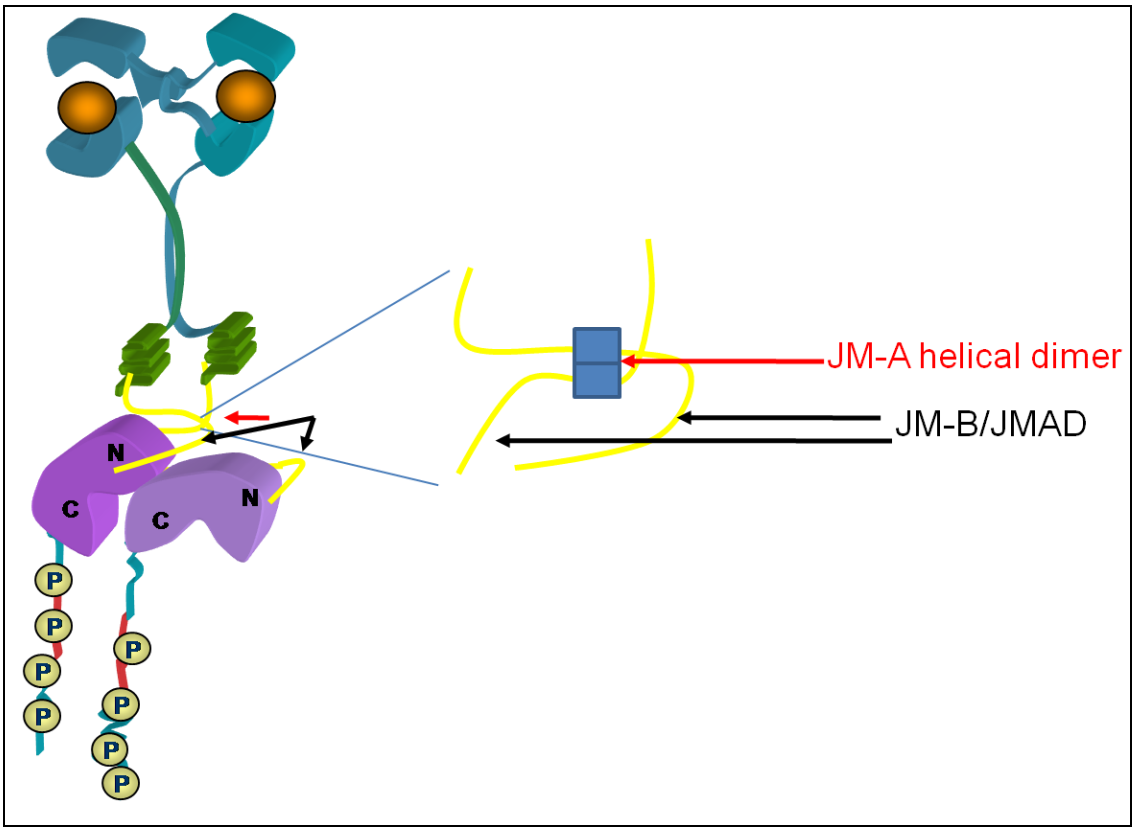

Figure 3.14: Formation of the asymmetric dimer. The JM-A forms an antiparallel helical dimer (interconnecting yellow lines) to allow and stabilise the formation of the asymmetric kinase dimer. The C lobe of the activator donor kinase interacts with the N lobe of the receiver/acceptor kinase leading to kinase activation of the receptor and phosphorylation of the carboxyl tail.

3.3.8 The L858R mutant does not require conformational change and allosteric activation

Despite the NLS123 mutant showing a complete lack of phosphorylation following both EGF, cisplatin or I.R, the LNLS123 showed only a reduction compared to its parental L858R. Fig 3.3, 3.4 and 3.11 showed LNLS123 phosphorylation activation on the PY1068 following EGF treatment and on the PY845 following I.R despite the

presence of the same NLS mutation as in the NLS123 responsible for its kinase inactivation. The LNLS123, and its parental construct (L858R), also bear a kinase point mutation (Leucine 858 into Arginine- L858R) that enhances the affinity of the ATP binding site to ATP like molecules rendering the receptor more prone to auto-phosphorylation. This mutation allows a thermodynamically stable conformation of the protein that enables autophosphorylation of the Y845 residue that resides in the same activation loop of the residue in position 858. (Yang et al, 2008) The reduced, rather than abolished, phosphorylation confirms that the L858R mutation of the receptor in non small cell lung cancer (NSCLC) confers to the EGF receptor a constitutive activation (Gazdar, 2009a). This study suggests that this mutation permits a mode of activation that escapes the necessity of undergoing a conformational change required by WT receptor. This would explain why, despite the mutation on its NLS sequence/p13+ peptide, the LNLS123 mutant still shows activation following ligand or IR treatment. The reduced activation requires further explanation. It has been reported that even minute amounts of EGFR receptor activation are sufficient to activate downstream signalling pathways and therefore also low levels must be taken into account (Arteaga, 2002; Bublil & Yarden, 2007). Moreover, although a clear reduction compared to its parental is observed, the phosphorylation levels presented by the LNLS123 are not negligible. Therefore, the activation potential of this construct will be categorised in this study as constitutive as with its parental L858R.

Structurally, the mutation to the nuclear localisation signal changed the arginine residues into alanine residues. As a result, the affinity to the importin molecule is lost and the receptor nuclear translocation is impaired. In addition, the mutation itself seems to be sufficient to disturb the conformational change necessary for the receptor activation as shown in the results.

3.3.9 EGFR nuclear localisation signal mutation impairs both nuclear translocation and protein activation

Our data have shown the successful mutation of the wtEGFR and L858R constructs NLS sequence. The mutated tripartite NLS signal of the NLS123 and LNLS123 constructs has resulted in marked reduction of EGFR nuclear localisation following EGF or IR treatment.

The western blot analysis on the protein lysate of the separated cellular compartments showed increase of wtEGFR nuclear translocation over time whereas in the other mutants only a significant impairment of nuclear translocation. On the other hand the results shown by the confocal microscopy following EGF treatment show clear lack of nuclear accumulation in NLS123, L858R, LNLS123 both at 30 and 60 minutes following EGF treatment. Therefore the residual EGFR expression detectable on the western blots of the nuclear compartments of NLS123, L858R and LNLS123 expressing cells, is most probably due to the reported cytoplasmic fraction contamination rather than the actual receptor translocation as confirmed by the densitometry analysis. This study also indicates that only phosphorylated wtEGFR on Y845 residue was found in the nucleus following IR treatment. However, both L858R and LNLS123 also undergo PY845 autophosphorylation, and the lack of PY845 signal within the nuclear fraction suggests that nuclear EGFR expression found in the blots from cells transfected with the other mutants is due to cytosolic contamination. This suggests that Y845 phosphorylation is not the post-translational modification causing the nuclear translocation but that it is a consequence of an *a priori* event that allows nuclear translocation. Taken together, the constitutive activation of the L858R and its lack of nuclear accumulation suggest that kinase activation *per se* is not sufficient for EGFR nuclear expression and that the mechanism is more complex.

The confocal microscopy analysis following EGF treatment shows a cytosolic and membrane accumulation of the receptor in the NLS mutants and in the L858R expressing cells as opposed to the gradual EGFR nuclear accumulation shown by the wtEGFR transfected cells. The EGFR staining pattern of the wtEGFR expressing cells shows EGFR localised primarily to endocytic vesicles in the perinuclear region at 30 minutes following treatment which is shown by the circle-like structure around the membrane and the nucleus. Differently from the other mutants, the cell membrane of wtEGFR expressing cells shows a punctuated staining since the receptor undergoes endocytosis and retrotranslocation. The nuclear distribution of the wild type receptor at 60 minutes shows again the circle-like internalisation pattern whereas the remaining mutants show a cytosolic accumulation. Considering the lack of kinase activation in NLS123 expressing cells, the cytosolic accumulation is most probably indicating receptor degradation in the lysosomal compartment

whereas the constitutive activation shown by the L858R and LNLS123 suggests that the receptors are reshuffled back to the transmembrane.

The impairment of nuclear localisation following EGF and IR could be explained by the reduction of affinity between the receptor molecule and the importin machinery due to a lack of conformational change and asymmetric dimer stabilisation due to the NLS123 mutation or to an alternative mode of activation.

3.3.10 NLS mutation impairs EGFR protein expression

Despite efforts to achieve equal protein expression (i.e. transfecting cells with 2-8 μg of plasmid DNA) the levels of the NLS123 are always different to its parental, wtEGFR, levels. This may reflect :

a) An intrinsic incapability of the cells to cope with this kinase mutant

b) The fact that the stable inactive (immature) conformation of the receptor renders the molecule more susceptible to degradation and/or reshuffling producing a reduced accumulation of the receptor both at the membrane and in the cytosol or

c) The inactivity of the receptor does not stimulate the degradation and synthesis of new receptor molecules.

3.3.11 CONCLUSION

This chapter has validated the NIH3T3 cellular system as a good model to study the effect of EGFR expression. The kinase activity of the constructs as well as their capability of translocating to the nucleus has been shown. Differently from the published mutants, the NLS123 mutation shows completely abolished nuclear translocation. Interestingly, the somatic mutant L858R and the LNLS123 mutant, have also shown inhibition of nuclear translocation suggesting that kinase activation does not determine nuclear import and that a specific receptor structural conformation is required to mediate the binding to the NLS sequence. The understanding of the different behaviour of these constructs is necessary to critically analyse their influence on DNA repair following IR or cisplatin (discussed in the next chapter).

CHAPTER 4:
NUCLEAR EGFR MODULATION OF DNA REPAIR

4.1 INTRODUCTION

EGFR nuclear localisation requires receptor allosteric conformational change. This is central to expose the NLS sequence for recognition and binding (Jura et al, 2009; Macdonald-Obermann & Pike, 2009; Red Brewer et al, 2009; Thiel & Carpenter, 2007). Although receptors, regardless of their active or inactive conformation will be internalised in the cytosol (Madshus & Stang, 2009), their nuclear translocation is dependent on the retrograde translocation through the sec61 translocon in the ER and the binding of importin to the NLS sequence (Liao & Carpenter, 2007). The NLS123 mutant not only showed lack of nuclear translocation but also ligand dependent or independent activation. This is because the EGFR NLS sequence is involved in dimer stabilisation and allosteric conformational change (Jura et al, 2009). The constitutive activation showed by the LNLS123 mutant suggested that the L858R mutation *per se*, within the kinase domain, is sufficient to determine a receptor mode of activation that escapes the allosteric conformational change requirement. This explains why the LNLS123 is active despite harbouring the NLS mutation that rendered the NLS123 kinase dead.

4.1.1 EGFR role in DNA repair

Increased EGFR activation has been strongly associated with tumorigenesis and cancer progression (Bublil & Yarden, 2007; Fischer et al, 2003; Lemmon & Schlessinger, 2010). Although EGFR already promotes the activation of survival, growth and proliferation signalling, EGFR inhibition by TKI (e.g. gefitinib and erlotonib) and monoclonal antibodies (e.g. cetuximab) have indicated a role for EGFR in the modulation of DNA repair following chemotherapy and radiotherapy (Gazdar, 2009a; Wheeler et al). Several studies have demonstrated the association of EGFR with DNAPKcs, the central component of the NHEJ pathway involved in the repair of DNA strand breaks (Dittmann et al, 2008a; Dittmann et al, 2007; Friedmann et al, 2006; Hsu et al, 2009; Mahaney et al, 2009; Mukherjee et al; Rodemann et al, 2007). Nuclear EGFR is found to correlate with worse prognosis in a variety of human cancers such as breast, head and neck and ovarian (Galleges Ruiz et al, 2009; Hoshino et al, 2007; Lo; Lo, 2010). Therefore, understanding the relationship between sensitivity to cancer therapy and EGFR sub-cellular distribution is necessary to design novel therapeutic combination strategies. While the interaction between EGFR and DNAPKcs has been demonstrated in response to IR (Rodemann et al,

2007), little is known about the role of EGFR in the modulation of repair following drug (e.g. cisplatin) treatment (Hsu et al, 2009). Having characterised the nuclear import and the activation potential of the different constructs the relationship between nuclear translocation and the kinetics of DNA repair following treatment with cisplatin or IR were characterised. This was achieved by the use of the alkaline single cell gel electrophoresis (comet) assay which determined the formation and repair of DNA strand breaks (both single and double) and interstrand crosslinks (ICLs) (Hartley et al, 1999).

4.1.2 Cisplatin damage and repair

Cisplatin can form intrastrand crosslinks, interstrand crosslinks (ICLs), DNA-protein crosslinks and monoadducts with DNA (Nojima et al, 2005) and inhibition of ribosomal RNA synthesis (Jordan & Carmo-Fonseca, 1998). Among all these lesions ICLs, although only 6-8% of the total lesions (Zdraveski et al, 2000), are considered to be the main determinant of toxicity of crosslinking agents. This is due to the difficulty to resolve the ICLs that can also result in blocked transcription and DNA replication and initiate apoptosis (Wang & Lippard, 2005).

The comet assay is designed as a method to measure DNA strand breaks in single cells (Olive, 1999) and can be modified for the purpose of measuring interstrand crosslink formation and repair (Spanswick et al) as described in the Materials and Methods section. Cisplatin repair in this study refers to the unhooking of the ICLs as measured using the comet assay.

4.1.3 IR damage and repair

IR exposure gives rise to multiple forms of direct DNA lesions including damage to the bases, cleavage of the DNA backbone to form single strand breaks (SSBs) and double strand breaks (DSBs) which can occur when two SSBs are formed at opposite strands or up to 10-20 bases apart (De Bont & van Larebeke, 2004; Jeggo & Lavin, 2009; Olive, 2009; Szumiel, 2008). Moreover, indirect damage due to ionisation, hydrated electrons and hydroxyl radicals, results in sugar derived product, additional single and double strand breaks and DNA-protein crosslinking (Ward, 1995). Exposure to one Gray of IR is known to produce 1000 SSBs and about 30 DSBs per diploid cell independently from the cell type (Jeggo, 2009). Unrepaired SSBs lead to blockage of DNA replication forks during S phase and possibly to the formation of

DSBs (Mahaney et al, 2009) Although cells have two non-competing repair pathways, NHEJ and HR, responsible for the repair of DSBs, acute levels of SSBs may saturate these pathways leading to genetic instability or cell death (van Gent & van der Burg, 2007). Alternatively, high levels of SSBs may induce cell death by excessive activation of the SSB sensor protein poly (ADP-ribose) polymerase1 (PARP1) whose prolonged activation leads to depletion of NAD and ATP and release of the apoptosis-inducing factor AIF from mitochondria (Hefferin & Tomkinson, 2005). DNA DSBs are considered the most lethal type of lesion. It has been shown that even 1 unrepaired DSB is sufficient to cause cell death (Jackson & Bartek, 2009).

4.1.4 Constructs utilised in this study

The investigation of the involvement of EGFR in the modulation of DNA repair and the mechanism that mediates this modulation requires a careful and detailed analysis of the different aspects of EGFR biology. For this reason five additional constructs were added to this study in addition to those described in the previous chapter. These are three EGFR NLS sequence mutants, 1 kinase mutant and a somatic mutant found in Glioma (EGFRvIII). While the addition of the three NLS mutants aims at mapping the extent of EGFR nuclear translocation required for repair, both the kinase mutant and EGFRvIII are needed to decipher the role of kinase activation in both nuclear translocation and repair.

4.1.5 CHAPTER AIMS:

- Test the hypothesis that nuclear localisation is required for the repair of cisplatin or IR induced damage and investigate the differential repair modulation of all the mutants.
- Investigate the relation between DNA repair modulation and intrinsic phosphorylation activity of the different transfected constructs.
- Determine the involvement of DNAPKcs in the repair of cisplatin-induced damage

4.2 RESULTS

4.2.1 EGFR constructs utilised for the DNA repair assays

The effect of both cisplatin and IR on EGFR expressing cell lines has been well described. However, the role and consequences of EGFR nuclear translocation and kinase activation in the repair of both ICLs and strand breaks have not been fully examined. To probe the differential EGFR modulation on DNA repair, the EGFR negative cell line, NIH3T3, was transfected with 10 different plasmids (wtEGFR, NLS123, L858R, LNLS123, EGFRvIII, VC, M1, M12, KMT or ΔNLS) and DNA repair was assessed via the alkaline comet assay. These contain mutations within the NLS sequence (NLS123, LNLS123, M1, M12, ΔNLS), the kinase domain (L858R, KMT) and the extracellular domain (EGFRvIII) (Fig 4.1). The M1 receptor bears the mutation of the first cluster of basic amino acids of the NLS sequence (RRRHIVRKRTLRR into AAAHIVRKRTLRR), the M12 receptor bearing the mutation of the first two clusters (RRRHIVRKRTLRR into AAAHIVAAATLRR), the ΔNLS having the NLS sequence deleted. KMT bears the mutation of the Lysine 721 into an Alanine (K721/A) and the EGFRvIII bears the deletion of exons 2-7. These affect the receptor kinase activity rendering the mutants: kinase dead (KMT) or constitutively active (EGFRvIII) respectively.

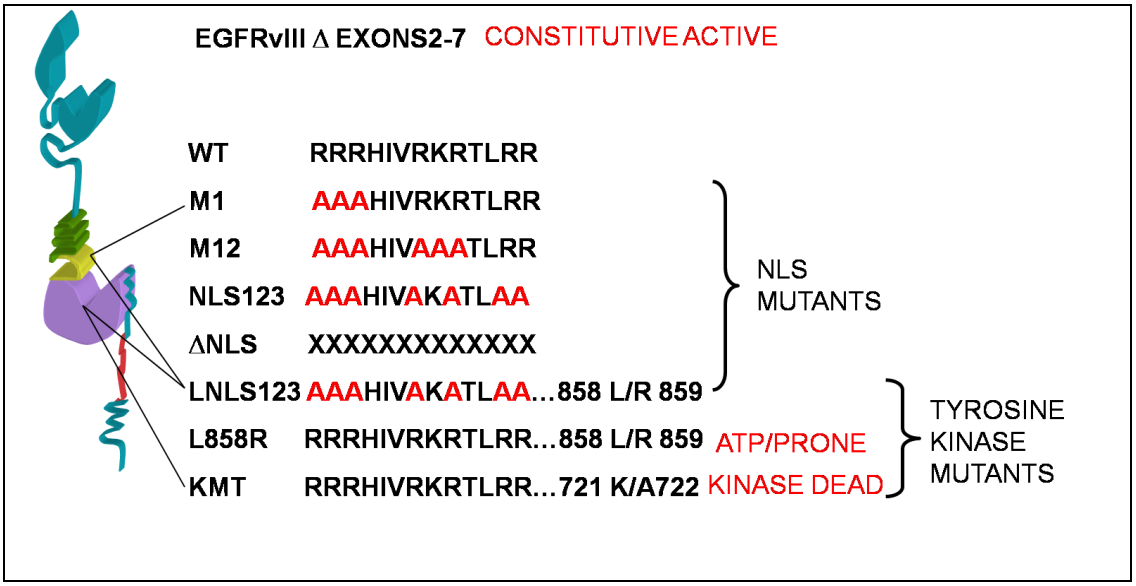

Figure 4.1: Graphic representation of the EGFR constructs employed in the study.

4.2.2 EGFR modulation of cisplatin-induced DNA damage repair.

4.2.2.1 50 μM cisplatin forms sufficient ICLs to study repair kinetics over time

Prior to investigating the repair of cisplatin adducts, the dose of cisplatin required to induce detectable DNA damage was calculated using a modification of the comet assay as previously described (Spanswick et al, 2002; Spanswick et al). Cells transfected with wtEGFR or VC were incubated with cisplatin at a dose up to 150 μM for 1 hour in serum-free media. It has been previously shown that cisplatin ICL formation peaks 9 hours after treatment with cisplatin. For this reason the cells were examined 9 hours following the treatment to determine the level of ICLs formed following drug treatment (Fig 4.2). The analysis of the comet assay showed that there was no difference in the formation of the crosslinks between cells transfected with wtEGFR or VC at all the time points. Levels of ICL formation, sufficient to investigate repair over time, were already detectable following 50 μM cisplatin. Higher doses (100-150 μM) showed a plateau effect for the formation of ICLs, suggesting that 50 μM was the optimal dose to determine repair over time.

Next, it was established whether the amount of damage inflicted by 50 μM cisplatin was reparable over a period of 48 hours in cell transfected with wtEGFR. Fig 4.3 shows a representative result of the % decrease in tail moment over a period of 48 hours in NIH3T3 cells transfected with wtEGFR following treatment with 50 μM cisplatin. The graph shows that ICLs start forming already at 1 hour and that the peak of ICLs is at 9 hours following treatment (71.7 +/-2.01%). The majority of the lesions are then resolved by 36 hours in wtEGFR expressing cells suggesting that the amount of ICLs formed is sufficient to investigate repair kinetics over a period of 48 hours.

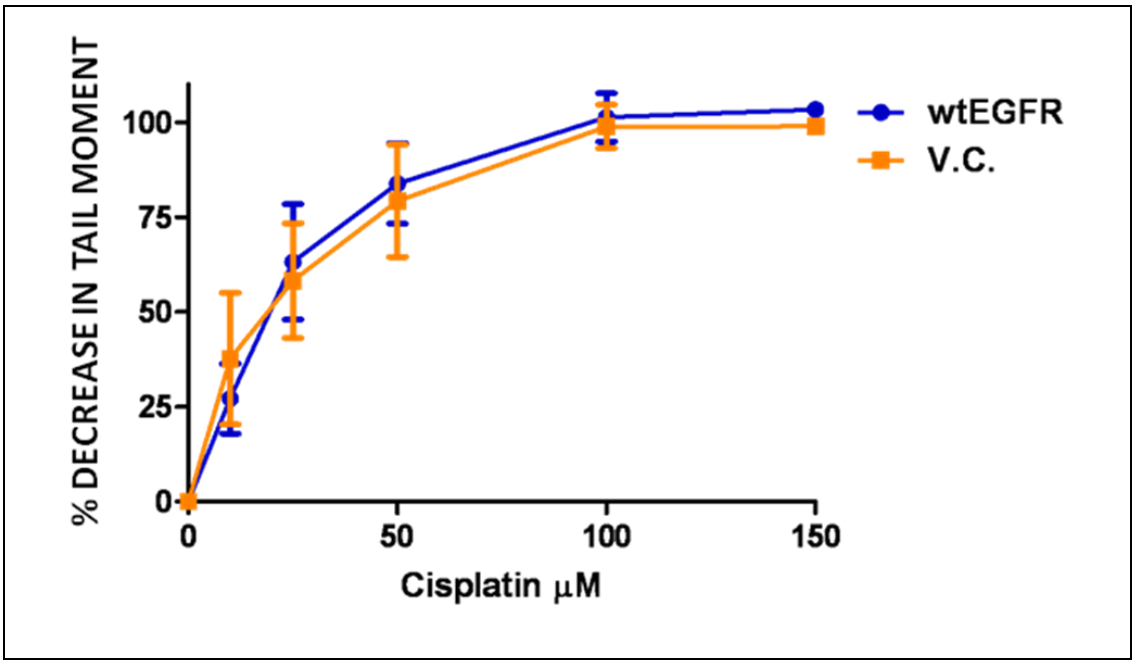

Figure 4.2: 50 µM cisplatin induces optimal levels of detectable DNA damage. Wild type and vector control expressing NIH3T3 were treated with 10, 25, 50, 100, 150 µM cisplatin 48 hour following transient transfection. Cells were then examined 9 hours following the treatment to determine the percentage of ICLs a major cytotoxic lesion produced following drug treatment. The graph shows the mean values from three independent experiments. Error bars represent standard deviation (SD).

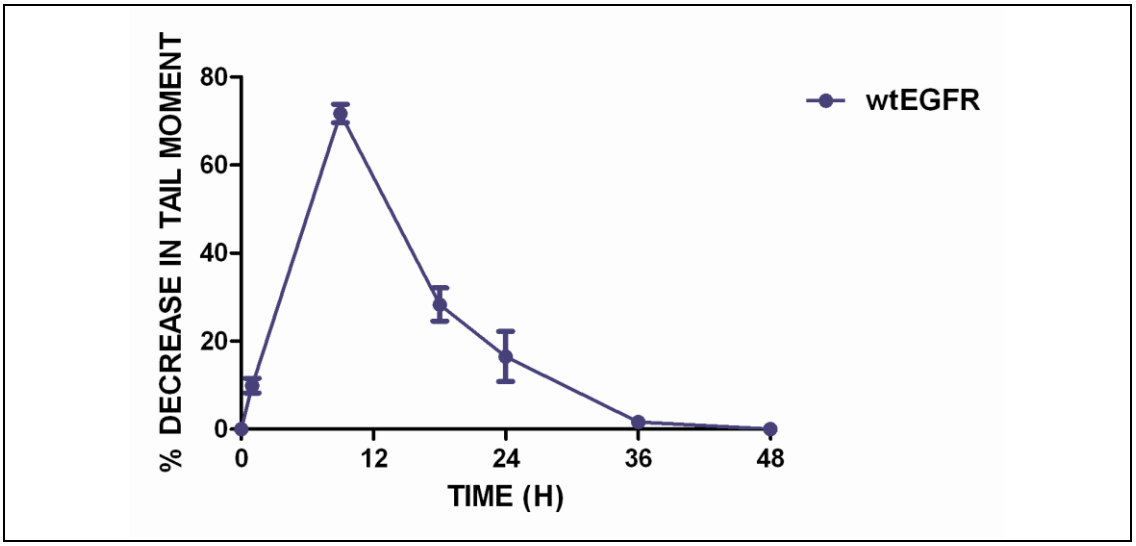

Figure 4.3: 50 µM cisplatin induces damage repairable over time. Cells expressing wtEGFR were treated with 50 µM cisplatin over 48 hour following transient transfection. Cells were then examined at different time points s following the treatment to determine the percentage decrease in tail moment as a measurement of ICLS unhooking. The graph shows the mean values from three independent experiments. Error bars represent standard deviation (SD).

4.2.2.1.1 Transfection of the EGFR mutants does not affect the peak of crosslinks

At this point, before evaluating the kinetics of repair of cisplatin induced ICLs, it was investigated whether the transfection of all the mutants in NIH3T3 cells could have an effect on the formation of ICLs following cisplatin treatment. Cells transfected with wtEGFR, NLS123, L858R, LNLS123, M1, M12, KMT, ΔNLS, EGFRvIII or VC were treated with 50 μM cisplatin for 1 hour and samples were obtained 9 hours following treatment. Fig 4.4 and table 4.1 show the peak of crosslink across all the transfected cell lines. There was no significant difference among the peaks of ICLs suggesting that the transfection of different EGFR mutants does not affect the amounts ICLs formed at 9 hours.

4.2.2.1.2 wtEGFR and EGFRvIII completely repair cisplatin crosslink 48 hours following treatment

Having determined the optimal dose of cisplatin to use during the comet assay, and after establishing that the transfection of different mutants in NIH3T3 cells was not affecting the formation of the crosslinks, NIH3T3 cells were transfected with all the mutants described in Fig 4.1 and cells were treated with 50μM cisplatin, for 1 hour in serum free media. Samples were then collected over a period of 48 hours to assess repair of ICLs. Since there was no alteration in the formation of ICL by cisplatin in cells expressing all constructs and no significant difference among the peak of crosslinks, the data collected over 48 hours were plotted as percentage of peak of crosslink. Fig 4.5 shows the graphical comparison of the repair kinetics between each individual construct and wtEGFR transfected cells. Only cells transfected with wtEGFR and EGFRvIII showed complete repair by 48 hours following cisplatin treatment. The repair kinetics of these transfected cells showed significant differences already by 18 hours following treatment establishing three different repair behaviours: greatly impaired repair (NLS123, LNLS123), intermediate repair (L858R, KMT, ΔNLS) and complete repair (wtEGFR, EGFRvIII, M1 and M12), shown together in Fig 4.6.

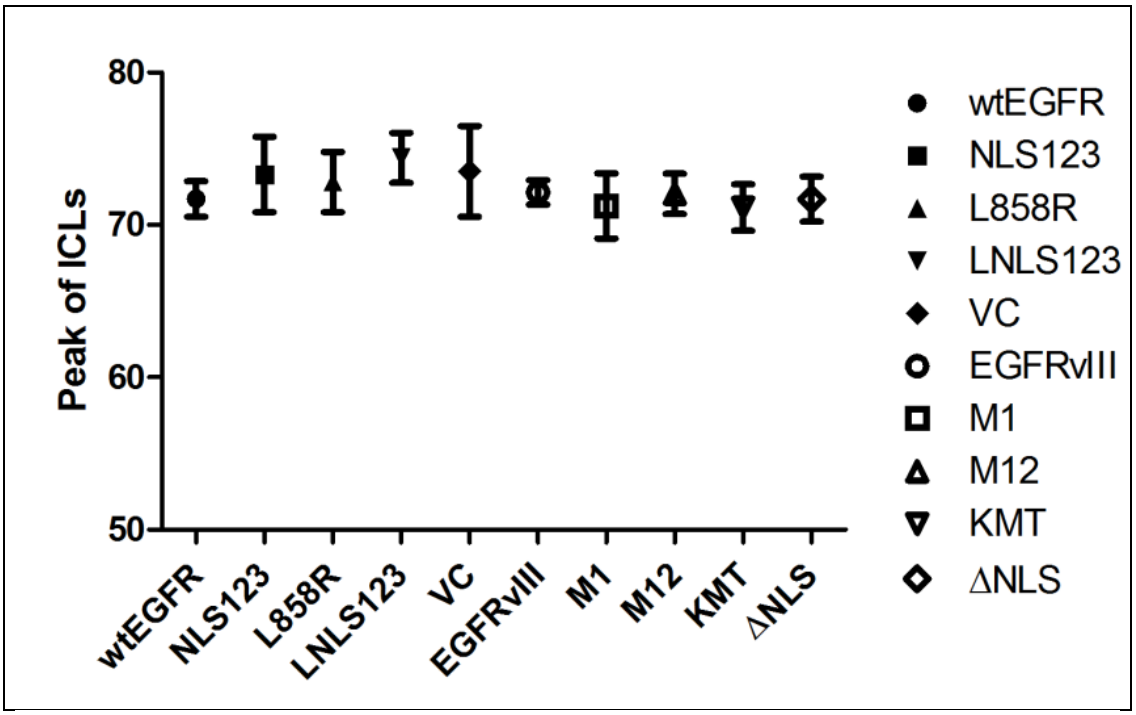

Figure 4.4: Percentage decrease of tail moment, at the peak of ICLs among the different constructs. The graph shows the average peak of ICLs, 9 hours following treatment with cisplatin, of NIH3T3 cells transfected with wtEGFR, NLS123, L858R, LNLS123, VC, EGFRvIII, M1, M12, KMT and ΔNLS. The average and the standard deviation of the data collected from 3 independent experiments are shown in the Table below.

	wtEGFR	NLS123	L858R	LNLS123	VC	EGFRvIII	M1	M12	KMT	ΔNLS
Average	71.70	73.31	72.80	74.40	73.51	72.14	71.25	72.04	71.13	71.69
SD(+/-)	2.01	4.29	3.42	2.82	5.16	1.38	3.71	2.28	2.65	2.55
P value	P>0.05	P>0.05	P>0.05	P>0.05	P>0.05	P>0.05	P>0.05	P>0.05	P>0.05	P>0.05

Table 4.1: Values and statistical analysis of the peak of crosslink. The average value from 3 independent experiments, the standard deviation and the statistical significance expressed as a P value are shown in the table

Unhooking of cisplatin–induced ICL was 60.14 ± 6.56 % and 61.32 ± 2.65 % unhooking by 24 hours in cell expressing wtEGFR and EGFRvIII and 100% after 36 hours in both cell lines. In contrast, cells expressing NLS123 and LNLS123 showed only 7.98 ± 1.76 % and 11.12 ± 2.59 % of unhooking by 18 hours and 26 ± 4.07% and 19.3 ± 4.8 % of unhooking at 48 hours. The intermediate repair group showed 19.23 ± 3.89 (L858R), 35.2 ± 6.87 % (KMT), 40.87 ± 8.37 % (ΔNLS) unhooking by 18 hours and 46.57 ± 2.13% (L858R), 54.95 ± 2,56% (KMT) and 57.21 ± 9.72% (ΔNLS) unhooking of ICLs by 48 hours following cisplatin treatment. M1 and M12

expressing cell lines showed 84.09 ± 4.87% and 97.41 ±2.73% unhooking of ICLs respectively at 48 hours following cisplatin treatment. All the numerical data are reported in Table 4.2, where the Statistical analysis by the 2 way ANOVA shows the average values of every single time point, the standard deviation and its statistical significance expressed as P value. Statistical significance (P value < 0.01/0.001) was found at 48 hours time points and/or at earlier time points when the kinetics of cells expressing wtEGFR were compared to the kinetics of cells expressing NLS123, L858R, LNLS123, M1, M12, KMT, ΔNLS or VC.

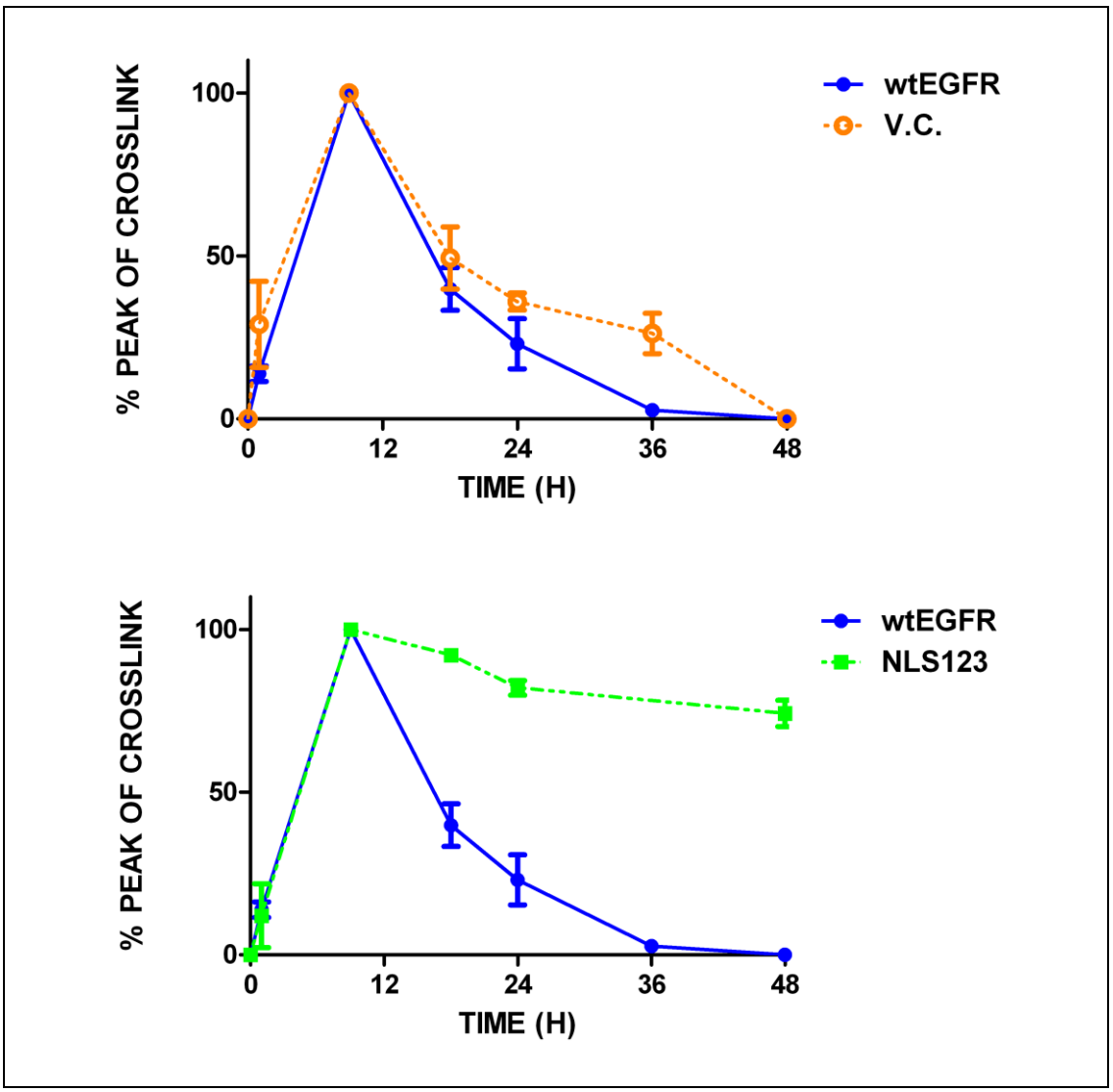

Figure 4.5: Effects of EGFR modulation in repair of ICLs. The modulation in repair of single mutants is compared to the modulation in repair by wtEGFR.

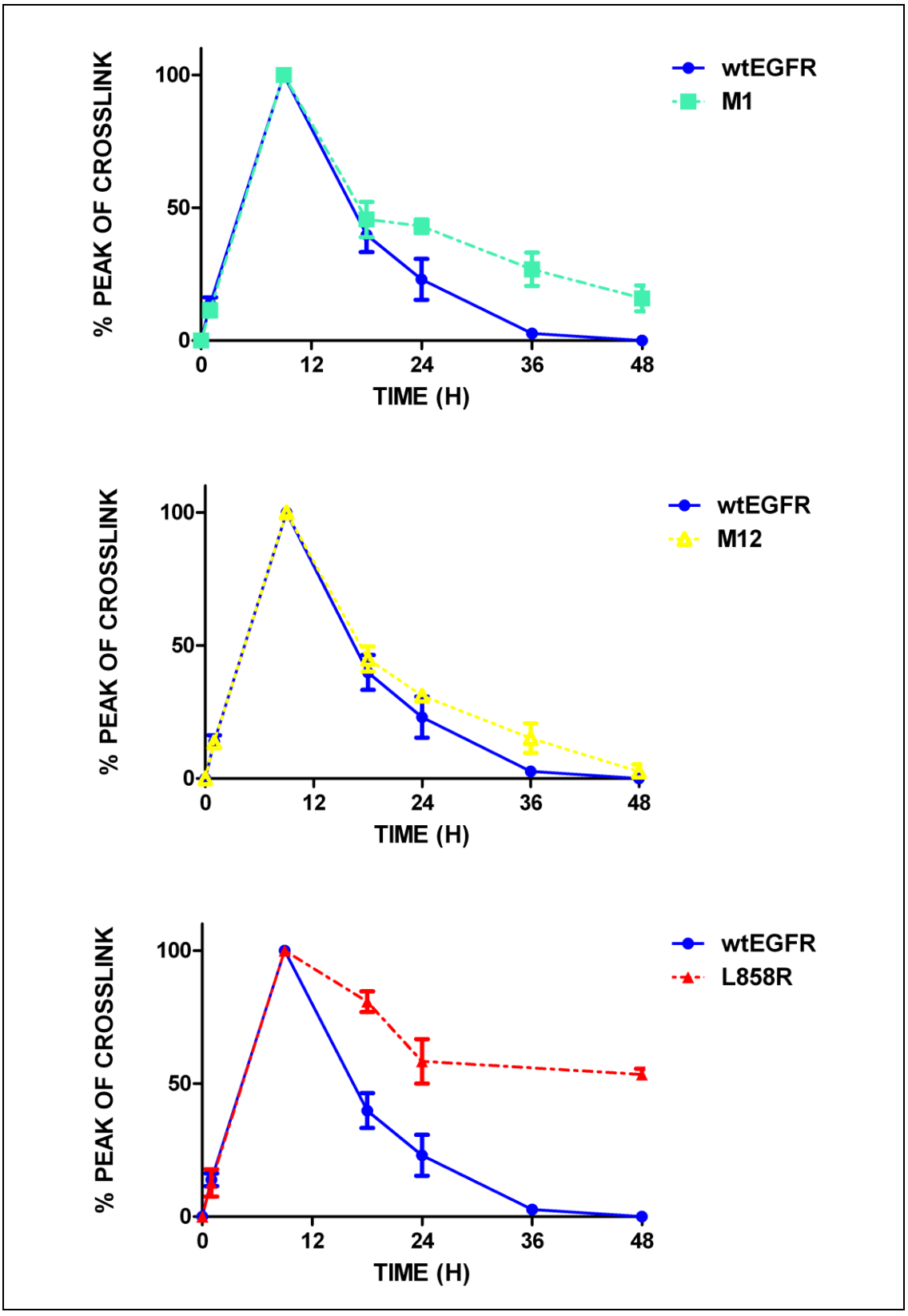

Figure 4.5: cont.

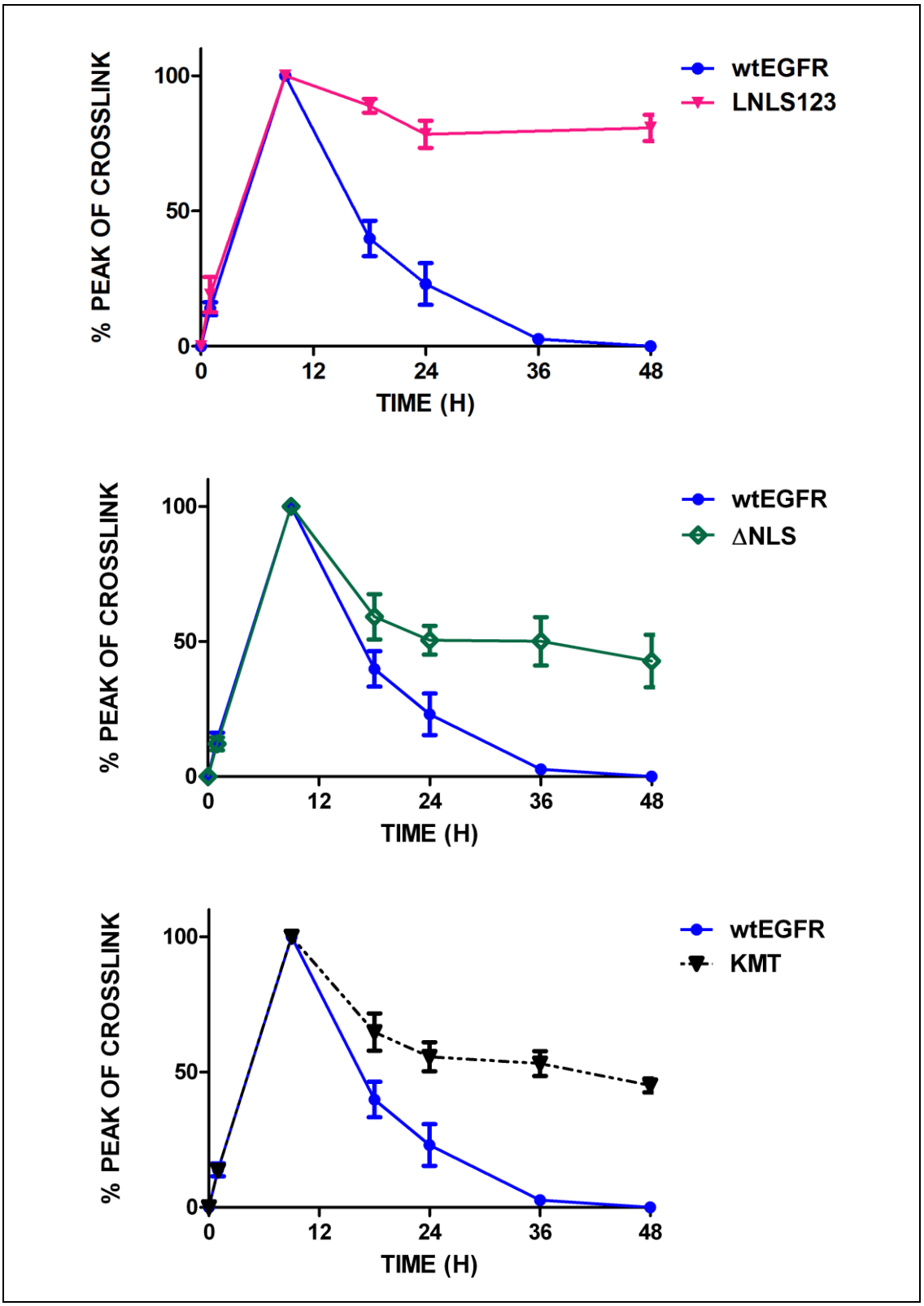

Figure 4.5: cont.

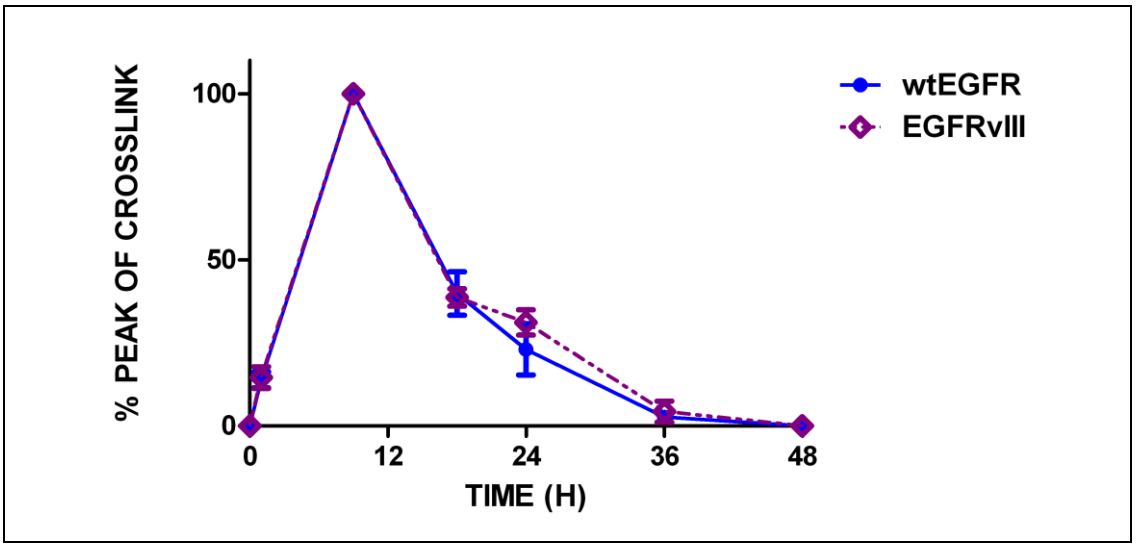

Fig 4.5: cont.

Cisplatin (50μM)	wtEGFR	
Time (h)	% Peak of ICLs	SD (±)
0.00	0.00	0.00
1.00	13.88	2.38
9.00	100.00	0.00
18.00	39.86	6.56
24.00	23.06	7.67
36.00	2.34	0.59
48.00	0.00	0.00

	VC			NLS123		
	% Peak of ICLs	SD (±)	P value	% Peak of ICLs	SD (±)	P value
	0.00	0.00	P > 0.05	0.00	0.00	P > 0.05
	29.01	13.16	P<0.001	12.04	9.83	P > 0.05
	100.00	0.00	P > 0.05	100.00	0.00	P > 0.05
	49.35	9.56	P > 0.05	92.12	1.76	P<0.001
	35.95	1.83	P<0.01	82.04	2.21	P<0.001
	26.24	6.19	P<0.001	77.46	4.07	P<0.001
	0.00	0.00	P > 0.05	74.21	4.07	P<0.001

Cisplatin (50μM)	L858R			LNLS123			EGFRvIII		
Time (h)	% Peak of ICLs	SD (±)	P value	% Peak of ICLs	SD (±)	P value	% Peak of ICLs	SD (±)	P value
0.00	0.00	0.00	P > 0.05	0.00	0.00	P > 0.05	0.00	0.00	P > 0.05
1.00	12.72	5.14	P > 0.05	19.11	6.48	P > 0.05	14.58	3.22	P > 0.05
9.00	100.00	0.00	P > 0.05	100.00	0.00	P > 0.05	100.00	0.00	P > 0.05
18.00	80.77	3.89	P<0.001	88.88	2.59	P<0.001	38.68	2.65	P > 0.05
24.00	58.36	8.34	P<0.001	78.34	5.05	P<0.001	31.16	3.81	P > 0.05
36.00	54.23	6.47	P<0.001	79.52	4.20	P<0.001	3.32	1.58	P > 0.05
48.00	53.43	2.13	P<0.001	80.70	4.82	P<0.001	0.00	0.00	P > 0.05

Cisplatin (50μM)	M1			M12			KMT		
Time (h)	% Peak of ICLs	SD (±)	P value	% Peak of ICLs	SD (±)	P value	% Peak of ICLs	SD (±)	P value
0.00	0.00	0.00	P > 0.05	0.00	0.00	P > 0.05	0.00	0.00	P > 0.05
1.00	11.42	2.33	P > 0.05	13.63	0.00	P > 0.05	13.64	1.00	P > 0.05
9.00	100.00	0.00	P > 0.05	100.00	0.00	P > 0.05	100.00	0.00	P > 0.05
18.00	45.56	6.64	P > 0.05	44.92	4.73	P > 0.05	64.80	6.87	P<0.001
24.00	43.04	2.58	P<0.001	31.16	1.71	P > 0.05	55.62	5.34	P<0.001
36.00	26.84	6.27	P<0.001	15.20	5.54	P<0.01	53.15	4.59	P<0.001
48.00	15.91	4.87	P<0.001	2.59	2.73	P > 0.05	45.05	2.56	P<0.001

Cisplatin (50μM)	ΔNLS		
Time (h)	% Peak of ICLs	SD (±)	P value
0.00	0.00	0.00	P > 0.05
1.00	12.11	2.38	P > 0.05
9.00	100.00	0.00	P > 0.05
18.00	59.13	8.37	P<0.001
24.00	50.45	5.29	P<0.001
36.00	50.06	8.95	P<0.001
48.00	42.79	9.72	P<0.001

Table 4.2: Statistical analysis of the cisplatin induced damage repair assay. Tables show the average value of three independent experiments. P values obtained with the 2-way Anova statistical analysis represent the comparison between all the mutants and to wtEGFR transfected cells

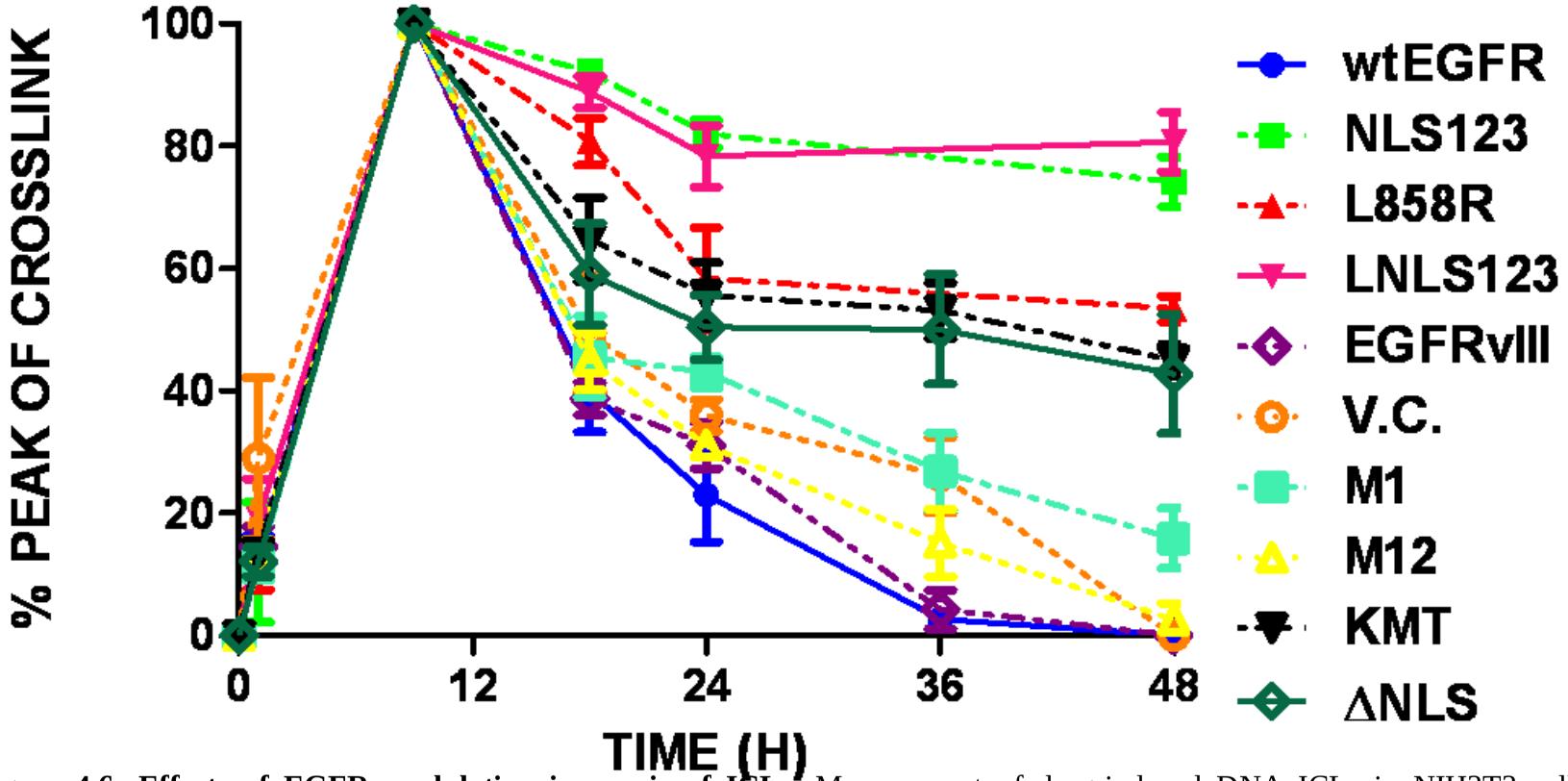

Figure 4.6: Effects of EGFR modulation in repair of ICLs. Measurement of drug-induced DNA ICLs in NIH3T3 cells transfected with wtEGFR, NLS123, L858R, LNLS123, EGFRvIII, Vector control, M1, M12, KMT, ΔNLS treated with 50μM cisplatin alone. Error bars represent standard deviation. The graph shows the average value of three independent experiments. The levels of ICL is normalised to the peak of ICL at 9 hours.

4.2.3 Effects of gefitinib on cisplatin induced ICLs formation and repair

The use of gefitinib in combination with cisplatin has shown to have a poor clinical outcome in tumours presenting EGFR overexpression and/or secondary acquired somatic mutations (Giaccone et al, 2004a; Normanno, 2005; Oliveras-Ferraros et al, 2008). The effect of the single agent gefitinib on the EGFR modulation of cisplatin DNA damage repair was therefore investigated. NIH3T3 cells transfected with wtEGFR, NLS123, L858R, LNLS123 or VC were pre-treated with 2μM gefitinib for 1hour prior to treatment with cisplatin as previously reported (Moasser et al, 2001). Following treatment of 50 μM cisplatin for 1 hour in serum free media containing 2 μM gefitinib, cells were further incubated in media containing 2 μM gefitinib and samples were collected over a period of 48 hours. Fig 4.7 shows the percentage of peak of crosslinks results obtained from the analysis of the comet assay. There was no difference in the peak formation of the ICLs in all the mutants. Despite treatment with gefitinib showed inhibition of cisplatin unhooking in cells expressing wtEGFR (66.18 ± 8.88 % unhooking by 48 hours), there was a significant difference when compared to unhooking in NLS123 (35.88 ± 1.74 %), L858R (41.74 ± 9.38%) and LNLS123 (25.48 ± 6.92%) expressing cells (Table 4.3). Statistical significance was also found when the unhooking of cisplatin ICLs in wtEGFR expressing cells was compared to VC expressing cells with wtEGFR expressing cells showing 22.57 % less unhooking (Table 4.3). Next, the results of the cisplatin unhooking in cells treated with gefitinib were compared to the unhooking of cells treated with cisplatin alone (Fig 4.8). Interestingly, only cells expressing wtEGFR treated with gefitinib showed significant differences at all the time points following peak of crosslinks (Table 4.4). L858R expressing cells showed statistical significance at 18 hours (19.43 % less unhooking in gefitinib treated cells) and at 24 hours (20.4% less unhooking in gefitinib treated cells) following cisplatin treatment. There was no statistical significant difference when treatment with gefitinib was compared to cisplatin alone in NLS123 or LNLS123 expressing cells (Table 4.4). Only the repair kinetics of wtEGFR transfected cells were impaired when cells were treated with cisplatin in combination with gefitinib.

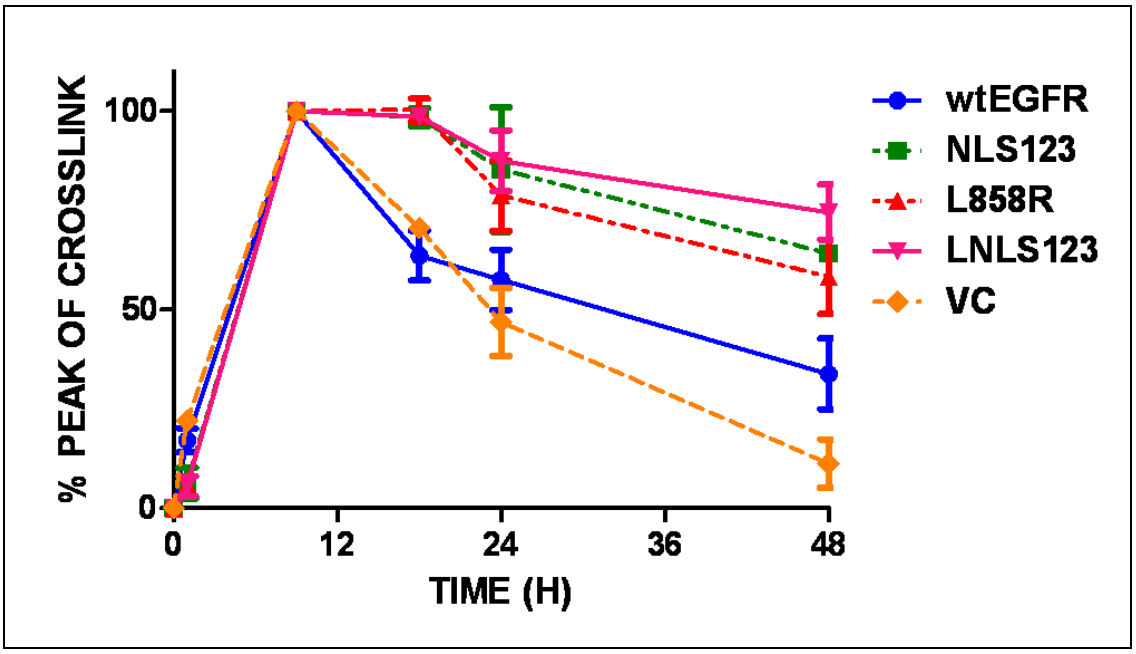

Figure 4.7: Effects of gefitinib on EGFR modulation in repair of ICLs. Measurement of drug-induced DNA ICLs in NIH3T3 cells transfected with wtEGFR, NLS123, L858R, LNLS123, and Vector control pre-treated with 2 μM gefitinib followed by 1 hour 50μM cisplatin with 2 μM gefitinib. Error bars represent standard deviation. The graph shows the average value of two independent experiments. ICL formation is represented as a percentage decrease of the peak of crosslink.

Cisplatin (50μM) + Gefitinib (2μM)	wtEGFR		VC			NLS123		
Time (h)	% Peak of ICLs	SD (±)	% Peak of ICLs	SD (±)	P value	% Peak of ICLs	SD (±)	P value
0.00	0.00	0.00	0.00	0.00	P > 0.05	0.00	0.00	P > 0.05
1.00	17.09	3.00	22.04	2.02	P > 0.05	6.27	3.93	P > 0.05
9.00	100.00	0.00	100.00	0.00	P > 0.05	100.00	0.00	P > 0.05
18.00	63.61	6.30	70.52	0.75	P > 0.05	98.39	2.31	P<0.001
24.00	57.56	7.61	46.87	8.52	P > 0.05	85.30	15.67	P<0.001
48.00	33.82	8.88	11.25	6.10	P<0.01	64.12	1.74	P<0.001

Cisplatin (50μM) + Gefitinib (2μM)	L858R			LNLS123		
Time (h)	% Peak of ICLs	SD (±)	P value	% Peak of ICLs	SD (±)	P value
0.00	0.00	0.00	P > 0.05	0.00	0.00	P > 0.05
1.00	5.93	1.34	P > 0.05	5.60	2.49	P > 0.05
9.00	100.00	0.00	P > 0.05	100.00	0.00	P > 0.05
18.00	100.20	2.89	P<0.001	98.57	1.79	P<0.001
24.00	78.76	8.83	P<0.01	87.45	7.66	P<0.001
48.00	58.26	9.38	P<0.001	74.52	6.92	P<0.001

Table 4.3: Statistical analysis of cisplatin induced damage repair assay in cells treated with 2μM gefitinib. Tables show the average value of 2 independent experiments. P values obtained with the 2-way Anova statistical analysis represent the comparison between all the mutants to the wtEGFR transfected cells.

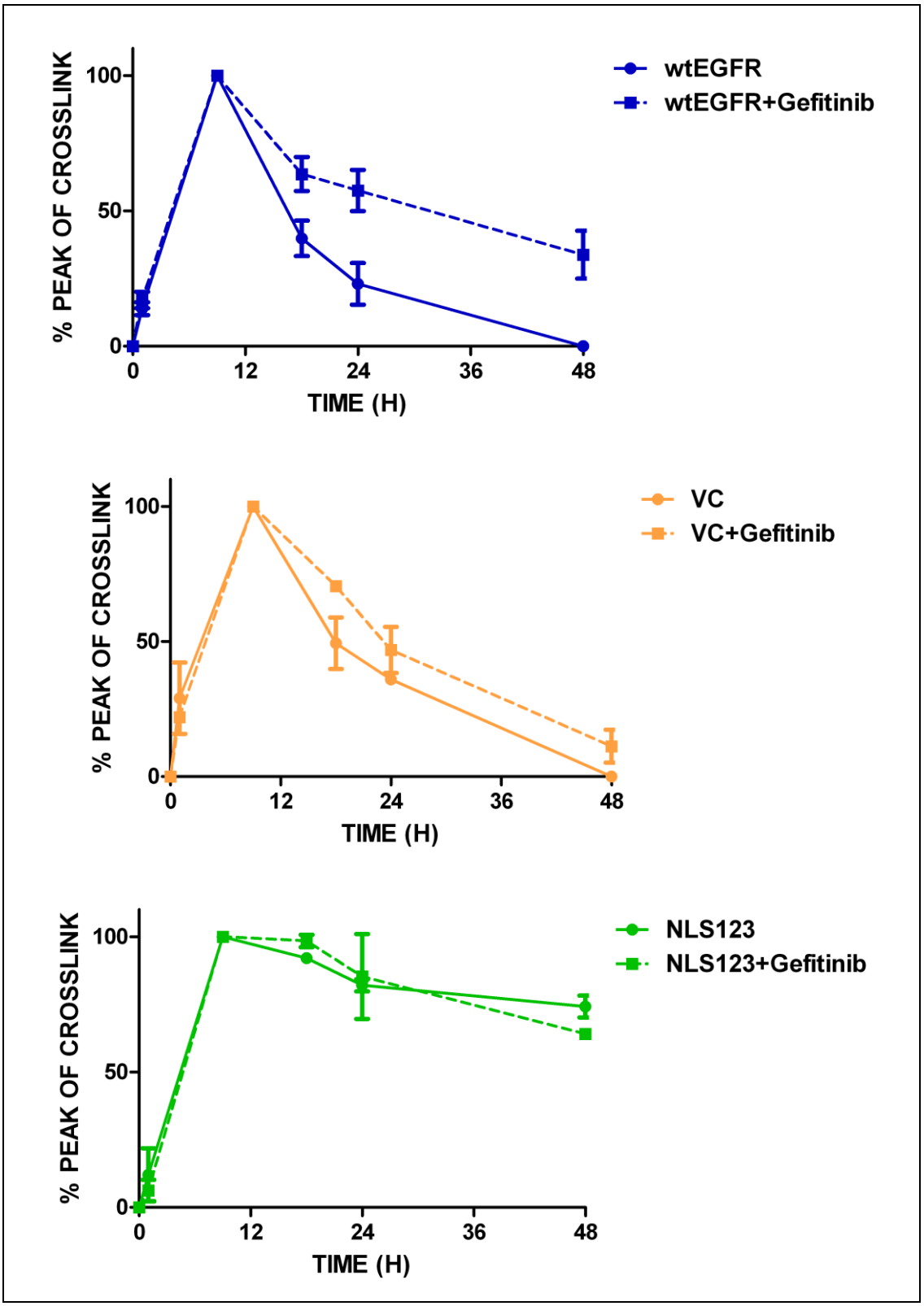

Figure 4.8: ICLs unhooking comparison between transfected cells treated (dotted line) and untreated (complete line) NIH3T3 cells. Error bars represent standard deviation. The graphs represent the single breakdown of the above shown comet assays. ICL formation is represented as a percentage decrease of the peak of crosslink.

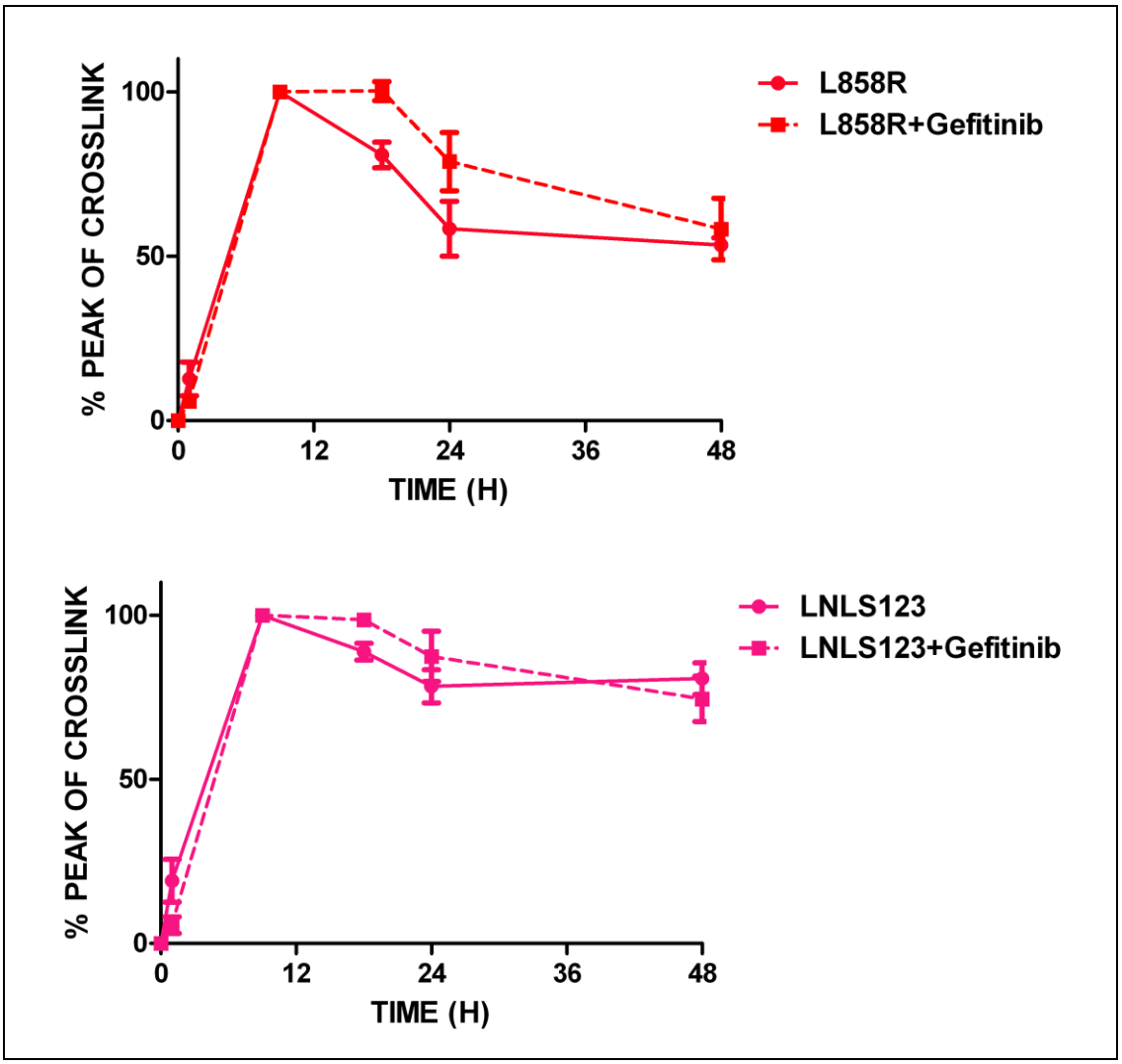

Figure 4.8: cont.

4.2.4 EGFR modulation of IR induced DNA damage repair

4.2.4.1 IR dose response

The dose of IR required to induce detectable DNA damage and sufficient to investigate its repair over time was determined by using the comet assay. NIH3T3 cells transfected with wtEGFR or VC were treated with IR at a dose up to 30 Gy. Since IR produces an immediate physical lesion to the DNA, treated cells were examined after the termination of the exposure. Fig 4.9 shows the results of the dose response obtained from the comet assay. The amount of strand breaks produced is shown as the mean tail moment value of three independent experiments. The data suggest that 15 Gy is the dose necessary to produce sufficient DNA strand breaks to asses repair over time and that EGFR expression does not influence the quantity of detectable DNA damage produced. For this reason the kinetics of repair will be shown as a percentage decrease of tail moment.

wtEGFR vs wtEGFR 2 µM Gefitinib

Cisplatin (50µM)	wtEGFR		wtEGFR Gef.		
Time (h)	% Peak of ICLs	SD (±)	% Peak of ICLs	SD (±)	P value
0.00	0	0.00	0	0	P > 0.05
1.00	13.88	2.38	17.09	2.999007	P > 0.05
9.00	100	0.00	100	7.6294E-06	P > 0.05
18.00	39.86	6.56	63.61	6.303628	P<0.001
24.00	23.06	7.67	57.56	7.608969	P<0.001
48.00	0	0.00	33.82	8.877351	P<0.001

VC vs VC 2 µM Gefitinib

Cisplatin (50µM)	VC		VC Gef.		
Time (h)	% Peak of ICLs	SD (±)	% Peak of ICLs	SD (±)	P value
0.00	0	0.00	0	0.00	P > 0.05
1.00	29.01	13.16	22.04	2.02	P > 0.05
9.00	100	0.00	100	0.00	P > 0.05
18.00	49.35	9.56	70.52	0.75	P<0.01
24.00	35.95	1.83	46.87	8.52	P > 0.05
48.00	0	0.00	11.25	6.10	P > 0.05

NLS123 vs NLS123 2 µM Gefitinib

Cisplatin (50µM)	NLS123		NLS123 Gef.		
Time (h)	% Peak of ICLs	SD (±)	% Peak of ICLs	SD (±)	P value
0.00	0	0.00	0	0.00	P > 0.05
1.00	12.04	9.83	6.272	3.93	P > 0.05
9.00	100	0.00	100	0.00	P > 0.05
18.00	92.12	1.76	98.39	2.31	P > 0.05
24.00	82.04	2.21	85.3	15.67	P > 0.05
48.00	74.21	4.07	64.12	1.74	P > 0.05

L858R vs L858R 2 µM Gefitinib

Cisplatin (50µM)	L858R		L858R Gef.		
Time (h)	% Peak of ICLs	SD (±)	% Peak of ICLs	SD (±)	P value
0.00	0	0.00	0	0.00	P > 0.05
1.00	12.72	5.14	5.93	1.34	P > 0.05
9.00	100	0.00	100	0.00	P > 0.05
18.00	80.77	3.89	100.2	2.89	P<0.01
24.00	58.36	8.34	78.76	8.83	P<0.01
48.00	53.43	2.13	58.26	9.38	P > 0.05

LNLS123 vs LNLS123 2 µM Gefitinib

Cisplatin (50µM)	LNLS123		LNLS123 Gef.		
Time (h)	% Peak of ICLs	SD (±)	% Peak of ICLs	SD (±)	P value
0.00	0	0.00	0	0.00	P > 0.05
1.00	19.11	6.48	5.597	2.49	P < 0.05
9.00	100	0.00	100	0.00	P > 0.05
18.00	88.88	2.59	98.57	1.79	P > 0.05
24.00	78.34	5.05	87.45	7.66	P > 0.05
48.00	80.7	4.82	74.52	6.92	P > 0.05

Table 4.4: Statistical analysis of cisplatin induced damage repair assay in cells treated with2 µM gefitinib compared to cells untreated with gefitinib. Tables show P values obtained with the 2 way Anova statistical analysis represent the comparison between cell treated vs untreated with gefitinib but transfected with the same construct.

4.2.4.2 DNA repair kinetics following IR treatment

Next, the effect of all the EGFR constructs (reported in Fig 4.1) on repair of stand breaks induced by IR was investigated. NIH3T3 cells were transfected with wtEGFR, NLS123, L858R, LNLS123, M1, M12, KMT, ΔNLS, EGFRvIII or VC. Following 48 hours transfection, cells were treated with 15 Gy IR and repair of IR-induced DNA-SB was examined. This is shown as percentage of tail moment calculated from the tail moment detected immediately following irradiation, over a period of 4 hours. Fig 4.10 shows the difference in repair kinetics between wtEGFR and single construct transfected cells. Following treatment with IR alone, repair of strand breaks was rapid in all the cell lines. Table 4.5 shows the statistical comparison between single constructs and wtEGFR transfected cells. Significant differences (P value <0.001) in repair kinetics between wtEGFR and NLS123, L858R, LNLS123, M1, M12, KMT or ΔNLS were found already at 30 minutes following radiation (Table 4.4). The decrease of tail moment was 100% in both wtEGFR and EGFRvIII-expressing cell lines at 4 hours following treatment, indicating repair of SB. In contrast, at 4 hours, cells expressing NLS123 and LNLS123 showed significant delay in repair of SBs with 22.48 ± 3.72 % and 24.94 ± 1.45 % of unrepaired SBs. Intermediate levels of repair were observed for cells expressing L858R (12.33 ±1.00 %), KMT (18.86±3.45%), ΔNLS (17.38±5.06 %), M1 (8.51±1.12%) and M12 (9.28±2.26%). The results are graphically grouped together in Fig 4.11 where the kinetics of all mutants are shown on the same graph.

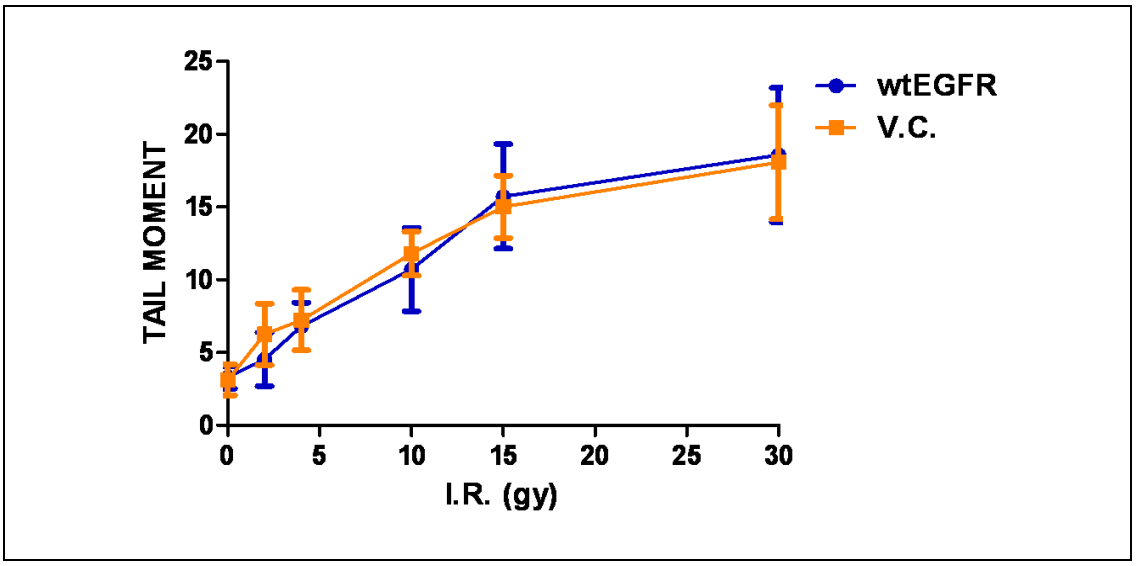

Figure 4.9: 15 Gy IR induces optimal levels of detectable DNA damage. NIH3T3 cells transfected with wtEGFR or VC were treated with 1, 3, 10, 15, 30 Gy IR. Cells were collected immediately following irradiation to determine the tail moment. The graph shows the average values from three independent experiments. Error bars represent standard deviation.

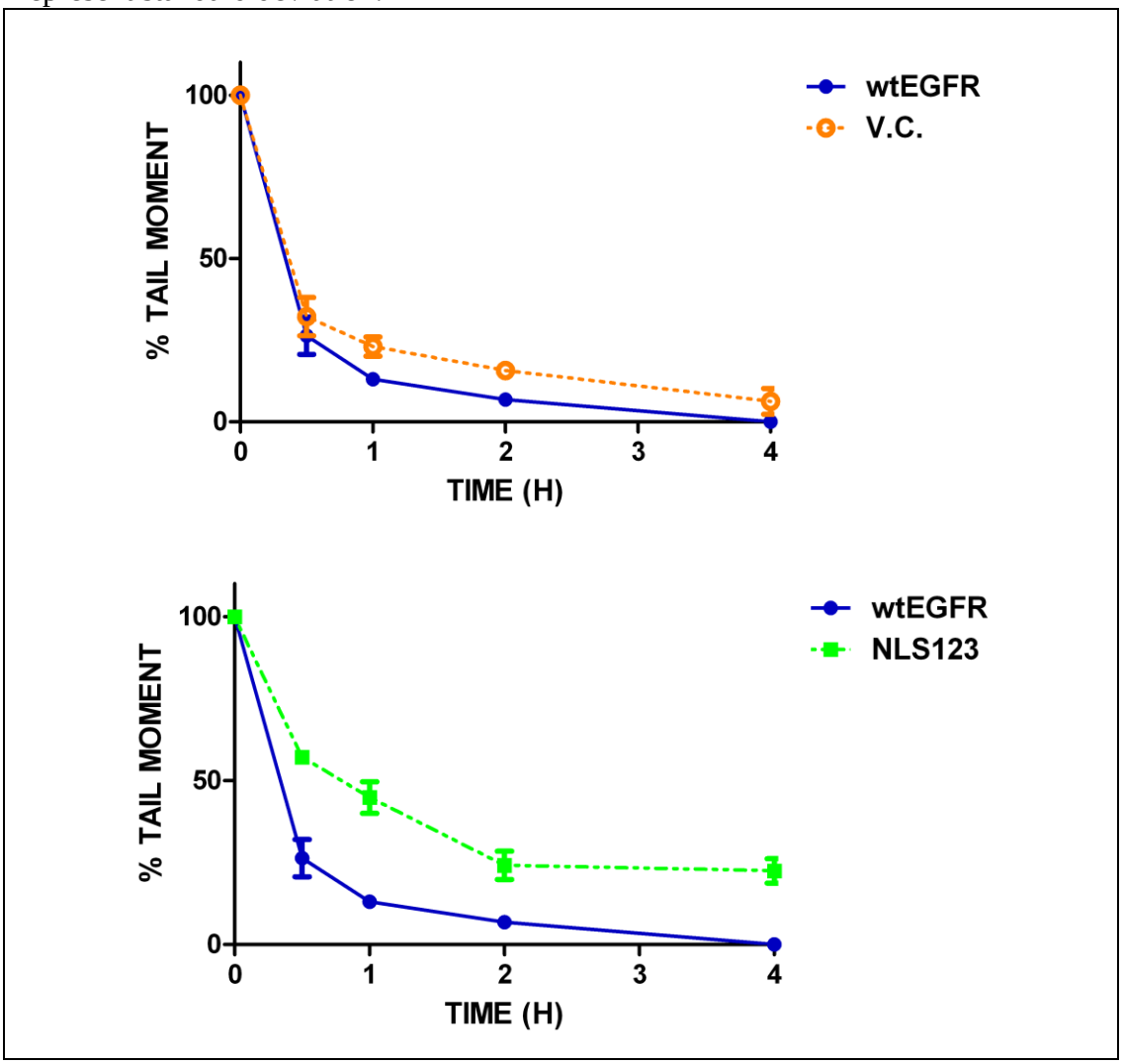

Figure 4.10: Effects of EGFR modulation on repair of Strand breaks. Repair of single mutants compared to repair by wtEGFR.

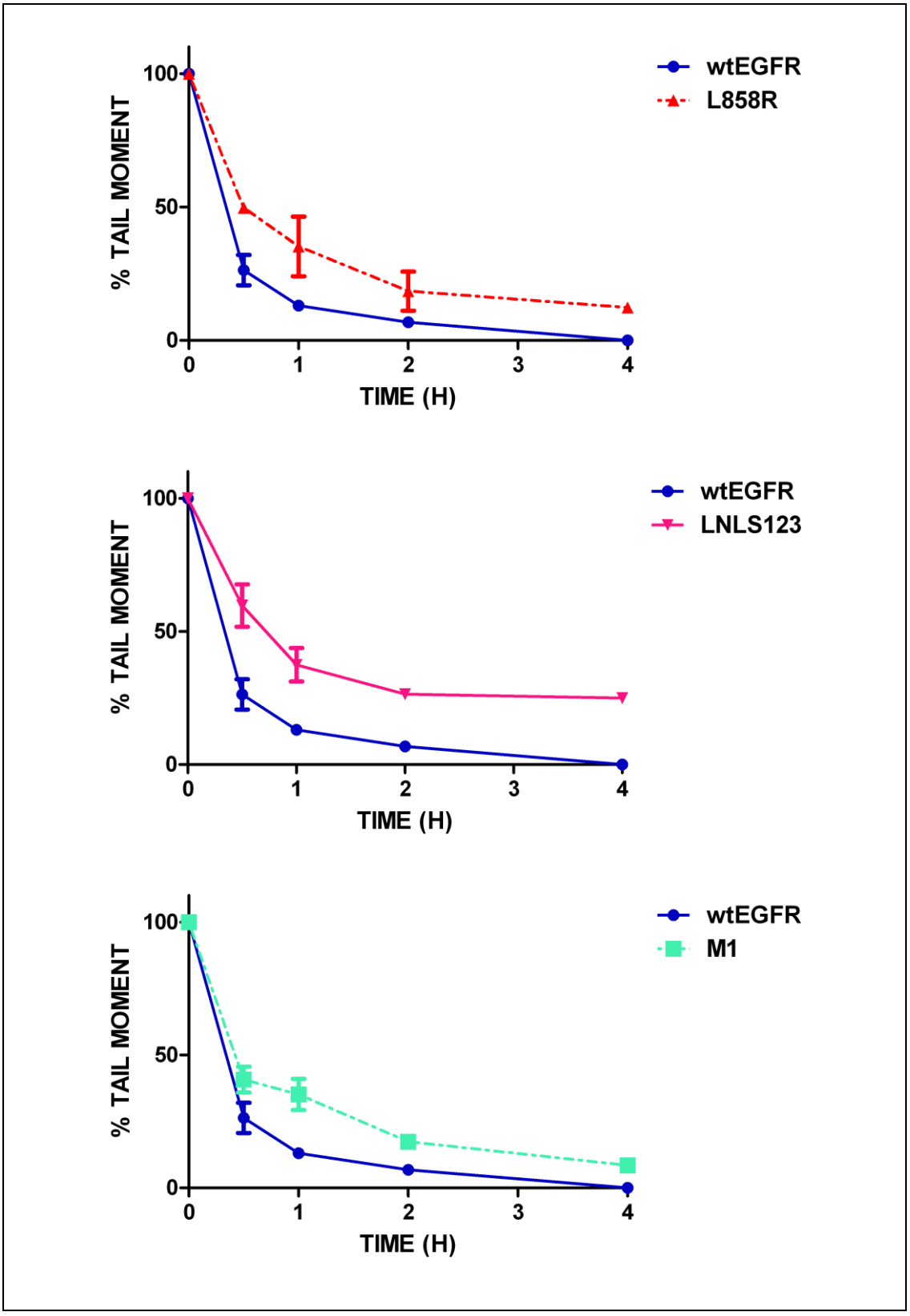

Figure 4.10: cont.

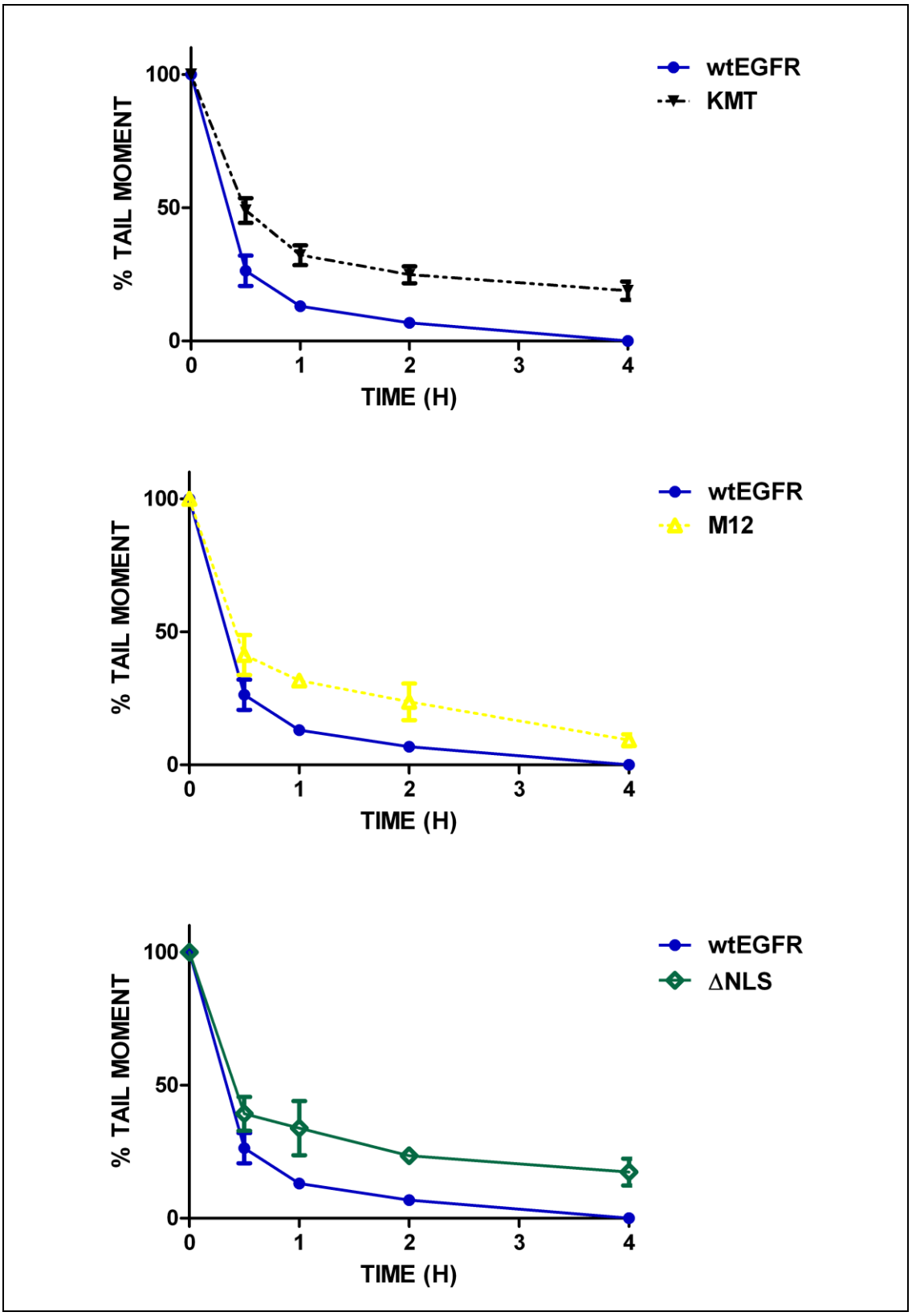

Figure 4.10: cont.

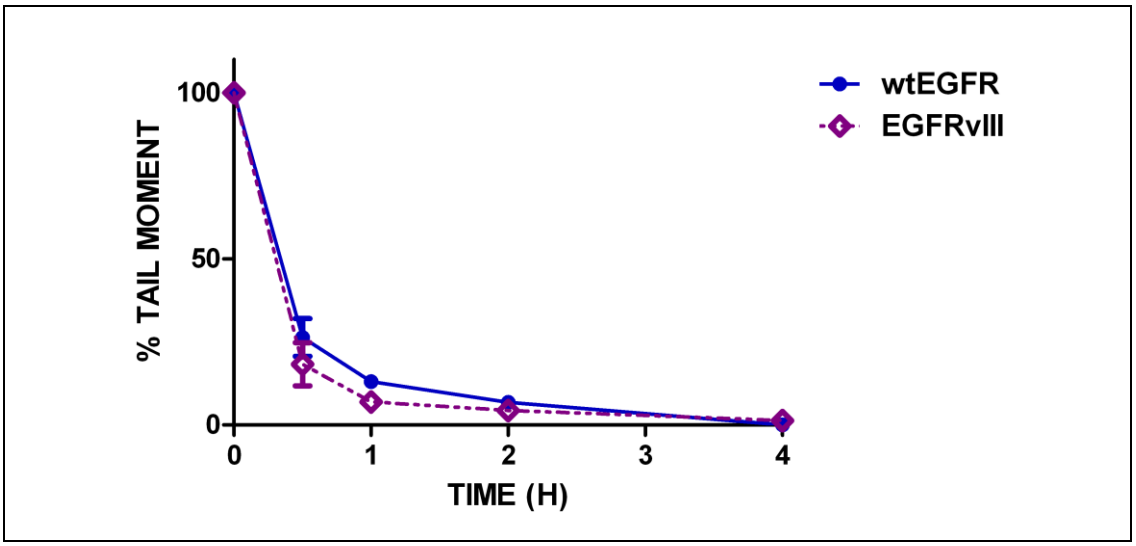

Figure 4.10: cont.

IR (15 Gy)	wtEGFR		
Time (h)	% Tail moment	SD (±)	
0.00	100.00	0.00	
0.50	27.98	6.00	
1.00	14.85	1.01	
2.00	6.81	1.17	
4.00	0.00	0.00	

	VC		
% Tail moment	SD (±)	P value	
100.00	0.00	P > 0.05	
33.92	3.20	P > 0.05	
25.81	0.91	P<0.01	
17.02	1.58	P < 0.05	
7.97	3.30	P > 0.05	

	NLS123		
% Tail moment	SD (±)	P value	
100.00	0.00	P > 0.05	
57.13	1.18	P<0.001	
44.84	4.80	P<0.001	
24.14	4.30	P<0.001	
22.48	3.72	P<0.001	

IR (15 Gy)	L858R		
Time (h)	% Tail moment	SD (±)	P value
0.00	100.00	0.00	P > 0.05
0.50	49.74	2.04	P<0.001
1.00	35.26	11.19	P<0.001
2.00	18.46	7.34	P<0.01
4.00	12.33	1.00	P<0.01

	LNLS123		
% Tail moment	SD (±)	P value	
100.00	0.00	P > 0.05	
59.75	7.97	P<0.001	
37.49	6.29	P<0.001	
26.48	1.88	P<0.001	
24.94	1.45	P<0.001	

	EGFRvIII		
% Tail moment	SD (±)	P value	
100.00	0.00	P > 0.05	
18.31	6.50	P < 0.05	
5.16	0.99	P < 0.05	
3.62	0.50	P > 0.05	
1.32	1.63	P > 0.05	

IR (15 Gy)	M1		
Time (h)	% Tail moment	SD (±)	P value
0.00	100.00	0.00	P > 0.05
0.50	40.74	4.85	P<0.01
1.00	35.14	5.88	P<0.001
2.00	17.35	0.98	P < 0.05
4.00	8.51	1.12	P > 0.05

	M12		
% Tail moment	SD (±)	P value	
100.00	0.00	P > 0.05	
41.29	7.51	P<0.001	
31.69	0.97	P<0.001	
23.69	6.84	P<0.001	
9.28	2.26	P < 0.05	

	KMT		
% Tail moment	SD (±)	P value	
100.00	0.00	P > 0.05	
48.98	4.62	P<0.001	
32.20	3.71	P<0.001	
24.88	3.17	P<0.001	
18.86	3.45	P<0.001	

IR (15 Gy)	ΔNLS		
Time (h)	% Tail moment	SD (±)	P value
0.00	100.00	0.00	P > 0.05
0.50	39.27	6.38	P<0.01
1.00	33.87	10.20	P<0.001
2.00	23.52	0.00	P<0.001
4.00	17.38	5.06	P<0.001

Table 4.4: Statistical analysis of IR-induced DNA SB repair assay in cells treated with 15 Gy IR. Tables show the average values of 3 independent experiments. P values obtained with the 2 way Anova statistical analysis represent the comparison between all the mutants to the wtEGFR transfected cells.

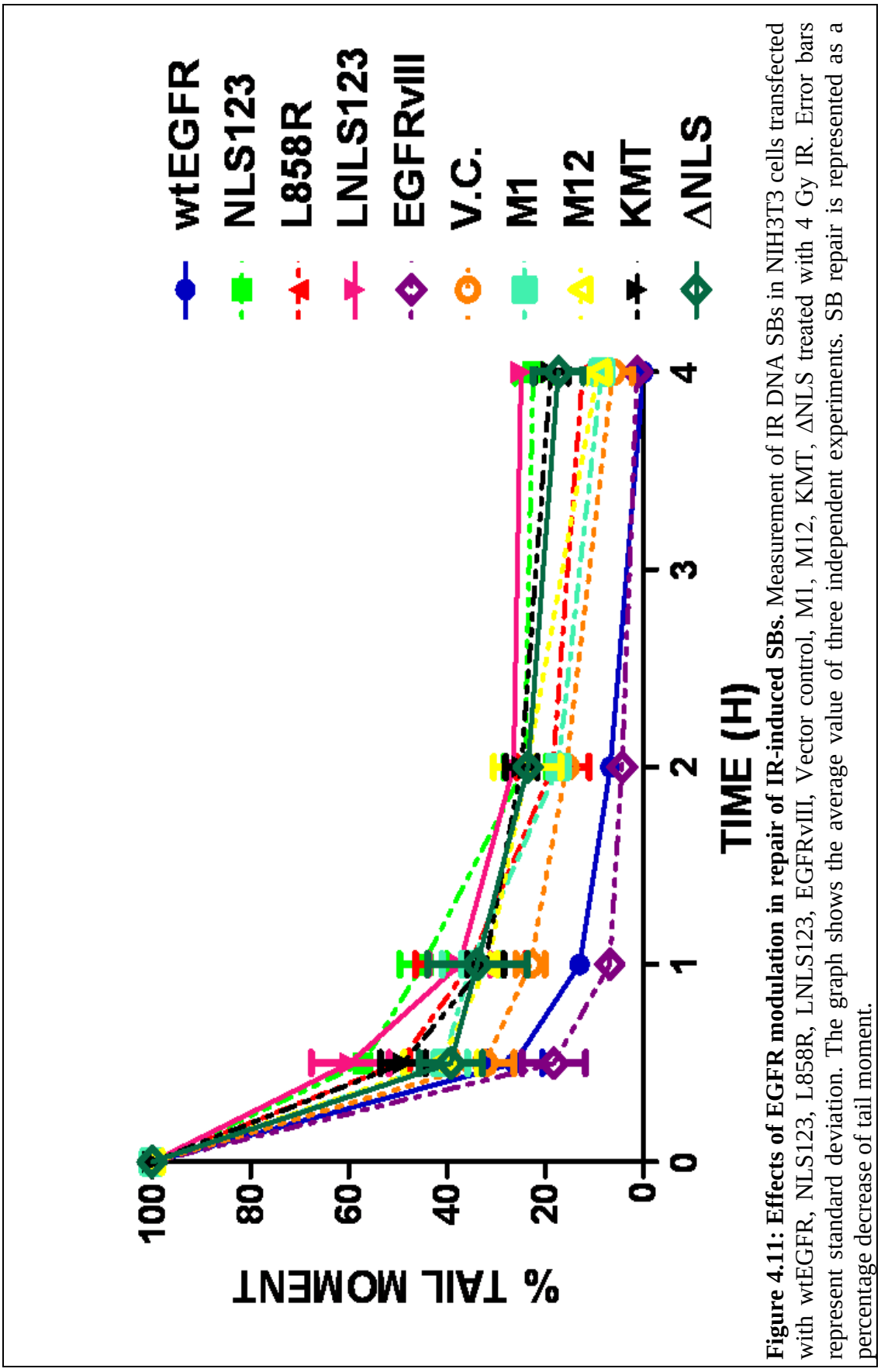

Figure 4.11: Effects of EGFR modulation in repair of IR-induced SBs. Measurement of IR DNA SBs in NIH3T3 cells transfected with wtEGFR, NLS123, L858R, LNLS123, EGFRvIII, Vector control, M1, M12, KMT, ΔNLS treated with 4 Gy IR. Error bars represent standard deviation. The graph shows the average value of three independent experiments. SB repair is represented as a percentage decrease of tail moment.

4.2.5 Cisplatin induced EGFR-DNAPKcs binding

Previous studies have demonstrated the association of EGFR and DNAPKcs following IR suggesting an intrinsic link between EGFR nuclear localisation and DNAPKcs association and activation (Dittmann et al, 2005a; Dittmann et al, 2008a; Golding et al, 2009; Rodemann et al, 2007). The timing of this association and its significance have not been described following cisplatin treatment, although already reported following cisplatin treatment (Hsu et al, 2009). EGFR-DNAPKcs association and its involvement in the mechanism of cisplatin repair was investigated. Since the modulation in repair kinetics in wtEGFR expressing cells was already detectable at 18 hours following cisplatin treatment the association between EGFR and DNAPKcs was investigated over a period of 24 hours following cisplatin treatment. NIH3T3 cells were transfected with wtEGFR and 48 hour following transfection they were treated with 50μM cisplatin. Cells were then collected at various time points up to 24 hours following treatment. Protein extracts were immunoprecipitated using an anti-DNAPKcs monoclonal antibody and blotted with an anti-EGFR antibody. Fig 4.12 shows a time dependent association of EGFR and DNAPKcs with a 2.7-fold increase at 18 hours following cisplatin treatment.

4.2.6 EGFR-DNAPKcs binding following cisplatin treatment does not correlate with EGFR activation

Next the cisplatin-induced activation in all the mutants and their binding with DNAPKcs was examined. NIH3T3 cells transfected with wtEGFR, M1, M12, NLS123, L858R, LNLS123, KMT, ΔNLS, EGFRvIII, or VC were treated with 50μM cisplatin. Cells were then collected 18 hours following treatment and protein lysates were immunoprecipitated with anti DNAPKcs and blotted for EGFR and DNAPKcs. Fig 4.13 shows EGFR and DNAPKcs association in wtEGFR, M1, M12 or EGFRvIII transfected cells. In contrast, L858R and LNLS123 transfected cells showed reduced EGFR-DNAPKcs binding whereas NLS123, KMT or ΔNLS transfected cells showed no binding. The previous chapter showed that EGFR nuclear localisation was not dependent on EGFR phosphorylation. Therefore the correlation between EGFR phosphorylation and EGFR-DNAPKcs binding was ivestigated. Cells transfected with wtEGFR, M1, M12, NLS123, L858R, LNLS123, KMT or ΔNLS were treated with cisplatin for one hour and cell lysates were immunoprecipitated with EGFR and blotted with PY20 and EGFR. In Fig 4.14,

wtEGFR, M1, M12, EGFRvIII showed phosphorylation activation following cisplatin treatment, L858R and LNLS123 transfected cells showed constitutive tyrosine phosphorylation. NLS123, KMT, ΔNLS transfected cells showed lack of kinase activation. There was no correlation between EGFR activation and EGFR-DNAPKcs binding as different constitutively active mutants showed pronounced (EGFRvIII) or reduced (L858R, LNLS123) association with DNAPKcs.

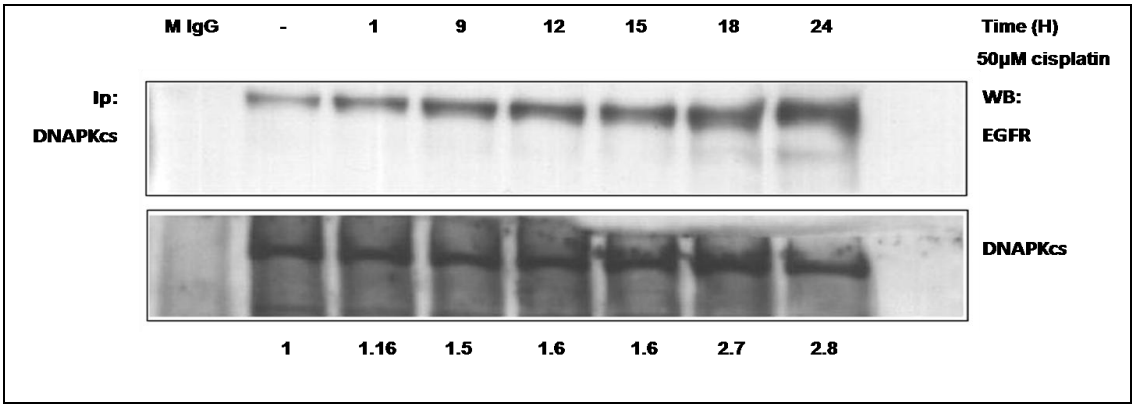

Figure 4.12: DNAPKcs-EGFR association over time. wtEGFR Transfected NIH3T3 cells were treated with 50μM cisplatin for 1 hour in serum free media. Cells were then lysed at 1, 9, 12, 15, 18, 24, hours following treatment. 750μg of protein lysate were immunoprecipitated using anti DNAPKcs and blotted with anti EGFR and anti DNAPKcs. EGFR pull down was quantified by 2D densitometry analysis and shown as a fold binding compared to the untreated control. Mouse unrelated antibody (M IGg) was used as negative control.

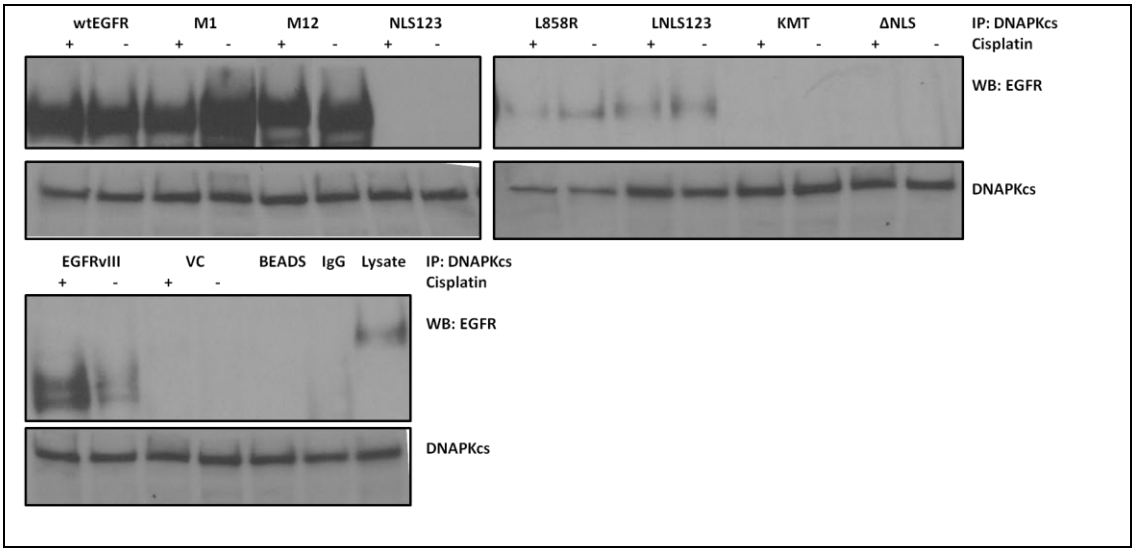

Figure 4.13: DNAPKcs-EGFR association. NIH3T3 cells were transfected with all the mutants reported in Fig 4.1. 48 hours following transfection cells were treated with 50μM cisplatin for 1 hour in serum free media. Cells were then lysed 18 hours following treatment. 750μg of protein lysate were immunoprecipitated using anti DNAPKcs and blotted with anti EGFR and anti DNAPKcs.

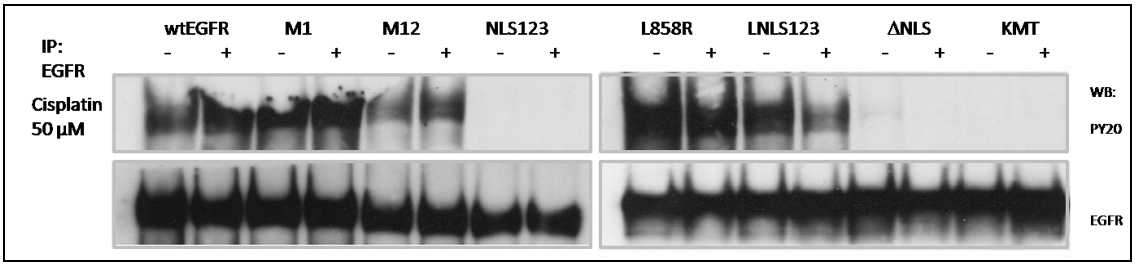

Figure 4.14: EGFR mutants' activation. NIH3T3 cells were transfected with all the mutants reported in Fig 4.1. 48 hours following transfection cells were treated with 50μM cisplatin for 1 hour in serum free media. Cells were then lysed immediately following treatment. 750μg of protein lysate were immunoprecipitated using anti EGFR and blotted with anti PY20 and anti EGFR.

4.2.7 EGFR and DNAPKcs cellular localisation following IR or cisplatin

Next, the cellular localisation of both EGFR and DNAPKcs following cisplatin (Fig 4.15 A-B) or IR (Fig 4.16 A-B) was investigated to determine whether the role of EGFR nuclear translocation in the repair of SB or ICL DNA damage was related also to and the EGFR-DNAPKcs binding. Cells transfected with wtEGFR, M1, M12, NLS123, L858R, LNLS123, KMT, ΔNLS, EGFRvIII, or VC were either fixed 18 hours following treatment with 50 μM cisplatin or serum starved for 24 hours and then fixed 20 minutes following 4 Gy IR. Fig 4.15 and 4.16 show the immunofluorescence results obtained via confocal analysis. Cells transfected with wtEGFR, M1, M12 and EGFRvIII showed EGFR nuclear expression following cisplatin or IR. DNAPKcs showed similar pattern of expression in cells transfected with these constructs. In wtEGFR and EGFRvIII transfected cells, EGFR was largely expressed in the nucleus following cisplatin or IR. In contrast M1 and M12 transfected cells showed reduced levels of EGFR nuclear expression.

L858R, KMT and ΔNLS transfected NIH3T3 showed only membrane/cytosolic EGFR localisation following cisplatin or IR. DNAPKcs nuclear expression in L858R cells was reduced compared to wtEGFR and EGFRvIII transfected cells following cisplatin or IR. In contrast, NLS123 and LNLS123 transfected cells showed lack of both DNAPKcs and EGFR nuclear expression.

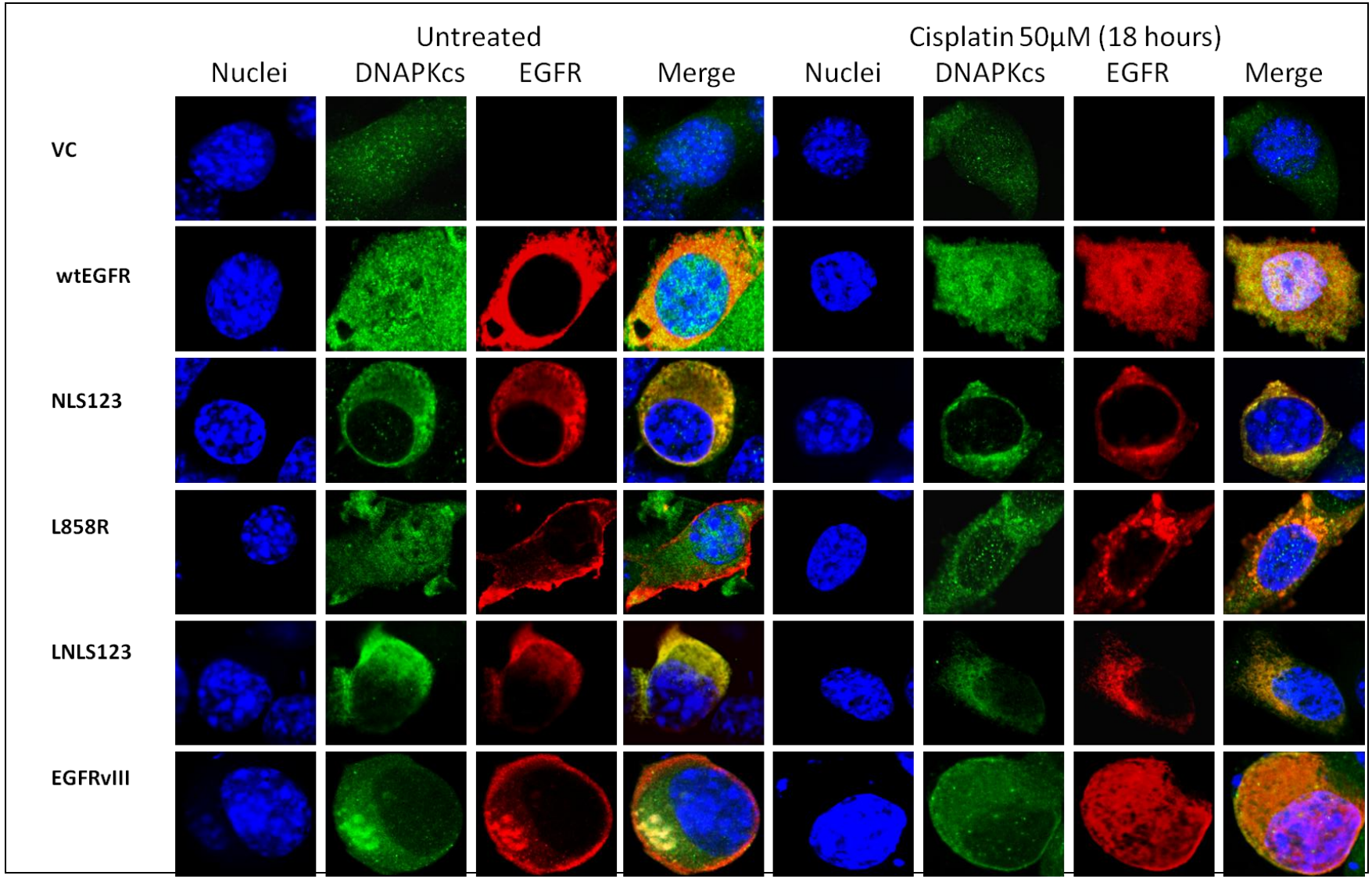
Untreated
Cisplatin 50µM (18 hours)
Nuclei
DNAPKcs
EGFR
Merge
Nuclei
DNAPKcs
EGFR
Merge
VC
wtEGFR
NLS123
L858R
LNLS123
EGFRvIII

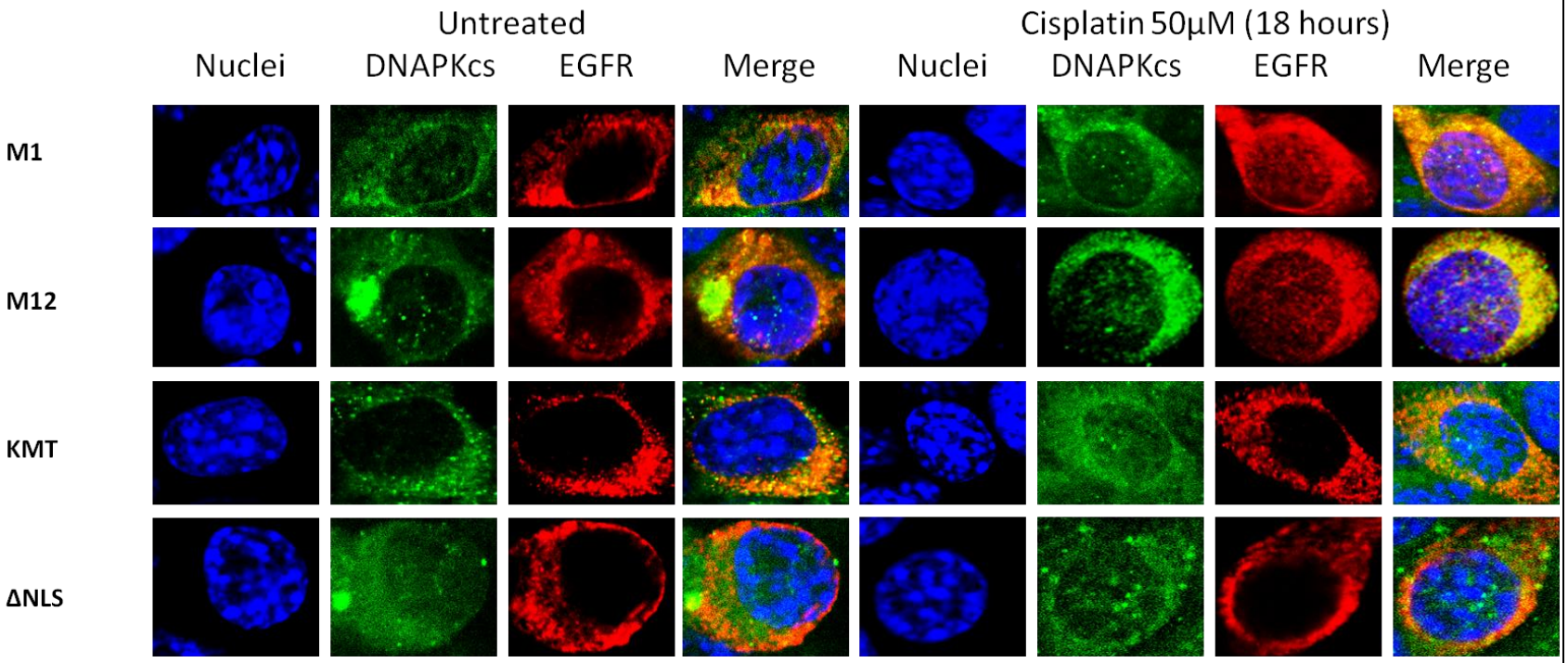

Figure 4.15: EGFR and DNAPKcs cellular localisation following cisplatin treatment. NIH3T3 cells transfected with wtEGFR, NL123, L858R, LNLS123,EGFRvIII, Vector control, M1, M12, KMT, and ΔNLS were treated with 50µM cisplatin for one hour in serum free media and then fixed with 4%PFA 18 hours following treatment.Cells were stained with Goat anti-Rabbit Alexa fluor 647 (EGFR),Goat anti-Mouse Alexa fluor 488 (DNAPKcs), and Dapi (nucleus).

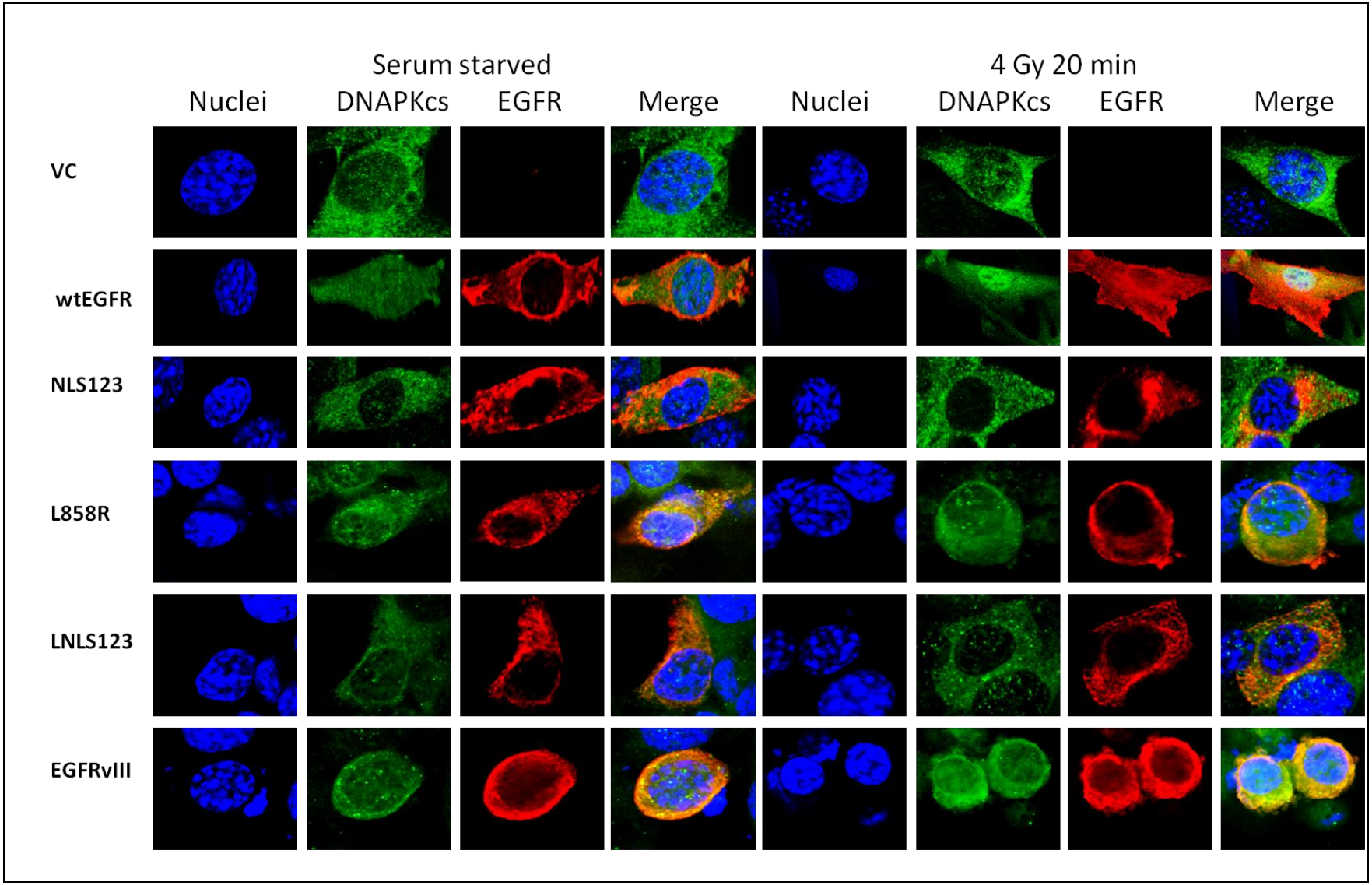
Serum starved
4 Gy 20 min
Nuclei
DNAPKcs
EGFR
Merge
Nuclei
DNAPKcs
EGFR
Merge
VC
wtEGFR
NLS123
L858R
LNLS123
EGFRvIII

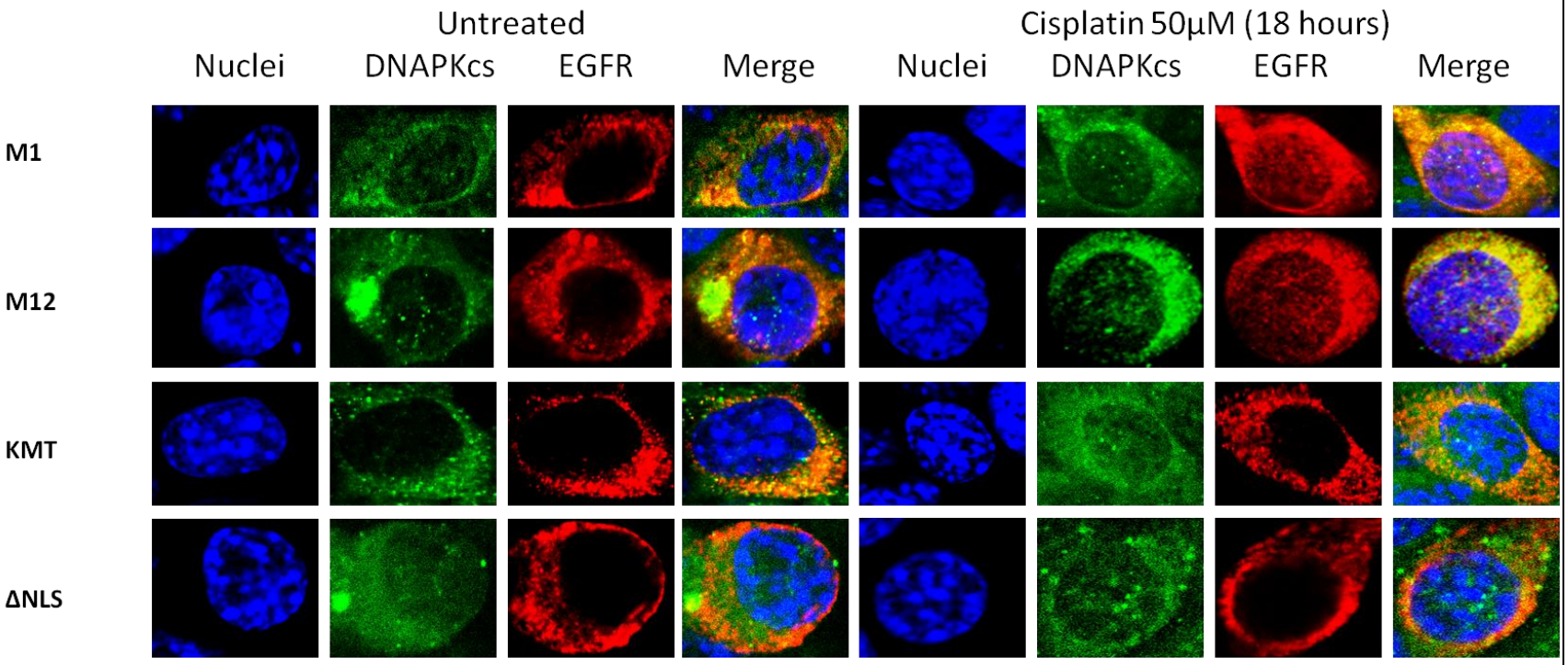

Figure 4.16: EGFR and DNAPKcs cellular localisation following IR treatment. NIH3T3 cells transfected with wtEGFR, NL123, L858R, LNLS123,EGFRvIII, Vector control, M1, M12, KMT, and ΔNLS were serum starved for 24 hours and then treated with 4 Gy and then fixed with 4%PFA 20 min following treatment.Cells were stained with Goat anti-Rabbit Alexa fluor 647 (EGFR),Goat anti-MouseAlexa fluor 488 (DNAPKcs), and Dapi (nucleus).

4.3 DISCUSSION

4.3.1 The NLS sequence is required for nuclear translocation and receptor activation

The data presented in Chapter 3 have confirmed the previously reported EGF and IR induced EGFR nuclear translocation and investigated the NLS123 mutation of the EGFR NLS sequence. The basic Arginine amino acids contained in the NLS/p13+ peptide sequence of the EGFR JX domain are necessary to achieve a conformational change that seems to be a prerequisite to achieve receptor activation. Upon any activating stimulus, the mutant receptors fail to achieve a conformational change that not only prevents activation but also stops the protein from binding to the importin machinery and achieve nuclear translocation. The NLS123 mutation has shown two effects in a wtEGFR background. Firstly it inhibits the protein translocation to the nucleus and secondly it interferes with EGFR phosphorylation, negatively affecting its downstream signalling pathways. This chapter provides evidence for an EGFR role in the modulation of DNA repair following cisplatin or IR induced DNA damage. The data show DNA repair kinetics modulated by the expression of EGFR and also by its capability to translocate to the nucleus. Receptor activation and kinase activity do not seem to be central in this modulation. It appears that binding and the similar localisation pattern with DNAPKcs within the nuclear compartment may be responsible for the enhanced repair kinetics.

4.3.1.2 EGFR modulates the repair of cisplatin-induced ICLs

4.3.1.2.1 DNA repair of cisplatin lesions

The effects of cisplatin and the repair pathways that may be involved in the repair of cisplatin damage are still debated and the literature emphasises that there is more than one pathway at work (Hlavin et al, 2010a; Martin et al, 2008; Wang & Lippard, 2005). It is, in fact, established that cisplatin not only binds to DNA but also to many cellular components that have soft nucleophilic sites such as cytoskeletal microfilaments, RNA, proteins. Only 5-10% of covalently bound associated cisplatin is found in the genomic DNA whereas 75-85% of the drug binds to proteins suggesting that the toxicity of this drug is also mediated by activation of specific signalling pathways that ultimately leads to cell death (Zdraveski et al, 2000).

Although there is evidence suggesting a strong effect on DNA replication it is not completely clear whether replication may be one of the consequences rather than the

reason of the lethality of the treatment (Zorbas and Keppler 2005).This is because in cycling cells the persistence of ICLs may also induce single and double DNA strand breaks (Smeaton et al, 2008; Smeaton et al, 2009). Therefore as a result, the cell machinery blocks replication and transcription allowing sufficient time for DNA repair mechanisms to resolve the crosslinks (Nojima et al, 2005). The pathway responsible for this cellular arrest is not completely characterised but EGFR seems to be involved in the mechanism (Ceppi et al, 2006; Chen et al, 2000; Hiraishi et al, 2008; Hsu et al, 2009; Kim et al, 2009b; Klass et al, 2009; Michaelis et al, 2008; Oliveras-Ferraros et al, 2008; Yoshida et al, 2008).

Because of the variety of DNA damage that arises from cross-linking agents, there are many pathways that are activated to repair these lesions. Their concerted activity is a key element to achieve complete DNA repair. Cross-links are well known to be repaired by Nucleotide excision repair (NER) and post replication repair (PRR) (Clingen et al, 2007; Clingen et al, 2005; De Silva et al, 2002; Hartley et al, 2004; McHugh et al, 2001). Cisplatin adducts are detected by the NER components Xpx/Hr23B and XPA. These then recruit the endonucleases Ercc1-Xpf and Xpg which are the catalytic NER proteins responsible for the dual incision process. The strand affected by the crosslink is incised 5' to the lesion by ERCC1-Xpf and 3'to the lesion by Xpg. Once the lesion is removed the gap is filled by repair synthesis.

In presence of a stalled replication machinery at the site of the lesion, both Translesion DNA synthesis (TLS) and HR are required to help restart replication. TLS fills the gap via RAD6/ RAD18 and specialised polymerases such as Polη, Polκ and Polζ complete repair. HR fills the gap left by the excised lesion by copying the other intact sister DNA as a template. HR could also be required to repair the induced DSB created as an indirect consequence of crosslinked DNA during replication. NHEJ can also be employed to relegate the strands broken as a result of the stalled replication machinery (Nojima et al. 2005c; Kartalou and Essigmann 2001; Cepeda et al. 2007). Some studies have shown that upon defective HR and TLS, mammalian cells seemed to be hypersensitive to crosslinking agents suggesting a minor role of NER (Nojima et al. 2005b), on the other hand there are some other studies that have clearly shown that upon inefficiency of NER components, cells are hypersensitive to cisplatin adducts (Nojima et al. 2005a; De, I et al. 2002; De, I et al. 2000).

4.3.1.2.2 Unhooking is the major determinant in interstrand crosslink repair

The ability of cisplatin to form covalent linkages between two strands of the double helix is without any doubt the basis for its high cellular cytotoxicity (Malinge et al, 1999). If left unrepaired, interstrand crosslinks prevent, virtually, all aspect of DNA metabolism, such as replication, transcription and recombination (Hlavin et al, 2010b). The capability of linking both the DNA strands renders bifunctional crosslinking agents the most genotoxic and mutagenic of compounds. This is, perhaps, the reason why their removal is the most complicated of DNA repair processes (Wang & Lippard, 2005). ICLs repair takes place in two ways. During the first, also called recombination-independent, the lesion is excised (unhooked) on one strand of the helix and the remaining gap is filled by TLS. This process converts the crosslink into a mono-adduct which is, subsequently, resolved by a second cycle of excision repair. In bacteria this process is carried out by NER and Pol II, however it remains unclear in mammalian cells. Although NER has been shown to be a major component, this repair mechanism seems to be clearly minor in cycling mammalian cells; however, in differentiated non-replicating cells it may represent the only way for the removal of ICLs. The second repair mode begins with the excision of the crosslinks and is followed by homologous recombination. This second pathway takes place during the S phase and it is the predominant pathway in cycling mammalian cells. Despite the different modality of DNA synthesis of these two systems, the central step in the repair of crosslinks is still the initial processing /unhooking (Hlavin et al, 2010a; Hlavin et al, 2010b; McCabe et al, 2009; Muniandy et al, 2010; Shrivastav et al, 2009; Smeaton et al, 2009; Tornaletti, 2009; Wang & Lippard, 2005). The context in which the ICL is recognised induces the recruitment of different repair proteins rendering this step incredibly complex.

4.3.1.2.3 Unhooking requires different protein complexes often dependent on the type of bifunctional alkylator

Although many proteins have been implicated the precise mechanism remains to be elucidated. Cycling cells treated with crosslinking reagents accumulate replication fork induced-breaks consisting in a DSB on one end, and a double stranded DNA cross-linked with a single strand in three stranded structure on the other. Different

from *E. coli* and *S. cervisiae*, ICL processing in mammalian cells only requires some of the protein involved in NER. XPF-ERCC1 are structure specific endonucleases capable of making 5' incision at the junction between double stranded DNA and a 3' single stranded region (Clingen et al, 2005). Cells deficient in XPF-ERCC1 show only 15% unhooking of nitrogen mustards (NH2) induced ICLs (assessed by the Comet assay). Other NER components do not seem to be required in the unhooking of NH2 ICLs. In contrast, little or no unhooking of cisplatin induced ICLs has been shown not only in cells deficient in XPF-ERCC1 but also in XPD, XPB or XPG deficient cells implicating all these NER proteins in the unhooking step of cisplatin ICLs (De Silva et al, 2000; McCabe et al, 2009). Interestingly, although all impaired in the unhooking, only cells deficient in XPF-ERCC1 have higher cisplatin sensitivity (37-40 fold more sensitive than their isogenic) compared to the other NER mutant cells (1.3-3.1 fold more sensitive than their parental line) (Hlavin et al, 2010a). In addition the observation that XRCC2 and XRCC3 deficient cells are also highly sensitive to cisplatin treatment, suggests that, as these two proteins, also XPF-ERCC1 may be (additionally) involved in recombinational repair (or DNA re-sysnthesis to fill the gap left by the DNA incision) (De Silva et al, 2002; Smeaton et al, 2009). It is therefore unclear whether the inhibition of unhooking observed in cells deficient in XPF-ERCC1 via the comet assay is actually the product of failed recombination intermediates that result in DNA migrating with the similar retarded mobility as cross-linked DNA (Fisher et al, 2008). Smeaton et al., have also shown NER independent 5' incision, unaffected by the absence of ERCC1-XPF suggesting alternative contributions of these proteins to the unhooking step. This was further confirmed by the finding that the ERCC1-XPF does not function alone and it has been found associated with the SLX4 protein that acts as a scaffolding for this complex as well as for two other nucleases: MUS81-EME1 and SLX1.

Cell free extracts and purified protein experiments have also shown contrasting results (Hlavin et al, 2010a; Smeaton et al, 2008; Smeaton et al, 2009). Bessho et al. have shown that the NER factors XPA, RPA, TFIIH XPC, XPG, ERCC1-XPF, were necessary and sufficient for the incision step and also that cells employ the incision step to relieve the DNA duplex from the distortion at either sides of the ICLs rather than removing the ICLs following its recognition (Bessho et al, 1997). Another study showed the requirement of RPA for both incision (unhooking) and re-synthesis and the essential role of PCNA for DNA synthesis and incision. The same group has also

shown the involvement of the complex containing the Pso4 pre mRNA splicing factor and the Werner Syndorme (WS) helicase activity (stimulated by BRAC1) in the initial ICL processing (Cheng et al, 2006). Recently there has been some evidence of the involvement of Fanconi Anemia (FA) complex in the unhooking of cisplatin ICLs. Although still not fully understood, it seems that FA complex recognises stalled replication forks created by ICLs, recruits protein complexes to this site and induces remodelling of the replication fork allowing repair to proceed. The role of FA proteins in unhooking is controversial. Although cells deficient in FANCA, B, C, D2, F and G or treated with antibodies against FANCA showed reduced incision, the suppression is generally not complete with the 3' incision being more resistant. Many other reports have shown partial or no requirement of these proteins (McCabe et al, 2009; McHugh et al, 2001; Muniandy et al, 2010; Nojima et al, 2005).

4.3.1.2.4 EGFR involvement in Cisplatin repair

The role of EGFR in the response to cisplatin treatment was firstly reported by Benhar M et al. Genotoxic stress induced by cisplatin activates DNA damage signals that culminate in EGFR autophosphorylation in a ligand independent mechanism. While initially it was proposed that EGFR activation induces downstream signalling responsible for cellular death, different groups have shown the contribution of EGFR in the repair of cisplatin lesions (Dittmann et al, 2005a; Friedmann et al, 2004; Friedmann et al, 2006; Oliveras-Ferraros et al, 2008). Recently, a study by Hsu et al., has suggested that nuclear EGFR is involved in the repair of cisplatin DNA damage (Hsu et al, 2009). The study looked at the phosphorylation of H2AX as a marker of DNA damage and of the repair of DSBs. Although their results pointed towards an involvement of nuclear EGFR in cisplatin toxicity, the phosphorylation of H2AX was determined only 12 hours following treatment (cisplatin crosslinks peak at nine hours following treatment) and repair of DSBs is not a good marker to asses the repair kinetics of cisplatin induced damage as DSBs are not directly caused by cisplatin.

4.3.1.3 EGFR constructs that translocate to the nucleus repair cisplatin lesions

This study confirms cisplatin-induced EGFR phosphorylation, shows enhanced repair kinetics in cells expressing EGFR constructs undergoing nuclear translocation and suggests that this mechanism is mediated by EGFR binding with DNAPKcs.

Three distinctive repair behaviours: complete repair, intermediate inhibition and highest inhibition of repair have been observed. Cells transfected with wtEGFR or EGFRvIII show complete repair both by 36 hours following cisplatin. Our data have demonstrated that both wtEGFR and EGFRvIII not only undergo nuclear translocation but that they also bind DNAPKcs following cisplatin. In addition the confocal analysis of wtEGFR and EGFRvIII expressing cells shows similar EGFR and DNAPKcs localisation pattern in the nucleus following cisplatin treatment. Cells that showed intermediate repair inhibition (L858R, KMT, ΔNLS) and highest inhibition of repair (NLS123, LNLS123) correlated to impaired EGFR nuclear translocation.

4.3.2 DNAPKcs involvement in the repair of cisplatin lesions

The matter of whether DNAPKcs promotes, amplifies, transmits stress signals, has been largely debated. The initial studies that looked at the involvement of DNAPKcs in the repair of cisplatin damage showed that cells deficient in DNAPKcs were hypersensitive to cisplatin treatment and that in the parental cell lines although showing quicker repair kinetics, DNAPKcs was not found at the site of the DNA lesion (Boeckman et al, 2005; Turchi et al, 1999; Turchi et al, 2000; Turchi et al, 1996). Subsequently it was reported that cisplatin adducts reduce the rate at which Ku, the subunit of the DNA-PK heterotrimeric complex, slides along the DNA duplex blocking its translocation from the DNA terminus (Pawelczak et al, 2005; Turchi et al, 2000). This resulted in a reduced association of Ku to DNAPKcs and also in the formation of inactive kinase complexes that are unable to resolve DNA breaks suggesting that cisplatin could be used to pre-sensitise cells to radiotherapy treatments (Turchi et al, 2000). However, in 2004 Glazer et al. showed that cells deficient in Ku80 and DNAPKcs were actually resistant to cisplatin treatment compared to the wild type but that such difference is only marked when cells were treated at high confluence (Jensen & Glazer, 2004). Moreover the authors showed that following cisplatin treatment DNA-PK trimeric complexes mediate death signals

within damaged cells via cell to cell contact through gap junction (Jensen & Glazer, 2004; Zorbas & Keppler, 2005). Subsequently, Shao et al. 2008 showed that high levels of DNAPKcs/Ku80 kinase activity in gliomas correlates with cisplatin resistance suggesting that activation of this trimeric complex could be utilised to screen for patients that would benefit from cisplatin treatment (Shao et al, 2008).

4.3.3 EGFR modulation of DNA repair following IR

The involvement of EGFR in the repair of IR-induced damage has been extensively reviewed in the introduction section. The characterised nuclear interaction of EGFR with DNAPKcs following IR is responsible for the DNA repair and resistance to IR treatment. Similarly, this study shows that cells expressing wtEGFR and EGFRvIII have completely repaired IR-induced SBs by 4 hours following treatment and this also correlates with EGFR nuclear translocation and similar DNAPKcs nuclear localisation pattern. EGFRvIII expressing cell line shows the highest rate of DNA SB repair (significantly higher to wtEGFR) suggesting that cancer cell expressing this mutant may present a more efficient DNA repair mechanism and therefore a higher resistance potential to IR.

4.3.3.1 EGFR modulation of SSBs and DSBs is shown at different time points

The differences in percentage tail moment among the different transfectants are smaller compared to the distinct patterns observed following cisplatin treatment. The type of damage conferred and the different repair pathways involved explain the significance of these differences. DNA SBs are formed immediately following IR treatment and therefore repair will act promptly upon their recognition. While SSBs are quickly repaired by the DNA repair machinery, the more complex double strand breaks will require a longer time. Therefore the differences observed at 4 hours following IR treatment represent the impairment of DSBs repair whereas the very early time points show the different kinetics in the repair of single strand breaks. The alkaline comet assay does not distinguish between the single and double strand breaks therefore it is unknown whether the percentage decrease in tail moment is due uniquely to inhibition of DSBs or to the accumulation of unrepaired SSBs and DSBs. This suggests that another DNA repair component, rather than DNAPKcs, involved in the EGFR modulation of IR induced repair cannot be excluded. Considering the

high biological significance and the great lethality of even one DSB the differences in percentage decrease of tail moment following IR among the mutants, although rather small numerically, have been still classified using the three categories (complete repair, intermediate inhibition and highest inhibition of repair) as for the cisplatin comet assay result.

4.3.4 The window of molecular intervention to determine DNA repair

The cisplatin comet assay also shows that the % unhooking obtained at the 18-hour time point could be very important to predict the overall repair response. Less than 50% of the unhooking at 18 hours will indicate that it is unlikely the ICLs will be successfully resolved within the 48 hours. This suggests that the binding between DNAPKcs and EGFR is only involved in the resolution of 50% of the unhooking however the immunoprecipitation analysis shows that the EGFR-DNAPKcs binding is progressive overtime therefore the earlier unhooking may still be due to this complex. Similarly, the reduction of tail moment at 30 minutes following IR treatment predicts clearly the rate of repair. More than 60% reduction of tail moment will result in complete repair within the following 4 hours. These data suggest that the initial 18 hours following cisplatin treatment and 30 minutes following IR treatment could be utilised to predict the overall repair kinetics following therapy

4.3.5 EGFR nuclear localisation expression does not quantitatively determine modulation of DNA repair

The IF analysis shows that despite the mutation in the NLS sequence, the nuclear translocation of both M1 and M12 show is only decreased. This, together with their ability to repair (shown in the comet assays), suggests that the amount of EGFR nuclear expression is not in linear relation with the repair kinetics. Even a small percentage of EGFR nuclear translocation results in sufficient repair. The difference in nuclear translocation as compared with wtEGFR and EGFRvIII, interestingly, suggests that the induction of EGFR nuclear expression following IR and cisplatin may not only be required for DNA purposes but also to exert some other biological functions. In addition, the comparison between the levels of M1/DNAPKcs, M12/DNAPKcs binding in relation to the levels of M1 and M12 nuclear expression and the levels of wtEGFR/DNAPKcs binding in relation to its nuclear expression, suggests a role for EGFR independent of DNAPKcs.

4.3.6 Kinase activity does not determine nuclear expression and it is not central to repair

KMT, L858R and ΔNLS show very similar intermediate levels of repair however their structural characteristics are quite different. The kinase dead mutant KMT bears the mutation K721A which is known to modify the kinase domain conformation hindering both dimerisation and receptor activation. The ΔNLS mutant lacks entirely the NLS sequence and in accordance to the allosteric model, (an EGFR receptor molecule lacking the p13+ peptide is unable of dimerise and activate) this receptor is kinase dead. Both these two mutants show impaired EGFR nuclear localisation. On the other hand, L858R bears the somatically acquired mutation of the Leucine 858 into an Arginine which renders the mutant 50 fold more active; 10-100 fold more sensitive to gefitinib and binds to gefitinib 20 times more tightly. In the inactive conformation Leucine 858 is exposed in the helical turn of the activation segment. Here it makes non-polar contact with the nearby Phenialanine 723 and the glycine-rich loop. Substitution with the positively charged amino acid Arginine is not compatible with the inactive conformation but is with the active conformation. This produces a lower affinity for ATP but higher affinity for TKI (Dixit & Verkhivker, 2009; Fassina et al, 2009). Moreover it has been shown that due to this mutation the residue Tyrosine 845 does not require SRC phosphorylation but undergoes constitutive autophosphorylation (Fu et al, 2008; Yang et al, 2008). Expression of the L858R mutant also resulted in impaired nuclear expression despite constitutive kinase activity (Das et al, 2007). This resulted in reduction of DNA strand break repair which is consistent with the observation that non-small cell lung cancer lines expressing L858R show increased sensitivity to IR and reduced nuclear expression. Moreover, the difference in repair between cells expressing L858R (kinase active but with impaired nuclear localization) and EGFRvIII (kinase active and expressed in the nucleus) suggests that, as a consequence of the lack of allosteric activation, the impaired nuclear EGFR accumulation and not kinase activity *per se* determines the reduced DNA repair in these models.

The confocal imaging shows that L858R, KMT or ΔNLS transfected cells still induce nuclear DNAPKcs following cisplatin and IR suggesting the presence of a backup signalling pathway that triggers some DNAPKcs nuclear accumulation however insufficient to determine complete repair. It is unknown whether the KMT mutant

undergoes a conformational change and therefore whether its lack of nuclear localisation is due to a sterically hindered NLS sequence or to an impaired kinase activation. Previous data have shown that inhibition of EGFR kinase activity is sufficient to inhibit the receptor nuclear translocation suggesting that despite an intact NLS sequence the kinase activity is also a requirement for nuclear translocation. Our data have shown that nuclear accumulation is the absolute requirement for efficient repair as kinase activity without nuclear accumulation can only account for intermediate levels of repair.

4.3.7 Maximal gefitinib inhibition of repair is shown only when EGFR translocates to the nucleus

The results obtained by the gefitinib treated cells following cisplatin suggest that nuclear localisation is central for the modulation of cisplatin repair modulation. Gefitinib showed maximal inhibition only in wtEGFR transfected cells whereas it had no significant effect on cells expressing NLS123 or LNLS123. Although wtEGFR cell treated with gefitinib showed significant inhibition compared to VC transfected cells (which do not express EGFR), the inhibition of repair was still significantly lower compared to cells with impaired EGFR nuclear translocation. Importantly, the intermediate levels of repair shown by wtEGFR expressing cells, treated with gefitinib, suggests that whilst not sufficient to determine a complete inhibition of repair, inhibition of EGFR kinase activity has a role in repair, however different from nuclear translocation.

The increased sensitivity shown in L858R transfected cells reflects the characteristic of this mutant to have a higher affinity to 4-anilinoquinazoline compounds such as gefitinib. Significant inhibition of repair was found only between 18 and 24 hours following cisplatin treatment. There was no significant difference in gefitinib treated cells at 48 hours. The effect of the inhibitor on the receptor activation was not determined therefore it cannot be concluded that the higher inhibition is directly determined by the peak of gefitinib-induced impairment of kinase activation. Interestingly, the time frame coincides with EGFR-DNAPKcs nuclear association shown in cells where EGFR translocates to the nucleus. It has been reported that gefitinib treatment induces cytosolic accumulation of DNAPKcs (Friedmann et al, 2004). The possibility that repair inhibition observed in L858R cells is due to other

factors rather than to an impaired kinase activity cannot be excluded. Future experiments will answer these important questions.

4.3.8 Gefitinib binds to EGFR active conformation

The necessity of a conformational change to allow recognition of the NLS sequence for nuclear translocation has been previously discussed. The impaired EGFR nuclear localisation has been explained as a result of an inactive conformation (NLS123) due to the lack of a dimer-dimer interface that initiates the allosteric mechanism and to a kinase mutation that achieves active conformation without requiring the conformational change (L858R). It has been shown that gefitinib binds only EGFR molecules in an active conformation. In line with this evidence, L858R and wtEGFR show gefitinib-induced inhibition of DNA repair. The lack of gefitinib-induced inhibition, in NLS123 cells, adds more evidence towards the argument that the NLS123 mutation impedes the allosteric conformational change necessary to achieve an active conformation. The fact that gefitinib treatment has shown no effect in LNS123 cells suggests that the mutation of all the arginines within the NLS sequence may impair the active conformation that the L858R receptor obtains via the arginine substitution at position 858. This underlines the importance of this stretch of amino acid and the necessity for further experiments to determine the correlation between the induction of impaired active conformation and DNA repair.

4.3.9 The NLS sequence is a target for molecular intervention

The NLS mutation (AAAHIVAKATLAA) contributed to an even greater delay of repair. The NLS123 mutant showed not only inhibition of nuclear translocation, abolished kinase activation and impaired DNAPKcs binding but also lack of DNAPKcs nuclear accumulation. The LNLS123 showed impaired EGFR nuclear accumulation and DNAPKcs binding, mirrored by the inhibition of DNAPKcs nuclear translocation maintaining, however, the receptor constitutive activation. The mutation of the three Arginine cores of the NLS sequence may have caused a structural change to the receptor obstructing the binding of other proteins and their trans-phosphorylation which results in the lack of DNAPKcs nuclear accumulation. A recent study has shown that targeting EGFR NLS sequence by a peptide corresponding to phosphorylated NLS resulted in abolished nuclear EGFR, reduced radiation-induced activation of DNAPK and reduced survival following IR (Dittmann et al, 2010a).

4.3.10 DNAPKcs subcellular distribution

These data clearly show that DNAPKcs is not only localised into the nucleus supporting other published data on the cytosolic functions of DNAPKcs. Moreover, in our EGFR overexpressing cellular system, DNAPKcs mirrors the EGFR cellular localisation suggesting that the behaviour of these two proteins is highly linked. In fact the inhibition of the nuclear translocation of the receptor is sufficient to mediate decreased DNAPKcs nuclear accumulation following cisplatin and IR. Previous data have shown that EGFR inhibition of gefitinib induce DNAPKcs accumulation in the cytosol (Friedmann et al, 2006). Although the gefitinib dose used in that study was greater the effects on EGFR kinase activity are comparable to those obtained with the NLS123 mutant. The statement that EGFR cellular localisation influences DNAPKcs subcellular distribution can be justified if one accepts the idea of EGFR being a kinase for DNAPKcs.

4.3.11 Conclusions

This chapter shows that nuclear EGFR plays an important role in modulating the repair of DNA damage caused by cisplatin and IR. Transfecting cells with wtEGFR and EGFRvIII showed an increased efficiency of the repair of DNA lesions, whereas the transfection of EGFR-NLS mutants demonstrated an impairment of DNA repair. Following cisplatin treatment there was a time dependent association of EGFR and DNAPKcs as assessed by immunoprecipitation assays. Confocal microscopy in cells transfected with wtEGFR or EGFRvIII showed similar localisation pattern of EGFR and DNAPKcs in the nucleus whereas the two proteins were exclusively detectable in the cytoplasm in cells transfected with EGFR NLS123 mutants. These results are in keeping with the observation that inhibitors of EGFR can inhibit DNA repair and demonstrates the importance of EGFR nuclear expression in this process.

It now needs to be demonstrated that both cisplatin and IR stimulate the formation of EGFR and DNAPKcs complex and therefore as a consequence of their physical interaction DNAPKcs undergoes a kinase modulation which is mediated only by nuclear EGFR.

CHAPTER 5:

THE MECHANISM OF EGFR MODULATION OF DNA REPAIR

5.1 INTRODUCTION

5.1.1 The role of EGFR nuclear translocation in the binding to DNAPKcs

EGFR modulation of DNA repair has been described in many reports with regards to the binding with DNAPKcs following IR. Although this interaction has been greatly discussed and characterised in the literature, there is no clear understanding as to whether EGFR nuclear expression is sufficient and necessary to determine this binding. The previous chapter has shown how EGFR can modulate ICL and SB repair. EGFR kinase activity and nuclear localization, despite appearing to rely both on the receptor active conformation, have distinct, non-mutually exclusive, roles in the repair of DNA damage.

Inhibition of EGFR (or other ERBB family receptors) kinase activity can either be achieved by TKI or by antibodies that impair the ligand binding to the receptor. When wtEGFR transfected cells were treated with gefitinib in combination with cisplatin the resulting effect on the DNA repair kinetics were similar to the behaviour of the KMT mutant. Cell expressing this kinase dead mutant showed impaired EGFR nuclear translocation and intermediate levels of ICL or SB repair. Our data have also shown that induced inhibition of EGFR nuclear translocation via the NLS123 mutation resulted in a consequent impaired kinase activity. However cells transfected with the NLS123 showed complete inhibition of repair suggesting that different targeting clearly has a more dramatic effect.

Confocal microscopy analysis suggested that mutation in the EGFR NLS sequence inhibits DNAPKcs nuclear localization without establishing a physical interaction. The question as to whether EGFR-DNAPKcs association takes place exclusively in the nucleus and whether EGFR kinase activity or nuclear translocation *per se* can induce this association remain unclear. The suggestion that EGFR acts as a kinase for DNAPKcs would explain DNAPKcs cytosolic localisation in presence of an EGFR NLS mutant. EGFR-DNAPKcs binding inhibition could interfere with DNAPKcs activation resulting in a DNAPKcs accumulation in the cytosol.

5.1.2 EGFR nuclear localisation and DNAPKcs kinase activity

Previous reports have shown a correlation between direct inhibition of EGFR kinase activity and consequent inhibition of DNA-PK kinase activity suggesting a relation between EGFR kinase activity and DNAPKcs. EGFR kinase inhibition by TKI (gefitinib) or mAB (cetuximab) have shown inhibition of DNA-PK kinase activity, DNAPKcs cytosolic accumulation and delayed repair (Dittmann et al, 2008a; Dittmann et al, 2005b; Friedmann et al, 2006; Golding et al, 2009). Recent reports have also shown a function for cytosolic DNAPKcs in apoptosis, activation of AKT and in cell-cell communication (Achanta et al, 2001; Gurley et al, 2009; Lu et al, 2006; Shi et al, 2009; Toulany et al, 2008b). Here it has been shown that inhibition of EGFR nuclear translocation via the NLS123 mutation also indirectly inhibits DNAPKcs nuclear accumulation following cisplatin and IR induced damage. This raised many questions on the induction of EGFR-DNAPKcs association and its consequences including whether this binding takes place exclusively in the nucleus, whether it is EGFR nuclear translocation, the treatments or EGFR allosteric conformational change that induce EGFR-DNAPKcs association and whether the complex can modulate DNAPK kinase activity. These are all central to decipher the mechanism that links EGFR with DNAPKcs and DNA repair, to provide substantial evidence to establish that nuclear EGFR is required for repair of cisplatin and IR induced DNA damage and that repair is mediated via binding to DNAPKcs.

5.1.3 Stable expression of EGFR constructs

The transient over-expression of the wtEGFR or other EGFR mutants has been utilised to determine the effect of EGFR on repair. In this chapter wtEGFR, NLS123, L858R, LNLS123, EGFRvIII were stably expressed in NIH3T3 cells and the mechanism of EGFR modulation of DNA repair was investigated. This allowed homogeneous EGFR- expressing populations of cells to be examined. The constructs within the stable transfectants represent, more significantly, the different DNA damage repair behaviours discussed in chapter 3 while presenting different EGFR characteristics in terms of nuclear translocation, kinase activation, and DNAPKcs binding.

5.1.4 Cisplatin cytotoxicity and survival

As detailed in the introduction chapter, cisplatin has been used in the clinic for over 30 years in the treatment of testicular, head and neck, cervix, ovary and lung cancer.

However, clinical responses to cisplatin are variable and there is substantial evidence suggesting that EGFR over-expression, as well as its nuclear expression, are major determinants of cisplatin-acquired resistance (Benhar et al, 2002; Eckstein et al, 2008; Wernyj & Morin, 2004; Winograd-Katz & Levitzki, 2006; Wynne et al, 2007). The general consensus is that the variety of platinum adducts underlie most of the cytotoxic effects of this drug (Malinge et al, 1999; Wang & Lippard, 2005). Besides EGFR, cisplatin activates a variety of cellular protein that exerts many crucial cellular functions such as p53, p73, c-abl, hence predicting signalling responses to cisplatin has been a challenge for many years (Boeckman et al, 2005; Laachi et al, 2009; Nojima et al, 2005; Patrick et al, 2008; Turchi, 2006; Wang et al, 2005; Winograd-Katz & Levitzki, 2006). It remains to elucidate the consequences of such high inhibition of repair in terms of survival. This is essential to assess the potential benefits of targeting EGFR nuclear localisation for therapeutic purposes.

5.1.4 Aims of this chapter:

- Investigate the induction of EGFR-DNAPKcs binding
- Determine the role of EGFR kinase activity in the binding with DNAPKcs.
- Determine the role of EGFR cellular localisation in relation to DNAPKcs cellular distribution.
- Identify the cellular compartment where EGFR-DNAPKcs association takes place.
- Study the consequence of EGFR-DNAPKcs association in terms of DNAPK kinase activity.
- Determine the survival of exponentially growing wtEGFR, NLS123, L858R, LNLS123, EGFRvIII or VC expressing cells following cisplatin treatment.

5.2 RESULTS

5.2.1 wtEGFR and EGFRvIII are expressed in the nucleus 18 hours following cisplatin treatment

In the previous chapter, confocal microscopy showed EGFR nuclear expression 18 hours following cisplatin treatment. Although immunofluorescence is the most reliable technique to determine the cellular localisation of any protein, wtEGFR and EGFRvIII nuclear translocation was confirmed by cellular fractionation. Cells expressing wtEGFR, EGFRvIII, NLS123 or VC were treated with 50μM cisplatin for one hour in serum-free media and cytosolic and nuclear compartments were separated 18 hours following cisplatin treatment (Fig 5.1). Densitometric analysis showed a 2.35-fold increase in EGFR nuclear expression in wtEGFR expressing cells and 3.28-fold increase in EGFRvIII expressing cells. EGFR nuclear translocation was impaired in NLS123 expressing cells. Fig 5.2 shows the graphical representation of the densitometric analysis

5.2.2 Ionising radiation or cisplatin induce EGFR-DNAPKcs binding

The timing of EGFR nuclear translocation following cisplatin was chosen according to the peak of EGFR-DNAPKcs binding following cisplatin. Interestingly, it has been shown that IR-induced EGFR-DNAPKcs binding also coincides with the time of IR-induced EGFR nuclear translocation (Das et al, 2007; Dittmann et al, 2008a). Although the formation of the EGFR- DNAPKcs complex and EGFR nuclear expression have always been related in the literature there is no clear understanding as to whether EGFR-DNAPKcs binding is a consequence of EGFR nuclear expression. Therefore the induction of this complex formation was invetsigated. Cells stably expressing wtEGFR, NLS123, L858R, LNLS123 or EGFRvIII were treated with 4 Gy IR or 50μM cisplatin or 100 ng EGF and samples were collected at the appropriate timing showing EGFR nuclear translocation. Cellular extracts were then immunoprecipitated using an anti-EGFR antibody and blotted with anti-DNAPKcs. The addition of the EGF treatment was necessary to determine whether the EGFR-DNAPKcs association is induced by nuclear translocation *per se*, by the induction of the allosteric conformational change that exposes the NLS sequence, or by the treatment. Fig 5.3 shows the western blot analysis of the EGFR pull-down

lysates blotted with anti-DNAPKcs. Cells expressing wtEGFR and EGFRvIII showed EGFR association with DNAPKcs only following treatment with IR or cisplatin. Cells expressing NLS123, L858R and LNLS123 showed no interaction between the mutant EGFR and DNAPKcs. This confirmed the results of the reciprocal DNAPKcs pull-down following cisplatin treatment shown in the previous chapter. EGF induction of EGFR nuclear translocation did not induce EGFR-DNAPKcs binding suggesting that the type of treatment induces EGFR-DNAPKcs binding. Since cisplatin, IR and EGF are potent activators of EGFR kinase activity, EGFR phosphorylation activation in relation to EGFR-DNAPKcs complex formationwas investigated. Fig 5.3 shows the analysis of the EGFR- pull down lysates blotted with the pan-phosphotyrosine PY20 antibody. Cells expressing wtEGFR showed maximal activation of the receptor following EGF treatment. Intermediate levels of activation were detected following IR or cisplatin. L858R, LNLS123 and EGFRvIII expressing cells showed a constitutive activation of the receptor whereas NLS123 showed no receptor activation. Despite maximal EGFR activation being achieved in wtEGFR expressing cells following EGF treatment, there was no correspondent EGFR-DNAPKcs binding. Kinase activity is therefore not sufficient to determine EGFR-DNAPKcs binding. This association is triggered by cisplatin or IR and not by the EGFR nuclear translocation *per se*.

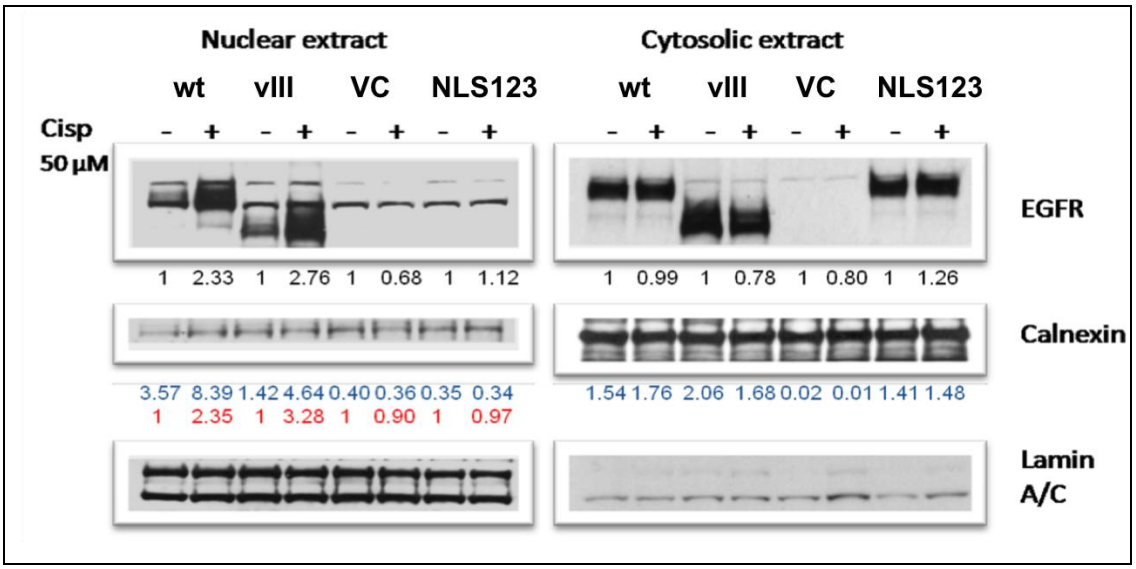

Figure 5.1: Cisplatin induces EGFR nuclear translocation. EGFR-null murine NIH3T3 cells were transfected with wtEGFR (wt), EGFRvIII (viii), M123, and vector control (VC). Cells were treated with 50µM cisplatin for one hour and nuclear extracts were obtained 18 hours following treatment. Nuclear extracts are prepared according to the Active Motif Nuclear extract kit and loaded relative to the cytosolic extracts and blotted with antibodies to EGFR or Calnexin or Lamin A/C. Numbers (black) represent fold increase compared to untreated, (blue) EGFR/Calnexin density ratio, (red) fold increase of nuclear EGFR once density of cytosolic contamination was substracted (blue underlined).

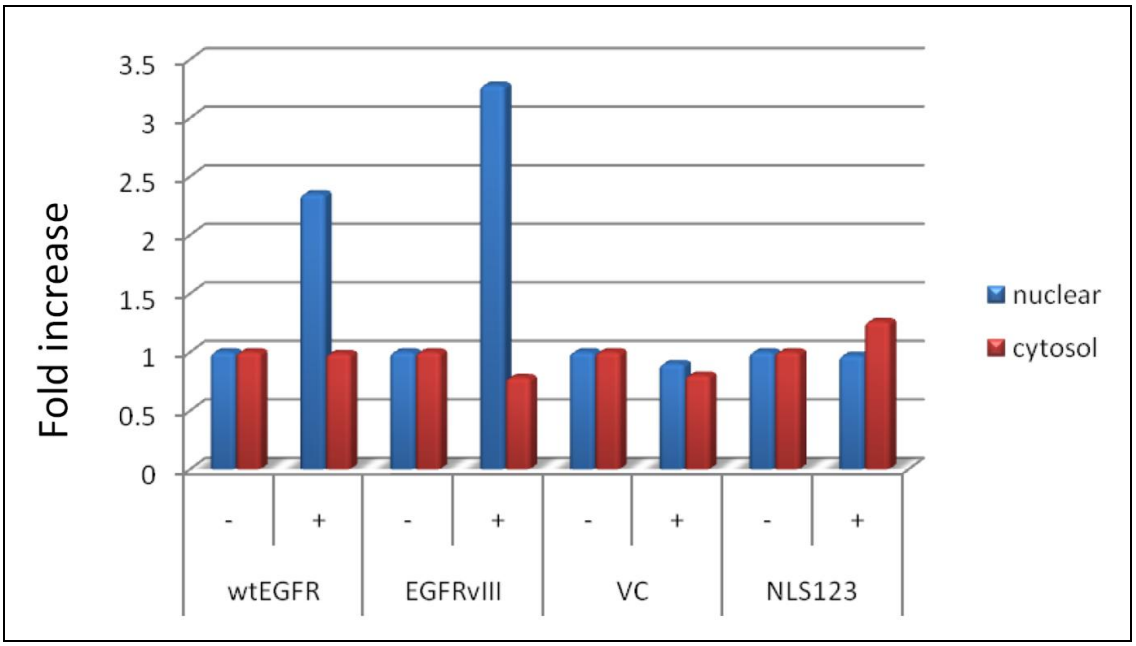

Figure 5.2: Cisplatin induces EGFR nuclear translocation. EGFR cellular distribution is shown in the graph. The bars show the graphical representation of the densitometric analysis of Fig 5.1.

5.2.3 Mutant EGFR associates with the heat shock protein 90 chaperone

The association of heat shock proteins (Hsps) to protein kinases has been shown in several reports (Citri et al, 2006; Pashtan et al, 2008; Sawai et al, 2008). Hsps are molecular chaperones whose expression increases in response to metabolic insults. Their most acknowledge function is to assist protein synthesis and folding (Young et al, 2001). In addition they have been shown to participate in protein assembly, secretion and trafficking and regulation of transcription factors (Citri et al, 2006). While Hsp70 have been shown to be involved in the nuclear translocation of EGFR (Liao & Carpenter, 2007), Hsp90 has been often shown to associate with EGFR somatic mutants. Previous reports have demonstrated that EGFRs harbouring mutation within the kinase domain require the Hsp90 chaperone for conformational maturation and stability. In fact, the inhibition of Hsp90 has been often associated with reduced expression of EGFR mutants and consequent sensitivity to treatment (Sawai et al, 2008). The cellular requirement for EGFR mutants to achieve post-translational maturity and proper folding induces HSp90 association with EGFR kinase mutants (Lavictoire et al, 2003). Since the NLS123 mutation interferes with EGFR allosteric conformation, the Hsp90-EGFR association in wtEGFR, NLS123, L858R, LNLS123, EGFRvIII or VC expressing cells was inevstigated to understand the relationship between HsP90, EGFR nuclear localisation and EGFR-DNAPKcs binding. Therefore, the EGFR pull-down samples were also blotted with anti-HSP90 antibody. Fig 5.3 shows the results of the western blot analysis. While, wtEGFR showed association with HSP90 only following cisplatin treatment, in contrast EGFRvIII expressing cell lines showed impaired association between EGFR and Hsp90. L858R, LNLS123 and NLS123expressing cells showed constitutive levels of association between EGFR and HSP90 following IR, cisplatin or EGF treatment, although weaker following IR treatment in L858R and NLS123 expressing cells (Fig 5.3).

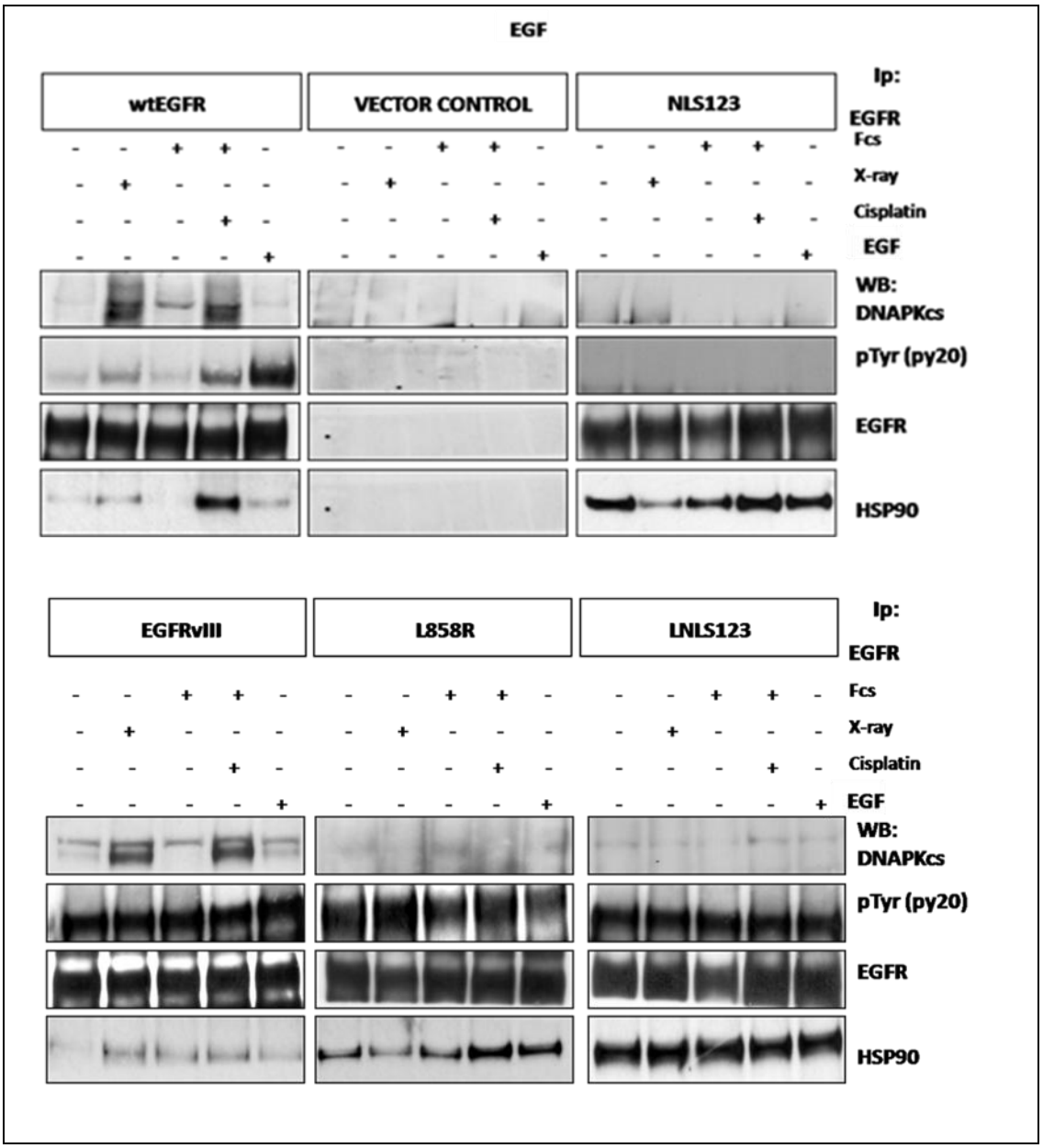

Figure 5.3: EGFR activation and binding to DNAPKcs and Hsp90. Stable NIH3T3 cells expressing wtEGFR, NLS123, L858R, LNLS123, EGFRvIII, and Vector control were treated with 50μM cisplatin or 4 G IR, or treated with 100ng/ml EGF as described in the materials and methods. 1.5mg of protein lysate was then immunoprecipitated using anti-EGFR monoclonal antibody and blotted with anti DNAPKcs, anti-PY20, anti-EGFR and anti-HSP90.

5.2.4 DNAPKcs and EGFR localise in the same cellular compartment following IR or cisplatin

Having established the levels of association between EGFR and DNAPKcs following either cisplatin or IR treatment, their cellular localisation by confocal microscopy following IR (Fig 5.4) or cisplatin (Fig 5.5) treatment was also validated in the stably transfected lines. Cells expressing wtEGFR, NLS123, L858R, LNLS123, EGFRvIII or VC were either fixed 18 hours following treatment with 50 μM cisplatin or serum

starved for 24 hours and then fixed 20 minutes following 4 Gy IR. Fig 5.4 and 5.5 show the immunofluorescence results obtained via confocal analysis. Cells expressing wtEGFR and EGFRvIII showed nuclear expression of both EGFR and DNAPKcs following IR or cisplatin treatment. In contrast, L858R-expressing cells showed impaired EGFR nuclear localisation following either treatment. This was associated with diminished expression of DNAPKcs within the nucleus. Expression of EGFR and DNAPKcs was exclusively cytosolic in NLS123 and LNLS123 expressing cell lines following either IR or cisplatin treatment (Fig 5.4 and 5.5). Inhibition of EGFR nuclear translocation impaired DNAPKcs nuclear translocation, confirming the results obtained in Chapter 4 with the transiently transfected cells.

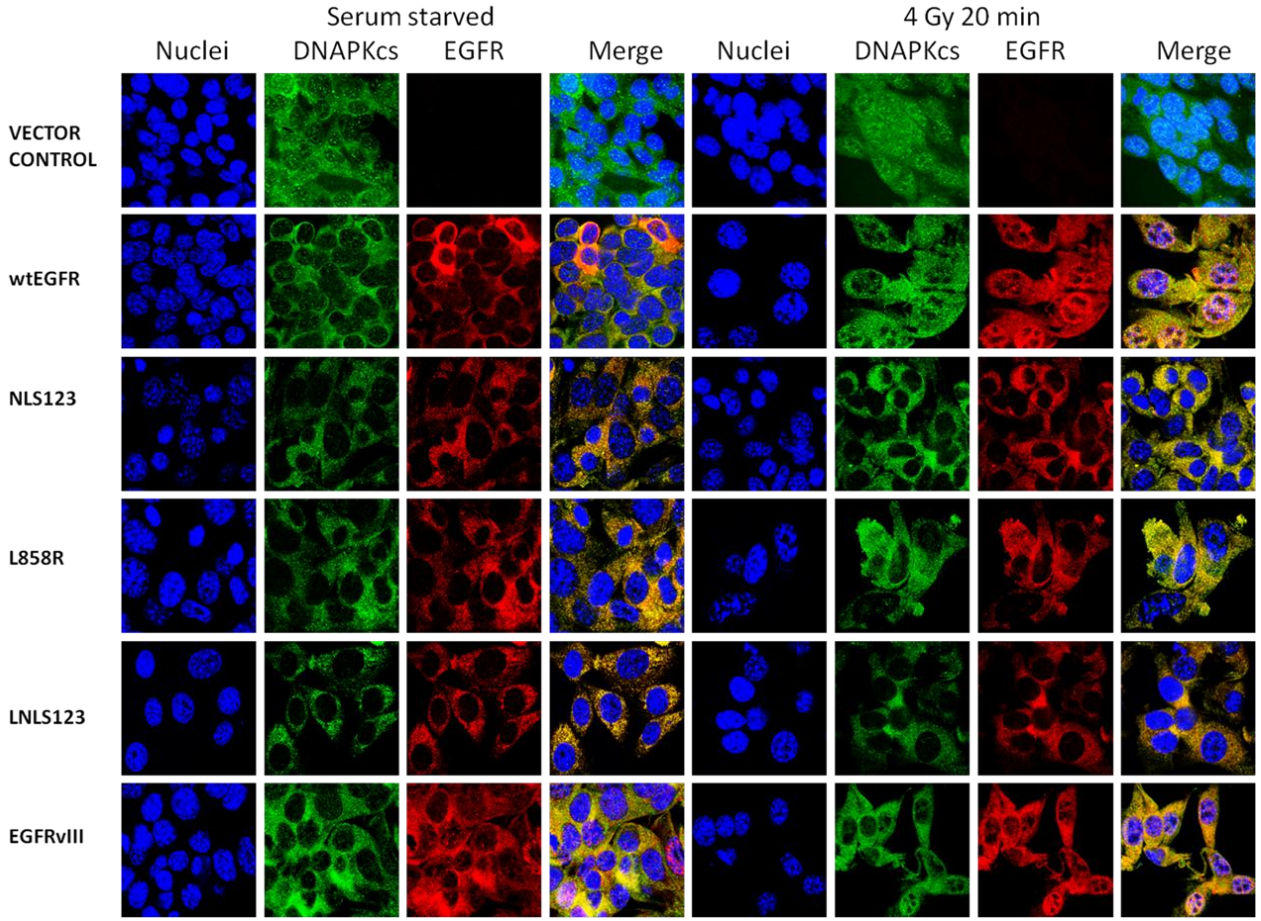

Figure 5.4: EGFR and DNAPKcs cellular localisation following IR treatment. Stable NIH3T3 cells expressing wtEGFR, NL123, L858R, LNLS123, EGFRvIII or VC were serum starved for 24 hours, treated with 4Gy Ionising radiation and then fixed with 4%PFA 20 minutes following treatment. Cells were stained with Goat anti-Rabbit Alexa fluor 647 (EGFR),Goat anti-Mouse Alexa fluor 488 (DNAPKcs), and Dapi (nucleus).

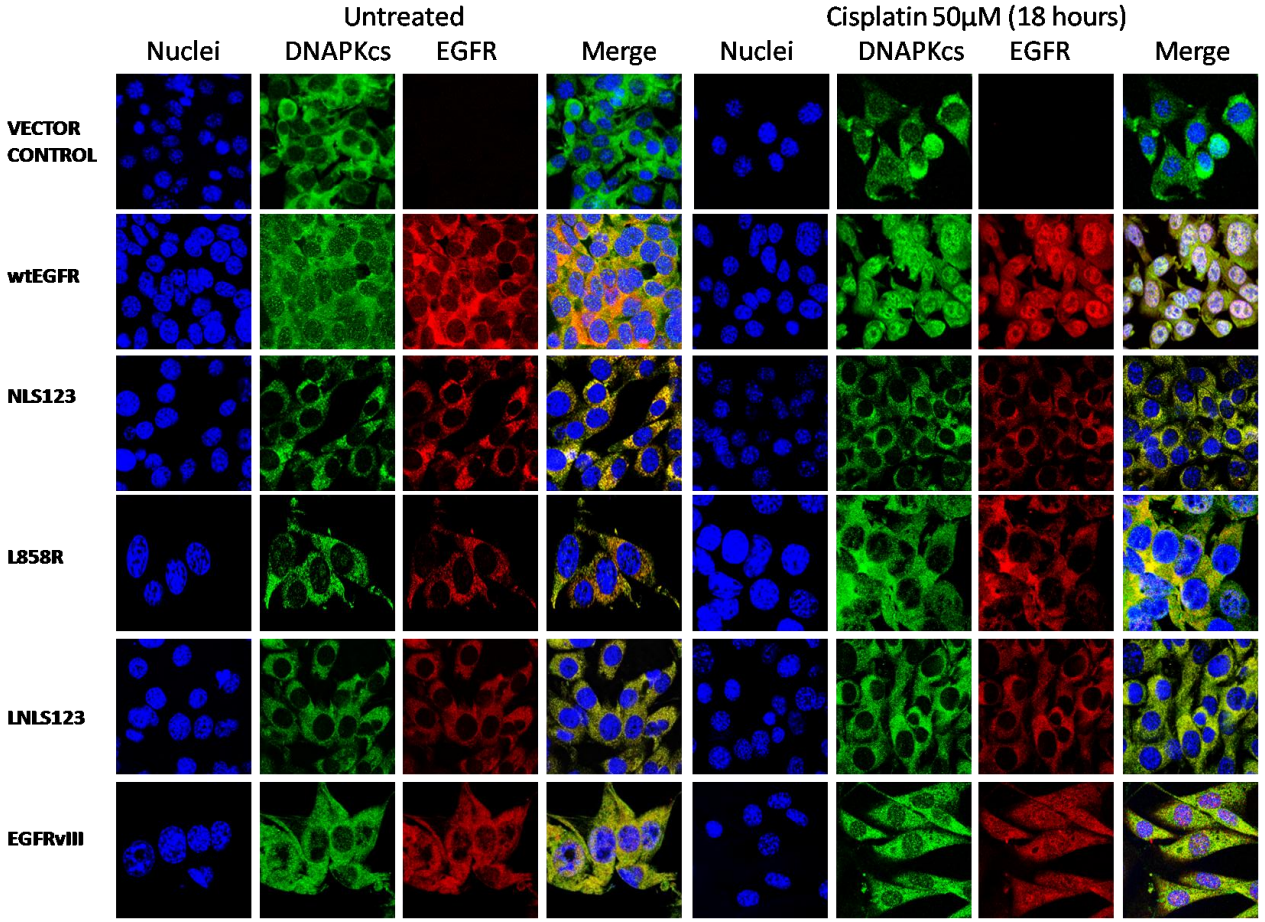

Figure 5.5: EGFR and DNAPKcs cellular localisation following cisplatin treatment. Stable NIH3T3 cells expressing wtEGFR, NL123, L858R, LNLS123, EGFRvIII or VC were serum starved for 24 hours, treated with with 50µM cisplatin and then fixed with 4% PFA 18 hours following treatment. Cells were stained with Goat anti-Rabbit Alexa fluor 647 (EGFR),Goat anti-Mouse Alexa fluor 488 (DNAPKcs), and Dapi (nucleus).

5.2.5 EGFR and DNAPKcs association following cisplatin or IR treatment

The time dependent association between EGFR and DNAPKcs showed a progressive formation of this complex following cisplatin treatment. EGFR is mainly a membrane/cytosolic protein, while DNAPKcs is principally found in the nucleus. Despite nuclear translocation and protein function, the most abundantly expressed nuclear protein will localise into the cytosol to be degraded. Although previous reports have shown DNAPKcs cytosolic accumulation following EGFR inhibition by gefitinib(Friedmann et al, 2006), the majority of the published data has investigated this complex formation almost exclusively in nuclear extracts (Dittmann et al, 2005a; Dittmann et al, 2008a; Dittmann et al, 2005b; Dittmann et al, 2007; Golding et al, 2009; Hsu et al, 2009; Mahaney et al, 2009). DNAPKcs has been shown to have diverse roles in the cytosol (discussed later). Our cellular fractionations have never achieved a nuclear fraction free from any cytosolic contamination, limiting the possibility to investigate EGFR-DNAPKcs association using fractionated cellular extracts. For this reason the cellular distribution of the EGFR-DNAPKcs complex formation via the proximity ligation assay was investigated. This assay allows fluorescent visualisation of the interaction between two proteins in fixed cells by labelling the secondary antibodies, used for the recognition of the protein involved in a complex, with two complementary oligos. Oligos from one secondary antibody will ligate only with oligos labelling the secondary antibody from different species (since they have been purposely made complementary) and within the proximity of 30nm. Ligation between two oligoes labelling the secondary antibody from the same species is therefore impossible. Therefore the formation of circular DNA molecule will be achievable only when two proteins are labelled by two secondary antibodies from different species and within the distance of 30nm. This is the distance recognised to be sufficient to determine physical interaction between two molecules. Before assessing the EGFR-DNAPKcs complex distribution in the NIH3T3 cells stably expressing wtEGFR or EGFR mutants, the assay and the antibody concentration required to prevent saturation were tested on A549 cells over expressing EGFR and DNAPKcs. Primary antibody concentration titration (1:50 - 1:150) was used to determine the most sensitive antibody concentration in cells treated with IR. Fig 5.6 shows the results of the confocal analysis of A549 cells blocked with anti-Rabbit EGFR antibody and anti-Mouse DNAPKcs and labelled using the proximity ligation

assay. Each interaction is represented via a single red fluorescent dot. There was a clear accumulation of red dots in the nuclei of A549 cells following treatment with IR at all the antibody dilutions. This confirmed the previously described EGFR-DNAPKcs association and established the optimal concentration of primary antibodies to use in wtEGFR, NLS123, EGFRvIII or VC expressing cells. Fig 5.6 shows that higher antibody dilutions (1:75, 1:100 and 1:150) produced less sensitivity in detecting nuclear complexes maintaining a discreet level of background complexes (serum starved) while the lower antibody dilution (1:50) showed a clear increase in nuclear fluorescent dots following IR treatment.

Next cells stably expressing wtEGFR, NLS123, EGFRvIII or VC were examined. Cells were treated with 50μM cisplatin or 4 Gy IR and then fixed 18 hours following treatment with cisplatin or 20 minutes following IR. Fig 5.7 shows the confocal analysis of the stable cells blocked with 1:50 anti-Rabbit EGFR antibody and 1:50 anti-Mouse DNAPKcs and labelled using the proximity ligation assay. In cells expressing vector or NLS123 constructs no interaction was detectable. In contrast, cells expressing wtEGFR or EGFRvIII showed interaction between EGFR and DNAPKcs following either IR or cisplatin. The pattern of interaction suggests that EGFR-DNAPKcs complex formation takes place both in the nucleus and cytoplasm.

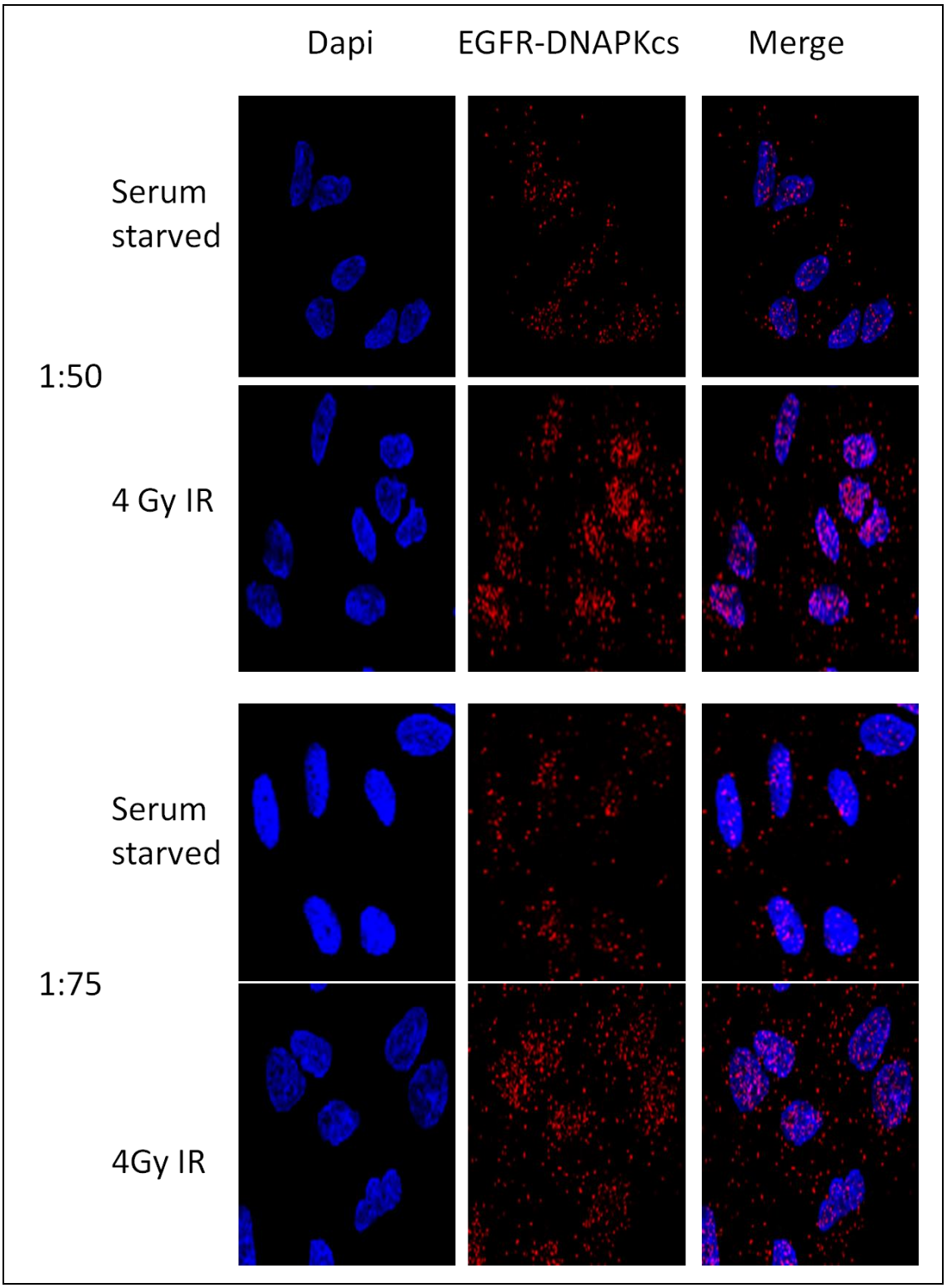

Figure 5.6: EGFR-DNAPKcs complex cellular localization. A549 cells were treated with 4 Gy IR and then fixed with 4%PFA 20 minutes follwowing radiation. Cells were then immuno blocked with anti-rabbit EGFR and anti-mouse DNAPKcs Dilution of the two antibodies are indicated (1:50-1:150). Interacting complexes were then visulised via the duo link proximity assay. Each red spot represent a single interaction.

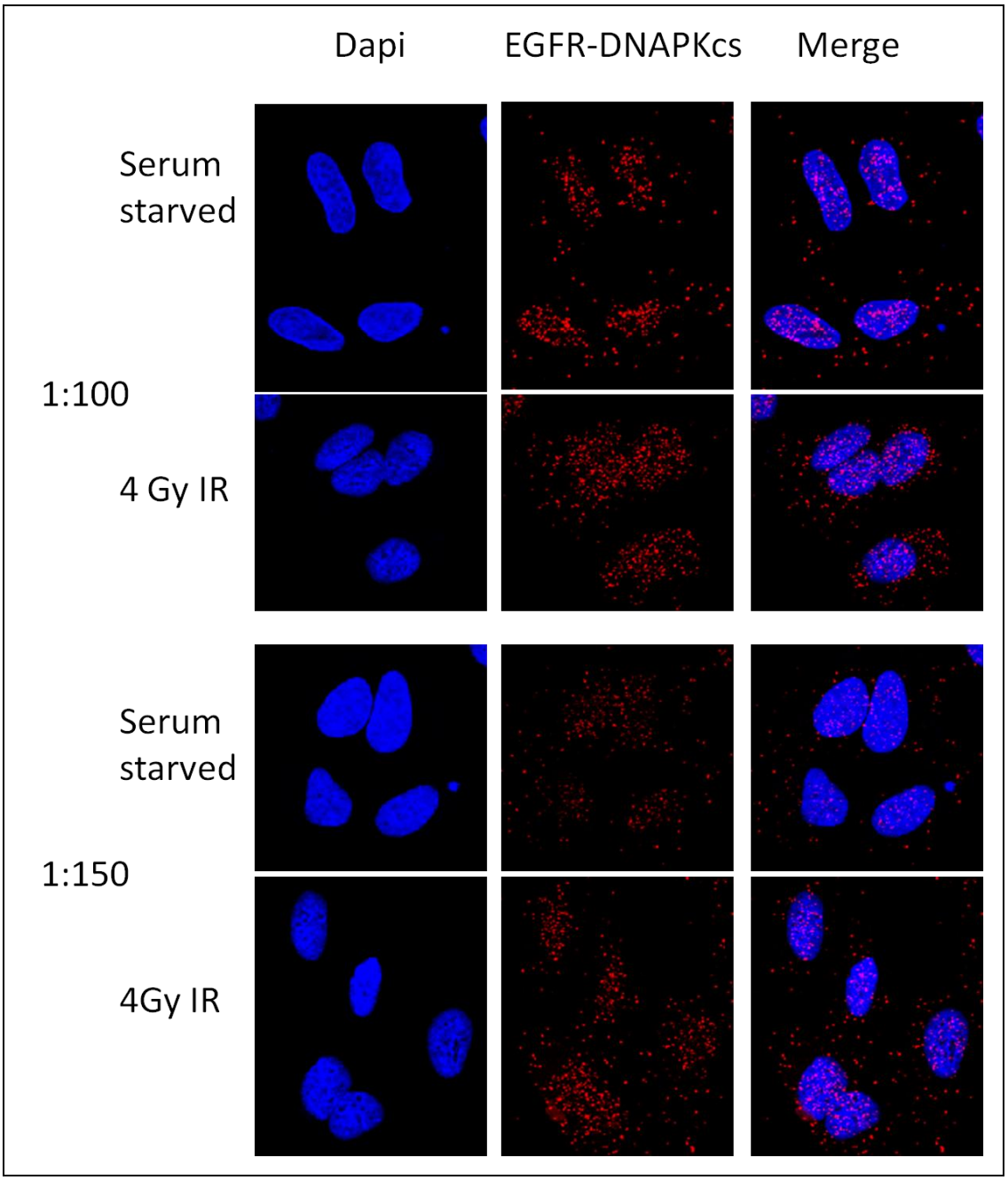

Figure 5.6 cont.

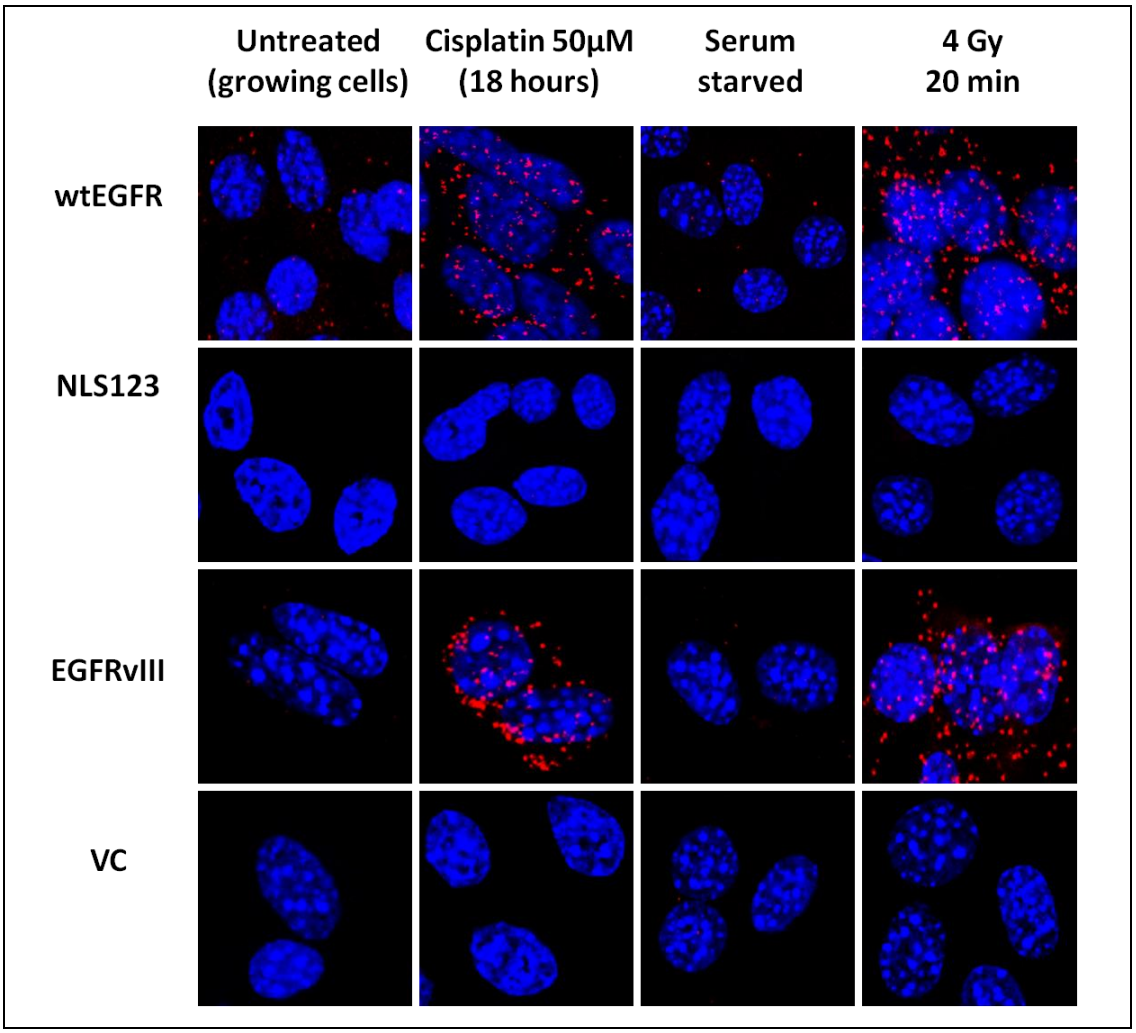

Figure 5.7: EGFR-DNAPKcs complex cellular localization. Stable NIH3T3 cells expressing wtEGFR, NLS123, EGFRvIII and Vector control were treated with 50µM cisplatin for one hour in serum free media and then fixed with 4%PFA 18 hours following treatment or 4 Gy and then fixed with 4%PFA 20 minutes follwowing radiation. Cells were then immuno blocked with anti-rabbit EGFR and anti-mouse DNAPKcs. Interacting complexes were then visulised via the duo link proximity assay. Each red spot represent a single interaction.

5.2.6 EGFR modulation of DNA-PK activity

Previous reports have shown that the association of EGFR and DNAPKcs stimulates DNA-PK kinase activity. The experiments detailed above demonstrated that EGFR kinase activity alone is not sufficient to determine EGFR-DNAPKcs association and that cisplatin or IR treatment was required to induce this complex formation. This is suggesting that cisplatin and IR may be responsible for DNAPKcs activation which would then allow binding. The modulation of repair observed during the study, however, suggests that treatment alone and putative activation of DNAPK is not sufficient to achieve complete repair (shown by the VC-expressing cells). Therefore

the effect of EGFR-DNAPKcs binding on the alteration of functional enzyme activity was investigated via the SignaTECT DNA-Dependent Protein Kinase Assay System. This assay utilises SAM^{2TM} Biotin Capture Membrane and overcomes the problem of non specific substrate binding by using a byotinylated DNA-PK p53-derived peptide substrate. The dose and the time to investigate the kinase activity were chosen according to the EGFR-DNAPKcs time of binding following IR (4 Gy, 20 minutes) or cisplatin (50 μM cisplatin, 18 hours). EGF induction of EGFR (100 ng/ml, 1 hour) was utilised to determine whether EGFR kinase activation *per se* were responsible for the effects on DNA-PK kinase activity.

Fig 5.8 shows the results of the DNA-PK kinase assay performed on extracts from cells expressing wtEGFR, NLS123, L858R, LNLS123, EGFRvIII or VC. Single treatment controls were used to determine the percentage change in DNA-PK kinase activity. As compared with EGFR-negative cells transfected with VC, cells expressing wtEGFR showed a 27.5 ± 7.22% increase in DNA-PK activity following IR (4Gy) and 37.52 ± 4.01 % increase following 50μM cisplatin treatment for 1 hour (Fig 5.7). Similarly, in cells expressing EGFRvIII there was 32.42 ± 16.58 % increase of DNAPK activity following IR and 26.6 ± 8.49% increase following the cisplatin treatment. In contrast, no significant change in DNA-PK activity compared to controls was found in L858R and LNLS123 expressing cell lines following IR (-5.29 ± 8.27% and 2.72 ± 7.06%) or cisplatin treatment (9.04 ±3.46% and 2.25 ±6.07%). Results are summarised in Table 5.1. Only cells expressing NLS123 showed a clear decrease in DNA-PK kinase activity compared to control. EGF treatment showed no statistical change in kinase activity suggesting that EGFR binding to DNAPKcs has a more significant role in determining DNA-PK kinase activity following cisplatin or IR.

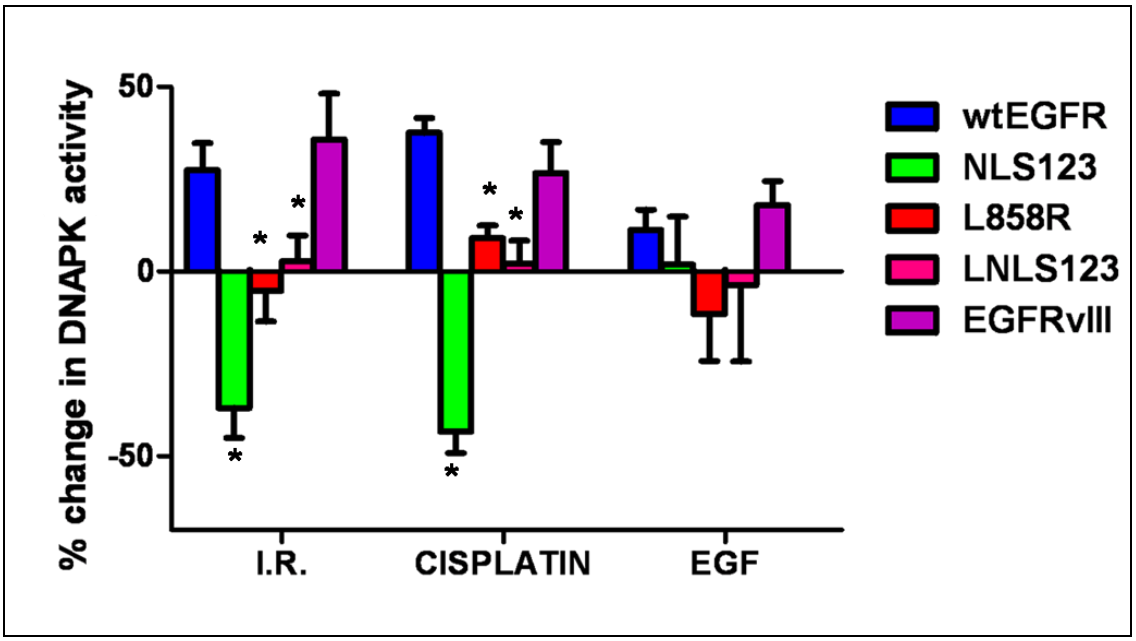

Figure 5.8: EGFR modulation of DNA-PK kinase activity. Stable NIH3T3 cells expressing wtEGFR, NLS123, L858R, LNLS123 or EGFRvIII were treated with 50μM cisplatin for one hour or 4 Gy or 100ng/ml EGF in serum free media. 18 hours following the treatment with cisplatin, 20 minutes following the treatment with IR and at the end of the EGF incubation cells were lsysed and samples prepared for the DNA-PK Kinase assay. The graph shows the percentage change in DNA-PK activity following each treatment compared to untreated.

	wtEGFR		NLS123			L858R			LNLS123			EGFRvIII		
	% CHANGE	S.D.	% CHANGE	S.D.	P value	% CHANGE	S.D.	P value	% CHANGE	S.D.	P value	% CHANGE	S.D.	P value
I.R.	27.50	7.222	-36.95	8.085	P<0.001	-5.29	8.266	P<0.001	2.72	7.062	P < 0.01	35.75	12.43	P > 0.05
CISPLATIN	37.52	4.009	-43.31	5.822	P<0.001	9.04	3.458	P<0.01	2.25	6.07	P<0.001	26.60	8.488	P > 0.05
EGF	11.28	5.472	1.88	12.96	P > 0.05	-11.60	12.67	P < 0.05	-3.60	20.76	P > 0.05	17.96	6.494	P > 0.05

Table 5.1: The table shows numerical values and statistical significance from the DNAPK kinase assay.

5.2.7 EGFR modulation of cellular survival

The DNA repair abilities observed in the cells expressing wtEGFR, somatic mutations and NLS mutations have underlined substantial differences in their repair kinetics following cisplatin and IR. The comet assay data, showed in result Chapter 4, suggested significant differences in the mechanism utlised by these cells to respond and repair the cisplatin and IR-induced DNA damage. To investigate whether the EGFR induced modulation of DNA repair has an effect on survival, wtEGFR, NLS123, L858R, LNLS123, EGFRvIII or VC expressing cells were treated with cisplatin and survival was assesed via the MTT assay. Cells were plated at a concentration that allows them to grow exponentially ($2.5x10^4$/ml) and then treated with 50μM cisplatin for one hour in serum free media. Survival was assessed via the MTT assay over a period of 72 hours Fig 5.9 shows the percentage

decrease in survival of each stable cell line as compared to their daily untreated control. The graph shows wtEGFR expressing cells comapred to single each cell line expressing different constructs. Cells expressing wtEGFR and EGFRvIII showed 61.99 ± 5.02 and 62.33 ± 6.82 % survival. L858R expressing cells showed 42.26 ± 1 % survival, statistically significant when compared to the wtEGFR % survival ($P<0.01$). NLS123 and LNLS123 showed 37.44 ± 2.26 and 33.76 ± 6.49 % survival, with high statistical significance when compared to wtEGFR % survival (P value < 0.001). Details of statistical analysis is reported in Table 5.2. These data are graphically grouped in Fig 5.10. Fig 5.11 shows only the survival 72 hours following cisplatin expressed as % survival.

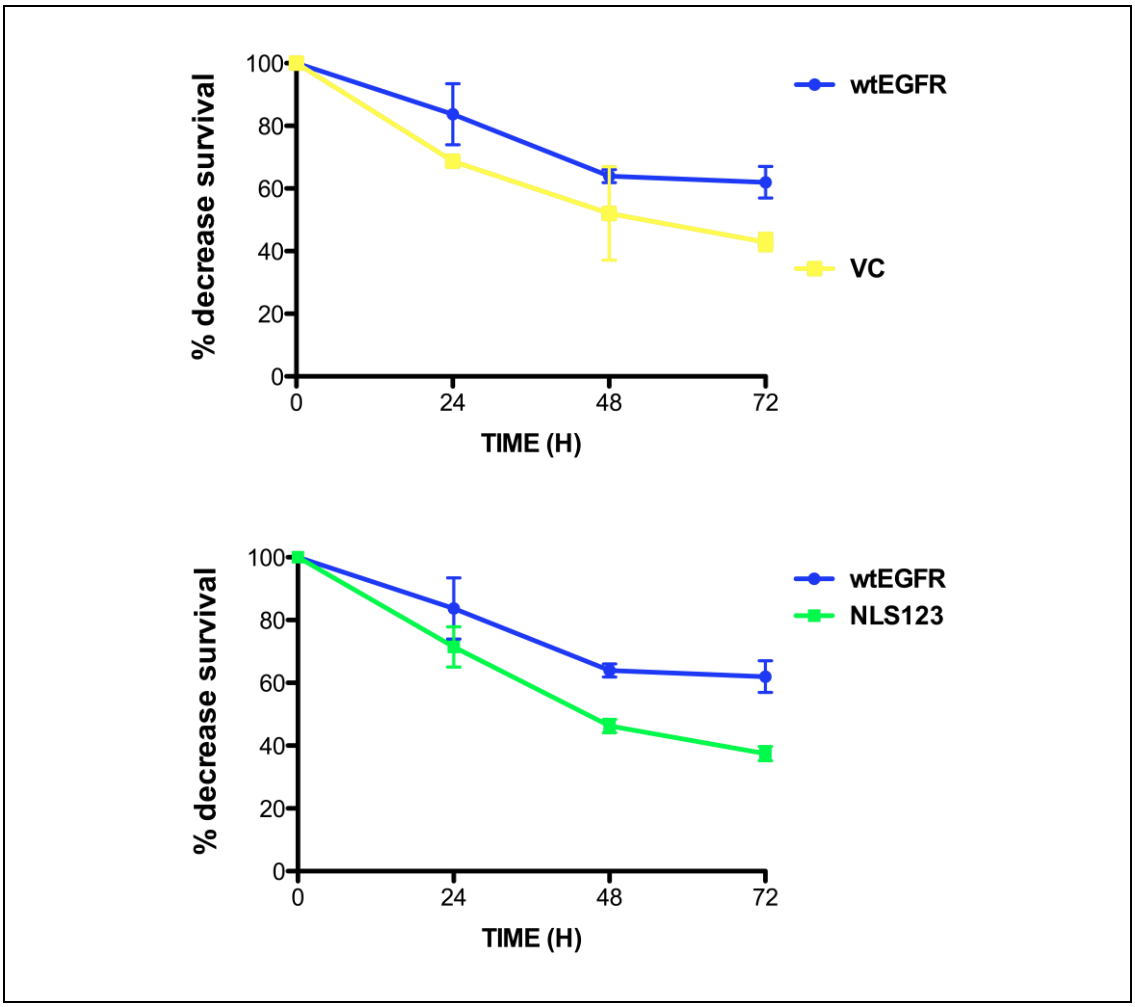

Figure 5.9: Cisplatin effects on cellular survival. Cells expressing wtEGFR, NLS123, L858R, LNLS123, EGFRvIII or VC were plated at 2.5 x10^4/ml. Then cells were treated with 50µM cisplatin for one hour in serum free media and then incubated over a period of 72 hours. Survival was assessed at 24 hours, 48 hours and 72 hours following cisplatin treatment. % decrease survival was calculated by comparing individually untreated cell lines with corresponding cisplatin treated. The graph shows mean % decrase survival of 3 independent experiments. The Fig shows comparison with wtEGFR expressing cells.

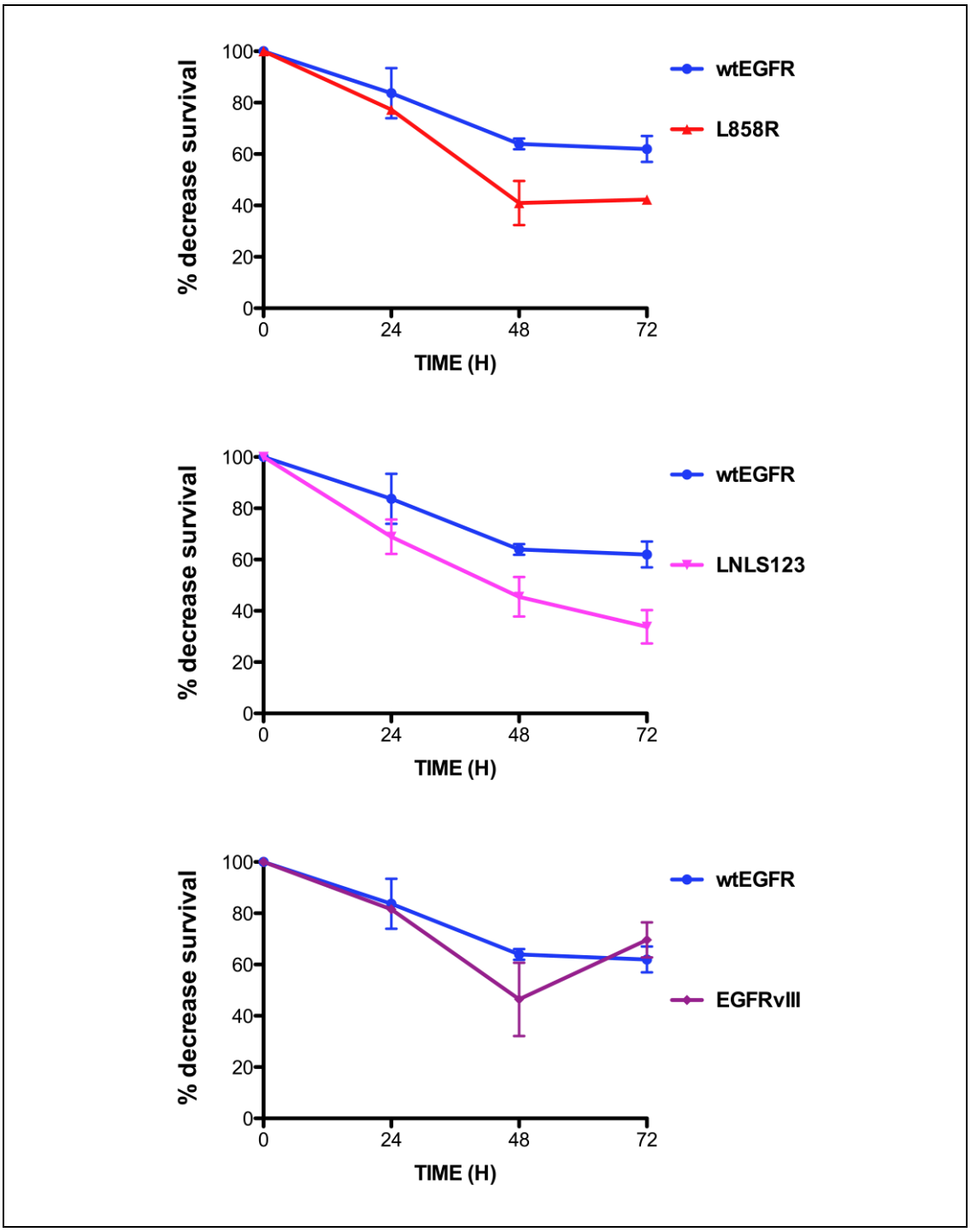

Figure 5.9: cont.

wtEGFR vs NLS123

time	wtEGFR		NLS123		P value
	Average	S.D.	Average	S.D.	
0	100	0.00	100	0.00	P > 0.05
24	83.72	9.77	71.49	6.42	P > 0.05
48	63.97	2.07	46.25	2.11	P < 0.05
72	61.99	5.02	37.44	2.26	P<0.001

wtEGFR vs L858R

time	wtEGFR		L858R		P value
	Average	S.D.	Average	S.D.	
0	100	0.00	100	0.00	P > 0.05
24	83.72	9.77	77.28	1.79	P > 0.05
48	63.97	2.07	40.95	8.56	P<0.01
72	61.99	5.02	42.26	1.00	P<0.01

wtEGFR vs LNLS123

time	wtEGFR		LNLS123		P value
	Average	S.D.	Average	S.D.	
0	100	0.00	100	0.00	P > 0.05
24	83.72	9.77	68.91	6.74	P > 0.05
48	63.97	2.07	45.48	7.73	P < 0.05
72	61.99	5.02	33.76	6.49	P<0.001

wtEGFR vs EGFRvIII

time	wtEGFR		EGFRvIII		P value
	Average	S.D.	Average	S.D.	
0	100	0.00	100	0.00	P > 0.05
24	83.72	9.77	81.52	0.85	P > 0.05
48	63.97	2.07	46.45	14.29	P<0.01
72	61.99	5.02	69.63	6.82	P > 0.05

wtEGFR vs V.C.

time	wtEGFR		V.C.		P value
	Average	S.D.	Average	S.D.	
0	100	0.00	100	0.00	P > 0.05
24	83.72	9.77	68.69	1.57	P > 0.05
48	63.97	2.07	52.06	14.92	P > 0.05
72	61.99	5.02	42.89	2.80	P<0.01

Table 6.1: Statistical analysis of the cisplatin effects on cellular survival. Table shows the average of three individual experiments, standard deviation (S.D.) of each individual cell line. All the cell lines were considered individually and compared to the wtEGFR expressing cell percentage of survival. P values were calculated using the 2 way ANOVA analysis and the Bonferroni post test. Difference were considered significant only for a P value < 0.01.

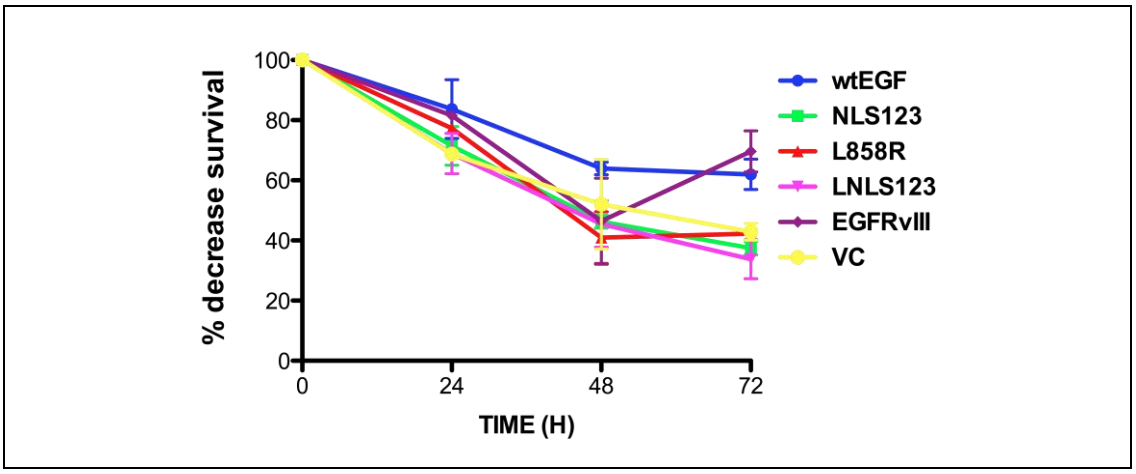

Figure 5.10: Percentage decrease survival following cisplatin treatment. The graph shows the effect of cisplatin on survival in all the cell lines grouped together

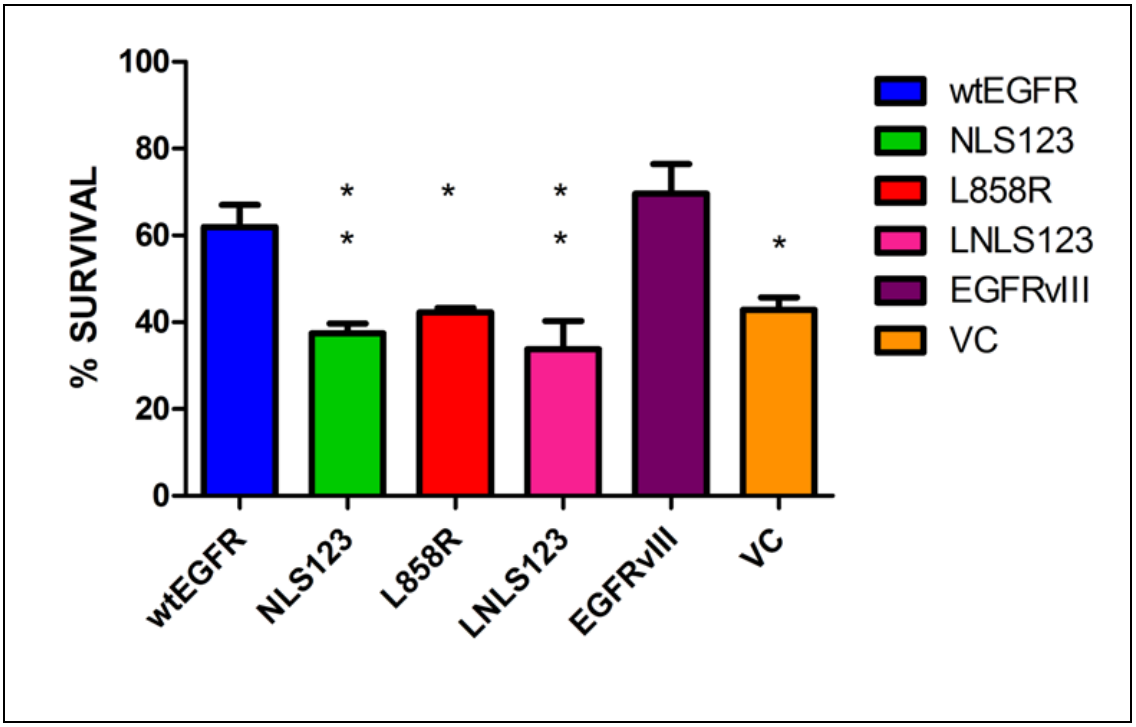

Figure 5.11: Percenatge survival following cisplatin treatment. The graph shows survival of all the cells lines 72 hours following cisplatin treatment Stars indicate statistical significance (*=P value <0.01, **= P value <0.001)

5.3 DISCUSSION

5.3.1 IR or cisplatin induces EGFR-DNAPKcs association

The association between EGFR and DNAPKcs has been shown in several reports however its induction has been controversial. The first study that shed light on this interaction demonstrated in fact that cetuximab inhibition of EGFR induced EGFR and DNAPKcs association resulting in a down-regulation of the DNA-PK kinase activity that impaired DNA repair (Bandyopadhyay et al, 1998). In contrast, multiple lines of evidence have since shown that EGFR is a major determinant of radiation-response and that this radio-protective function is exerted via its ability to bind DNAPKcs and mediate DNA repair (Dittmann et al, 2005a; Dittmann et al, 2007; Rodemann et al, 2007). These studies also demonstrated that EGFR inhibition via mAB or TKI treatment inhibits EGFR nuclear translocation and also association with DNAPKcs rendering cells sensitive to radiotherapy (Baumann et al, 2007; Das et al, 2007; Dittmann et al, 2008a; Nyati et al, 2006; Rodemann & Blaese, 2007; Toulany et al, 2005; Wanner et al, 2008). This study has shown that EGF, IR and cisplatin mediated EGFR nuclear translocation however only treatment with IR and cisplatin induce EGFR-DNAPKcs binding. Nuclear expression *per se* is therefore not sufficient to mediate this association suggesting that EGFR-DNAPKcs binding is specifically induced in response to DNA damage confirming the involvement of EGFR in modulation of DNA repair. As highlighted in the Introduction Chapter the role of EGFR nuclear expression is not uniquely related to DNA repair. EGFR stimulation by ligand has been shown to modulate gene expression and contribute to a variety of important transcription related cellular mechanisms such as proliferation (cyclinD1 expression) or oxidative stress (iNos expression) (Lo et al, 2005a; Wang & Hung, 2009). This highlights the complexity of EGFR nuclear localisation mechanism and its modularity to different inputs. Although, the molecular targeting of the pathway involved in EGFR nuclear translocation can still represent a good candidate for molecular intervention, these results have shown that EGFR nuclear translocation is not directly responsible for the binding with DNAPKcs.

5.3.2 wtEGFR and EGFRvIII associate to DNAPKcs

Despite the great number of reports discussing EGFR-DNAPKcs association and the lack of this complex formation in cells expressing L858R, the criteria necessary for

this binding and the EGFR characteristics required to allow this association have not been described. In this study there is not sufficient data to outline the mechanism that leads to this complex formation, however, the analysis of these results have lead to a few hypotheses.

While the nuclear expression of wtEGFR has been shown in several reports, nuclear expression of EGFRvIII has been controversial in the literature. EGFRvIII and STAT3 localisation within the nucleus was demonstrated in some studies (de la Iglesia et al, 2008), whereas other studies have reported lack of nuclear expression in glioma models (Mukherjee et al, 2009). The understanding that EGFRvIII, following internalisation, is recycled rather then sent to the lysosomal compartment supports the EGFR nuclear localisation mechanism. As previously discussed the nuclear translocation can take place only if the receptor escapes degradation. This study confirms that wtEGFR and EGFRvIII are expressed in the nucleus and also shows that they bind to DNAPKcs following cisplatin or IR treatment. If originally the constitutive activation may have been accounted as a determinant of EGFR-DNAPKcs binding, the hypothesis is now excluded since EGFR-DNAPKcs binding takes place only following cisplatin or IR treatment, despite constitutive activation throughout the conditions (EGFRvIII, L858R, LNLS123) and EGF-induced EGFR phosphorylation. Another hypothesis was that cisplatin or IR may induce EGFR phosphorylation on specific residues that favour EGFR-DNAPKcs interaction. Although this could be valid for wtEGFR receptor, the EGFRvIII constitutive activation suggests that EGFR-DNAPKcs binding is not determined by a specific phosphorylation event or by the up-regulation of the kinase activity of the receptor. Moreover, the lack of EGFR-DNAPKcs binding shown in L858R expressing cells only confirms that EGFR kinase activation is not central to determine EGFR-DNAPKcs binding. The previous chapters has already suggested that the impaired EGFR nuclear translocation in L858R-expressing cells is probably due to a lack of conformational change that does not expose the NLS for recognition. EGFRvIII is always in a dimerised active conformation suggesting that, differently from the L858R mutant, EGFRvIII constitutive activation is a consequence of a constitutive, structural, and active allosteric conformation. Recently, it has been shown that induced phosphorylation by peptide targeting of the residue T654 within the EGFR NLS sequence results in EGFR phosphorylated NLS which abolishes EGFR nuclear localisation and DNAPK activation inhibiting repair of IR induced-DNA damage

(Huang et al, 1997; Li et al, 2004). These results suggest that IR or cisplatin treatment may either induce the activation of a secondary molecule that prevents T654 EGFR phosphorylation or induce an EGFR conformational change that prevents this phosphorylation event and favours DNAPKcs-EGFR association.

5.3.3 EGFR-Hsp90 binding

HSP90 is one of the most abundant proteins in the cell. It is widely involved in biogenesis, stability and activity of its binding partners also called client proteins. It participates in the maturation of nascent proteins and in the regulation of signalling events as it is often found bound to a protein effector domain (e.g.: hormone binding domain or kinase domain) (Young et al, 2001). In many cases Hsp90 binding is characterised by repeated cycles of low affinity binding and release (Lavictoire et al, 2003). The literature suggests that Hsp90, rather than recognising specific motifs, binds to features that are common to unstable proteins, such as unveiled hydrophobic patches, gaining a higher level of affinity to the client protein via co-chaperones such as CDC37 (Prince & Matts, 2005). Pharmacological inhibition of Hsp90, via ansamycin antibiotics such as Geldanamycin, results in the degradation of client proteins showing that this chaperone is involved in protein stability (Sawai et al, 2008). As with other Hsps, it responds to stressful conditions (mainly metabolic insults) by assuring stability of key proteins and preventing their degradation. Hsp90 functions have been exploited by molecular intervention to target the over-expression of proteins that are involved in tumorigenesis such as EGFR and Her2 (Citri et al, 2004b; Yang et al, 2006). While EGFR requires Hsp90 for the maturation of nascent protein, but becomes independent of it once matured, Her2 stability depends on Hsp90 binding (Citri et al, 2004a). Wild type EGFR is quickly internalised following ligand activation and ubiquitinated by Cbl. In addition Cbl also promotes EGFR internalisation via its interaction with CIN85, which interacts with endophilins, the regulatory component of the clathrin coated pits. Recognition and internalisation of active EGFR by the Cin85/Cbl complex is necessary to regulate the distribution of the receptor and also its signal input. EGFR somatic mutations in NSCLC such as L858R have been shown to escape the ligand induced receptor down-regulation and present a strong association with Hsp90 and unphosphorylated Cbl. This impairs the Cbl mediated recruitment of CIN85 to the endocytic complex preventing the receptor degradation (Sawai et al, 2008;

Shimamura et al, 2005; Yang et al, 2006). The data showed in Fig 5.3 confirmed the binding between Hsp90 and L858R however IR treatment seemed to weaken this interaction. Similarly, NLS123 expressing cells showed the same pattern of interaction. This confirms the previously discussed data suggesting that the NLS123 mutation destabilises the receptor conformation. This semi-constitutive association with Hsp90 seems to be a signature for EGFR conformational instability. It is difficult to determine whether the weaker association shown following IR is due to timing or indicates receptor degradation. Future experiments will be able to shed more light on this open question.

Interestingly, LNLS123 expressing cells do not show weakening of the association following IR treatment; in contrast the Hsp90 binding does not seem to be modulated by any particular treatment suggesting a mechanism of interaction that may involve both conformational change and receptor activation. It has been shown that mutations that occur within or near the M5 loop region (αC-β4 region) of the EGFR protein, are likely to favour the binding with Hsp90 by affecting the conformation of this loop or altering the conformation of other parts of the kinase domain that interacts with Hsp90. All the mutations that expose the kinase domain to structural stresses require the chaperone stabilisation and, as a consequence, Hsp90 clients will boast an overall positive or neutral charge within the binding region. In contrast, proteins that do not require chaperone regulation will normally bear an overall negative charge (Citri et al, 2006). The change of all the arginine residues within the NLS sequence into alanines changes the positive signal of that stretch of amino acid into a neutral signal; therefore the change in charge is not the determinant factor. However, as shown in the previous chapter, the NLS123 mutation is altering the conformational change of the receptor impeding the allosteric activation and the dimer interface formation. Therefore, the structural stress imposed on the receptor may be responsible for the Hsp90 binding to the NLS123 mutant. The impact of the NLS123 mutation on protein stability is also shown by the LNLS123 mutant that shows higher binding affinity with Hsp90 as compared to the L858R.

It is difficult to comment on the interaction observed between Hsp90 and wtEGFR following cisplatin treatment. Although, the literature suggests mainly that Hsp90 binding confers stability to the client protein, the main role of heat shock proteins is to respond to cellular shocks favouring survival. Cisplatin-induced binding of wtEGFR to Hsp90 could prevent EGFR degradation and maintain a constitutive

function required in the response to cisplatin treatment. A very recent study showed dependence of wtEGFR and EGFRvIII on Hsp90 binding (Pines et al) . It is clear from Fig 5.3 that, although greatly weaker compared to the other mutants, both wtEGFR and EGFRvIII show association with Hsp90. Future studies will determine the relevance of this dependence and its degree in the context of DNA repair.

5.3.4 DNAPKcs subcellular localisation in response to IR or cisplatin is influenced by EGFR subcellular distribution.

In line with previous published evidence, this study shows EGFR and DNAPKcs association. The confocal analysis of the stable cells expressing constructs confirms the results shown in the previous chapter. Only wtEGFR and EGFRvIII are expressed in the nucleus following cisplatin or IR and this is induced by the treatments and not by a transient over-expression of the wtEGFR and EGFRvIII expressing plasmids. Interestingly, not only does DNAPKcs co-localise in the nucleus with wtEGFR and EGFRvIII but the impaired nuclear localisation shown by the remaining mutants seems to indirectly determine DNAPKcs cytosolic accumulation. Moreover, in L858R expressing cells DNAPKcs seems to be capable of localising within the nucleus despite the lack of L858R nuclear localisation. This explains why L858R cells showed intermediate repair following IR and cisplatin. In addition, this suggests that the NLS123 mutation may further, sterically, obstruct the receptor direct or indirect mediation of DNAPKcs nuclear localisation. EGFR may indirectly signal for DNAPKcs cellular distribution by activation of a secondary messenger or by physical interaction with another protein. The NLS123 mutation within the wtEGFR (NLS123) and the L858R (LNLS123) may interfere with this mechanism supporting the evidence that targeting the NLS inhibits DNAPKcs-EGFR binding and its function in repair (Dittmann et al)

5.3.5 EGFR–DNAPKcs interaction takes place both in the nucleus and in the cytoplasm

It was clearly demonstrated that EGFR binds to DNAPKcs and that they both co-localise within the same cellular compartments following cisplatin and IR. Since EGFR-DNAPKcs association has been reported this binding has only been shown by co-immunoprecipitating these two proteins from nuclear extracts. Although this answer the question relative to modulation in DNA repair, it does not characterise

this association with regards to whether these two proteins come into contact before entering the nucleus, whether this association is exclusively nuclear and therefore dependent of EGFR nuclear translocation. This is central to fully understand how molecular intervention can effectively target this interaction and modulate repair response and kinetics. The precise distance between two proteins sufficient to allow a physical interaction has not yet been defined. The proximity ligation assay determines whether the physical space between two proteins is smaller than 40 nm, which is acknowledged to be sufficient to allow protein-protein interaction. Fig 5.7 confirms the result of the immunoprecipitation by showing that only in wtEGFR and EGFRvIII expressing cells EGFR and DNAPKcs are in the proximity sufficient to interact. Moreover, it also shows that this interaction takes place both in the nucleus and in the cytoplasm suggesting that DNAPKcs recruitment by EGFR is most probably a cytosolic event that precedes the nuclear translocation. The time course immunoprecipitation discussed in the previous chapter showed that the binding between these two proteins increases over time and peaks at 18 following cisplatin treatment. The time course experiment also shows interaction already at 1 hour following cisplatin treatment, suggesting a recruitment that anticipates the DNA damage response. The possibility that EGFR-DNAPKcs complex forms in the cytosol and then migrates to the nucleus cannot be excluded. Similarly, the possibility that the cytosolic portion of this complex may have another secondary function still involved in response to therapy cannot be excluded.

5.3.6 EGFR modulates DNAPKcs kinase activity

EGFR modulation of DNAPK kinase activity has been shown in several reports. Cetuximab-induced reduction in DNA-PK kinase has been correlated not only with inhibited EGFR kinase activation but also with EGFR nuclear localisation (Dittmann et al, 2005b; Li et al, 2008; Perez-Torres et al, 2006). This has supported the experimental evidence that IR induces EGFR-DNAPKcs association leading to enhanced kinase activity of the NHEJ DNA-PK complex (Chen & Nirodi, 2007). This study showed that expression of EGFR modulates DNAPK kinase activity only in cells expressing wtEGFR or EGFRvIII. This did not occur in cells expressing EGFR constructs deficient in EGFR nuclear translocation and DNAPKcs binding. These data show that EGFR modulation of DNA repair is mediated via DNAPK pathways and requires EGFR-DNAPKcs binding and EGFR nuclear localisation.

The decrease of DNAPK activity in NLS123 expressing cells confirms the previously published data where EGFR inhibition by cetuximab or via Src knockdown also induced inhibition of DNAPK kinase activity (Andersen et al, 2009; Dittmann et al, 2008a; Dittmann et al, 2009; Gueven et al, 1998; Wheeler et al, 2009). Interestingly these down-regulations were highly statistically significant when compared to cells not expressing EGFR. The possibility that the NLS123 mutant indirectly inhibits the activation of signalling pathway involved in DNAPK kinase activity cannot be excluded. Future experiments utilising EGFR inhibitors and/or a kinase dead mutant will address this issue. There was no change in the kinase activity of cells expressing L858R or LNLS123 expressing cells. This suggests that, although nuclear translocation and the binding are determining the increment of DNAPK kinase activity, receptor kinase activation may also influence, indirectly, DNAPK. It has been shown that activation of AKT may lead to DNAPKcs activation as AKT has been shown to act as a kinase of DNAPKcs (Bozulic et al, 2008; Shi et al, 2009; Toulany et al, 2008b). The role of EGFR as a direct kinase activator of DNAPKcs via their physical interaction or as an indirect activator needs to be elucidated. It is arguable that EGFR recruits cytosolic DNAPKcs inducing DNAPKcs nuclear accumulation. This would then enhance the DNAPKcs-DNA interaction and therefore the kinase activity of the DNAPK complex. In EGFRvIII expressing cells both the binding and/or the nuclear translocation and the possible activation of a putative AKT back-up activation pathway may trigger the enhanced DNAPK kinase activity significantly higher than in wtEGFR expressing cells allowing a faster rate of DNA SB repair following IR.

5.3.7 Cisplatin toxicity

Cisplatin is one of the most widely used anticancer drugs. Although it is generally accepted that the binding of cisplatin to genomic DNA is the main event responsible for its anti-tumor property, nearly 90% of platinum is bound to plasma proteins (Turchi et al, 1999; Wang & Lippard, 2005; Wernyj & Morin, 2004). This leads to the activation of many signalling pathways which many line of evidence have shown to either confer sensitivity or resistance to the treatment. The activation of DNA repair mechanisms in response to cisplatin treatment has already been reviewed both in the introduction and in result chapter 2. Therefore the transduction of DNA damage signals on cellular signalling and survival will be briefly reviewed with

regards to the cisplatin induction of cell death and the involvement of AKT, MAPK/JNK/ERK in the response to cisplatin and how EGFR has been shown to modulate these pathways.

5.3.7.1 Cisplatin-induced cell death

Several lines of evidence have shown that cisplatin induces two different modes of cellular death: necrosis and apoptosis. A cytosolic swelling and loss of plasma membrane integrity characterize necrosis. It is initialized by the DNA damage-induced activation of PARP-1 that cleaves the glycolytic coenzyme NAD^+. Loss of NAD^+ inhibits the glycolytic production of ATP with subsequent depletion of cellular ATP leading to cell death via necrosis. In contrast, cells undergoing apoptosis show shrinkage, chromatin condensation and DNA fragmentation. Apoptotic death results from the activation of the caspases (aspartate specific family of proteases). The activation of the upstream CASP8 or CASP9 leads to the activation of downstream caspases such as CASP3 and CASP7. This induces the cleavage and subsequent degradation of many cellular proteins leading to apoptosis. Although in resistant cell lines cisplatin seems to produce characteristic features of necrosis there is evidence suggesting that within the same population of cells, platinum can induce both necrosis and apoptosis. Moreover the cooperation of these two pathways has been shown by the caspase activation and induction of apoptosis in presence of PARP1 induced NAD^+ cleavage inhibition (Fishel et al, 2005; Lee et al, 2005; Wernyj & Morin, 2004).

5.3.7.2 Pro-survival AKT signalling

AKT promotes cell survival via the down regulation of apoptotic pathways. It phosphorylates the X-linked inhibitor of apoptosis XIAP and inhibits the auto-ubiquitylation of this protein and the cisplatin induced ubiquitylation activities. Increased levels of XIAP have been shown to correlate with decreased levels of CASP3 and down regulation of apoptosis(Fraser et al, 2003a; Fraser et al, 2003b). In addition AKT has been shown to induce activation of NFkB (Asselin et al, 2001; Dan et al, 2004). Increased activity of NFkB correlates with decreased apoptosis whereas its inhibition has been shown to augment cisplatin cytoxicity. It has been demonstrated that cisplatin-induced T308 phosphorylation of AKT in MDA-MB-468

is dependent on Src and EGFR with EGFR being the initiator of the signal transduction that leads to the activation of this pro-survival signal (Yang et al, 2004).

5.3.7.3 p38MAPK/MAPK/JNK role in cisplatin resistance

There is a growing body of evidence suggesting that p38MAPK has a central role in the response to cisplatin treatment. Cisplatin activates p38MAPK for 8-12 hours in sensitive cells and for 1-3 hours in resistant cells suggesting that the different kinetics may explain the differential cytotoxicity (Mansouri et al, 2003). There is instead conflicting evidence on the role of ERK in influencing cellular survival following cisplatin treatment. Some studies indicate that ERK activation is associated with enhanced survival (Hayakawa et al, 1999). However the use of the MEK1 inhibitor has been shown to be effective only in certain cell line suggesting a more complex and cell line dependent response to cisplatin (Mandic et al, 2001). In addition elevated activation of RAS, an upstream component of the ERK signaling pathway has been shown to confer sensitivity to cisplatin (Wang & Lippard, 2005).

Far from being clear is also the JNK mediated response to cisplatin treatment. Several studied have shown evidence that activation of the JNK pathway contributes to cisplatin induced apoptosis (Mansouri et al, 2003) whereas some other have shown a protective response necessary for cell survival (Davis, 2000). Interestingly one study has shown that duration of the signalling pathway activation might be central for the decision between cellular proliferation or death (Chen et al, 1996).

It has been shown that phosphorylation of the T669 by p38MAPK leads to cisplatin induced-EGFR internalization. This event seems to be mediated by ERK inducing the abrogation of EGFR signalling to JNK (Winograd-Katz & Levitzki, 2006). At the same time, this study has suggested that EGFR signalling to JNK is dependent on receptor internalization. Since internalization defective EGFR was shown to increase cell proliferation and lead to ERK down- regulation it has been suggested that internalized EGFR may form signalling complexes within the endosomes triggering a switch in signalling from proliferation to survival (Grandal & Madshus, 2008).

5.3.7.4 EGFR is required for cisplatin resistance

In line with these studies the MTT assay have shown that wtEGFR or EGFRvIII expression confers survival to cells following cisplatin treatment. Our analysis does not verify whether the cisplatin induced EGFR activation (wtEGFR) or the

constitutive kinase activation (EGFRvIII) may be responsible for induction of pro-survival signalling. These data suggest that by 36 hours following cisplatin treatment, cells expressing wtEGFR and EGFRvIII have already repaired all the crosslinks induced by cisplatin treatment (Result Chapter 4) and also that by 18 hours both the wt receptor and the EGFRvIII mutant are expressed in the nucleus and associate with DNAPKcs resulting in up-regulation of DNAPK activity. The EGFR kinase activation alone does not seem to be responsible for the survival response. Cells expressing the constitutive kinase active L858R mutant, which does not translocates to the nucleus, show less than 50% survival, suggesting that both EGFR nuclear expression and binding to DNAPKcs modulation of DNA repair could correlate with the pro-survival response. This is confirmed also by the results obtained in cell expressing NLS123 and LNLS123 where cisplatin toxicity is clearly compromising cellular viability. Further experiments will show whether it is a direct effect of DNA repair inhibition or whether this is the result of signalling events in response to DNA damage or both.

CHAPTER 6: CONCLUSION

EGFR is commonly expressed in human tumours and has been an important target for therapy. Although several small molecules inhibitors and antibodies are currently utilised in the clinic in combination with chemotherapy and IR, the successfulness of these treatments has been limited. EGFR nuclear expression has been a source of important insights in the biology of this oncogene. This study investigated the role of nuclear EGFR in the modulation of DNA repair following treatment with cisplatin and IR.

Chapter 3 focused on the construction of two NLS mutants, one in the background of wtEGFR and the other one in the background of the somatic mutation L858R often found in lung cancer. Then nuclear expression of EGFR following IR treatment and EGF induction was confirmed. Evidence was provided showing that the mutation of all arginine residues of EGFR NLS sequence induced inhibition of nuclear translocation in the NLS123 and LNLS123 mutant. In line with published data, also L858R showed impaired nuclear translocation. The characterisation of the constructs within the NIH3T3 murine fibroblast (negative for the expression of EGFR) showed that the NLS123 mutation impairs EGFR kinase activity. Recent studies have shown the importance of the NLS sequence in EGFR activation and binding to the importin machinery. This suggested that the inhibition of nuclear translocation was due to the lack of an allosteric change required by EGFR to adopt an active conformation. Only EGFR molecules undergoing this conformational change expose the NLS sequence for recognition. Interestingly LNLS123 expressing cells showed EGFR constitutive activation suggesting that the impaired EGFR nuclear translocation observed in L858R is due to the receptor conformation. The kinase mutation at position 858 induces a modification within the active loop that allows constitutive kinase activation without requiring kinase domain juxtaposition. This explains why the single amino acid mutation is sufficient to impair EGFR nuclear translocation in L858R and LNLS123 expressing cells. **Chapter 4** showed EGFR modulation of DNA repair kinetics following cisplatin and IR using the alkaline single-cell gel electrophoresis (comet assay). Constructs expressing point mutation within the NLS sequence, a deletion of the NLS sequence, an EGFR kinase death mutant and the somatic EGFRvIII were utilised to compare and contrast the different modulation of the unhooking of cisplatin interstrand crosslinks and the repair of DNA strand breaks. Three different repair behaviours were observed. Whilst wtEGFR and EGFRvIII showed complete repair by 36 hours following

cisplatin and 4 hour following IR treatment, intermediate levels of repair were observed in cells expressing L858R, KMT and ΔNLS. Complete inhibition of repair was observed in cell expressing NLS123 and LNLS123. The result obtained by the comet assays suggested that EGFR kinase activity is not central to the modulation of repair and that the inhibition of nuclear translocation via the NLS mutation was central to the repair inhibition. The impaired receptor dimerisation and the lack of an active conformation seem to be critical for this mechanism. The confocal analysis on the transient transfectants showed that the impaired nuclear localisation of EGFR and DNAPKcs (NLS123 and LNLS123 expressing cells) correlated with complete inhibition of repair. Interestingly, while low levels of EGFR nuclear accumulation (M1 and M12) corresponded to DNA repair, low levels of DNAPKcs nuclear accumulation but complete inhibition of EGFR nuclear expression (L858R, KMT and ΔNLS expressing cells) resulted only in intermediate levels of repair. The difference in modulation shown with the comet assay and the nuclear expression of the different constructs shown in the confocal analysis confirms that the repair is mediated by EGFR and that is modulated by EGFR nuclear translocation.

Chapter 5 investigated the mechanism involved in the EGFR mediated modulation of DNA repair. The association between EGFR and DNAPKcs, induced by IR and cisplatin, correlated with DNA repair. EGFR interaction with DNAPKcs was shown only in wtEGFR and EGFRvIII expressing cells. Although EGFR nuclear translocation *per se* was not sufficient to mediate binding with DNAPKcs, nuclear expression was required for repair. The confocal analysis showed that the nls123 mutation not only inhibited EGFR nuclear translocation (NLS123 and LNLS123 expressing cells) but also binding to DNAPKcs and, indirectly, DNAPKcs nuclear accumulation. The formation of this complex was shown to take place both in the nucleus and in the cytoplasm and seemed to require EGFR allosteric active conformational change. The association between EGFR and DNAPKcs is central to repair as shown by the DNAPK kinase assay. While, in cells expressing wtEGFR and EGFRvIII there was a clear upregulation in DNAPK kinase activity, L858R and LNLS123 expressing cells showed no upregulation. In line with previous study that showed that Gefitinib-induced EGFR inhibition resulted in down regulation of DNAPK kinase activity and also in DNAPKcs cytosolic accumulation, the impaired binding to DNAPKcs and impaired kinase activity shown in NLS123 expressing cells correlated with a significant downregulation in DNAPK kinase activity. These

data suggest that EGFR inhibition by targeting EGFR NLS sequence inhibits EGFR nuclear accumulation and EGFR kinase activity via the impairment of its allosteric activation. As a consequence, the binding to DNAPKcs and DNAPK kinase activity are significantly impaired leading to inhibition of DNA repair following cisplatin and IR. Our data have also shown that the impairment of EGFR nuclear translocation and the consequent modulation of DNA repair via the inhibition of DNAPK kinase activity correlate with cellular survival following cisplatin. The mechanism of nuclear translocation, following treatment with cisplatin or IR can therefore be accounted as a cellular response that cells employ to overcome DNA damage and survive treatment toxicity.

6.1 EGFR and DNAPKcs physical interaction

This study validates the importance of EGFR-DNAPKcs interaction following treatment with cisplatin and IR. Deletion constructs expressing either protein can be generated and used to determine the domain involved in this interaction. This could have potential implication in the design of novel drugs with relevance to the EGFR-DNAPKcs association. Our initial work on the construction of deletion mutants has led to the conclusion that EGFR subcellular distribution and allosteric conformation are determinant to the binding. Although, deletion mutants would be ideal to underpin the exact stretch of amino acid responsible for EGFR-DNAPKcs binding, the impaired association observed in the NLS mutants suggests that other regions within EGFR may indirectly impair this association. DNAPKcs deletion mutants are therefore the only viable option.

Despite the *in vitro* success of many EGFR inhibitors clinical outcomes are still poor. This study points out that dimerisation and conformational change, being events upstream of kinase activation, may be better targets for EGFR directed therapy. The validation of EGFR allosteric conformational change as an absolute requirement for DNAPKcs binding can be evaluated by analysing EGFR dimer formations following treatment in wtEGFR or EGFR mutants expressing cells. This together with a pharmacological inhibition of EGFR dimer formation will shed some light on other modalities to inhibit EGFR and DNAPKcs that may result in better therapeutic outcome.

6.2 Novel partners involved in EGFR modulation of repair

The repair of SBs shown by the comet assay suggest that the most significant difference in repair kinetics among all the mutants is within the first 30 minutes following IR. Many studies have discussed the type of breaks detected by the comet assay and although it primarily detects singles strand breaks, double strand breaks are not to be excluded. Despite being difficult to detect via the comet assay, the clustering formation of DNA damage following IR implies that statistically the formation of DSBs is inevitable. Considering their complexity as opposed to SSBs, DSBs are regarded as being the subject of 'late repair'. While the early and immediate repair shows the kinetics of SSBs, the difference in kinetics of the late repair highlights the repair inhibition of DSBs. DNAPKcs is the central component of NHEJ the pathway involved in the repair DSBs, therefore the observed differences in the early repair kinetics may be the result of EGFR interaction with other DNA repair proteins involved in SSB repair. Our preliminary data on the gliomas model MO59J and M059K suggest that in absence of DNAPKcs, Gefitinib-induced EGFR inhibition results in slower repair kinetic following IR treatment. This suggests a role for EGFR in repair independent of DNAPKcs. The study of alternative interactions by immunoprecipitation and confocal imaging in cells expressing wtEGFR and EGFR mutants in the NLS sequence may reveal novel mechanisms of EGFR modulation of DNA repair.

6.3 EGFR mediated transcription

EGFR nuclear expression following ligand activation has been shown to induce iNOS, cyclin D1, Aurora A, and RNA helicase A expression. Binding with the STAT family of transcription factors is central to the modulation of gene expression. Although here and in previous studies cisplatin and IR treatments have been shown to induce EGFR nuclear translocation, little is known about the modulation of gene expression mediated by EGFR following these treatments. Further studies should be designed to address this point and to determine a read out of all the genes whose expression is mediated by EGFR. The Hsp90 binding to wtEGFR following cisplatin treatment (chapter 5) is indicative of a stress response mechanism that may involve transcriptional regulation. The system validated in this study will allow the investigation of the EGFR characteristics involved in transcriptional activation and unveil novel mechanisms involved in resistance to cisplatin and IR.

6.4 Conclusion

These results highlight the importance of understanding the events that lead to EGFR subcellular distribution and its involvement in mediating DNA response following cisplatin and IR. The molecular mechanisms of EGFR nuclear translocation and binding with DNAPKcs will form the design of future molecular targeted therapy and point the way for further studies to investigate the role of EGFR in cancer therapy.

References

Achanta G, Pelicano H, Feng L, Plunkett W, Huang P (2001) Interaction of p53 and DNA-PK in response to nucleoside analogues: potential role as a sensor complex for DNA damage. *Cancer Res* **61:** 8723-8729

Adair GM, Rolig RL, Moore-Faver D, Zabelshansky M, Wilson JH, Nairn RS (2000) Role of ERCC1 in removal of long non-homologous tails during targeted homologous recombination. *EMBO J* **19:** 5552-5561

Adrain C, Martin SJ (2009) Apoptosis: calling time on apoptosome activity. *Sci Signal* **2:** pe62

Agelaki S, Spiliotaki M, Markomanolaki H, Kallergi G, Mavroudis D, Georgoulias V, Stournaras C (2009) Caveolin-1 regulates EGFR signaling in MCF-7 breast cancer cells and enhances gefitinib-induced tumor cell inhibition. *Cancer Biol Ther* **8:** 1470-1477

Aifa S, Frikha F, Miled N, Johansen K, Lundstrom I, Svensson SP (2006a) Phosphorylation of Thr654 but not Thr669 within the juxtamembrane domain of the EGF receptor inhibits calmodulin binding. *Biochem Biophys Res Commun* **347:** 381-387

Aifa S, Miled N, Frikha F, Aniba MR, Svensson SP, Rebai A (2006b) Electrostatic interactions of peptides flanking the tyrosine kinase domain in the epidermal growth factor receptor provides a model for intracellular dimerization and autophosphorylation. *Proteins* **62:** 1036-1043

Akaboshi M, Kawai K, Maki H, Akuta K, Ujeno Y, Miyahara T (1992) The number of platinum atoms binding to DNA, RNA and protein molecules of HeLa cells treated with cisplatin at its mean lethal concentration. *Jpn J Cancer Res* **83:** 522-526

Allen C, Halbrook J, Nickoloff JA (2003) Interactive competition between homologous recombination and non-homologous end joining. *Mol Cancer Res* **1:** 913-920

Alvarado D, Klein DE, Lemmon MA (2009) ErbB2 resembles an autoinhibited invertebrate epidermal growth factor receptor. *Nature* **461:** 287-291

Amit I, Citri A, Shay T, Lu Y, Katz M, Zhang F, Tarcic G, Siwak D, Lahad J, Jacob-Hirsch J, Amariglio N, Vaisman N, Segal E, Rechavi G, Alon U, Mills GB, Domany E, Yarden Y (2007a) A module of negative feedback regulators defines growth factor signaling. *Nat Genet* **39:** 503-512

Amit I, Wides R, Yarden Y (2007b) Evolvable signaling networks of receptor tyrosine kinases: relevance of robustness to malignancy and to cancer therapy. *Mol Syst Biol* **3:** 151

Andersen P, Villingshoj M, Poulsen HS, Stockhausen MT (2009) Improved response by co-targeting EGFR/EGFRvIII and Src family kinases in human cancer cells. *Cancer Invest* **27:** 178-183

Andressoo JO, Hoeijmakers JH, de Waard H (2005) Nucleotide excision repair and its connection with cancer and ageing. *Adv Exp Med Biol* **570:** 45-83

Andressoo JO, Hoeijmakers JH, Mitchell JR (2006) Nucleotide excision repair disorders and the balance between cancer and aging. *Cell Cycle* **5:** 2886-2888

Armour AA, Watkins CL The challenge of targeting EGFR: experience with gefitinib in nonsmall cell lung cancer. *Eur Respir Rev* **19:** 186-196

Arteaga CL (2002) Epidermal growth factor receptor dependence in human tumors: more than just expression? *Oncologist* **7 Suppl 4:** 31-39

Asselin E, Mills GB, Tsang BK (2001) XIAP regulates Akt activity and caspase-3-dependent cleavage during cisplatin-induced apoptosis in human ovarian epithelial cancer cells. *Cancer Res* **61:** 1862-1868

Azevedo F, Marques F, Fokt H, Oliveira R, Johansson B Measuring oxidative DNA damage and DNA repair using the yeast comet assay. *Yeast* **28:** 55-61

Azqueta A, Shaposhnikov S, Collins AR (2009) DNA oxidation: investigating its key role in environmental mutagenesis with the comet assay. *Mutat Res* **674:** 101-108

Bae JH, Schlessinger J (2010) Asymmetric tyrosine kinase arrangements in activation or autophosphorylation of receptor tyrosine kinases. *Mol Cells* **29:** 443-448

Bailey SM, Brenneman MA, Halbrook J, Nickoloff JA, Ullrich RL, Goodwin EH (2004) The kinase activity of DNA-PK is required to protect mammalian telomeres. *DNA Repair (Amst)* **3:** 225-233

Bandyopadhyay D, Mandal M, Adam L, Mendelsohn J, Kumar R (1998) Physical interaction between epidermal growth factor receptor and DNA-dependent protein kinase in mammalian cells. *J Biol Chem* **273:** 1568-1573

Bassermann F, Pagano M (2010) Dissecting the role of ubiquitylation in the DNA damage response checkpoint in G2. *Cell Death Differ* **17:** 78-85

Batty DP, Wood RD (2000) Damage recognition in nucleotide excision repair of DNA. *Gene* **241:** 193-204

Baumann M, Krause M, Dikomey E, Dittmann K, Dorr W, Kasten-Pisula U, Rodemann HP (2007) EGFR-targeted anti-cancer drugs in radiotherapy: preclinical evaluation of mechanisms. *Radiother Oncol* **83:** 238-248

Bean J, Brennan C, Shih JY, Riely G, Viale A, Wang L, Chitale D, Motoi N, Szoke J, Broderick S, Balak M, Chang WC, Yu CJ, Gazdar A, Pass H, Rusch V, Gerald W, Huang SF, Yang PC, Miller V, Ladanyi M, Yang CH, Pao W (2007) MET amplification occurs with or without T790M mutations in EGFR mutant lung tumors with acquired resistance to gefitinib or erlotinib. *Proc Natl Acad Sci U S A* **104:** 20932-20937

Benavente S, Huang S, Armstrong EA, Chi A, Hsu KT, Wheeler DL, Harari PM (2009) Establishment and characterization of a model of acquired resistance to epidermal growth factor receptor targeting agents in human cancer cells. *Clin Cancer Res* **15:** 1585-1592

Benhar M, Engelberg D, Levitzki A (2002) Cisplatin-induced activation of the EGF receptor. *Oncogene* **21:** 8723-8731

Bentzen SM (2003) Repopulation in radiation oncology: perspectives of clinical research. *Int J Radiat Biol* **79:** 581-585

Bessho T, Sancar A, Thompson LH, Thelen MP (1997) Reconstitution of human excision nuclease with recombinant XPF-ERCC1 complex. *J Biol Chem* **272:** 3833-3837

Bitler BG, Goverdhan A, Schroeder JA (2010) MUC1 regulates nuclear localization and function of the epidermal growth factor receptor. *J Cell Sci* **123:** 1716-1723

Boeckman HJ, Trego KS, Turchi JJ (2005) Cisplatin sensitizes cancer cells to ionizing radiation via inhibition of nonhomologous end joining. *Mol Cancer Res* **3:** 277-285

Borst P, Rottenberg S, Jonkers J (2008) How do real tumors become resistant to cisplatin? *Cell Cycle* **7:** 1353-1359

Bose R, Zhang X (2009) The ErbB kinase domain: structural perspectives into kinase activation and inhibition. *Exp Cell Res* **315:** 649-658

Bozulic L, Surucu B, Hynx D, Hemmings BA (2008) PKBalpha/Akt1 acts downstream of DNA-PK in the DNA double-strand break response and promotes survival. *Mol Cell* **30:** 203-213

Branzei D, Foiani M (2008) Regulation of DNA repair throughout the cell cycle. *Nat Rev Mol Cell Biol* **9:** 297-308

Breen L, Heenan M, Amberger-Murphy V, Clynes M (2007) Investigation of the role of p53 in chemotherapy resistance of lung cancer cell lines. *Anticancer Res* **27:** 1361-1364

Bublil EM, Yarden Y (2007) The EGF receptor family: spearheading a merger of signaling and therapeutics. *Curr Opin Cell Biol* **19:** 124-134

Caldecott KW (2008) Single-strand break repair and genetic disease. *Nat Rev Genet* **9:** 619-631

Carpenter G (1993) EGF: new tricks for an old growth factor. *Curr Opin Cell Biol* **5:** 261-264

Carter CA, Kelly RJ, Giaccone G (2009) Small-molecule inhibitors of the human epidermal receptor family. *Expert Opin Investig Drugs* **18:** 1829-1842

Cepeda V, Fuertes MA, Castilla J, Alonso C, Quevedo C, Perez JM (2007) Biochemical mechanisms of cisplatin cytotoxicity. *Anticancer Agents Med Chem* **7:** 3-18

Ceppi P, Volante M, Novello S, Rapa I, Danenberg KD, Danenberg PV, Cambieri A, Selvaggi G, Saviozzi S, Calogero R, Papotti M, Scagliotti GV (2006) ERCC1 and RRM1 gene expressions but not EGFR are predictive of shorter survival in advanced non-small-cell lung cancer treated with cisplatin and gemcitabine. *Ann Oncol* **17:** 1818-1825

Chabner BA, Roberts TG, Jr. (2005) Timeline: Chemotherapy and the war on cancer. *Nat Rev Cancer* **5:** 65-72

Chan DW, Chen BP, Prithivirajsingh S, Kurimasa A, Story MD, Qin J, Chen DJ (2002) Autophosphorylation of the DNA-dependent protein kinase catalytic subunit is required for rejoining of DNA double-strand breaks. *Genes Dev* **16:** 2333-2338

Chang JW, Chou CL, Huang SF, Wang HM, Hsieh JJ, Hsu T, Cheung YC (2007) Erlotinib response of EGFR-mutant gefitinib-resistant non-small-cell lung cancer. *Lung Cancer* **58:** 414-417

Chang YC, Wu W, Zhang JL, Huang Y (2009) Allosteric activation mechanism of the cys-loop receptors. *Acta Pharmacol Sin* **30:** 663-672

Chen BP, Chan DW, Kobayashi J, Burma S, Asaithamby A, Morotomi-Yano K, Botvinick E, Qin J, Chen DJ (2005) Cell cycle dependence of DNA-dependent protein kinase phosphorylation in response to DNA double strand breaks. *J Biol Chem* **280:** 14709-14715

Chen DJ, Nirodi CS (2007) The epidermal growth factor receptor: a role in repair of radiation-induced DNA damage. *Clin Cancer Res* **13:** 6555-6560

Chen YR, Fu YN, Lin CH, Yang ST, Hu SF, Chen YT, Tsai SF, Huang SF (2006) Distinctive activation patterns in constitutively active and gefitinib-sensitive EGFR mutants. *Oncogene* **25:** 1205-1215

Chen YR, Wang X, Templeton D, Davis RJ, Tan TH (1996) The role of c-Jun N-terminal kinase (JNK) in apoptosis induced by ultraviolet C and gamma radiation. Duration of JNK activation may determine cell death and proliferation. *J Biol Chem* **271:** 31929-31936

Chen Z, Ke LD, Yuan XH, Adler-Storthz K (2000) Correlation of cisplatin sensitivity with differential alteration of EGFR expression in head and neck cancer cells. *Anticancer Res* **20:** 899-902

Cheng WH, Kusumoto R, Opresko PL, Sui X, Huang S, Nicolette ML, Paull TT, Campisi J, Seidman M, Bohr VA (2006) Collaboration of Werner syndrome protein and BRCA1 in cellular responses to DNA interstrand cross-links. *Nucleic Acids Res* **34:** 2751-2760

Choong NW, Dietrich S, Seiwert TY, Tretiakova MS, Nallasura V, Davies GC, Lipkowitz S, Husain AN, Salgia R, Ma PC (2006) Gefitinib response of erlotinib-refractory lung cancer involving meninges--role of EGFR mutation. *Nat Clin Pract Oncol* **3:** 50-57; quiz 51 p following 57

Choowongkomon K, Carlin CR, Sonnichsen FD (2005) A structural model for the membrane-bound form of the juxtamembrane domain of the epidermal growth factor receptor. *J Biol Chem* **280:** 24043-24052

Choowongkomon K, Hobert ME, He C, Carlin CR, Sonnichsen FD (2004) Aqueous and micelle-bound structural characterization of the epidermal growth factor receptor juxtamembrane domain containing basolateral sorting motifs. *J Biomol Struct Dyn* **21:** 813-826

Chuderland D, Konson A, Seger R (2008) Identification and characterization of a general nuclear translocation signal in signaling proteins. *Mol Cell* **31:** 850-861

Citri A, Alroy I, Lavi S, Rubin C, Xu W, Grammatikakis N, Patterson C, Neckers L, Fry DW, Yarden Y (2002) Drug-induced ubiquitylation and degradation of ErbB receptor tyrosine kinases: implications for cancer therapy. *EMBO J* **21:** 2407-2417

Citri A, Gan J, Mosesson Y, Vereb G, Szollosi J, Yarden Y (2004a) Hsp90 restrains ErbB-2/HER2 signalling by limiting heterodimer formation. *EMBO Rep* **5:** 1165-1170

Citri A, Harari D, Shohat G, Ramakrishnan P, Gan J, Lavi S, Eisenstein M, Kimchi A, Wallach D, Pietrokovski S, Yarden Y (2006) Hsp90 recognizes a common surface on client kinases. *J Biol Chem* **281:** 14361-14369

Citri A, Kochupurakkal BS, Yarden Y (2004b) The achilles heel of ErbB-2/HER2: regulation by the Hsp90 chaperone machine and potential for pharmacological intervention. *Cell Cycle* **3:** 51-60

Citri A, Yarden Y (2006) EGF-ERBB signalling: towards the systems level. *Nat Rev Mol Cell Biol* **7:** 505-516

Clingen PH, Arlett CF, Hartley JA, Parris CN (2007) Chemosensitivity of primary human fibroblasts with defective unhooking of DNA interstrand cross-links. *Exp Cell Res* **313:** 753-760

Clingen PH, De Silva IU, McHugh PJ, Ghadessy FJ, Tilby MJ, Thurston DE, Hartley JA (2005) The XPF-ERCC1 endonuclease and homologous recombination contribute to the repair of minor groove DNA interstrand crosslinks in mammalian cells produced by the pyrrolo[2,1-c][1,4]benzodiazepine dimer SJG-136. *Nucleic Acids Res* **33:** 3283-3291

Collins AR (2004) The comet assay for DNA damage and repair: principles, applications, and limitations. *Mol Biotechnol* **26:** 249-261

Collis SJ, DeWeese TL, Jeggo PA, Parker AR (2005) The life and death of DNA-PK. *Oncogene* **24:** 949-961

Corbett AH, Krebber H (2004) Hot trends erupting in the nuclear transport field. Workshop on mechanisms of nuclear transport. *EMBO Rep* **5:** 453-458

Costa DB, Nguyen KS, Cho BC, Sequist LV, Jackman DM, Riely GJ, Yeap BY, Halmos B, Kim JH, Janne PA, Huberman MS, Pao W, Tenen DG, Kobayashi S (2008) Effects of erlotinib in EGFR mutated non-small cell lung cancers with resistance to gefitinib. *Clin Cancer Res* **14:** 7060-7067

Croce CM (2008) Oncogenes and cancer. *N Engl J Med* **358:** 502-511

Cyert MS (2001) Regulation of nuclear localization during signaling. *J Biol Chem* **276:** 20805-20808

Dan HC, Sun M, Kaneko S, Feldman RI, Nicosia SV, Wang HG, Tsang BK, Cheng JQ (2004) Akt phosphorylation and stabilization of X-linked inhibitor of apoptosis protein (XIAP). *J Biol Chem* **279:** 5405-5412

Darzynkiewicz Z, Traganos F, Wlodkowic D (2009) Impaired DNA damage response--an Achilles' heel sensitizing cancer to chemotherapy and radiotherapy. *Eur J Pharmacol* **625:** 143-150

Das AK, Chen BP, Story MD, Sato M, Minna JD, Chen DJ, Nirodi CS (2007) Somatic mutations in the tyrosine kinase domain of epidermal growth factor receptor (EGFR) abrogate EGFR-mediated radioprotection in non-small cell lung carcinoma. *Cancer Res* **67:** 5267-5274

Davis RJ (2000) Signal transduction by the JNK group of MAP kinases. *Cell* **103:** 239-252

Dawson JP, Bu Z, Lemmon MA (2007) Ligand-induced structural transitions in ErbB receptor extracellular domains. *Structure* **15:** 942-954

De Bont R, van Larebeke N (2004) Endogenous DNA damage in humans: a review of quantitative data. *Mutagenesis* **19:** 169-185

de la Iglesia N, Konopka G, Puram SV, Chan JA, Bachoo RM, You MJ, Levy DE, Depinho RA, Bonni A (2008) Identification of a PTEN-regulated STAT3 brain tumor suppressor pathway. *Genes Dev* **22:** 449-462

De Silva IU, McHugh PJ, Clingen PH, Hartley JA (2000) Defining the roles of nucleotide excision repair and recombination in the repair of DNA interstrand cross-links in mammalian cells. *Mol Cell Biol* **20:** 7980-7990

De Silva IU, McHugh PJ, Clingen PH, Hartley JA (2002) Defects in interstrand cross-link uncoupling do not account for the extreme sensitivity of ERCC1 and XPF cells to cisplatin. *Nucleic Acids Res* **30:** 3848-3856

Debucquoy A, Machiels JP, McBride WH, Haustermans K Integration of epidermal growth factor receptor inhibitors with preoperative chemoradiation. *Clin Cancer Res* **16:** 2709-2714

DePinho RA (2000) The age of cancer. *Nature* **408:** 248-254

Di Fiore PP, Pierce JH, Fleming TP, Hazan R, Ullrich A, King CR, Schlessinger J, Aaronson SA (1987) Overexpression of the human EGF receptor confers an EGF-dependent transformed phenotype to NIH 3T3 cells. *Cell* **51:** 1063-1070

DiBiase SJ, Zeng ZC, Chen R, Hyslop T, Curran WJ, Jr., Iliakis G (2000) DNA-dependent protein kinase stimulates an independently active, nonhomologous, end-joining apparatus. *Cancer Res* **60:** 1245-1253

Dick JE (2008) Stem cell concepts renew cancer research. *Blood* **112:** 4793-4807

Dikomey E, Franzke J (1986a) DNA repair kinetics after exposure to X-irradiation and to internal beta-rays in CHO cells. *Radiat Environ Biophys* **25:** 189-194

Dikomey E, Franzke J (1986b) Three classes of DNA strand breaks induced by X-irradiation and internal beta-rays. *Int J Radiat Biol Relat Stud Phys Chem Med* **50:** 893-908

Dittmann K, Mayer C, Fehrenbacher B, Schaller M, Kehlbach R, Rodemann HP Nuclear EGFR shuttling induced by ionizing radiation is regulated by phosphorylation at residue Thr654. *FEBS Lett*

Dittmann K, Mayer C, Fehrenbacher B, Schaller M, Kehlbach R, Rodemann HP (2010a) Nuclear EGFR shuttling induced by ionizing radiation is regulated by phosphorylation at residue Thr654. *FEBS Lett* **584:** 3878-3884

Dittmann K, Mayer C, Fehrenbacher B, Schaller M, Raju U, Milas L, Chen DJ, Kehlbach R, Rodemann HP (2005a) Radiation-induced epidermal growth factor receptor nuclear import is linked to activation of DNA-dependent protein kinase. *J Biol Chem* **280:** 31182-31189

Dittmann K, Mayer C, Kehlbach R, Rodemann HP (2008a) Radiation-induced caveolin-1 associated EGFR internalization is linked with nuclear EGFR transport and activation of DNA-PK. *Mol Cancer* **7:** 69

Dittmann K, Mayer C, Kehlbach R, Rothmund MC, Peter Rodemann H (2009) Radiation-induced lipid peroxidation activates src kinase and triggers nuclear EGFR transport. *Radiother Oncol* **92:** 379-382

Dittmann K, Mayer C, Rodemann HP Nuclear EGFR as novel therapeutic target: insights into nuclear translocation and function. *Strahlenther Onkol* **186:** 1-6

Dittmann K, Mayer C, Rodemann HP (2005b) Inhibition of radiation-induced EGFR nuclear import by C225 (Cetuximab) suppresses DNA-PK activity. *Radiother Oncol* **76:** 157-161

Dittmann K, Mayer C, Rodemann HP (2010b) Nuclear EGFR as novel therapeutic target: insights into nuclear translocation and function. *Strahlenther Onkol* **186:** 1-6

Dittmann K, Mayer C, Wanner G, Kehlbach R, Rodemann HP (2007) The radioprotector O-phospho-tyrosine stimulates DNA-repair via epidermal growth factor receptor- and DNA-dependent kinase phosphorylation. *Radiother Oncol* **84:** 328-334

Dittmann KH, Mayer C, Ohneseit PA, Raju U, Andratschke NH, Milas L, Rodemann HP (2008b) Celecoxib induced tumor cell radiosensitization by inhibiting radiation induced nuclear EGFR transport and DNA-repair: a COX-2 independent mechanism. *Int J Radiat Oncol Biol Phys* **70:** 203-212

Dixit A, Verkhivker GM (2009) Hierarchical modeling of activation mechanisms in the ABL and EGFR kinase domains: thermodynamic and mechanistic catalysts of kinase activation by cancer mutations. *PLoS Comput Biol* **5:** e1000487

Djordjevic S, Driscoll PC (2002) Structural insight into substrate specificity and regulatory mechanisms of phosphoinositide 3-kinases. *Trends Biochem Sci* **27:** 426-432

Domagala T, Konstantopoulos N, Smyth F, Jorissen RN, Fabri L, Geleick D, Lax I, Schlessinger J, Sawyer W, Howlett GJ, Burgess AW, Nice EC (2000) Stoichiometry, kinetic and binding analysis of the interaction between epidermal growth factor (EGF) and the extracellular domain of the EGF receptor. *Growth Factors* **18:** 11-29

Douglas P, Gupta S, Morrice N, Meek K, Lees-Miller SP (2005) DNA-PK-dependent phosphorylation of Ku70/80 is not required for non-homologous end joining. *DNA Repair (Amst)* **4:** 1006-1018

Eckstein N, Servan K, Girard L, Cai D, von Jonquieres G, Jaehde U, Kassack MU, Gazdar AF, Minna JD, Royer HD (2008) Epidermal growth factor receptor pathway analysis identifies amphiregulin as a key factor for cisplatin resistance of human breast cancer cells. *J Biol Chem* **283:** 739-750

Engelman JA (2009) Targeting PI3K signalling in cancer: opportunities, challenges and limitations. *Nat Rev Cancer* **9:** 550-562

Engelman JA, Zejnullahu K, Gale CM, Lifshits E, Gonzales AJ, Shimamura T, Zhao F, Vincent PW, Naumov GN, Bradner JE, Althaus IW, Gandhi L, Shapiro GI, Nelson JM, Heymach JV, Meyerson M, Wong KK, Janne PA (2007) PF00299804, an irreversible pan-ERBB inhibitor, is effective in lung cancer models with EGFR and ERBB2 mutations that are resistant to gefitinib. *Cancer Res* **67:** 11924-11932

Epperly MW, Franicola D, Zhang X, Nie S, Greenberger JS (2006) Effect of EGFR antagonists gefitinib (Iressa) and C225 (Cetuximab) on MnSOD-plasmid liposome transgene radiosensitization of a murine squamous cell carcinoma cell line. *In Vivo* **20:** 791-796

Evers B, Helleday T, Jonkers J (2010) Targeting homologous recombination repair defects in cancer. *Trends Pharmacol Sci* **31:** 372-380

Fassina A, Gazziero A, Zardo D, Corradin M, Aldighieri E, Rossi GP (2009) Detection of EGFR and KRAS mutations on trans-thoracic needle aspiration of lung nodules by high resolution melting analysis. *J Clin Pathol* **62:** 1096-1102

Feng FY, Lopez CA, Normolle DP, Varambally S, Li X, Chun PY, Davis MA, Lawrence TS, Nyati MK (2007) Effect of epidermal growth factor receptor inhibitor class in the treatment of head and neck cancer with concurrent radiochemotherapy in vivo. *Clin Cancer Res* **13:** 2512-2518

Fenstermaker RA, Ciesielski MJ (2000) Deletion and tandem duplication of exons 2 - 7 in the epidermal growth factor receptor gene of a human malignant glioma. *Oncogene* **19:** 4542-4548

Fischer OM, Hart S, Gschwind A, Ullrich A (2003) EGFR signal transactivation in cancer cells. *Biochem Soc Trans* **31:** 1203-1208

Fishel ML, Newell DR, Griffin RJ, Davison R, Wang LZ, Curtin NJ, Zuhowski EG, Kasza K, Egorin MJ, Moschel RC, Dolan ME (2005) Effect of cell cycle inhibition on Cisplatin-induced cytotoxicity. *J Pharmacol Exp Ther* **312:** 206-213

Fisher LA, Bessho M, Bessho T (2008) Processing of a psoralen DNA interstrand cross-link by XPF-ERCC1 complex in vitro. *J Biol Chem* **283:** 1275-1281

Fiske WH, Threadgill D, Coffey RJ (2009) ERBBs in the gastrointestinal tract: recent progress and new perspectives. *Exp Cell Res* **315:** 583-601

Fojo T (2001) Cancer, DNA repair mechanisms, and resistance to chemotherapy. *J Natl Cancer Inst* **93:** 1434-1436

Fraser M, Leung B, Jahani-Asl A, Yan X, Thompson WE, Tsang BK (2003a) Chemoresistance in human ovarian cancer: the role of apoptotic regulators. *Reprod Biol Endocrinol* **1:** 66

Fraser M, Leung BM, Yan X, Dan HC, Cheng JQ, Tsang BK (2003b) p53 is a determinant of X-linked inhibitor of apoptosis protein/Akt-mediated chemoresistance in human ovarian cancer cells. *Cancer Res* **63:** 7081-7088

Frederick L, Wang XY, Eley G, James CD (2000) Diversity and frequency of epidermal growth factor receptor mutations in human glioblastomas. *Cancer Res* **60:** 1383-1387

Friedmann B, Caplin M, Hartley JA, Hochhauser D (2004) Modulation of DNA repair in vitro after treatment with chemotherapeutic agents by the epidermal growth factor receptor inhibitor gefitinib (ZD1839). *Clin Cancer Res* **10:** 6476-6486

Friedmann BJ, Caplin M, Savic B, Shah T, Lord CJ, Ashworth A, Hartley JA, Hochhauser D (2006) Interaction of the epidermal growth factor receptor and the DNA-dependent protein kinase pathway following gefitinib treatment. *Mol Cancer Ther* **5:** 209-218

Fry WH, Kotelawala L, Sweeney C, Carraway KL, 3rd (2009) Mechanisms of ErbB receptor negative regulation and relevance in cancer. *Exp Cell Res* **315:** 697-706

Fu YN, Yeh CL, Cheng HH, Yang CH, Tsai SF, Huang SF, Chen YR (2008) EGFR mutants found in non-small cell lung cancer show different levels of sensitivity to suppression of Src: implications in targeting therapy. *Oncogene* **27:** 957-965

Fyles AW, Milosevic M, Pintilie M, Hill RP (1998) Cervix cancer oxygenation measured following external radiation therapy. *Int J Radiat Oncol Biol Phys* **42:** 751-753

Galleges Ruiz MI, Floor K, Steinberg SM, Grunberg K, Thunnissen FB, Belien JA, Meijer GA, Peters GJ, Smit EF, Rodriguez JA, Giaccone G (2009) Combined assessment of EGFR pathway-related molecular markers and prognosis of NSCLC patients. *Br J Cancer* **100:** 145-152

Gandhi J, Zhang J, Xie Y, Soh J, Shigematsu H, Zhang W, Yamamoto H, Peyton M, Girard L, Lockwood WW, Lam WL, Varella-Garcia M, Minna JD, Gazdar AF (2009) Alterations in genes of the EGFR signaling pathway and their relationship to EGFR tyrosine kinase inhibitor sensitivity in lung cancer cell lines. *PLoS One* **4:** e4576

Gao M, Mayr NA, Huang Z, Zhang H, Wang JZ (2010) When tumor repopulation starts? The onset time of prostate cancer during radiation therapy. *Acta Oncol* **49:** 1269-1275

Gazdar AF (2009a) Activating and resistance mutations of EGFR in non-small-cell lung cancer: role in clinical response to EGFR tyrosine kinase inhibitors. *Oncogene* **28 Suppl 1:** S24-31

Gazdar AF (2009b) Personalized medicine and inhibition of EGFR signaling in lung cancer. *N Engl J Med* **361:** 1018-1020

Gazdar AF, Minna JD (2008) Deregulated EGFR signaling during lung cancer progression: mutations, amplicons, and autocrine loops. *Cancer Prev Res (Phila Pa)* **1:** 156-160

Gazdar AF, Shigematsu H, Herz J, Minna JD (2004) Mutations and addiction to EGFR: the Achilles 'heal' of lung cancers? *Trends Mol Med* **10:** 481-486

Gelibter A, Ceribelli A, Milella M, Mottolese M, Vocaturo A, Cognetti F (2003) Clinically meaningful response to the EGFR tyrosine kinase inhibitor gefitinib ('Iressa', ZD1839) in non small cell lung cancer. *J Exp Clin Cancer Res* **22:** 481-485

Giaccone G (2005) EGFR point mutation confers resistance to gefitinib in a patient with non-small-cell lung cancer. *Nat Clin Pract Oncol* **2:** 296-297

Giaccone G, Gonzalez-Larriba JL, van Oosterom AT, Alfonso R, Smit EF, Martens M, Peters GJ, van der Vijgh WJ, Smith R, Averbuch S, Fandi A (2004a) Combination therapy with gefitinib, an epidermal growth factor receptor tyrosine kinase inhibitor, gemcitabine and cisplatin in patients with advanced solid tumors. *Ann Oncol* **15:** 831-838

Giaccone G, Herbst RS, Manegold C, Scagliotti G, Rosell R, Miller V, Natale RB, Schiller JH, Von Pawel J, Pluzanska A, Gatzemeier U, Grous J, Ochs JS, Averbuch SD, Wolf MK, Rennie P, Fandi A, Johnson DH (2004b) Gefitinib in combination with gemcitabine and cisplatin in advanced non-small-cell lung cancer: a phase III trial--INTACT 1. *J Clin Oncol* **22:** 777-784

Glei M, Hovhannisyan G, Pool-Zobel BL (2009) Use of Comet-FISH in the study of DNA damage and repair: review. *Mutat Res* **681:** 33-43

Golding SE, Morgan RN, Adams BR, Hawkins AJ, Povirk LF, Valerie K (2009) Pro-survival AKT and ERK signaling from EGFR and mutant EGFRvIII enhances DNA double-strand break repair in human glioma cells. *Cancer Biol Ther* **8:** 730-738

Golsteyn RM (2004) The story of gefitinib, an EGFR kinase that works in lung cancer. *Drug Discov Today* **9:** 587

Gramaglia D, Gentile A, Battaglia M, Ranzato L, Petronilli V, Fassetta M, Bernardi P, Rasola A (2004) Apoptosis to necrosis switching downstream of apoptosome

formation requires inhibition of both glycolysis and oxidative phosphorylation in a BCL-X(L)- and PKB/AKT-independent fashion. *Cell Death Differ* **11:** 342-353

Grandal MV, Madshus IH (2008) Epidermal growth factor receptor and cancer: control of oncogenic signalling by endocytosis. *J Cell Mol Med* **12:** 1527-1534

Grandal MV, Zandi R, Pedersen MW, Willumsen BM, van Deurs B, Poulsen HS (2007) EGFRvIII escapes down-regulation due to impaired internalization and sorting to lysosomes. *Carcinogenesis* **28:** 1408-1417

Grant S, Qiao L, Dent P (2002) Roles of ERBB family receptor tyrosine kinases, and downstream signaling pathways, in the control of cell growth and survival. *Front Biosci* **7:** d376-389

Griffiths LM, Swartzlander D, Meadows KL, Wilkinson KD, Corbett AH, Doetsch PW (2009) Dynamic compartmentalization of base excision repair proteins in response to nuclear and mitochondrial oxidative stress. *Mol Cell Biol* **29:** 794-807

Gu J, Li S, Zhang X, Wang LC, Niewolik D, Schwarz K, Legerski RJ, Zandi E, Lieber MR (2010) DNA-PKcs regulates a single-stranded DNA endonuclease activity of Artemis. *DNA Repair (Amst)* **9:** 429-437

Gueven N, Dittmann K, Mayer C, Rodemann HP (1998) Bowman-Birk protease inhibitor reduces the radiation-induced activation of the EGF receptor and induces tyrosine phosphatase activity. *Int J Radiat Biol* **73:** 157-162

Gurley KE, Moser R, Gu Y, Hasty P, Kemp CJ (2009) DNA-PK suppresses a p53-independent apoptotic response to DNA damage. *EMBO Rep* **10:** 87-93

Hammel M, Yu Y, Mahaney BL, Cai B, Ye R, Phipps BM, Rambo RP, Hura GL, Pelikan M, So S, Abolfath RM, Chen DJ, Lees-Miller SP, Tainer JA (2010) Ku and DNA-dependent protein kinase dynamic conformations and assembly regulate DNA binding and the initial non-homologous end joining complex. *J Biol Chem* **285:** 1414-1423

Hanada N, Lo HW, Day CP, Pan Y, Nakajima Y, Hung MC (2006) Co-regulation of B-Myb expression by E2F1 and EGF receptor. *Mol Carcinog* **45:** 10-17

Hanahan D, Weinberg RA (2000) The hallmarks of cancer. *Cell* **100:** 57-70

Harada T, Lopez-Chavez A, Xi L, Raffeld M, Wang Y, Giaccone G Characterization of epidermal growth factor receptor mutations in non-small-cell lung cancer patients of African-American ancestry. *Oncogene*

Hartley JA, Spanswick VJ, Brooks N, Clingen PH, McHugh PJ, Hochhauser D, Pedley RB, Kelland LR, Alley MC, Schultz R, Hollingshead MG, Schweikart KM, Tomaszewski JE, Sausville EA, Gregson SJ, Howard PW, Thurston DE (2004) SJG-136 (NSC 694501), a novel rationally designed DNA minor groove interstrand cross-linking agent with potent and broad spectrum antitumor activity: part 1: cellular

pharmacology, in vitro and initial in vivo antitumor activity. *Cancer Res* **64:** 6693-6699

Hartley JM, Spanswick VJ, Gander M, Giacomini G, Whelan J, Souhami RL, Hartley JA (1999) Measurement of DNA cross-linking in patients on ifosfamide therapy using the single cell gel electrophoresis (comet) assay. *Clin Cancer Res* **5:** 507-512

Hayakawa J, Ohmichi M, Kurachi H, Ikegami H, Kimura A, Matsuoka T, Jikihara H, Mercola D, Murata Y (1999) Inhibition of extracellular signal-regulated protein kinase or c-Jun N-terminal protein kinase cascade, differentially activated by cisplatin, sensitizes human ovarian cancer cell line. *J Biol Chem* **274:** 31648-31654

Hefferin ML, Tomkinson AE (2005) Mechanism of DNA double-strand break repair by non-homologous end joining. *DNA Repair (Amst)* **4:** 639-648

Helleday T (2010) Homologous recombination in cancer development, treatment and development of drug resistance. *Carcinogenesis* **31:** 955-960

Helleday T, Lo J, van Gent DC, Engelward BP (2007) DNA double-strand break repair: from mechanistic understanding to cancer treatment. *DNA Repair (Amst)* **6:** 923-935

Helleday T, Petermann E, Lundin C, Hodgson B, Sharma RA (2008) DNA repair pathways as targets for cancer therapy. *Nat Rev Cancer* **8:** 193-204

Hiraishi Y, Wada T, Nakatani K, Tojyo I, Matsumoto T, Kiga N, Negoro K, Fujita S (2008) EGFR inhibitor enhances cisplatin sensitivity of oral squamous cell carcinoma cell lines. *Pathol Oncol Res* **14:** 39-43

Hlavin EM, Smeaton MB, Miller PS (2010a) Initiation of DNA interstrand cross-link repair in mammalian cells. *Environ Mol Mutagen* **51:** 604-624

Hlavin EM, Smeaton MB, Noronha AM, Wilds CJ, Miller PS (2010b) Cross-link structure affects replication-independent DNA interstrand cross-link repair in mammalian cells. *Biochemistry* **49:** 3977-3988

Hoeijmakers JH (2001) Genome maintenance mechanisms for preventing cancer. *Nature* **411:** 366-374

Hoeijmakers JH (2007) Genome maintenance mechanisms are critical for preventing cancer as well as other aging-associated diseases. *Mech Ageing Dev* **128:** 460-462

Hoeijmakers JH (2009) DNA damage, aging, and cancer. *N Engl J Med* **361:** 1475-1485

Hoshino M, Fukui H, Ono Y, Sekikawa A, Ichikawa K, Tomita S, Imai Y, Imura J, Hiraishi H, Fujimori T (2007) Nuclear expression of phosphorylated EGFR is associated with poor prognosis of patients with esophageal squamous cell carcinoma. *Pathobiology* **74:** 15-21

Hsu SC, Hung MC (2007) Characterization of a novel tripartite nuclear localization sequence in the EGFR family. *J Biol Chem* **282:** 10432-10440

Hsu SC, Miller SA, Wang Y, Hung MC (2009) Nuclear EGFR is required for cisplatin resistance and DNA repair. *Am J Transl Res* **1:** 249-258

Huang CL, Yang CH, Yeh KH, Hu FC, Chen KY, Shih JY, Lin ZZ, Yu CJ, Cheng AL, Yang PC (2009) EGFR intron 1 dinucleotide repeat polymorphism is associated with the occurrence of skin rash with gefitinib treatment. *Lung Cancer* **64:** 346-351

Huang F, Goh LK, Sorkin A (2007a) EGF receptor ubiquitination is not necessary for its internalization. *Proc Natl Acad Sci U S A* **104:** 16904-16909

Huang F, Sorkin A (2005) Growth factor receptor binding protein 2-mediated recruitment of the RING domain of Cbl to the epidermal growth factor receptor is essential and sufficient to support receptor endocytosis. *Mol Biol Cell* **16:** 1268-1281

Huang HS, Nagane M, Klingbeil CK, Lin H, Nishikawa R, Ji XD, Huang CM, Gill GN, Wiley HS, Cavenee WK (1997) The enhanced tumorigenic activity of a mutant epidermal growth factor receptor common in human cancers is mediated by threshold levels of constitutive tyrosine phosphorylation and unattenuated signaling. *J Biol Chem* **272:** 2927-2935

Huang WC, Hsu RM, Chi LM, Leu YL, Chang YS, Yu JS (2007b) Selective downregulation of EGF receptor and downstream MAPK pathway in human cancer cell lines by active components partially purified from the seeds of Livistona chinensis R. Brown. *Cancer Lett* **248:** 137-146

Hubbard SR (2001) Theme and variations: juxtamembrane regulation of receptor protein kinases. *Mol Cell* **8:** 481-482

Hubbard SR (2004) Juxtamembrane autoinhibition in receptor tyrosine kinases. *Nat Rev Mol Cell Biol* **5:** 464-471

Hubbard SR (2009) The juxtamembrane region of EGFR takes center stage. *Cell* **137:** 1181-1183

Hung LY, Tseng JT, Lee YC, Xia W, Wang YN, Wu ML, Chuang YH, Lai CH, Chang WC (2008) Nuclear epidermal growth factor receptor (EGFR) interacts with signal transducer and activator of transcription 5 (STAT5) in activating Aurora-A gene expression. *Nucleic Acids Res* **36:** 4337-4351

Huo L, Wang YN, Xia W, Hsu SC, Lai CC, Li LY, Chang WC, Wang Y, Hsu MC, Yu YL, Huang TH, Ding Q, Chen CH, Tsai CH, Hung MC RNA helicase A is a DNA-binding partner for EGFR-mediated transcriptional activation in the nucleus. *Proc Natl Acad Sci U S A* **107:** 16125-16130

Husvik C, Bryne M, Halstensen TS (2009) Epidermal growth factor-induced cyclooxygenase-2 expression in oral squamous cell carcinoma cell lines is mediated

through extracellular signal-regulated kinase 1/2 and p38 but is Src and nuclear factor-kappa B independent. *Eur J Oral Sci* **117:** 528-535

Hynes NE, Lane HA (2005) ERBB receptors and cancer: the complexity of targeted inhibitors. *Nat Rev Cancer* **5:** 341-354

Ibrahim SO, Lillehaug JR, Johannessen AC, Liavaag PG, Nilsen R, Vasstrand EN (1999) Expression of biomarkers (p53, transforming growth factor alpha, epidermal growth factor receptor, c-erbB-2/neu and the proliferative cell nuclear antigen) in oropharyngeal squamous cell carcinomas. *Oral Oncol* **35:** 302-313

Jackson SP (2009) The DNA-damage response: new molecular insights and new approaches to cancer therapy. *Biochem Soc Trans* **37:** 483-494

Jackson SP, Bartek J (2009) The DNA-damage response in human biology and disease. *Nature* **461:** 1071-1078

Jakupec MA, Galanski M, Keppler BK (2003) Tumour-inhibiting platinum complexes--state of the art and future perspectives. *Rev Physiol Biochem Pharmacol* **146:** 1-54

Jeggo P, Lavin MF (2009) Cellular radiosensitivity: how much better do we understand it? *Int J Radiat Biol* **85:** 1061-1081

Jeggo PA (2009) Risks from low dose/dose rate radiation: what an understanding of DNA damage response mechanisms can tell us. *Health Phys* **97:** 416-425

Jeggo PA, Lobrich M (2007) DNA double-strand breaks: their cellular and clinical impact? *Oncogene* **26:** 7717-7719

Jensen R, Glazer PM (2004) Cell-interdependent cisplatin killing by Ku/DNA-dependent protein kinase signaling transduced through gap junctions. *Proc Natl Acad Sci U S A* **101:** 6134-6139

Jordan P, Carmo-Fonseca M (1998) Cisplatin inhibits synthesis of ribosomal RNA in vivo. *Nucleic Acids Res* **26:** 2831-2836

Jorissen RN, Walker F, Pouliot N, Garrett TP, Ward CW, Burgess AW (2003) Epidermal growth factor receptor: mechanisms of activation and signalling. *Exp Cell Res* **284:** 31-53

Jura N, Endres NF, Engel K, Deindl S, Das R, Lamers MH, Wemmer DE, Zhang X, Kuriyan J (2009) Mechanism for activation of the EGF receptor catalytic domain by the juxtamembrane segment. *Cell* **137:** 1293-1307

Kaffman A, O'Shea EK (1999) Regulation of nuclear localization: a key to a door. *Annu Rev Cell Dev Biol* **15:** 291-339

Kamat A, Carpenter G (1997) Phospholipase C-gamma1: regulation of enzyme function and role in growth factor-dependent signal transduction. *Cytokine Growth Factor Rev* **8:** 109-117

Kamio T, Shigematsu K, Sou H, Kawai K, Tsuchiyama H (1990) Immunohistochemical expression of epidermal growth factor receptors in human adrenocortical carcinoma. *Hum Pathol* **21:** 277-282

Kang D, Gridley G, Huang WY, Engel LS, Winn DM, Brown LM, Bravo-Otero E, Wu T, Diehl SR, Hayes RB (2005) Microsatellite polymorphisms in the epidermal growth factor receptor (EGFR) gene and the transforming growth factor-alpha (TGFA) gene and risk of oral cancer in Puerto Rico. *Pharmacogenet Genomics* **15:** 343-347

Kartalou M, Essigmann JM (2001a) Mechanisms of resistance to cisplatin. *Mutat Res* **478:** 23-43

Kartalou M, Essigmann JM (2001b) Recognition of cisplatin adducts by cellular proteins. *Mutat Res* **478:** 1-21

Katz M, Amit I, Yarden Y (2007) Regulation of MAPKs by growth factors and receptor tyrosine kinases. *Biochim Biophys Acta* **1773:** 1161-1176

Kersting C, Agelopoulos K, Schmidt H, Korsching E, August C, Gosheger G, Dirksen U, Juergens H, Winkelmann W, Brandt B, Bielack S, Buerger H, Gebert C (2008) Biological importance of a polymorphic CA sequence within intron 1 of the epidermal growth factor receptor gene (EGFR) in high grade central osteosarcomas. *Genes Chromosomes Cancer* **47:** 657-664

Khanna KK, Jackson SP (2001) DNA double-strand breaks: signaling, repair and the cancer connection. *Nat Genet* **27:** 247-254

Kil SJ, Hobert M, Carlin C (1999) A leucine-based determinant in the epidermal growth factor receptor juxtamembrane domain is required for the efficient transport of ligand-receptor complexes to lysosomes. *J Biol Chem* **274:** 3141-3150

Kim HH, Sierke SL, Koland JG (1994) Epidermal growth factor-dependent association of phosphatidylinositol 3-kinase with the erbB3 gene product. *J Biol Chem* **269:** 24747-24755

Kim HP, Yoon YK, Kim JW, Han SW, Hur HS, Park J, Lee JH, Oh DY, Im SA, Bang YJ, Kim TY (2009a) Lapatinib, a dual EGFR and HER2 tyrosine kinase inhibitor, downregulates thymidylate synthase by inhibiting the nuclear translocation of EGFR and HER2. *PLoS One* **4:** e5933

Kim JS, Kim MA, Kim TM, Lee SH, Kim DW, Im SA, Kim TY, Kim WH, Yang HK, Heo DS, Bang YJ, Lee KU, Choe KJ, Kim NK (2009b) Biomarker analysis in stage III-IV (M0) gastric cancer patients who received curative surgery followed by adjuvant 5-fluorouracil and cisplatin chemotherapy: epidermal growth factor receptor (EGFR) associated with favourable survival. *Br J Cancer* **100:** 732-738

Klass CM, Choe MS, Hurwitz SJ, Tighiouart M, Zhang X, Chen ZG, Shin DM (2009) Sequence dependence of cell growth inhibition by EGFR-tyrosine kinase inhibitor ZD1839, docetaxel, and cisplatin in head and neck cancer. *Head Neck* **31:** 1263-1273

Klein P, Mattoon D, Lemmon MA, Schlessinger J (2004) A structure-based model for ligand binding and dimerization of EGF receptors. *Proc Natl Acad Sci U S A* **101:** 929-934

Klein S, Levitzki A (2009) Targeting the EGFR and the PKB pathway in cancer. *Curr Opin Cell Biol* **21:** 185-193

Kondo N, Tsukuda M, Ishiguro Y, Kimura M, Fujita K, Sakakibara A, Takahashi H, Toth G, Matsuda H Antitumor effects of lapatinib (GW572016), a dual inhibitor of EGFR and HER-2, in combination with cisplatin or paclitaxel on head and neck squamous cell carcinoma. *Oncol Rep* **23:** 957-963

Kwak EL, Sordella R, Bell DW, Godin-Heymann N, Okimoto RA, Brannigan BW, Harris PL, Driscoll DR, Fidias P, Lynch TJ, Rabindran SK, McGinnis JP, Wissner A, Sharma SV, Isselbacher KJ, Settleman J, Haber DA (2005) Irreversible inhibitors of the EGF receptor may circumvent acquired resistance to gefitinib. *Proc Natl Acad Sci U S A* **102:** 7665-7670

Laachi N, Cho J, Dorfman KD (2009) DNA unhooking from a single post as a deterministic process: insights from translocation modeling. *Phys Rev E Stat Nonlin Soft Matter Phys* **79:** 031928

Lange A, Mills RE, Lange CJ, Stewart M, Devine SE, Corbett AH (2007) Classical nuclear localization signals: definition, function, and interaction with importin alpha. *J Biol Chem* **282:** 5101-5105

Lavictoire SJ, Parolin DA, Klimowicz AC, Kelly JF, Lorimer IA (2003) Interaction of Hsp90 with the nascent form of the mutant epidermal growth factor receptor EGFRvIII. *J Biol Chem* **278:** 5292-5299

Lazzara MJ, Lauffenburger DA (2009) Quantitative modeling perspectives on the ErbB system of cell regulatory processes. *Exp Cell Res* **315:** 717-725

Lee BJ, Chon KM, Kim YS, An WG, Roh HJ, Goh EK, Wang SG (2005) Effects of cisplatin, 5-fluorouracil, and radiation on cell cycle regulation and apoptosis in the hypopharyngeal carcinoma cell line. *Chemotherapy* **51:** 103-110

Lee YS, Huang K, Quiocho FA, O'Shea EK (2008) Molecular basis of cyclin-CDK-CKI regulation by reversible binding of an inositol pyrophosphate. *Nat Chem Biol* **4:** 25-32

Lemmon MA (2009) Ligand-induced ErbB receptor dimerization. *Exp Cell Res* **315:** 638-648

Lemmon MA, Schlessinger J Cell signaling by receptor tyrosine kinases. *Cell* **141:** 1117-1134

Lemmon MA, Schlessinger J (2010) Cell signaling by receptor tyrosine kinases. *Cell* **141:** 1117-1134

Li B, Yuan M, Kim IA, Chang CM, Bernhard EJ, Shu HK (2004) Mutant epidermal growth factor receptor displays increased signaling through the phosphatidylinositol-3 kinase/AKT pathway and promotes radioresistance in cells of astrocytic origin. *Oncogene* **23:** 4594-4602

Li J, Li Y, Feng ZQ, Chen XG (2009) Anti-tumor activity of a novel EGFR tyrosine kinase inhibitor against human NSCLC in vitro and in vivo. *Cancer Lett* **279:** 213-220

Li JZ, Zheng JW, Zhang ZY (2008) Evaluation of Cetuximab in combination with radiotherapy or chemotherapy against advanced squamous cell carcinoma of the head and neck. *Shanghai Kou Qiang Yi Xue* **17:** 1-5

Li W, Hesabi B, Babbo A, Pacione C, Liu J, Chen DJ, Nickoloff JA, Shen Z (2000) Regulation of double-strand break-induced mammalian homologous recombination by UBL1, a RAD51-interacting protein. *Nucleic Acids Res* **28:** 1145-1153

Liang J, Zubovitz J, Petrocelli T, Kotchetkov R, Connor MK, Han K, Lee JH, Ciarallo S, Catzavelos C, Beniston R, Franssen E, Slingerland JM (2002) PKB/Akt phosphorylates p27, impairs nuclear import of p27 and opposes p27-mediated G1 arrest. *Nat Med* **8:** 1153-1160

Liao HJ, Carpenter G (2007) Role of the Sec61 translocon in EGF receptor trafficking to the nucleus and gene expression. *Mol Biol Cell* **18:** 1064-1072

Liao HJ, Carpenter G (2009) Cetuximab/C225-induced intracellular trafficking of epidermal growth factor receptor. *Cancer Res* **69:** 6179-6183

Liaw YS, Yang PC, Yu CJ, Kuo SH, Luh KT, Lin YJ, Wu ML (1998) PKC activation is required by EGF-stimulated Na(+)-H+ exchanger in human pleural mesothelial cells. *Am J Physiol* **274:** L665-672

Lieber MR (2010) The mechanism of double-strand DNA break repair by the nonhomologous DNA end-joining pathway. *Annu Rev Biochem* **79:** 181-211

Lin SY, Makino K, Xia W, Matin A, Wen Y, Kwong KY, Bourguignon L, Hung MC (2001) Nuclear localization of EGF receptor and its potential new role as a transcription factor. *Nat Cell Biol* **3:** 802-808

Linardou H, Dahabreh IJ, Bafaloukos D, Kosmidis P, Murray S (2009) Somatic EGFR mutations and efficacy of tyrosine kinase inhibitors in NSCLC. *Nat Rev Clin Oncol* **6:** 352-366

Lind MJ, Ardiet C (1993) Pharmacokinetics of alkylating agents. *Cancer Surv* **17:** 157-188

Lo HW EGFR-targeted therapy in malignant glioma: novel aspects and mechanisms of drug resistance. *Curr Mol Pharmacol* **3:** 37-52

Lo HW Nuclear mode of the EGFR signaling network: biology, prognostic value, and therapeutic implications. *Discov Med* **10:** 44-51

Lo HW (2010) Nuclear mode of the EGFR signaling network: biology, prognostic value, and therapeutic implications. *Discov Med* **10:** 44-51

Lo HW, Ali-Seyed M, Wu Y, Bartholomeusz G, Hsu SC, Hung MC (2006a) Nuclear-cytoplasmic transport of EGFR involves receptor endocytosis, importin beta1 and CRM1. *J Cell Biochem* **98:** 1570-1583

Lo HW, Cao X, Zhu H, Ali-Osman F (2010) Cyclooxygenase-2 is a novel transcriptional target of the nuclear EGFR-STAT3 and EGFRvIII-STAT3 signaling axes. *Mol Cancer Res* **8:** 232-245

Lo HW, Hsu SC, Ali-Seyed M, Gunduz M, Xia W, Wei Y, Bartholomeusz G, Shih JY, Hung MC (2005a) Nuclear interaction of EGFR and STAT3 in the activation of the iNOS/NO pathway. *Cancer Cell* **7:** 575-589

Lo HW, Hsu SC, Hung MC (2006b) EGFR signaling pathway in breast cancers: from traditional signal transduction to direct nuclear translocalization. *Breast Cancer Res Treat* **95:** 211-218

Lo HW, Hung MC (2006) Nuclear EGFR signalling network in cancers: linking EGFR pathway to cell cycle progression, nitric oxide pathway and patient survival. *Br J Cancer* **94:** 184-188

Lo HW, Xia W, Wei Y, Ali-Seyed M, Huang SF, Hung MC (2005b) Novel prognostic value of nuclear epidermal growth factor receptor in breast cancer. *Cancer Res* **65:** 338-348

Lo S, Tolner B, Taanman JW, Cooper JM, Gu M, Hartley JA, Schapira AH, Hochhauser D (2005c) Assessment of the significance of mitochondrial DNA damage by chemotherapeutic agents. *Int J Oncol* **27:** 337-344

Lobrich M, Jeggo PA (2007) The impact of a negligent G2/M checkpoint on genomic instability and cancer induction. *Nat Rev Cancer* **7:** 861-869

Lowe SW, Lin AW (2000) Apoptosis in cancer. *Carcinogenesis* **21:** 485-495

Lu D, Huang J, Basu A (2006) Protein kinase Cepsilon activates protein kinase B/Akt via DNA-PK to protect against tumor necrosis factor-alpha-induced cell death. *J Biol Chem* **281:** 22799-22807

Luo KQ, Yu VC, Pu Y, Chang DC (2003) Measuring dynamics of caspase-8 activation in a single living HeLa cell during TNFalpha-induced apoptosis. *Biochem Biophys Res Commun* **304:** 217-222

Macdonald-Obermann JL, Pike LJ (2009) The intracellular juxtamembrane domain of the epidermal growth factor (EGF) receptor is responsible for the allosteric regulation of EGF binding. *J Biol Chem* **284:** 13570-13576

Madrid AS, Weis K (2006) Nuclear transport is becoming crystal clear. *Chromosoma* **115:** 98-109

Madshus IH, Stang E (2009) Internalization and intracellular sorting of the EGF receptor: a model for understanding the mechanisms of receptor trafficking. *J Cell Sci* **122:** 3433-3439

Maemondo M, Inoue A, Kobayashi K, Sugawara S, Oizumi S, Isobe H, Gemma A, Harada M, Yoshizawa H, Kinoshita I, Fujita Y, Okinaga S, Hirano H, Yoshimori K, Harada T, Ogura T, Ando M, Miyazawa H, Tanaka T, Saijo Y, Hagiwara K, Morita S, Nukiwa T Gefitinib or chemotherapy for non-small-cell lung cancer with mutated EGFR. *N Engl J Med* **362:** 2380-2388

Mahaney BL, Meek K, Lees-Miller SP (2009) Repair of ionizing radiation-induced DNA double-strand breaks by non-homologous end-joining. *Biochem J* **417:** 639-650

Malinge JM, Giraud-Panis MJ, Leng M (1999) Interstrand cross-links of cisplatin induce striking distortions in DNA. *J Inorg Biochem* **77:** 23-29

Mandic A, Viktorsson K, Molin M, Akusjarvi G, Eguchi H, Hayashi SI, Toi M, Hansson J, Linder S, Shoshan MC (2001) Cisplatin induces the proapoptotic conformation of Bak in a deltaMEKK1-dependent manner. *Mol Cell Biol* **21:** 3684-3691

Mansouri A, Ridgway LD, Korapati AL, Zhang Q, Tian L, Wang Y, Siddik ZH, Mills GB, Claret FX (2003) Sustained activation of JNK/p38 MAPK pathways in response to cisplatin leads to Fas ligand induction and cell death in ovarian carcinoma cells. *J Biol Chem* **278:** 19245-19256

Marais R, Light Y, Mason C, Paterson H, Olson MF, Marshall CJ (1998) Requirement of Ras-GTP-Raf complexes for activation of Raf-1 by protein kinase C. *Science* **280:** 109-112

Marti U, Burwen SJ, Wells A, Barker ME, Huling S, Feren AM, Jones AL (1991) Localization of epidermal growth factor receptor in hepatocyte nuclei. *Hepatology* **13:** 15-20

Marti U, Ruchti C, Kampf J, Thomas GA, Williams ED, Peter HJ, Gerber H, Burgi U (2001) Nuclear localization of epidermal growth factor and epidermal growth factor receptors in human thyroid tissues. *Thyroid* **11:** 137-145

Martin GS (2003) Cell signaling and cancer. *Cancer Cell* **4:** 167-174

Martin LP, Hamilton TC, Schilder RJ (2008) Platinum resistance: the role of DNA repair pathways. *Clin Cancer Res* **14:** 1291-1295

Massie C, Mills IG (2006) The developing role of receptors and adaptors. *Nat Rev Cancer* **6:** 403-409

Masunaga S, Hirayama R, Uzawa A, Kashino G, Suzuki M, Kinashi Y, Liu Y, Koike S, Ando K, Ono K (2009) The effect of post-irradiation tumor oxygenation status on recovery from radiation-induced damage in vivo: with reference to that in quiescent cell populations. *J Cancer Res Clin Oncol* **135:** 1109-1116

Mattoon D, Klein P, Lemmon MA, Lax I, Schlessinger J (2004) The tethered configuration of the EGF receptor extracellular domain exerts only a limited control of receptor function. *Proc Natl Acad Sci U S A* **101:** 923-928

McArt DG, Wasson GR, McKerr G, Saetzler K, Reed M, Howard CV (2009) Systematic random sampling of the comet assay. *Mutagenesis* **24:** 373-378

McCabe KM, Olson SB, Moses RE (2009) DNA interstrand crosslink repair in mammalian cells. *J Cell Physiol* **220:** 569-573

McCune JS, Slattery JT (2002) Pharmacological considerations of primary alkylators. *Cancer Treat Res* **112:** 323-345

McHugh PJ, Spanswick VJ, Hartley JA (2001) Repair of DNA interstrand crosslinks: molecular mechanisms and clinical relevance. *Lancet Oncol* **2:** 483-490

McKinnon PJ, Caldecott KW (2007) DNA strand break repair and human genetic disease. *Annu Rev Genomics Hum Genet* **8:** 37-55

Meek DW (2009) Tumour suppression by p53: a role for the DNA damage response? *Nat Rev Cancer* **9:** 714-723

Merlo LM, Pepper JW, Reid BJ, Maley CC (2006) Cancer as an evolutionary and ecological process. *Nat Rev Cancer* **6:** 924-935

Michaelis M, Bliss J, Arnold SC, Hinsch N, Rothweiler F, Deubzer HE, Witt O, Langer K, Doerr HW, Wels WS, Cinatl J, Jr. (2008) Cisplatin-resistant neuroblastoma cells express enhanced levels of epidermal growth factor receptor (EGFR) and are sensitive to treatment with EGFR-specific toxins. *Clin Cancer Res* **14:** 6531-6537

Middleton MR, Margison GP (2003) Improvement of chemotherapy efficacy by inactivation of a DNA-repair pathway. *Lancet Oncol* **4:** 37-44

Mitchell JR, Hoeijmakers JH, Niedernhofer LJ (2003) Divide and conquer: nucleotide excision repair battles cancer and ageing. *Curr Opin Cell Biol* **15:** 232-240

Miyashita T, Krajewski S, Krajewska M, Wang HG, Lin HK, Liebermann DA, Hoffman B, Reed JC (1994) Tumor suppressor p53 is a regulator of bcl-2 and bax gene expression in vitro and in vivo. *Oncogene* **9:** 1799-1805

Moasser MM, Basso A, Averbuch SD, Rosen N (2001) The tyrosine kinase inhibitor ZD1839 ("Iressa") inhibits HER2-driven signaling and suppresses the growth of HER2-overexpressing tumor cells. *Cancer Res* **61:** 7184-7188

Modjtahedi H, Moscatello DK, Box G, Green M, Shotton C, Lamb DJ, Reynolds LJ, Wong AJ, Dean C, Thomas H, Eccles S (2003) Targeting of cells expressing wild-type EGFR and type-III mutant EGFR (EGFRvIII) by anti-EGFR MAb ICR62: a two-pronged attack for tumour therapy. *Int J Cancer* **105:** 273-280

Morandell S, Stasyk T, Skvortsov S, Ascher S, Huber LA (2008) Quantitative proteomics and phosphoproteomics reveal novel insights into complexity and dynamics of the EGFR signaling network. *Proteomics* **8:** 4383-4401

Morgan S, Grandis JR (2009) ErbB receptors in the biology and pathology of the aerodigestive tract. *Exp Cell Res* **315:** 572-582

Morita S, Okamoto I, Kobayashi K, Yamazaki K, Asahina H, Inoue A, Hagiwara K, Sunaga N, Yanagitani N, Hida T, Yoshida K, Hirashima T, Yasumoto K, Sugio K, Mitsudomi T, Fukuoka M, Nukiwa T (2009) Combined survival analysis of prospective clinical trials of gefitinib for non-small cell lung cancer with EGFR mutations. *Clin Cancer Res* **15:** 4493-4498

Moroianu J (1999) Nuclear import and export pathways. *J Cell Biochem* **Suppl 32-33:** 76-83

Mosesson Y, Mills GB, Yarden Y (2008) Derailed endocytosis: an emerging feature of cancer. *Nat Rev Cancer* **8:** 835-850

Mosesson Y, Shtiegman K, Katz M, Zwang Y, Vereb G, Szollosi J, Yarden Y (2003) Endocytosis of receptor tyrosine kinases is driven by monoubiquitylation, not polyubiquitylation. *J Biol Chem* **278:** 21323-21326

Moynahan ME, Jasin M (2010) Mitotic homologous recombination maintains genomic stability and suppresses tumorigenesis. *Nat Rev Mol Cell Biol* **11:** 196-207

Mukherjee B, Choy H, Nirodi C, Burma S Targeting nonhomologous end-joining through epidermal growth factor receptor inhibition: rationale and strategies for radiosensitization. *Semin Radiat Oncol* **20:** 250-257

Mukherjee B, McEllin B, Camacho CV, Tomimatsu N, Sirasanagandala S, Nannepaga S, Hatanpaa KJ, Mickey B, Madden C, Maher E, Boothman DA, Furnari F, Cavenee WK, Bachoo RM, Burma S (2009) EGFRvIII and DNA double-strand break repair: a molecular mechanism for radioresistance in glioblastoma. *Cancer Res* **69:** 4252-4259

Muniandy PA, Liu J, Majumdar A, Liu ST, Seidman MM (2010) DNA interstrand crosslink repair in mammalian cells: step by step. *Crit Rev Biochem Mol Biol* **45:** 23-49

Murray S, Dahabreh IJ, Linardou H, Manoloukos M, Bafaloukos D, Kosmidis P (2008) Somatic mutations of the tyrosine kinase domain of epidermal growth factor receptor and tyrosine kinase inhibitor response to TKIs in non-small cell lung cancer: an analytical database. *J Thorac Oncol* **3:** 832-839

Mustafa M, Mirza A, Kannan N (2011) Conformational regulation of the EGFR kinase core by the juxtamembrane and C-terminal tail: a molecular dynamics study. *Proteins* **79:** 99-114

Nakamura K, Mitamura T, Takahashi T, Kobayashi T, Mekada E (2000) Importance of the major extracellular domain of CD9 and the epidermal growth factor (EGF)-like domain of heparin-binding EGF-like growth factor for up-regulation of binding and activity. *J Biol Chem* **275:** 18284-18290

Nevins JR (2001) The Rb/E2F pathway and cancer. *Hum Mol Genet* **10:** 699-703

Nicholson KM, Anderson NG (2002) The protein kinase B/Akt signalling pathway in human malignancy. *Cell Signal* **14:** 381-395

Nojima K, Hochegger H, Saberi A, Fukushima T, Kikuchi K, Yoshimura M, Orelli BJ, Bishop DK, Hirano S, Ohzeki M, Ishiai M, Yamamoto K, Takata M, Arakawa H, Buerstedde JM, Yamazoe M, Kawamoto T, Araki K, Takahashi JA, Hashimoto N, Takeda S, Sonoda E (2005) Multiple repair pathways mediate tolerance to chemotherapeutic cross-linking agents in vertebrate cells. *Cancer Res* **65:** 11704-11711

Normanno N (2005) Gefitinib and cisplatin-based chemotherapy in non-small-cell lung cancer: simply a bad combination? *J Clin Oncol* **23:** 928-930; author reply 930-921

Nowell PC (1976) The clonal evolution of tumor cell populations. *Science* **194:** 23-28

Nyati MK, Morgan MA, Feng FY, Lawrence TS (2006) Integration of EGFR inhibitors with radiochemotherapy. *Nat Rev Cancer* **6:** 876-885

Olive PL (1999) DNA damage and repair in individual cells: applications of the comet assay in radiobiology. *Int J Radiat Biol* **75:** 395-405

Olive PL (2009) Impact of the comet assay in radiobiology. *Mutat Res* **681:** 13-23

Olive PL, Banath JP (2006) The comet assay: a method to measure DNA damage in individual cells. *Nat Protoc* **1:** 23-29

Oliveras-Ferraros C, Vazquez-Martin A, Lopez-Bonet E, Martin-Castillo B, Del Barco S, Brunet J, Menendez JA (2008) Growth and molecular interactions of the

anti-EGFR antibody cetuximab and the DNA cross-linking agent cisplatin in gefitinib-resistant MDA-MB-468 cells: new prospects in the treatment of triple-negative/basal-like breast cancer. *Int J Oncol* **33:** 1165-1176

Oved S, Yarden Y (2002) Signal transduction: molecular ticket to enter cells. *Nature* **416:** 133-136

Ozcan F, Klein P, Lemmon MA, Lax I, Schlessinger J (2006) On the nature of low- and high-affinity EGF receptors on living cells. *Proc Natl Acad Sci U S A* **103:** 5735-5740

Paez JG, Janne PA, Lee JC, Tracy S, Greulich H, Gabriel S, Herman P, Kaye FJ, Lindeman N, Boggon TJ, Naoki K, Sasaki H, Fujii Y, Eck MJ, Sellers WR, Johnson BE, Meyerson M (2004) EGFR mutations in lung cancer: correlation with clinical response to gefitinib therapy. *Science* **304:** 1497-1500

Pallis AG, Voutsina A, Kalikaki A, Souglakos J, Briasoulis E, Murray S, Koutsopoulos A, Tripaki M, Stathopoulos E, Mavroudis D, Georgoulias V (2007) 'Classical' but not 'other' mutations of EGFR kinase domain are associated with clinical outcome in gefitinib-treated patients with non-small cell lung cancer. *Br J Cancer* **97:** 1560-1566

Paques F, Haber JE (1999) Multiple pathways of recombination induced by double-strand breaks in Saccharomyces cerevisiae. *Microbiol Mol Biol Rev* **63:** 349-404

Park EJ, Min HY, Chung HJ, Hong JY, Kang YJ, Hung TM, Youn UJ, Kim YS, Bae K, Kang SS, Lee SK (2009) Down-regulation of c-Src/EGFR-mediated signaling activation is involved in the honokiol-induced cell cycle arrest and apoptosis in MDA-MB-231 human breast cancer cells. *Cancer Lett* **277:** 133-140

Pashtan I, Tsutsumi S, Wang S, Xu W, Neckers L (2008) Targeting Hsp90 prevents escape of breast cancer cells from tyrosine kinase inhibition. *Cell Cycle* **7:** 2936-2941

Patrick SM, Tillison K, Horn JM (2008) Recognition of cisplatin-DNA interstrand cross-links by replication protein A. *Biochemistry* **47:** 10188-10196

Pawelczak KS, Andrews BJ, Turchi JJ (2005) Differential activation of DNA-PK based on DNA strand orientation and sequence bias. *Nucleic Acids Res* **33:** 152-161

Pedersen MW, Pedersen N, Ottesen LH, Poulsen HS (2005) Differential response to gefitinib of cells expressing normal EGFR and the mutant EGFRvIII. *Br J Cancer* **93:** 915-923

Perez-Torres M, Guix M, Gonzalez A, Arteaga CL (2006) Epidermal growth factor receptor (EGFR) antibody down-regulates mutant receptors and inhibits tumors expressing EGFR mutations. *J Biol Chem* **281:** 40183-40192

Pines G, Huang PH, Zwang Y, White FM, Yarden Y EGFRvIV: a previously uncharacterized oncogenic mutant reveals a kinase autoinhibitory mechanism. *Oncogene* **29:** 5850-5860

Powers MA, Dasso M (2004) Nuclear transport erupts on the slopes of Mount Etna. *Nat Cell Biol* **6:** 82-86

Prat A, Baselga J (2008) The role of hormonal therapy in the management of hormonal-receptor-positive breast cancer with co-expression of HER2. *Nat Clin Pract Oncol* **5:** 531-542

Prince T, Matts RL (2005) Exposure of protein kinase motifs that trigger binding of Hsp90 and Cdc37. *Biochem Biophys Res Commun* **338:** 1447-1454

Psyrri A, Egleston B, Weinberger P, Yu Z, Kowalski D, Sasaki C, Haffty B, Rimm D, Burtness B (2008) Correlates and determinants of nuclear epidermal growth factor receptor content in an oropharyngeal cancer tissue microarray. *Cancer Epidemiol Biomarkers Prev* **17:** 1486-1492

Puri C, Tosoni D, Comai R, Rabellino A, Segat D, Caneva F, Luzzi P, Di Fiore PP, Tacchetti C (2005) Relationships between EGFR signaling-competent and endocytosis-competent membrane microdomains. *Mol Biol Cell* **16:** 2704-2718

Qiu C, Tarrant MK, Choi SH, Sathyamurthy A, Bose R, Banjade S, Pal A, Bornmann WG, Lemmon MA, Cole PA, Leahy DJ (2008) Mechanism of activation and inhibition of the HER4/ErbB4 kinase. *Structure* **16:** 460-467

Reade CA, Ganti AK (2009) EGFR targeted therapy in non-small cell lung cancer: potential role of cetuximab. *Biologics* **3:** 215-224

Red Brewer M, Choi SH, Alvarado D, Moravcevic K, Pozzi A, Lemmon MA, Carpenter G (2009) The juxtamembrane region of the EGF receptor functions as an activation domain. *Mol Cell* **34:** 641-651

Reiter M, Welz C, Baumeister P, Schwenk-Zieger S, Harreus U Mutagen sensitivity and DNA repair of the EGFR gene in oropharyngeal cancer. *Oral Oncol* **46:** 519-524

Rivera F, Vega-Villegas ME, Lopez-Brea MF, Marquez R (2008) Current situation of Panitumumab, Matuzumab, Nimotuzumab and Zalutumumab. *Acta Oncol* **47:** 9-19

Rodemann HP, Blaese MA (2007) Responses of normal cells to ionizing radiation. *Semin Radiat Oncol* **17:** 81-88

Rodemann HP, Dittmann K, Toulany M (2007) Radiation-induced EGFR-signaling and control of DNA-damage repair. *Int J Radiat Biol* **83:** 781-791

Rossler J, Odenthal E, Geoerger B, Gerstenmeyer A, Lagodny J, Niemeyer CM, Vassal G (2009) EGFR inhibition using gefitinib is not active in neuroblastoma cell lines. *Anticancer Res* **29:** 1327-1333

Rout MP, Aitchison JD (2001) The nuclear pore complex as a transport machine. *J Biol Chem* **276:** 16593-16596

Russo A, Rizzo S, Bronte G, Silvestris N, Colucci G, Gebbia N, Bazan V, Fulfaro F (2009) The long and winding road to useful predictive factors for anti-EGFR therapy in metastatic colorectal carcinoma: the KRAS/BRAF pathway. *Oncology* **77 Suppl 1:** 57-68

Ruzzo A, Graziano F, Canestrari E, Magnani M Molecular predictors of efficacy to anti-EGFR agents in colorectal cancer patients. *Curr Cancer Drug Targets* **10:** 68-79

Savage P, Stebbing J, Bower M, Crook T (2009) Why does cytotoxic chemotherapy cure only some cancers? *Nat Clin Pract Oncol* **6:** 43-52

Sawai A, Chandarlapaty S, Greulich H, Gonen M, Ye Q, Arteaga CL, Sellers W, Rosen N, Solit DB (2008) Inhibition of Hsp90 down-regulates mutant epidermal growth factor receptor (EGFR) expression and sensitizes EGFR mutant tumors to paclitaxel. *Cancer Res* **68:** 589-596

Schlessinger J (2002) Ligand-induced, receptor-mediated dimerization and activation of EGF receptor. *Cell* **110:** 669-672

Schlessinger J (2003) Signal transduction. Autoinhibition control. *Science* **300:** 750-752

Schmidt-Ullrich RK, Contessa JN, Dent P, Mikkelsen RB, Valerie K, Reardon DB, Bowers G, Lin PS (1999) Molecular mechanisms of radiation-induced accelerated repopulation. *Radiat Oncol Investig* **7:** 321-330

Schmiedel J, Blaukat A, Li S, Knochel T, Ferguson KM (2008) Matuzumab binding to EGFR prevents the conformational rearrangement required for dimerization. *Cancer Cell* **13:** 365-373

Sebastian T, Malik R, Thomas S, Sage J, Johnson PF (2005) C/EBPbeta cooperates with RB:E2F to implement Ras(V12)-induced cellular senescence. *EMBO J* **24:** 3301-3312

Seger R, Rodeck U, Yarden Y (2008) Receptor tyrosine kinases: the emerging tip of systems control. *IET Syst Biol* **2:** 1-4

Selvanayagam CS, Davis CM, Cornforth MN, Ullrich RL (1995) Latent expression of p53 mutations and radiation-induced mammary cancer. *Cancer Res* **55:** 3310-3317

Sequist LV, Martins RG, Spigel D, Grunberg SM, Spira A, Janne PA, Joshi VA, McCollum D, Evans TL, Muzikansky A, Kuhlmann GL, Han M, Goldberg JS, Settleman J, Iafrate AJ, Engelman JA, Haber DA, Johnson BE, Lynch TJ (2008) First-line gefitinib in patients with advanced non-small-cell lung cancer harboring somatic EGFR mutations. *J Clin Oncol* **26:** 2442-2449

Sergina NV, Rausch M, Wang D, Blair J, Hann B, Shokat KM, Moasser MM (2007) Escape from HER-family tyrosine kinase inhibitor therapy by the kinase-inactive HER3. *Nature* **445:** 437-441

Shackleton M, Quintana E, Fearon ER, Morrison SJ (2009) Heterogeneity in cancer: cancer stem cells versus clonal evolution. *Cell* **138:** 822-829

Shan B, Durfee T, Lee WH (1996) Disruption of RB/E2F-1 interaction by single point mutations in E2F-1 enhances S-phase entry and apoptosis. *Proc Natl Acad Sci U S A* **93:** 679-684

Shao CJ, Fu J, Shi HL, Mu YG, Chen ZP (2008) Activities of DNA-PK and Ku86, but not Ku70, may predict sensitivity to cisplatin in human gliomas. *J Neurooncol* **89:** 27-35

Sharma SV, Settleman J (2009) ErbBs in lung cancer. *Exp Cell Res* **315:** 557-571

Shi F, Telesco SE, Liu Y, Radhakrishnan R, Lemmon MA ErbB3/HER3 intracellular domain is competent to bind ATP and catalyze autophosphorylation. *Proc Natl Acad Sci U S A* **107:** 7692-7697

Shi M, Vivian CJ, Lee KJ, Ge C, Morotomi-Yano K, Manzl C, Bock F, Sato S, Tomomori-Sato C, Zhu R, Haug JS, Swanson SK, Washburn MP, Chen DJ, Chen BP, Villunger A, Florens L, Du C (2009) DNA-PKcs-PIDDosome: a nuclear caspase-2-activating complex with role in G2/M checkpoint maintenance. *Cell* **136:** 508-520

Shi Y (2002) Apoptosome: the cellular engine for the activation of caspase-9. *Structure* **10:** 285-288

Shiloh Y (2003) ATM and related protein kinases: safeguarding genome integrity. *Nat Rev Cancer* **3:** 155-168

Shimamura T, Lowell AM, Engelman JA, Shapiro GI (2005) Epidermal growth factor receptors harboring kinase domain mutations associate with the heat shock protein 90 chaperone and are destabilized following exposure to geldanamycins. *Cancer Res* **65:** 6401-6408

Shrivastav M, De Haro LP, Nickoloff JA (2008) Regulation of DNA double-strand break repair pathway choice. *Cell Res* **18:** 134-147

Shrivastav M, Miller CA, De Haro LP, Durant ST, Chen BP, Chen DJ, Nickoloff JA (2009) DNA-PKcs and ATM co-regulate DNA double-strand break repair. *DNA Repair (Amst)* **8:** 920-929

Shtiegman K, Kochupurakkal BS, Zwang Y, Pines G, Starr A, Vexler A, Citri A, Katz M, Lavi S, Ben-Basat Y, Benjamin S, Corso S, Gan J, Yosef RB, Giordano S, Yarden Y (2007) Defective ubiquitinylation of EGFR mutants of lung cancer confers prolonged signaling. *Oncogene* **26:** 6968-6978

Sibanda BL, Chirgadze DY, Blundell TL (2010) Crystal structure of DNA-PKcs reveals a large open-ring cradle comprised of HEAT repeats. *Nature* **463:** 118-121

Sigismund S, Argenzio E, Tosoni D, Cavallaro E, Polo S, Di Fiore PP (2008) Clathrin-mediated internalization is essential for sustained EGFR signaling but dispensable for degradation. *Dev Cell* **15:** 209-219

Sigismund S, Woelk T, Puri C, Maspero E, Tacchetti C, Transidico P, Di Fiore PP, Polo S (2005) Clathrin-independent endocytosis of ubiquitinated cargos. *Proc Natl Acad Sci U S A* **102:** 2760-2765

Smeaton MB, Hlavin EM, McGregor Mason T, Noronha AM, Wilds CJ, Miller PS (2008) Distortion-dependent unhooking of interstrand cross-links in mammalian cell extracts. *Biochemistry* **47:** 9920-9930

Smeaton MB, Hlavin EM, Noronha AM, Murphy SP, Wilds CJ, Miller PS (2009) Effect of cross-link structure on DNA interstrand cross-link repair synthesis. *Chem Res Toxicol* **22:** 1285-1297

Soh J, Toyooka S, Ichihara S, Suehisa H, Kobayashi N, Ito S, Yamane M, Aoe M, Sano Y, Kiura K, Date H (2007) EGFR mutation status in pleural fluid predicts tumor responsiveness and resistance to gefitinib. *Lung Cancer* **56:** 445-448

Sorkin A, Goh LK (2008) Endocytosis and intracellular trafficking of ErbBs. *Exp Cell Res* **314:** 3093-3106

Sorscher SM (2004) EGFR mutations and sensitivity to gefitinib. *N Engl J Med* **351:** 1260-1261; author reply 1260-1261

Spanswick VJ, Craddock C, Sekhar M, Mahendra P, Shankaranarayana P, Hughes RG, Hochhauser D, Hartley JA (2002) Repair of DNA interstrand crosslinks as a mechanism of clinical resistance to melphalan in multiple myeloma. *Blood* **100:** 224-229

Spanswick VJ, Hartley JM, Hartley JA Measurement of DNA interstrand crosslinking in individual cells using the Single Cell Gel Electrophoresis (Comet) assay. *Methods Mol Biol* **613:** 267-282

Stang E, Blystad FD, Kazazic M, Bertelsen V, Brodahl T, Raiborg C, Stenmark H, Madshus IH (2004) Cbl-dependent ubiquitination is required for progression of EGF receptors into clathrin-coated pits. *Mol Biol Cell* **15:** 3591-3604

Stracker TH, Williams BR, Deriano L, Theunissen JW, Adelman CA, Roth DB, Petrini JH (2009) Artemis and nonhomologous end joining-independent influence of DNA-dependent protein kinase catalytic subunit on chromosome stability. *Mol Cell Biol* **29:** 503-514

Strambio-De-Castillia C, Niepel M, Rout MP The nuclear pore complex: bridging nuclear transport and gene regulation. *Nat Rev Mol Cell Biol* **11:** 490-501

Sugawara N, Paques F, Colaiacovo M, Haber JE (1997) Role of Saccharomyces cerevisiae Msh2 and Msh3 repair proteins in double-strand break-induced recombination. *Proc Natl Acad Sci U S A* **94:** 9214-9219

Sundberg AL, Almqvist Y, Tolmachev V, Carlsson J (2003) Treatment of cultured glioma cells with the EGFR-TKI gefitinib ("Iressa", ZD1839) increases the uptake of astatinated EGF despite the absence of gefitinib-mediated growth inhibition. *Eur J Nucl Med Mol Imaging* **30:** 727-729

Swartzlander DB, Griffiths LM, Lee J, Degtyareva NP, Doetsch PW, Corbett AH Regulation of base excision repair: Ntg1 nuclear and mitochondrial dynamic localization in response to genotoxic stress. *Nucleic Acids Res* **38:** 3963-3974

Swartzlander DB, Griffiths LM, Lee J, Degtyareva NP, Doetsch PW, Corbett AH (2010) Regulation of base excision repair: Ntg1 nuclear and mitochondrial dynamic localization in response to genotoxic stress. *Nucleic Acids Res* **38:** 3963-3974

Szumiel I (2008) Intrinsic radiation sensitivity: cellular signaling is the key. *Radiat Res* **169:** 249-258

Tam IY, Leung EL, Tin VP, Chua DT, Sihoe AD, Cheng LC, Chung LP, Wong MP (2009) Double EGFR mutants containing rare EGFR mutant types show reduced in vitro response to gefitinib compared with common activating missense mutations. *Mol Cancer Ther* **8:** 2142-2151

Tanos B, Pendergast AM (2006) Abl tyrosine kinase regulates endocytosis of the epidermal growth factor receptor. *J Biol Chem* **281:** 32714-32723

Thiel KW, Carpenter G (2007) Epidermal growth factor receptor juxtamembrane region regulates allosteric tyrosine kinase activation. *Proc Natl Acad Sci U S A* **104:** 19238-19243

Tornaletti S (2009) DNA repair in mammalian cells: Transcription-coupled DNA repair: directing your effort where it's most needed. *Cell Mol Life Sci* **66:** 1010-1020

Toulany M, Baumann M, Rodemann HP (2007) Stimulated PI3K-AKT signaling mediated through ligand or radiation-induced EGFR depends indirectly, but not directly, on constitutive K-Ras activity. *Mol Cancer Res* **5:** 863-872

Toulany M, Dittmann K, Baumann M, Rodemann HP (2005) Radiosensitization of Ras-mutated human tumor cells in vitro by the specific EGF receptor antagonist BIBX1382BS. *Radiother Oncol* **74:** 117-129

Toulany M, Dittmann K, Fehrenbacher B, Schaller M, Baumann M, Rodemann HP (2008a) PI3K-Akt signaling regulates basal, but MAP-kinase signaling regulates radiation-induced XRCC1 expression in human tumor cells in vitro. *DNA Repair (Amst)* **7:** 1746-1756

Toulany M, Kasten-Pisula U, Brammer I, Wang S, Chen J, Dittmann K, Baumann M, Dikomey E, Rodemann HP (2006) Blockage of epidermal growth factor receptor-phosphatidylinositol 3-kinase-AKT signaling increases radiosensitivity of K-RAS mutated human tumor cells in vitro by affecting DNA repair. *Clin Cancer Res* **12:** 4119-4126

Toulany M, Kehlbach R, Florczak U, Sak A, Wang S, Chen J, Lobrich M, Rodemann HP (2008b) Targeting of AKT1 enhances radiation toxicity of human tumor cells by inhibiting DNA-PKcs-dependent DNA double-strand break repair. *Mol Cancer Ther* **7:** 1772-1781

Tsujimoto Y (2003) Cell death regulation by the Bcl-2 protein family in the mitochondria. *J Cell Physiol* **195:** 158-167

Turchi JJ (2006) Nitric oxide and cisplatin resistance: NO easy answers. *Proc Natl Acad Sci U S A* **103:** 4337-4338

Turchi JJ, Henkels KM, Hermanson IL, Patrick SM (1999) Interactions of mammalian proteins with cisplatin-damaged DNA. *J Inorg Biochem* **77:** 83-87

Turchi JJ, Henkels KM, Zhou Y (2000) Cisplatin-DNA adducts inhibit translocation of the Ku subunits of DNA-PK. *Nucleic Acids Res* **28:** 4634-4641

Turchi JJ, Li M, Henkels KM (1996) Cisplatin-DNA binding specificity of calf high-mobility group 1 protein. *Biochemistry* **35:** 2992-3000

Tvorogov D, Carpenter G (2002) EGF-dependent association of phospholipase C-gamma1 with c-Cbl. *Exp Cell Res* **277:** 86-94

Ushiki A, Koizumi T, Kobayashi N, Kanda S, Yasuo M, Yamamoto H, Kubo K, Aoyagi D, Nakayama J (2009) Genetic heterogeneity of EGFR mutation in pleomorphic carcinoma of the lung: response to gefitinib and clinical outcome. *Jpn J Clin Oncol* **39:** 267-270

Vallbohmer D, Zhang W, Gordon M, Yang DY, Yun J, Press OA, Rhodes KE, Sherrod AE, Iqbal S, Danenberg KD, Groshen S, Lenz HJ (2005) Molecular determinants of cetuximab efficacy. *J Clin Oncol* **23:** 3536-3544

van Gent DC, van der Burg M (2007) Non-homologous end-joining, a sticky affair. *Oncogene* **26:** 7731-7740

van Vugt MA, Bras A, Medema RH (2005) Restarting the cell cycle when the checkpoint comes to a halt. *Cancer Res* **65:** 7037-7040

Viana-Pereira M, Lopes JM, Little S, Milanezi F, Basto D, Pardal F, Jones C, Reis RM (2008) Analysis of EGFR overexpression, EGFR gene amplification and the EGFRvIII mutation in Portuguese high-grade gliomas. *Anticancer Res* **28:** 913-920

Vogelstein B, Kinzler KW (2004) Cancer genes and the pathways they control. *Nat Med* **10:** 789-799

Wang D, Lippard SJ (2005) Cellular processing of platinum anticancer drugs. *Nat Rev Drug Discov* **4:** 307-320

Wang Q, Greene MI (2005) EGFR enhances Survivin expression through the phosphoinositide 3 (PI-3) kinase signaling pathway. *Exp Mol Pathol* **79:** 100-107

Wang Q, Zhu F, Wang Z (2007) Identification of EGF receptor C-terminal sequences 1005-1017 and di-leucine motif 1010LL1011 as essential in EGF receptor endocytosis. *Exp Cell Res* **313:** 3349-3363

Wang SC, Hung MC (2009) Nuclear translocation of the epidermal growth factor receptor family membrane tyrosine kinase receptors. *Clin Cancer Res* **15:** 6484-6489

Wang SE, Narasanna A, Perez-Torres M, Xiang B, Wu FY, Yang S, Carpenter G, Gazdar AF, Muthuswamy SK, Arteaga CL (2006) HER2 kinase domain mutation results in constitutive phosphorylation and activation of HER2 and EGFR and resistance to EGFR tyrosine kinase inhibitors. *Cancer Cell* **10:** 25-38

Wang WD, Li R, Chen ZT, Li DZ, Duan YZ, Cao ZH (2005) Cisplatin-controlled p53 gene therapy for human non-small cell lung cancer xenografts in athymic nude mice via the CArG elements. *Cancer Sci* **96:** 706-712

Wang YN, Wang H, Yamaguchi H, Lee HJ, Lee HH, Hung MC (2010a) COPI-mediated retrograde trafficking from the Golgi to the ER regulates EGFR nuclear transport. *Biochem Biophys Res Commun* **399:** 498-504

Wang YN, Yamaguchi H, Hsu JM, Hung MC (2010b) Nuclear trafficking of the epidermal growth factor receptor family membrane proteins. *Oncogene* **29:** 3997-4006

Wang YN, Yamaguchi H, Huo L, Du Y, Lee HJ, Lee HH, Wang H, Hsu JM, Hung MC The translocon Sec61beta localized in the inner nuclear membrane transports membrane-embedded EGF receptor to the nucleus. *J Biol Chem* **285:** 38720-38729

Wang YN, Yamaguchi H, Huo L, Du Y, Lee HJ, Lee HH, Wang H, Hsu JM, Hung MC (2010c) The translocon Sec61beta localized in the inner nuclear membrane transports membrane-embedded EGF receptor to the nucleus. *J Biol Chem* **285:** 38720-38729

Wang Z, Zhang L, Yeung TK, Chen X (1999) Endocytosis deficiency of epidermal growth factor (EGF) receptor-ErbB2 heterodimers in response to EGF stimulation. *Mol Biol Cell* **10:** 1621-1636

Wanner G, Mayer C, Kehlbach R, Rodemann HP, Dittmann K (2008) Activation of protein kinase Cepsilon stimulates DNA-repair via epidermal growth factor receptor nuclear accumulation. *Radiother Oncol* **86:** 383-390

Ward JF (1995) Radiation mutagenesis: the initial DNA lesions responsible. *Radiat Res* **142:** 362-368

Warren CM, Landgraf R (2006) Signaling through ERBB receptors: multiple layers of diversity and control. *Cell Signal* **18:** 923-933

Waterman H, Yarden Y (2001) Molecular mechanisms underlying endocytosis and sorting of ErbB receptor tyrosine kinases. *FEBS Lett* **490:** 142-152

Weis K (1998) Importins and exportins: how to get in and out of the nucleus. *Trends Biochem Sci* **23:** 185-189

Weis K (2007) The nuclear pore complex: oily spaghetti or gummy bear? *Cell* **130:** 405-407

Weisz L, Damalas A, Liontos M, Karakaidos P, Fontemaggi G, Maor-Aloni R, Kalis M, Levrero M, Strano S, Gorgoulis VG, Rotter V, Blandino G, Oren M (2007) Mutant p53 enhances nuclear factor kappaB activation by tumor necrosis factor alpha in cancer cells. *Cancer Res* **67:** 2396-2401

Wells A, Marti U (2002) Signalling shortcuts: cell-surface receptors in the nucleus? *Nat Rev Mol Cell Biol* **3:** 697-702

Wente SR, Rout MP The Nuclear Pore Complex and Nuclear Transport. *Cold Spring Harb Perspect Biol*

Wernyj RP, Morin PJ (2004) Molecular mechanisms of platinum resistance: still searching for the Achilles' heel. *Drug Resist Updat* **7:** 227-232

Weterings E, Chen DJ (2007) DNA-dependent protein kinase in nonhomologous end joining: a lock with multiple keys? *J Cell Biol* **179:** 183-186

Wheeler DL, Dunn EF, Harari PM Understanding resistance to EGFR inhibitors-impact on future treatment strategies. *Nat Rev Clin Oncol* **7:** 493-507

Wheeler DL, Dunn EF, Harari PM (2010) Understanding resistance to EGFR inhibitors-impact on future treatment strategies. *Nat Rev Clin Oncol* **7:** 493-507

Wheeler DL, Iida M, Kruser TJ, Nechrebecki MM, Dunn EF, Armstrong EA, Huang S, Harari PM (2009) Epidermal growth factor receptor cooperates with Src family kinases in acquired resistance to cetuximab. *Cancer Biol Ther* **8:** 696-703

Wheeler SE, Suzuki S, Thomas SM, Sen M, Leeman-Neill RJ, Chiosea SI, Kuan CT, Bigner DD, Gooding WE, Lai SY, Grandis JR Epidermal growth factor receptor variant III mediates head and neck cancer cell invasion via STAT3 activation. *Oncogene* **29:** 5135-5145

Williams RT, den Besten W, Sherr CJ (2007) Cytokine-dependent imatinib resistance in mouse BCR-ABL+, Arf-null lymphoblastic leukemia. *Genes Dev* **21:** 2283-2287

Winograd-Katz SE, Levitzki A (2006) Cisplatin induces PKB/Akt activation and p38(MAPK) phosphorylation of the EGF receptor. *Oncogene* **25:** 7381-7390

Woelk T, Sigismund S, Penengo L, Polo S (2007) The ubiquitination code: a signalling problem. *Cell Div* **2:** 11

Wojda I (2000) [The group of protein kinases CKI]. *Postepy Biochem* **46:** 140-147

Wong AJ, Ruppert JM, Bigner SH, Grzeschik CH, Humphrey PA, Bigner DS, Vogelstein B (1992) Structural alterations of the epidermal growth factor receptor gene in human gliomas. *Proc Natl Acad Sci U S A* **89:** 2965-2969

Wu JY, Wu SG, Yang CH, Chang YL, Chang YC, Hsu YC, Shih JY, Yang PC Comparison of gefitinib and erlotinib in advanced NSCLC and the effect of EGFR mutations. *Lung Cancer*

Wynne P, Newton C, Ledermann JA, Olaitan A, Mould TA, Hartley JA (2007) Enhanced repair of DNA interstrand crosslinking in ovarian cancer cells from patients following treatment with platinum-based chemotherapy. *Br J Cancer* **97:** 927-933

Xia W, Wei Y, Du Y, Liu J, Chang B, Yu YL, Huo LF, Miller S, Hung MC (2009) Nuclear expression of epidermal growth factor receptor is a novel prognostic value in patients with ovarian cancer. *Mol Carcinog* **48:** 610-617

Xu K, Chang CM, Gao H, Shu HK (2009a) Epidermal growth factor-dependent cyclooxygenase-2 induction in gliomas requires protein kinase C-delta. *Oncogene* **28:** 1410-1420

Xu Y, Liu H, Chen J, Zhou Q Acquired resistance of lung adenocarcinoma to EGFR-tyrosine kinase inhibitors gefitinib and erlotinib. *Cancer Biol Ther* **9:** 572-582

Xu Y, Shao Y, Zhou J, Voorhees JJ, Fisher GJ (2009b) Ultraviolet irradiation-induces epidermal growth factor receptor (EGFR) nuclear translocation in human keratinocytes. *J Cell Biochem* **107:** 873-880

Yang L, Dan HC, Sun M, Liu Q, Sun XM, Feldman RI, Hamilton AD, Polokoff M, Nicosia SV, Herlyn M, Sebti SM, Cheng JQ (2004) Akt/protein kinase B signaling inhibitor-2, a selective small molecule inhibitor of Akt signaling with antitumor activity in cancer cells overexpressing Akt. *Cancer Res* **64:** 4394-4399

Yang S, Park K, Turkson J, Arteaga CL (2008) Ligand-independent phosphorylation of Y869 (Y845) links mutant EGFR signaling to stat-mediated gene expression. *Exp Cell Res* **314:** 413-419

Yang S, Qu S, Perez-Tores M, Sawai A, Rosen N, Solit DB, Arteaga CL (2006) Association with HSP90 inhibits Cbl-mediated down-regulation of mutant epidermal growth factor receptors. *Cancer Res* **66:** 6990-6997

Yano S, Yamaguchi M, Dong RP (2003) EGFR tyrosine kinase inhibitor "gefitinib (Iressa)" for cancer therapy. *Nippon Yakurigaku Zasshi* **122:** 491-497

Yeo WL, Riely GJ, Yeap BY, Lau MW, Warner JL, Bodio K, Huberman MS, Kris MG, Tenen DG, Pao W, Kobayashi S, Costa DB Erlotinib at a dose of 25 mg daily for non-small cell lung cancers with EGFR mutations. *J Thorac Oncol* **5:** 1048-1053

Yoshida T, Okamoto I, Iwasa T, Fukuoka M, Nakagawa K (2008) The anti-EGFR monoclonal antibody blocks cisplatin-induced activation of EGFR signaling mediated by HB-EGF. *FEBS Lett* **582:** 4125-4130

Young JC, Moarefi I, Hartl FU (2001) Hsp90: a specialized but essential protein-folding tool. *J Cell Biol* **154:** 267-273

Yu X, Sharma KD, Takahashi T, Iwamoto R, Mekada E (2002) Ligand-independent dimer formation of epidermal growth factor receptor (EGFR) is a step separable from ligand-induced EGFR signaling. *Mol Biol Cell* **13:** 2547-2557

Yu Z, Boggon TJ, Kobayashi S, Jin C, Ma PC, Dowlati A, Kern JA, Tenen DG, Halmos B (2007) Resistance to an irreversible epidermal growth factor receptor (EGFR) inhibitor in EGFR-mutant lung cancer reveals novel treatment strategies. *Cancer Res* **67:** 10417-10427

Zaczek A, Brandt B, Bielawski KP (2005) The diverse signaling network of EGFR, HER2, HER3 and HER4 tyrosine kinase receptors and the consequences for therapeutic approaches. *Histol Histopathol* **20:** 1005-1015

Zaidi SK, Young DW, Choi JY, Pratap J, Javed A, Montecino M, Stein JL, Lian JB, van Wijnen AJ, Stein GS (2004) Intranuclear trafficking: organization and assembly of regulatory machinery for combinatorial biological control. *J Biol Chem* **279:** 43363-43366

Zandi R, Larsen AB, Andersen P, Stockhausen MT, Poulsen HS (2007) Mechanisms for oncogenic activation of the epidermal growth factor receptor. *Cell Signal* **19:** 2013-2023

Zdraveski ZZ, Mello JA, Farinelli CK, Essigmann JM, Marinus MG (2002) MutS preferentially recognizes cisplatin- over oxaliplatin-modified DNA. *J Biol Chem* **277:** 1255-1260

Zdraveski ZZ, Mello JA, Marinus MG, Essigmann JM (2000) Multiple pathways of recombination define cellular responses to cisplatin. *Chem Biol* **7:** 39-50

Zhang X, Gureasko J, Shen K, Cole PA, Kuriyan J (2006) An allosteric mechanism for activation of the kinase domain of epidermal growth factor receptor. *Cell* **125:** 1137-1149

Zhou BB, Elledge SJ (2000) The DNA damage response: putting checkpoints in perspective. *Nature* **408:** 433-439

Zhou BB, Peyton M, He B, Liu C, Girard L, Caudler E, Lo Y, Baribaud F, Mikami I, Reguart N, Yang G, Li Y, Yao W, Vaddi K, Gazdar AF, Friedman SM, Jablons DM, Newton RC, Fridman JS, Minna JD, Scherle PA (2006) Targeting ADAM-mediated ligand cleavage to inhibit HER3 and EGFR pathways in non-small cell lung cancer. *Cancer Cell* **10:** 39-50

Zhu JQ, Zhong WZ, Zhang GC, Li R, Zhang XC, Guo AL, Zhang YF, An SJ, Mok TS, Wu YL (2008) Better survival with EGFR exon 19 than exon 21 mutations in gefitinib-treated non-small cell lung cancer patients is due to differential inhibition of downstream signals. *Cancer Lett* **265:** 307-317

Zorbas H, Keppler BK (2005) Cisplatin damage: are DNA repair proteins saviors or traitors to the cell? *Chembiochem* **6:** 1157-1166

Zwang Y, Yarden Y (2009) Systems biology of growth factor-induced receptor endocytosis. *Traffic* **10:** 349-363

Reference List

Cepeda V, Fuertes MA, Castilla J, Alonso C, Quevedo C and Perez JM. (2007). *Anticancer Agents Med Chem*, **7,** 3-18.

De S, I, McHugh PJ, Clingen PH and Hartley JA. (2000). *Mol Cell Biol,* **20,** 7980-7990.

De S, I, McHugh PJ, Clingen PH and Hartley JA. (2002). *Nucleic Acids Res,* **30,** 3848-3856.

Kartalou M and Essigmann JM. (2001). *Mutat Res,* **478,** 1-21.

Nojima K, Hochegger H, Saberi A, Fukushima T, Kikuchi K, Yoshimura M, Orelli BJ, Bishop DK, Hirano S, Ohzeki M, Ishiai M, Yamamoto K, Takata M, Arakawa H, Buerstedde JM, Yamazoe M, Kawamoto T, Araki K, Takahashi JA, Hashimoto N, Takeda S and Sonoda E. (2005a). *Cancer Res,* **65,** 11704-11711.

Nojima K, Hochegger H, Saberi A, Fukushima T, Kikuchi K, Yoshimura M, Orelli BJ, Bishop DK, Hirano S, Ohzeki M, Ishiai M, Yamamoto K, Takata M, Arakawa H, Buerstedde JM, Yamazoe M, Kawamoto T, Araki K, Takahashi JA, Hashimoto N, Takeda S and Sonoda E. (2005b). *Cancer Res,* **65,** 11704-11711.

Nojima K, Hochegger H, Saberi A, Fukushima T, Kikuchi K, Yoshimura M, Orelli BJ, Bishop DK, Hirano S, Ohzeki M, Ishiai M, Yamamoto K, Takata M, Arakawa H, Buerstedde JM, Yamazoe M, Kawamoto T, Araki K, Takahashi JA, Hashimoto N, Takeda S and Sonoda E. (2005c). *Cancer Res,* **65,** 11704-11711.

Zorbas H and Keppler BK. (2005). *Chembiochem,* **6,** 1157-1166.